ISSN 0918-4597

NRIM

Research Activities

1992

National Research Institute for Metals

Japan

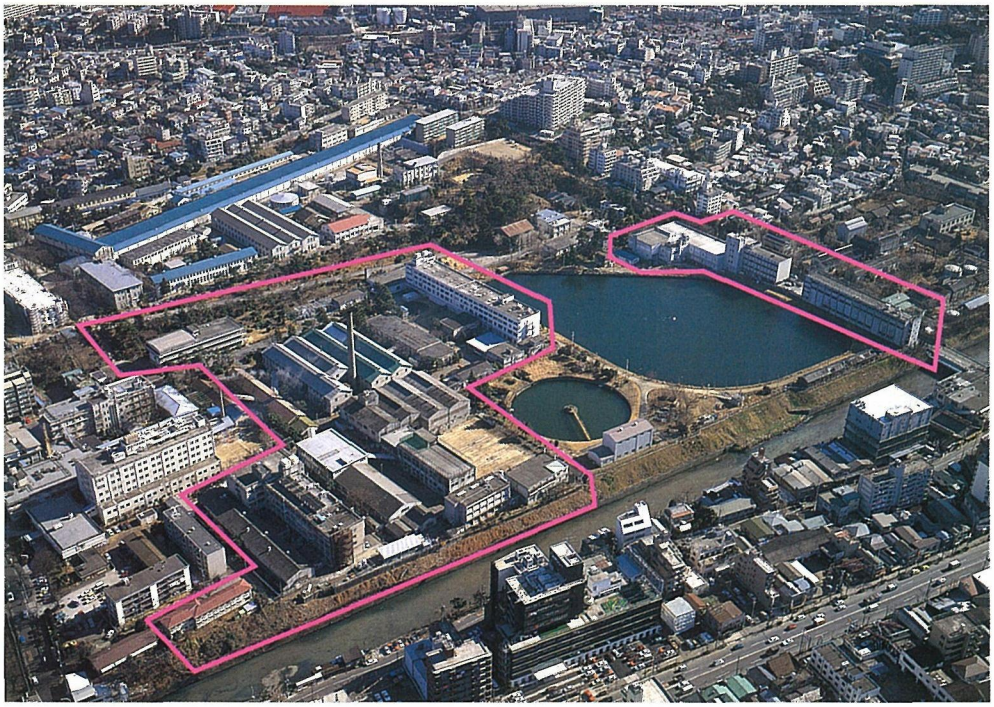

Meguro Main Site

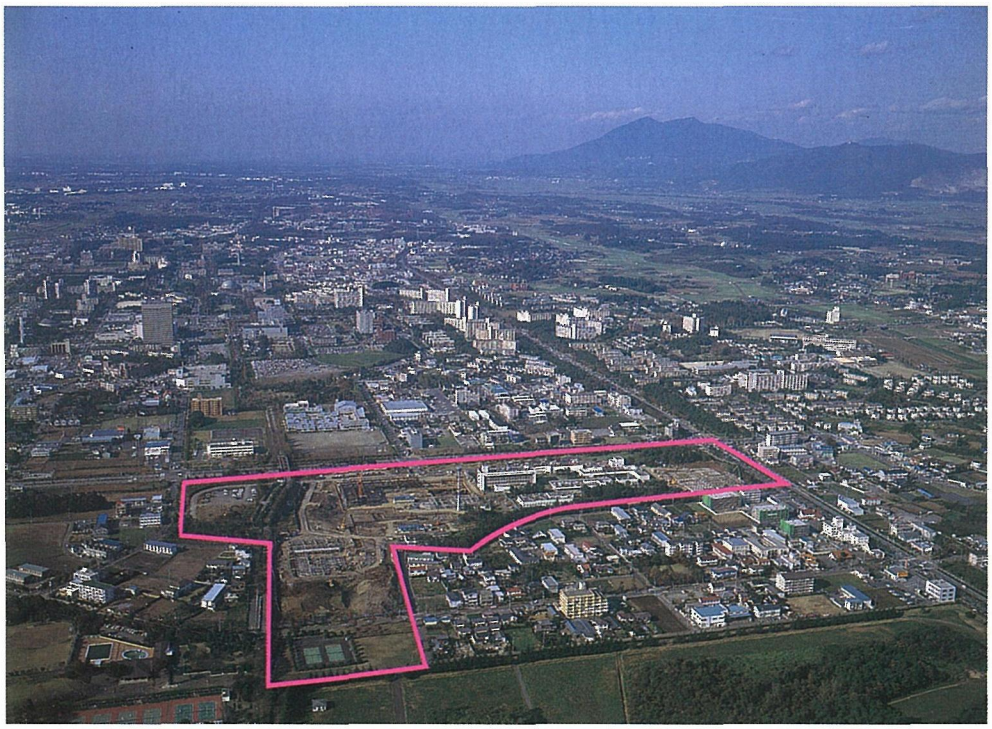

Tsukuba Laboratories

NRIM Research Activities

1992

National Research Institute for Metals, Japan

For the last several years, international scientific exchange between the National Research Institute for Metals (NRIM) and foreign research organizations through joint projects and exchange of scientists and information has increased considerably. We intend NRIM to be an open research center interacting even more actively with other research organizations all over the world. For this purpose, NRIM was to publish a new *annual report "NRIM Research Activities" instead of the former English publication* "Transactions of NRIM" in 1991. This new journal is arranged to present, up-to-date research activities in NRIM and other information such as its organization and budget. We hope that "NRIM Research Activities" will indeed be useful for your understanding of NRIM and will promote mutual scientific relationship.

Preface

National Research Institute for Metals was established in 1956 as a research organization attached to the Science and Technology Agency of the Japanese Government. Since then, our Institute has played an important role in research and development of metals and alloys in Japan. Now NRIM has research staffs of over 300 people with a budget of about 7.5 billion yen (FY 1992) and is located at two sites; the main site in Tokyo and the branch in Tsukuba City.

The research activities of NRIM are concentrated on two fields. One is fundamental and applied research for advanced materials such as metallic and oxide superconductors, heat-resisting alloys, structural intermetallic compounds, etc. The other is research on reliability of materials to ensure safety of structural components and facilities. It includes the production of standard creep and fatigue data of Japanese commercial alloys, research on the failure mechanism, life prediction method and so on.

During the past 36 years, we have made several contributions to materials science and technology, especially in the fields of superconducting materials and superalloys. We have developed the bronze method to draw wires of metallic superconducting materials, and in 1988 our colleague found a new superconducting material of Bi-Sr-Ca-Cu oxide, which has T_c higher than 100K. The computer aided alloy design method for superalloys was constructed, and several excellent heat-resisting alloys have been successfully developed. In the research on reliability of materials, we have been conducting the very long-term research programs on creep and fatigue properties, including creep rupture testing over 100,000 hr. We have published these data as the series of NRIM Creep and Fatigue Data Sheets, which we think are one of the most reliable sets of creep and fatigue data of commercial alloys. Through these programs, we have contributed to the progress in the life prediction technology and advanced materials assessment technology.

We are now concentrating the whole Institute in Tsukuba City, and the new site will be completed in 1994. We will take this occasion to extend our materials research in the various fields, especially researches in high magnetic field, in ultra-high vacuum and in excited state assisted by high energy beams, and currently we are building their facility base. We expect this extension will bring about a new development of NRIM.

Kazuyoshi Nii

Dr. NII, Kazuyoshi
Director-General

NRIM Research Activities 1992

Contents

❒ Pressure Effect on T_c of $YBa_2Cu_4O_8$

T. Matsumoto, Materials Physics Division

Keywords: electrical resistance, structure, neutron diffraction, Madelung energy, charge redistribution model

Since the discovery of the high T_c superconducting oxide, there are many works which have attempted to synthesize new materials with layered structure. Among these oxides, $YBa_2Cu_4O_8$ (Y124) is regarded as a unique material. The parent oxides of many superconductors are generally insulator without carrier doping. However, $[Cu\text{-}O]^+$ holes are self-doped in an as-prepared Y124 which becomes superconducting with T_c=80 K. Furthermore, this oxide is characterized by not only the absence of oxygen defects, but also the perfect ordering of constituent elements.

The high pressure technique is often regarded as a useful tool for understanding the physical properties of materials. So, in the context of the study of pressure effects on oxide superconductors, we measured the change in T_c for Y124 as a function of pressure. The T_c of Y124 rises markedly with an increase of pressure and exceeds 100K above 4 GPa as shown in figure 1. Compared with the result for $YBa_2Cu_3O_{7-\delta}$ (Y123), the pressure dependence of T_c for Y124 is considerably different. The initial values of dT_c/dP for Y123 and Y124 are reported to be about 0.7 and 5.5 K/GPa, respectively.

Although the structure of Y123 is closely related to that of Y124, it has not yet been understood why there appears the large difference between their dT_c/dP values. We also performed a structural study of Y124 at high pressure[1] by neutron diffraction in order to clarify the enhancement of T_c by pressure. As shown in figure 2, the fundamental unit of their structures is a five-coordinated CuO_2 plane and a four-coordinated CuO chain. The corner-shared CuO chain in Y123 (not shown) is replaced by the edge-shared double CuO chain in Y124. In this work, the special attention has been drawn to the pressure induced change in the position of apical oxygen located above or below Cu atom in the CuO_2 plane. This plays a dominant role for the superconducting properties.

Linear compressibilities of Y124 were estimated from the present result of neutron diffraction as follows:

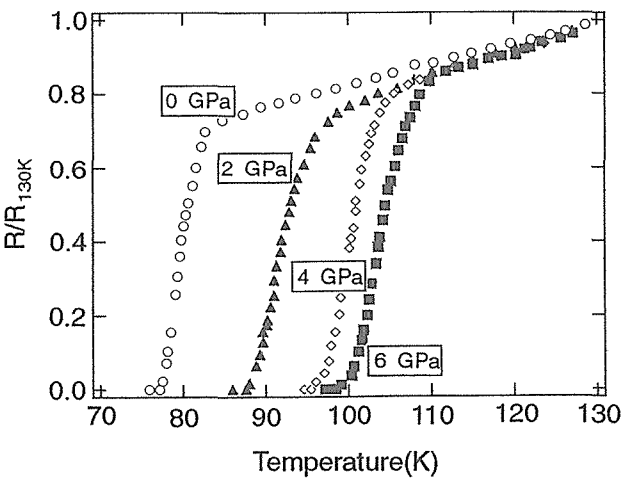

Fig. 1. Pressure dependence of electrical resistance for $YBa_2Cu_4O_8$ normalized at 130 K.

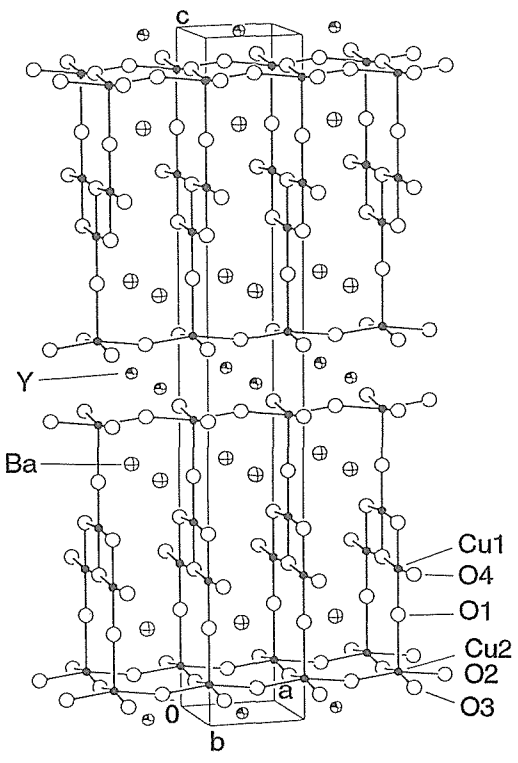

Fig. 2. Crystal structure of $YBa_2Cu_4O_8$. Cu and O atoms are connected with bonds

$-(da/dP)/a_o = 3.05 \times 10^{-3}$/GPa
$-(db/dP)/b_o = 1.45 \times 10^{-3}$
$-(dc/dP)/c_o = 4.00 \times 10^{-3}$

As shown in figure 3, the bond length l(Cu(2)-O(1)) (the interatomic distance between an in-plane Cu and an apical oxygen) decreases continuously with increasing pressure. We could not find any drastic change in the behavior of the apical oxygen as a function of pressure. The change in l(Cu(2)-O(1)) which is parallel to the c-axis is estimated to be about 0.9%/GPa, which is twice that along the c-axis. The decrease in l(Cu(2)-O(1)) must be associated with hole-transfer from the CuO chain to the CuO_2 plane. The enhancement of the hole concentration in the CuO_2 plane is also deduced from the pressure dependence of other bond lengths, for example, l(Ba-O(4)) and l(Cu(2)-Cu(2)).

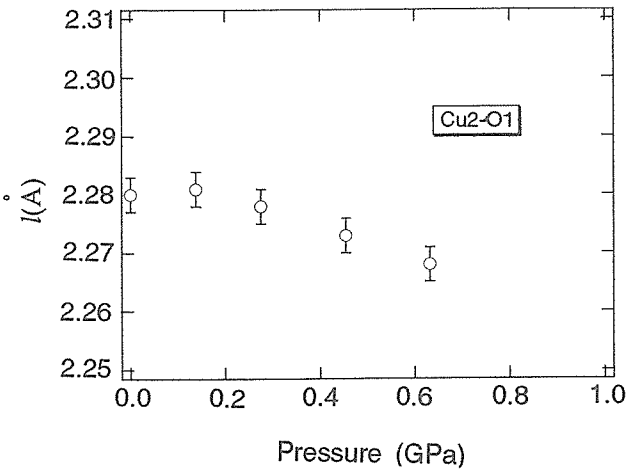

Fig. 3. Pressure dependence of Cu(2)-O(1) bond length for $YBa_2Cu_4O_8$

The Madelung energy (E_M) was calculated as a function of the hole concentration in the CuO_2 plane. As shown in figure 4, the optimum hole number, n_M, which gives the minimum E_M increases with an increase in pressure. The relative change in n_M, Δn by pressure was estimated to be 0.025/GPa from this result. Compared with other reports[2],(3) indicating the hole-concentration dependence of T_c, this value was concluded to correspond to the change in T_c of 5.5K/GPa.

The calculation of the Madelung energy was carried out in the pressure range up to about 5GPa by using the structural data obtained from X-ray experiment at high pressure[4]. The pressure dependence of n_M is shown in figure 5 along with the pressure dependence of T_c. As shown in this figure, the qualitative change of n_M coincides with that of T_c. From these results, the change in T_c of Y124 under pressure is generally explained by the pressure-induced charge redistribution model through the inhomogeneous displacement of all constituent elements including the apical oxygen.

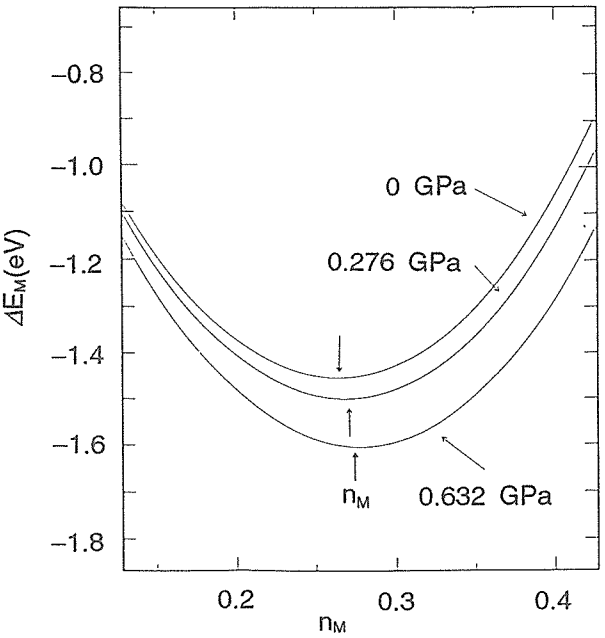

Fig. 4. Relative changes in Madelung energy of $YBa_2Cu_4O_8$ as a function of the number of holes per Cu in the CuO_2 plane

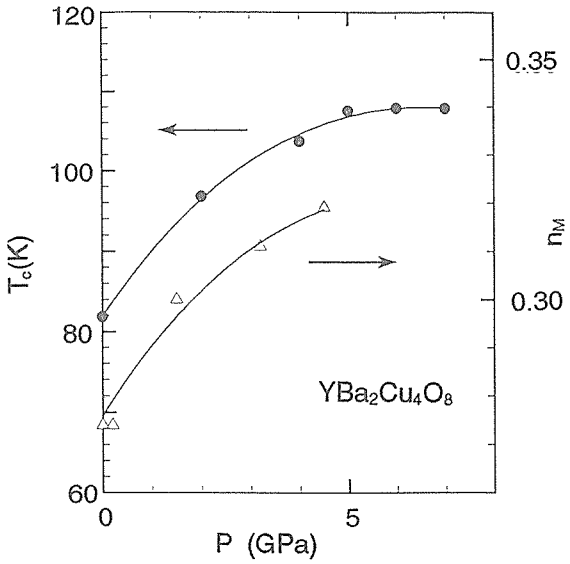

Fig. 5. Pressure dependence of T_c and n_M for $YBa_2Cu_4O_8$

References

1. *Experiment of neutron diffraction at high pressure* was done at the neutron facility (Leader, J.D. Jorgensen) of Argonne National Laboratory, Argonne, Illinois, U.S.A.
2. Jorgensen, J.D., Veal, B.W., Paulikas, A.P., Nowicki, L.J., Crabtree, G.W., Claus, H. and Kwok, W.K. Phys. Rev. B41 (1990): 1863.
3. Tokura, Y., Torrance, J.B., Huang, T.C. and Nazzal, A.I. Phys. Rev. B38 (1988): 7156.
4. Nelmes, R.J., Loveday, J.S., Kaldis, E. and Karpinski, J. Physica C172 (1990): 311.

❒ Modeling of α/α_2 Phase Equilibrium in the Ti-Al system by the Cluster Variation Method

H. Onodera and T. Yokokawa, Materials Design Division

Keywords: cluster variation method, DO_{19} structure, HCP, Ti-Al system, Lennard-Jones potential

The use of the ordered α_2 phase (Ti_3Al) to strengthen the α (hcp) phase of titanium is one of the possible approaches to develop new high temperature titanium alloys. In order to design such alloys, the present authors have applied a sublattice regular solution model to the calculation of the α-α_2 phase equilibrium in the Ti-Al-Sn-Zr system[1]. However, as long as the random mixing is assumed in that model, the atom configuration in compounds may be quite different from reality. The cluster variation method (CVM) can calculate the probabilities of atom configurations in the same and different sublattices in a most reliable manner. Although the CVM is well established for cubic structures such as fcc and bcc, it has not been applied to the hcp structure. In the present study, equations needed in the CVM calculation for the hcp structure are derived based on the tetrahedron approximation with the Lennard-Jones (L-J) pair potential. Subsequently, the method is applied to the calculation of the α-α_2 phase equilibrium in the Ti-Al binary system.

Configurational Entropy for the DO_{19} structure (Ordered hcp)

The nearest neighbor tetrahedron approximation of the CVM in the fcc lattice has been shown to provide an accurate description of the $L1_0$ and $L1_2$ ordering reactions in the binary and ternary model system. In the case of hcp lattice, four sets of the probabilities, Z_{ijkl}^{pqmn} (pqmn = abcd, bcda, cdab and dabc) are needed to express arrangements of the different atomic species on the four four-point clusters shown in figure 1. Figure 1 also shows four simple hexagonal sublattices, labeled a, b, c and d. The symmetry of the DO_{19} structure requires that sublattices b, c and d be indistinguishable. rs and rl are the nearest neighbor and the second neighbor atomic distances, respectively. If a c/a ratio is the ideal value of $(8/3)^{1/2}$, rs is equal to rl, and the four sets of clusters are equivalent.

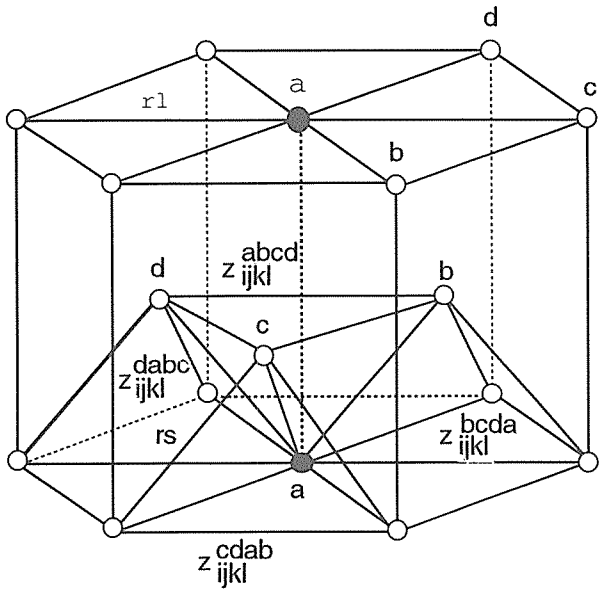

Fig. 1. DO_{19} structure unit cell with four simple hexagonal sublattices, a, b, c and d, and four sets of tetrahedrons used in the CVM approximation

The entropy per each lattice point is obtained by the procedure proposed by Sanchez and de Fontaine as

$$S = -k\left[\frac{1}{2}\sum_{ijkl}\left\{\sum_{pqmn} L\left(Z_{ijkl}^{pqmn}\right)\right\} - \frac{1}{2}\sum_{ijkl}\left\{\sum_{pq} L\left({}^{s}y_{ij}^{pq}\right)+\sum_{pq} L\left({}^{l}y_{ij}^{pq}\right)\right\} + \frac{5}{4}\sum_{i}\left\{\sum_{p} L\left(x_i^p\right)\right\}\right] \quad (1)$$

where x_i^p is the concentration of i atoms in sublattice p, ${}^{s}y_{ij}$ and ${}^{l}y_{ij}$ are the nearest neighbor and the second neighbor pair probabilities of finding an i atom at p sublattice and a j atom at q sublattice, respectively. Z_{ijkl}^{pqmn} is the probability of finding i, j, k and l atoms at p, q, m and n sublattices, respectively. The function L(x) in equation (1) is defined as $L(x)=x\ln(x) - x$.

Free Energy of DO_{19} structure

It is assumed that the enthalphy is given by the sum of the nearest neighbor and the second neighbor pair interactions as

$$H = \frac{1}{2}\sum_{ij}\left\{\sum_{pq} e_{ij}(rs)\cdot {}^{s}y_{ij}^{pq} + \sum_{pq} e_{ij}(rl)\cdot {}^{l}y_{ij}^{pq}\right\} \quad (2)$$

where the pair energy $e_{ij}(r)$ is dependent upon the interatomic distance, r.

The pair interactions are expressed by the L-J potential of the form,

$$e_{ij}(r) = e_{ij}^{O}(rs)\left[\left(\frac{r_{ij}}{r}\right)^{8} - 2\left(\frac{r_{ij}}{r}\right)^{4}\right] \quad (3)$$

The values of the L-J potential parameters are evaluated in principle in the same manner as used by Sigli and Sanchez. Approximate values for the parameters e_{TiAl}^{o} and r_{TiAl} were determined from experimentally determined cohesive energies and lattice parameters of Ti and Al, and from the energy of formation and lattice parameters of stoichiometric Ti_3Al (DO_{19}).

In order to obtain the most probable atom configuration at equilibrium, the grand potential of the system defined as

$$\Omega = H - TS + PV - \sum_{i} \mu_i x_i \quad (4)$$

is minimized with respect to both Z_{ijkl}^{pqmn} and the atomic volume, V, namely, the atomic distance, at the constant temperature, T, pressure, P, and the chemical potential of the i atom, μ_i under the normalization conditions, i.e.,

$$\sum_{ijkl} z_{ijkl}^{pqmn} = 1 \quad (pqmn = abcd,\ bcda,\ cdab,\ \text{and}\ dabc).$$

The pair and point probabilities can be written in terms of the Z_{ijkl}^{pqmn} as

$${}^{S}y_{ij}^{ab} = \sum_{kl} z_{ijkl}^{abcd} = \sum_{kl} z_{jkli}^{bcda},\quad x_i^a = \sum_{jkl} z_{ijkl}^{abcd},\ \text{etc.}, \quad (5)$$

For the cubic structures such as fcc and bcc, the relationships, equation (5) hold inherently. In the case of the DO_{19} structure, however, the relationships do not always hold inherently because the total energy of formation of each tetrahedron is generally different, for example, between an atom configuration of {2111} at {abcd} tetrahedron and that of {1112} at {bcda} tetrahedron. Thus, in order to take in the relationships extrinisically, which is a demand of the lattice structure, the minimization has been done by introducing the proper Lagrange multipliers, λ_i and λ_{ij}^{k}. The minimization of Ω yields

$$z_{ijkl}^{abcd} = Ya^{\frac{1}{2}} \cdot Xa^{\frac{-5}{8}} \exp\left(-Q_{ijkl}/2kT\right) \cdot \exp(2Ma/kT),\ \text{etc.}, \quad (6)$$

where $Q_{ijkl} = U_{ijkl} - \frac{1}{4}\left(\mu_i + \mu_j + \mu_k + \mu_l\right)$,

$$U_{ijkl} = e_{ij}(rs) + e_{ik}(rs) + e_{il}(rs) + e_{jk}(rl) + e_{jl}(rl) + e_{kl}(rl),$$

$$Ya = {}^{S}y_{ij}^{ab}\ {}^{S}y_{ik}^{ac}\ {}^{S}y_{il}^{ad}\ {}^{1}y_{jk}^{bc}\ {}^{1}y_{jl}^{bd}\ {}^{1}y_{kl}^{cd},$$

$$Xa = x_i^a x_j^b x_k^c x_l^d,$$

$$Ma = \lambda_1 - \lambda_{ij}^{1} - \lambda_{ik}^{2} - \lambda_{il}^{3}.$$

Equilibrium rs and rl are calculated from the equation, $dH/dV = -P$.

Titanium-Aluminum System

The initial attempts to fit the experimental α/α_2 phase boundaries, which were summarized by Murray and Wriedt, resulted in considerable deviation from them. Especially, the calculated temperature for the congruent transformation from the disorder state to the ordered DO_{19} structure is considerably lower than experimentally determined one. The values of e_{TiAl}^{o} and r_{TiAl} were used as the variables to fit the experimental diagram. The Ti-Ti and Al-Al parameters were kept constant and equal to the initial values as listed in table 1. The parameters for the Ti-Al pair potential providing the optimal fit to the experimental diagram are listed in table 1. Calculated α/α_2 phase boundaries in the Ti-rich region were in good agreement with the experimental diagram within the experimental scatter as shown in figure 2. The effects of a c/a ratio and the type of pair potential on the CVM calculations may be the subjects of future studies.

Table 1 Lennard-Jones potential parameters

i-j	Parameters	
	e_{ij}^{o} (KJ/mol)	r_{ij} (nm)
Ti-Ti	78.3	0.2922
Al-Al	53.9	0.2864
Ti-Al (best fit)	78.3	0.3032
Ti-Al (experimental)	75.3	0.2831

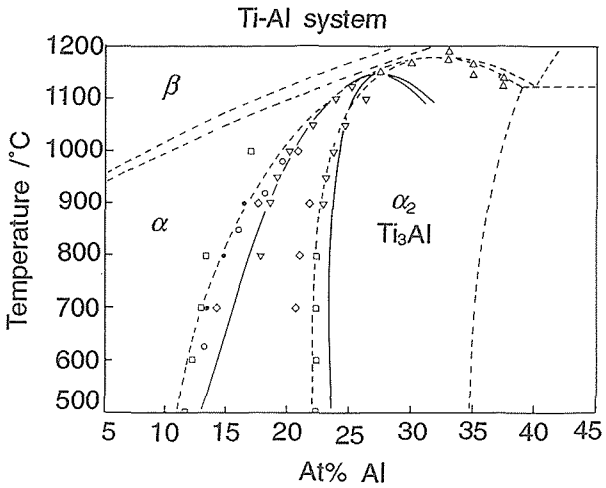

Fig. 2. The α/α_2 phase boundaries in the Ti-Al system calculated with the CVM using the Lennard-Jones approximation for the energy (solid lines). The experimental boundaries are shown by dashed lines.

Reference

1. Onodera, H., Nakazawa, S., Ohno, K., Yamagata, T. and Yamazaki, M. ISIJ International 31 (1991): 875.

❒ Characterization of Optical Microstructure by Sensory Test

Y. Kurihara

Keywords: microstructure, sensory test, multi-dimensional scaling method, Ti-6Al-4V, mechanical properties

Introduction

The microstructure is one of the most important factors for material design which affecting the physical, chemical and mechanical properties of materials. Among microstructural information, numeric data such as a grain size have been used for the analysis of the relationship between the microstructure and mechanical properties. However, image data such as a morphology of transformation products do not seems to be used fully for materials design because of the difficulty of obtaining as numerical data. In that case, specialists in the field of materials science seem to judge a usefulness of microstructure qualitatively on the basis of their experiences. If such image data of microstructures could be obtained as numeric ones, more precise prediction of materials properties would be realized.

The sensory test, which has been widely used to characterize such properties as color and taste which are evaluated by human senses, seems to be one of effective methods to analyze image data such as microstructures. Then, in the present study, the sensory test was applied to microstructural evaluations to extract view points of specialists. Results of the sensory test were analyzed by the multi-dimensional scaling method to obtain numeric parameters. As the next step, extracted parameters were used for analyzing the relationship between the microstructure and mechanical properties.

Sensory test on microstructures

Six kinds of microstructure with different morphology in a Ti-6Al-4V alloy were used in the sensory test figure 2. These microstructures were prepared by six kinds of heat treatments. The sensory test were performed by judging the degree of similarity between two microstructures which were selected from the six ones. The degree of similarity was ranked as 7 steps, (1) very similar, (2) similar, (3) a little similar, (4) less similar, (5) a little different, (6) different, (7) quite different. Panelists who judged the similarity consisted of 4 specialists, who were researchers on titanium alloys and 57 non-specialists. Non-specialists were researchers of this laboratory and students in engineering divisions of universities. The test was carried out without showing chemical composition of the alloy and the heat treatment in an effort to improve the objectivity of judgements.

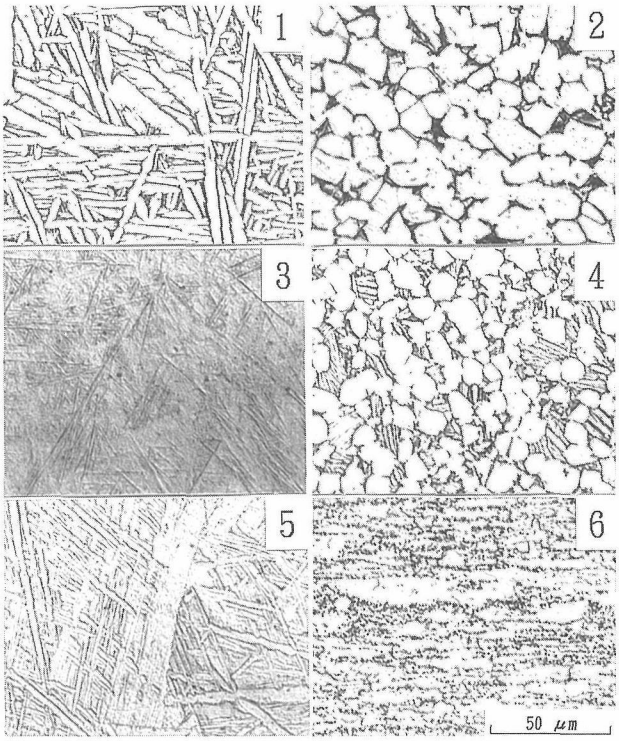

Photo. 1. Optical microstructure of Ti-6Al-4V alloy used in the sensory tests.

1. *1050 °C × 5min→WQ + 950 °C × 1.5h→AC*
2. *950° C × 1.5h→FC*
3. *1050 °C × 5min →WQ*
4. *950 °C ×1.5h→WQ + 700 °C × 2.0h→AC*
5. *1050 °C × 5min→AC*
6. *700 °C × 2.0h→AC*

Analysis of results of the sensory test by the multi-dimensional scaling method

Three characteristic vectors of microstructure were extracted from the results of the sensory test for the specialists by the multi-dimensional scaling analysis as shown in figure 1, suggesting that the specialists evaluated microstructures mainly from three factors. Although the characteristics these three axes mean are not so definitely apprehensible, they can be interpreted qualitatively by referring the coordinates of the points in the figure and the microstructures as follows:

1. Three characteristic vectors of microstructure were extracted in the analysis of results for specialists as shown in figure 1, suggesting that

specialists evaluated microstructures mainly from three factors.

2. The first factor (C1 axis) represents the geometrical variation of morphology from spherical to needle. The second one (C2 axis) represents the anisotropy change from lamellar to granular (massive), and the third one represents the size variation of microstructures from fine to coarse. Thus, it can be concluded that the specialist evaluates the microstructure of the Ti-6Al-4V alloy from the geometry, the anisotropy and the size. Furthermore, each characteristic of microstructure can be obtained as a numerical datum corresponding to each characteristics vector in figure 1.

Analysis for non-specialists gave almost the same results as those for specialists suggesting that non-specialists evaluated microstructures from the same factors.

However, the specialists' evaluations of microstructure are based on the metallurgical knowledge about mechanical properties and processes such as heat treatments hot rolling, as well as the geometrical pattern. So that, the knowledge of specialists will deserve storing along with the above microstructural information to construct a more accurate and efficient expert system for materials design or selection.

Thus, a more accurate and efficient expert system for materials design or selection would be constructed by storing both the above microstructural information and the knowledge of specialists.

Application of numerical data representing characteristics of the microstructure to the analysis of mechanical properties

Relationships between the microstructure and tensile properties were examined by the multiple regression analysis using the characteristic vectors for each microstructure. The regression equations are

$$0.2\%\ \text{Proof Stress (MPa)} = 954 + 81C1 + 170C2,$$

$$\text{Tensile Strength (MPa)} = 1046 - 75C1 + 53C2 + 164C3,$$

$$\text{Elongation (\%)} = 15.6 + 11.2C1 - 9.7C3,$$

$$\text{Reduction of Area (MPa)} = 13.0 + 21.9C1.$$

The multiple correlation coefficient for each equation was more than 0.9. These equations will be used effectively in the expert system for predicting tensile properties of Ti-6Al-4V alloy if the microstructure of it can be characterized by the vectors C1, C2 and C3.

These equations can be used effectively in the expert system for predicting tensile properties based on the microstructure.

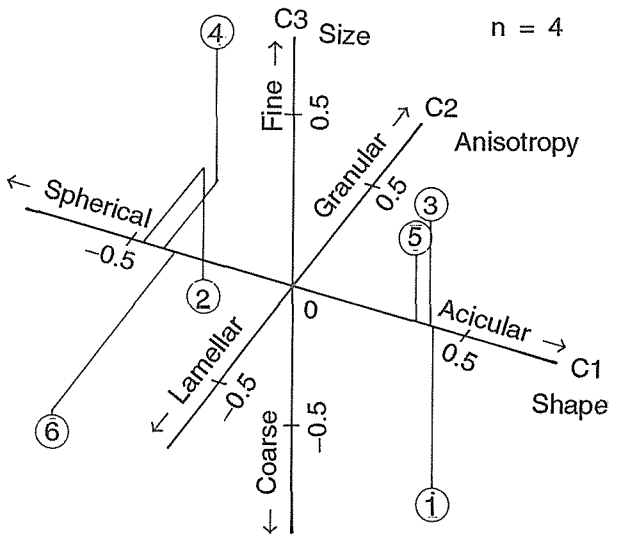

Fig. 1. Results of analysis using multi-dimensional scaling method on the sensory tests for specialists having deep knowledge of Ti-6Al-4V alloys. Each point is plotted with a line parallel to each axis (C1, C2, C3). The number of each point corresponds to that of the microstructure in Photo. 1.

References

1. *Application of Multivariate Statistical Analysis to Alloy Design of Secondary-Hardening High Strength Steel*, Kurihara, Y. and Fujita, J. J. Mater. Sci. Soc. Jpn. 24 (1988): 150–57 (in Japanese).
2. *Characterization of Optical Microstructure by Sensory Test*, Kurihara, Y., Kaneko, T., Hoshimoto, H., Yamasaki, M. and Fujita, M. J. Mater. Sci. Soc. Jpn. 28 (1991): 245–51 (in Japanese).

❒ Improvement of Room-Temperature Ductility of Ni_3Al by Unidirectional Solidification

T. Hirano, Chemical Processing Division

Keywords: unidirectional solidification, floating zone method, Ni_3Al, room-temperature ductility

Ni_3Al

We have found that unidirectional solidification of Ni_3Al using a floating zone method is remarkably effective in improving the room-temperature ductility without addition of alloying elements[(1)-(5)]. We call this method FZ-UDS.

Ordered intermetallic compounds are attractive for high temperature structural applications due to their high strength retention at high temperatures, combined with good oxidation resistance. In particular, Ni_3Al is one of the most attractive compounds. Apart from having superior room- temperature strength, it exhibits an unusual characteristic of increase in yield strength with temperature which is different from conventional materials. However, polycrystalline Ni_3Al has a big drawback as engineering materials. It is extremely brittle at room temperature because of intrinsic grain-boundary brittleness. In particular, it easily fractures at grain boundaries in tensile deformation.

Aoki and Izumi have found a dramatic effect of a amount of boron addition on the room-temperature ductility. Unfortunately the boron doping is effective only in Ni-rich Ni_3Al. From an engineering point of view stoichiometric and Al-rich Ni_3Al is more attractive than Ni-rich Ni_3Al since the formers have such higher high-temperature strength and oxidation resistance than the latter. It is almost impossible to enhance the room-temperature ductility of stoichiometric and Al-rich Ni_3Al, and up until now no one has succeeded.

Unidirectional solidification of Ni_3Al by a floating zone method (FZ-UDS)

Unidirectional solidification were carried out in a flowing argon gas atmosphere by a floating zone method. The growth rate, which was the most important factor to control the solidification structure, was 24 mm/h. As-grown alloys were 12 mm in diameter and 120 mm in length. Figure 1 shows the optical micrographs of the Ni_3Al grown by FZ-UDS. The solidification structure is strongly dependent on the growth rate. The stoichiometric Ni_3Al has a columnar-grained and single-phase structure of Ni_3Al at this growth rate, whereas the Al-rich Ni_3Al has martensite-like precipitates in the Ni_3Al matrix. These precipitates are considered to be NiAl.

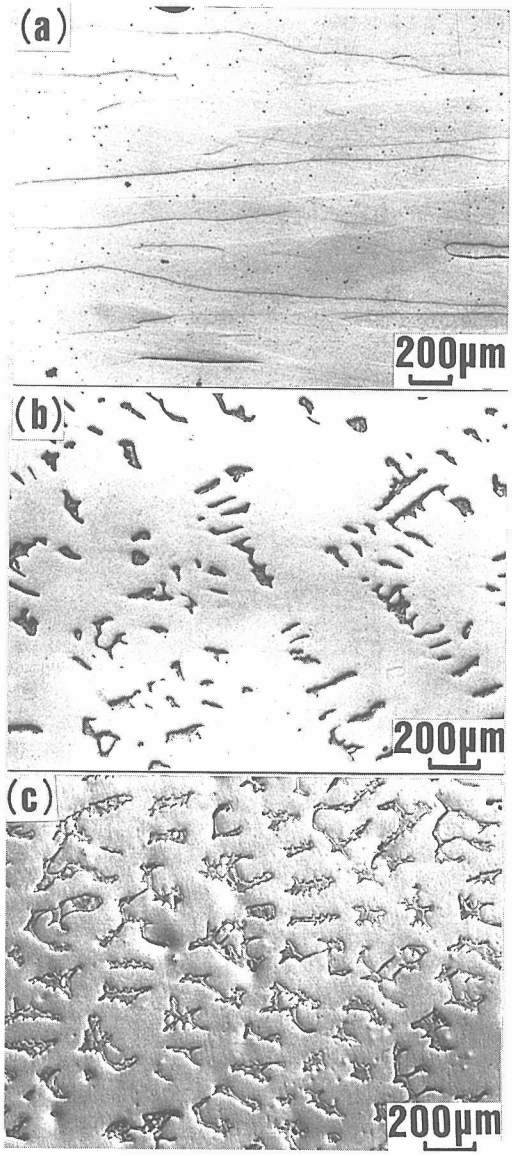

Fig. 1. Optical micrographs of the Ni_3Al grown by FZ-UDS. (a) Ni-25at%Al, (b) Ni-26at%Al, and (c) Ni-27at%Al

Room-temperature Ductility

All the alloys grown by FZ-UDS exhibit a large tensile elongation at room temperature, as shown in figure 2. It is a quite contrast to the brittleness of the equiaxed-grained Ni_3Al which is conventionally cast. A uniform tensile elongation throughout the entire gauge section was obtained without necking. It should be noted that even Al-rich Ni_3Al exhibit ductility. Figure 3 compares the present results with the boron-doping method. In the boron-doping method tensile elongation decrease rapidly with increasing Al concentration and al-

most no ductility is observed for stoichiometric and Al-rich Ni_3Al. Compared with the boron-doping method, FZ-UDS has a remarkable improving effect of ductility for both alloys.

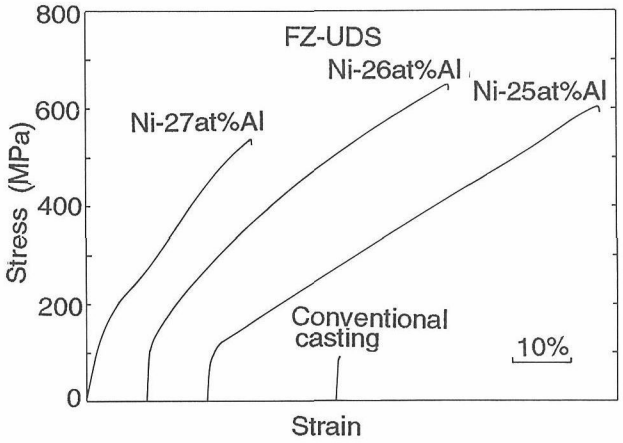

Fig. 2. Stress-Strain curves of the Ni_3Al grown by FZ-UDS at room temperature

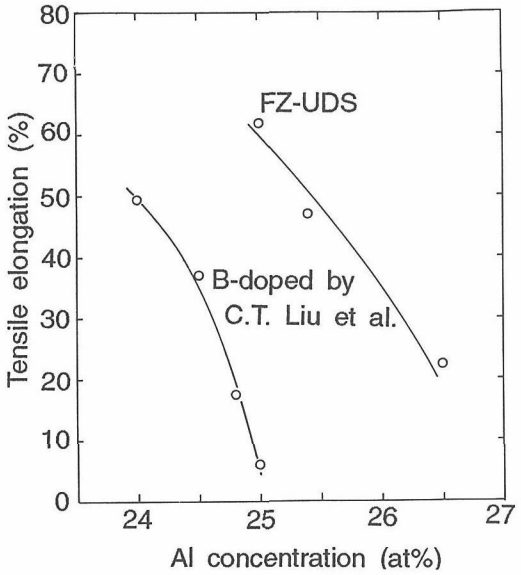

Fig. 3. Plot of room-temperature tensile elongation as a function of Al concentration, comparing with the results of boron-doped Ni_3Al

Figure 4 shows the SEM micrographs of the fracture surface of the stoichiometric Ni_3Al (a) grown by FZ-UDS and (b) fabricated by conventional casting. Complete transgranular fracture is observed in the Ni_3Al grown by FZ-UDS, whereas intergranular fracture is observed in the conventionally cast Ni_3Al. These results prove that grain boundary brittleness in polycrystalline Ni_3Al (responsible for the lack of ductility of Ni_3Al) can be remarkably improved by the control of the solidification structure.

The columnar-grained structure as shown in figure 1 may allow one to predict poor ductility in the transverse direction of the columnar structure, i.e. perpendicular to the growth direction. The tensile tests of stoichiometric Ni_3Al along this direction showed a large tensile elongation of about 15% at room temperature. Cold rolling of this alloy is also possible. It was cold-rolled to about 25% reduction without intermediate annealing.

These data indicate that FZ-UDS is a promising method to improve the ductility of intermetallic compounds.

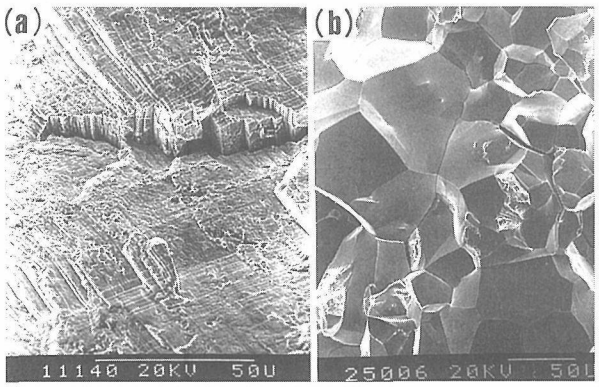

Fig. 4. SEM fractographs of the Ni-25at%Al (a) grown by FZ-UDS, comparing with that (b) fabricated by conventional casting.

References

1. *Improvement of Room Temperature Ductility of Stoichiometric Ni_3Al by Unidirectional Solidification*, Hirano, T. Acta Metall. Mater. 38 (1990): 2667–71.
2. *Improvement of Room Temperature Ductility of Stoichiometric Ni_3Al by Unidirectional Solidification*, Hirano, T. and Kainuma, T. ISIJ International 31 (1991): 1134–38.
3. *Improvement of Room Temperature Ductility of Ni_3Al by Unidirectional Solidification*, Hirano, T., Chung, S.S., Mishima, Y. and Suzuki, T. Mat. Res. Soc. Proc. 213 (1991): 635–40.
4. *Tensile Properties of Stoichiometric Ni_3Al Grown by Unidirectional Solidification*, Hirano, T. Scripta Metall. Mater. 25 (1991): 1747–50.
5. *Cold Rolling of Boron-Free Polycrystalline Ni_3Al Grown by Unidirectional Solidification*, Hirano, T. and Mawari, T., ibid. 26 (1992): 597–600.

❒ Fundamental Phenomena in Spray Deposition of Surface Coatings

S. Kuroda, Advanced Materials Processing Division

Keywords: plasma spray, temperature measurement, velocity measurement, rapid quenching, residual stress

Needs for Scientific Understanding in Process Technology

Spray deposition of surface coatings has been finding a wide range of industrial applications covering automobiles, steel and ship-building industry, as well as aerospace and biological applications because of its unique capability to form thick coatings of various materials such as metals, ceramics, cermets and composites. To meet such intensifying requirements for the quality of sprayed coatings, various spraying technologies have been emerging such as LPPS (low pressure plasma spray), HVOF (high velocity oxy-fuel) spray, RF plasma spray and so on. In contrast to those technological developments, scientific understanding of the process fundamentals has been somewhat lagging behind and choice of spray process and its operating conditions still seem to rely on experience. To clarify the process fundamentals, we have done a series of study on the process of plasma spraying, the most widely used spraying technology today.

What Happens When a Molten Particle Strikes a Solid Surface?

The essence of the coating formation process is the collision of a sprayed powder particle onto a solid surface. It is a phenomenon similar to what we observe through a glass window struck by falling rain drops in foul weather. When the incident particle is a molten metal or ceramic particle with diameter in the range of 10 to 100 μm with velocity like 100 m/s, it becomes a fascinating but very fast and complicated phenomenon, involving heat and momentum transfer, wetting, disintegration of liquid sheets and threads, rapid solidification, and elasto-plastic deformation. Figure 1 shows examples of morphology of (a) Ni-20Cr alloy and (b) ZrO_2-8% Y_2O_3 ceramic particles struck onto a polished stainless steel plate and observed under SEM. Such morphology changes sensitively with the temperature and velocity of the impinging particles as well as the surface condition and temperature of the substrate. Since a sprayed coating is made of layered lamellae of such splats, it is essential to (1) define the characteristics of the incident particles such as their velocity and temperature and then (2) examine the resultant coating properties.

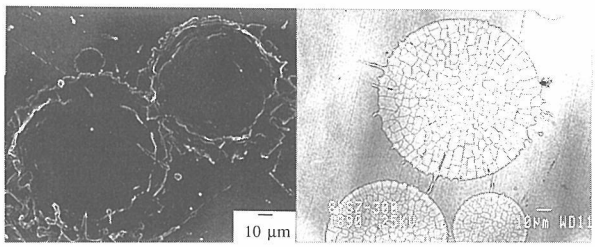

Fig. 1. Morphology of sprayed splats observed under SEM: (a) Ni-20Cr alloy, (b) ZrO_2-8%Y_2O_3 ceramic

Particle Monitoring Reveals Complex Behavior of Sprayed Powders in Flight

Figure 2 shows a schematic illustration of a typical plasma torch together with the change in the temperature and velocity of Mo particles sprayed in air along the distance from the torch outlet. Powder material is fed into a plasma jet generated by an arc discharge with typical flow velocity of 300 m/s and temperature of 10,000K at the torch outlet. The measuring method developed is to use the thermal radiation emitted by sprayed particles at high temperature: particle velocity determined by the so-called spatial filtering method (a modified time-of flight method) and particle temperature determined by color pyrometry.

As can be seen in the temperature and the velocity profiles, size of powder has a significant effect; finer powders can be accelerated to a higher velocity and heated to a higher temperature but decelerated and cooled with a greater rate once they come out of the hot core of a plasma jet. Even though this is not a surprising result from the viewpoint of hydrodynamics, it implies the difficulty of changing one characteristic of impinging particles such as particle size without affecting other properties such as velocity and temperature. The process has a number of parameters to be controlled, i.e. composition of plasma gas and its flow rate, arc current, arc voltage, powder size, powder feed rate, electrode design, spray distance and others. By changing one process parameter, one may find a change in a property of the formed coating. But to explain the phenomenon, data on the characteristics of sprayed particles will be essential.

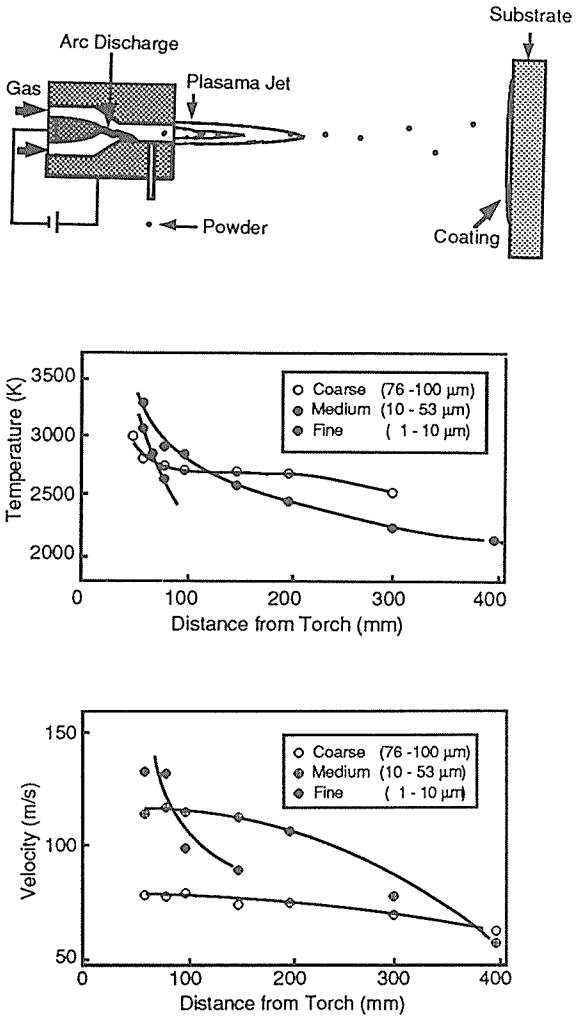

Fig. 2. A schematic illustration of plasma spraying process together with the temperature and velocity profiles of sprayed Mo powder with different size distribution

Quenching Stress—a Unique Source of Internal Stress in Sprayed Deposits

The time required for a particle to spread and solidify after impact is estimated to be in the order of 10 μs. As each splat cools down after solidification, its thermal contraction is constrained by the underlying solid, which is the substrate at the beginning of coating formation and the coating-substrate couple thereafter. As a result, in-plane tensile stress develops within each splat. This is a unique source of internal stress in spray deposition and termed as the "quenching stress".

In almost all coating applications, the mechanical stability of a coating is the most fundamental requirement and stresses within a coating are very important in this aspect. By continuously measuring the curvature of a substrate *in-situ* during spraying, it has become possible to quantify the average value of quenching stress within a number of particles deposited. As the coating-substrate couple cools down after deposition, macroscopic thermal stress due to mismatch in thermal contraction between the two materials is superimposed on this quenching stress. This is why only *in-situ* measurement of stress during deposition can quantify the quenching stress. Figure 3 shows the values of measured quenching stress for a range of spray materials sprayed onto a substrate held at a wide range of temperatures. The substrate temperature is normalized by the melting point of the powder material. The quenching stress of soft f.c.c. metals such as Ni and Al decreases readily with increase in T_s. Creep and plastic yielding are considered to be responsible for this drop in the stress with temperature. For materials with a higher yield strength and creep resistance such as Ni-20Cr alloy, much higher stress well above 100 MPa can be frozen into the splats. Stress relaxation becomes effective at a very high temperature for these materials. For ceramic materials such as alumina and zirconia, the quenching stress is usually much lower because of microcracking as shown in figure 1(b).

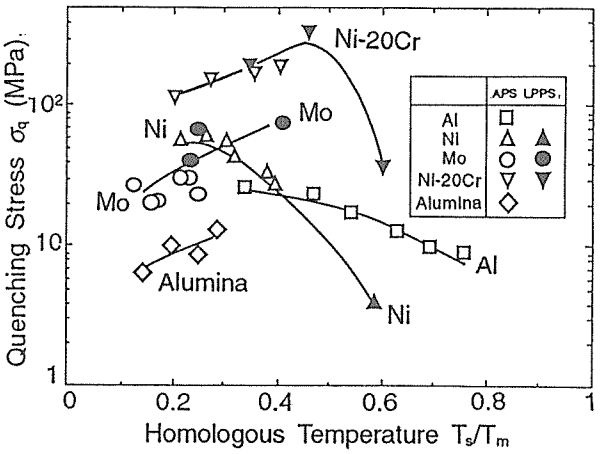

Fig. 3. Measured values of quenching stress for various spray materials as a function of substrate temperature T_s normalized by the melting point T_m of each spray material

The quenching stress is a factor which determines the maximum thickness of a coating that can be deposited. As the coating becomes thicker, the shear stress at the coating/substrate boundary increases and could result in spontaneous delamination. Even though industrial fabricators have known by experience that some spray materials can be sprayed to a great thickness while others cannot, it is through such measurement that the reasons can be clarified and quantified.

The quenching stress is only one aspect of the deposition phenomena and there are more questions to be answered, such as the adhesion mechanisms of sprayed coatings. It is hoped that as these fundamental aspects of coating technology become better understood, rational selection of spray technology, operating conditions, and materials will be possible, and a next-generation spray process will emerge.

❒ Development of New Moiré Method Using Electron Beam Lithography and Electron Beam Scan

S. Kishimoto, M. Egashira and N. Shinya, Failure Physics Division

Keywords: Moiré fringe, electron beam lithography, electron beam scan, electron Moiré method

To analyze the damage formation process, a new Moiré method for the measurement of micro-deformation has been developed. This new Moiré method (Electron Moiré Method) makes it possible to determine the highly localized micro-deformation, and also to observe the scanning electron microscope (SEM) image and the electron Moiré fringe at the same time. Using this method, micro-creep deformation has been measured.

Principle of Electron Moiré Method

A principle of this new Moiré method[1] is shown in figure 1. In this method, a fine model grid is formed by metal depositing on the specimen's surface using an electron beam lithography, and a primary electron beam in a SEM is used as a master grid. Exposure of the scanning electron beam on the model grid produces electron Moiré fringes of bright and dark lines in response to the amount of the emitted secondary electrons per primary electron.

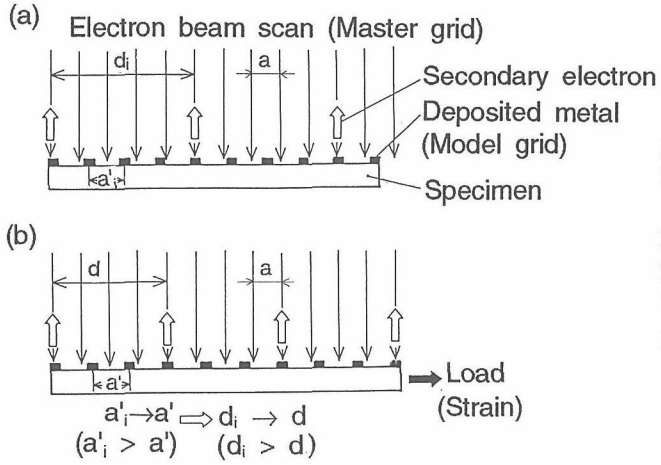

Fig. 1. Schematic for formation of electron Moiré fringe

In figure 1(a), **a**, $\acute{a}_i$ and $\mathbf{d}_i$ are the distance between two neighboring electron beam scan, the initial distance between two neighboring model grid lines and the initial distance between Moiré fringes, respectively. The strain which causes the increase of model grid spacing from $\acute{a}_i$ to $\acute{a}$ is accompanied with the decrease of Moiré fringe spacing from $\mathbf{d}_i$ to **d** (figure 1(b)).

Electron Moiré Fringe

In this work, a SEM equipped with a beam blanking device and a pattern generator for beam control was used to produce the model grid and to observe the Moiré fringes.

A typical electron Moiré fringe is shown in figure 2. The model grid consisting of parallel gold lines was prepared by the electron beam lithography around a hold of the polyimide resin specimen. And then the scanning electron beam exposure on the model grid produces this fine electron Moiré fringe in a small area (about 500 μm square) without image processing system. This Moiré fringe shows strain concentration around a hole of a tensile tested polyimide resin specimen.

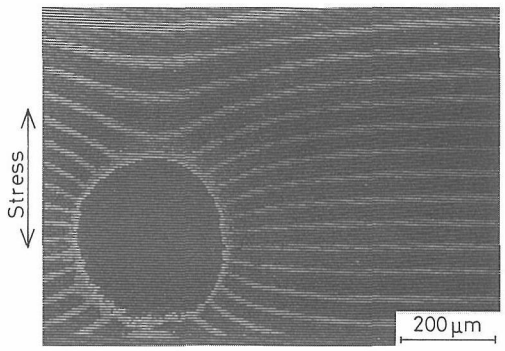

Fig. 2. Electron Moiré fringe around a hole formed by electron beam scan

Application of New Moiré Method for Measurement of High Temperature Deformation

1. Strain distribution

Some model grids of about 4 μm spacing consisting parallel gold lines perpendicular to the stress axis were prepared on the copper specimen's surface. The specimen was crept for 21h at 723K and 30MPa.

A typical photograph of the Moiré fringe pattern is shown in figure 3. The spacing of the Moiré fringe was measured in the direction parallel to the stress axis, and the strain was calculated from the spacing[2]. The strain distribution within the central grain in figure 3 is shown in figure 4.

The strain distribution is non-uniform even in a same grain, and the regions of strain may be divided into areas of high strain (upper part of the grain), low strain (lower part of the grain)

and medium strain (middle part between the upper and lower). The triple point cracks are surrounded with low tensile strain areas. This indicates that the formation of triple point cracks releases the stress or strain concentration.

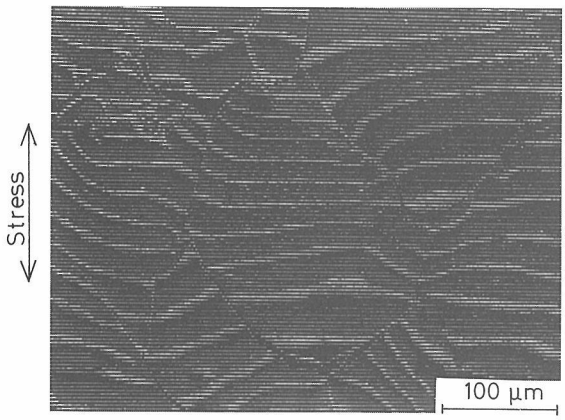

Fig. 3. Moiré fringe pattern of a copper specimen crept for 21h at 723K and 30MPa

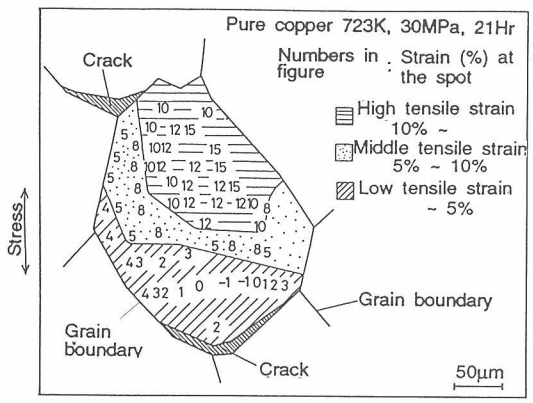

Fig. 4. Strain distribution in a copper specimen crept for 21h at 723K and 30MPa

2. Grain boundary sliding and coarse slip

Figure 5 shows the Moiré fringe pattern and a SEM image around a grain boundary in a copper specimen crept for 15h at 723K and 30MPa. Offsets of the Moiré fringe can be seen along the grain boundary **A** and point **c**, where grain boundary sliding and a coarse slip occurs, respectively. The grain boundary displacement parallel to the stress axis was calculated from the offsets of the Moiré fringes[3], and the displacement along the grain boundary **A** is shown in figure 6.

The grain boundary displacement becomes smaller near the both triple points **a** and **b**, and large and uniform at the middle section of the grain boundary **A**. The surface step caused by the coarse slip at the point **c** was also measured and the displacement of the surface step was about 0.6 μm.

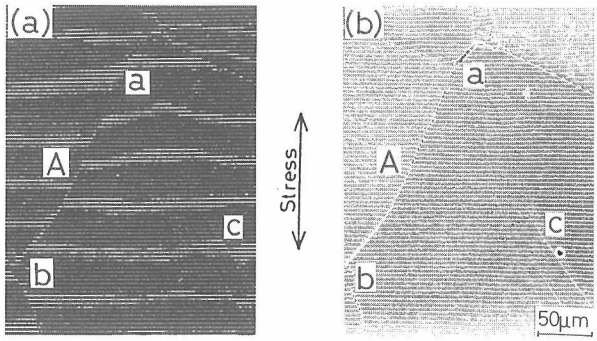

Fig. 5. Moiré fringe pattern (a) and SEM image (b) of a copper specimen crept for 15h at 723K and 30MPa

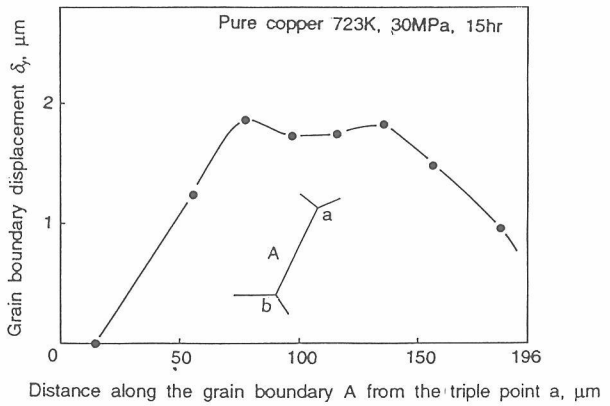

*Fig. 6. Distribution of grain boundary sliding along the grain boundary **A** measured from Moiré fringe in Fig. 5*

This electron Moiré method offers a highly sensitive means of detecting highly localized micro-deformation, and it is useful to analyze damage formation process of materials.

References

1. *Observation of Micro-Deformation by Moiré Method Using a Scanning Electron Microscope*, Kishimoto, S., Egashira, M. and Shinya, N. J. Soc. Mater. Sci. Jpn. 40 (1991): 637–41 (in Japanese).
2. *Use of the Moiré Effect to Measure Plastic Strains*, Vincker, A. and Dechaene, R. Trans. ASME, ser. D 82 (1960): 426–34.
3. *Observation of Grain Boundary Sliding of Aluminum Bicrystals by Thermostable Moiré Method*, Obata, M. and Shimada H. J. Jpn. Inst. Met. 42 (1976): 112–17 (in Japanese).

❒ NRIM Fatigue Data Sheet Project on Japanese Materials

S. Nishijima, Failure Physics Division

Keywords: fatigue of metals, data sheets, engineering materials, standard reference basis, fatigue mechanisms

Since 1975, NRIM has been engaged on the establishment of standard reference data on fatigue properties of Japanese engineering steels and alloys for mechanical and structural applications. Results of the work have been published as NRIM Fatigue Data Sheets, and widely referred to, as the most valuable basis for reliable and effective use of metallic materials.

The project has been conducted as a nation-wide program, in conjunction with NRIM Creep Data Sheets project, both being supported by industrial, academic and governmental societies. The work is promoted in parallel with the basic researches to understand fundamental mechanisms of fatigue and thus to validate the acquired data. These activities can be categorized into three fields, namely, ambient-, intermediate- and elevated-temperature properties fields, according to the range of material applications.

Ambient temperature fatigue properties are studied mostly on typical steels and aluminium alloys for machine structural use. Test materials are sampled arbitrarily from ordinary products of representative companies, with multiple heats or batches for each class of materials, so as to cover the range of variations normally allowed by the material specification.

Fatigue strength at infinite number of cycles is generally considered as the limiting stress for the propagation of small cracks at material surface, where controlling factor is the crack closure which is more or less influenced by the environments.

In case of high strength materials, however, the crack can be initiated at the sub-surface, mostly at non-metallic inclusions or grain boundary irregularities. Fatigue limit is then decreased with variable degrees depending on the severity of internal flaws and materials strength. A unified analysis is attempted referring to the working stress intensity factor at the crack initiation site.

Aluminum alloys and their welded joints are examined for high- and low-cycle behavior and crack growth properties, in a standard atmosphere of 23 °C and 50% of relative humidity. Recent results showed that the fatigue lives of butt-welded joints are coincident for 5083-O alloy and for 780 MPa grade steel plates of different thicknesses, when they are expressed with nominal elastic strain range, $\Delta\sigma/E$, where $\Delta\sigma$ represents the stress range and E Young's modulus.

It is suggested that the fatigue process in the welded joints consists mostly of crack growth rather than crack initiation, since their life property can be well predicted from the crack growth rate

Table 1 Summary of NRIM Fatigue Data Sheets Published

Subthemes and Subject Issues			Materials Classes	No. Issued
Ambient Temperature Properties for Machine Structural Materials	High-Cycle Fatigue with Multi-Heat Variations		Carbon Steels, Low Alloy Steels, Stainless Steels	15
			Carburizing Steels, Spring Steels, Tool Steels, Aluminium Alloys	7
	Low-Cycle Fatigue with Multi-Heat Variations		Carbon Steels, Low Alloy Steels	6
			Aluminium Alloys	1
Properties for Welded Joints of Structural Materials	Specimen Dimension & Standardization		Butt Joints of 490/570/780MPa Steels, Cruciform Joints of 490 MPa Steels	5
	Welding Methods & Procedures		Butt Joints of 490/780 MPa Steels, Cruciform Joints of 490 MPa Steels	5
	Stress Ratio, Weld Metal and HAZ		Butt Joints of 410/610 MPa Steels and 304 Stainless Steels	9
	Aluminium Alloys		Butt Joints of 5083 Aluminium Alloys	1
Elevated Temperature Properties for Steels and Alloys	High-Cycle Fatigue		Carbon & Low Alloy Steels, Stainless Steels, Heat-Resisting Alloys	9
		Time Dependence	Low Alloy Steels	1
	Low-Cycle Fatigue		Low Alloy Steels, Stainless Steels	5
		Time Dependence	Low Alloy Steels, Stainless Steels, Heat-Resisting Alloys	5

data expressed in terms of $\Delta K/E$, with ΔK denoting stress intensity range.

Intermediate temperature properties are studied on pressure vessel steels and their welded joints, looking at their high- and low-cycle lives and crack growth performances. Two approaches are being made: standard specimens tests to obtain basic data on time-temperature dependence of the materials, and large-sized specimens tests to acquire engineering data for practical applications.

Standard specimens tests on a carbon steel for boilers, SB450, have shown that the fatigue strength takes its maximum value around 300 °C due to dynamic strain aging, and that the elapse of time during fatigue presents an analogous effect to the increase of temperature.

Oxidation seems to have positive effects, in this case, by constraining the crack initiation with formation of hard surface layers, on one hand, and by decreasing the crack growth rate with reducing crack tip opening range, on the other. Detailed observation of fish-eye type failure and analysis of surface oxides are in progress to understand these complex behaviors.

Large-sized joint specimens give in general shorter fatigue lives than in smaller ones, because the high tensile residual stresses due to welding are better preserved in larger members. A simulated tests was performed, using ordinary specimens, by setting the maximum stress at yield strength of material and changing the stress range. This new method proved its effectiveness.

Similarly, the crack growth rates are independent of applied stress ratios, in large center-cracked type joint specimens, as the crack tip is subjected to high tensile residual stresses and is always free from closure. This can be best simulated, with smaller specimens, by P_{max} constant tests where the maximum load is kept constant during ΔK decreasing tests.

Elevated temperature performance is investigated for a variety of material ranging from low alloy steels to super alloys. One of the latest topics is a proposal of parametric representation for time-dependent low-cycle fatigue lives at elevated temperatures, which might be extended to predict long-term materials behaviors.

The new parameter, P, comprises the temperature, T (K), the fatigue life under triangular strain wave, N_{25}, and the strain rate, $\dot{\varepsilon}(s^{-1})$, and is expressed with an asymptotic function of total strain range, $\Delta\varepsilon_t$:

$$P = T(\log N_{25} - A\log\dot{\varepsilon} + B)$$
$$= A_0 + A_1\log(\Delta\varepsilon_t - \Delta\varepsilon_0)$$

Here, A, B, A_0, A_1 and $\Delta\varepsilon_0$ are constants, to be optimized for a given set of observed data, by minimizing the least squares error on log-life.

Figure 1 shows an example 'master curve' by the proposed method, for a 2.25Cr-1Mo steel, where A = 0.174, B = −2.372, A_0 = 1240, A_1 = 975 and $\Delta\varepsilon_0$ = 0.039. Similar results are obtained for austenitic alloys, with similar degree of fitness, but of course with different values of constants, likely reflecting the intrinsic property of each material.

Results from the Project have been published yearly as series of NRIM Fatigue Data Sheets, for which a summary is given in table 1. In total 68 issues have been published so far and exchanged worldwide with related scientific and technical organizations. An on-line data service is currently available through Japan Information Center of Science and Technology for domestic use.

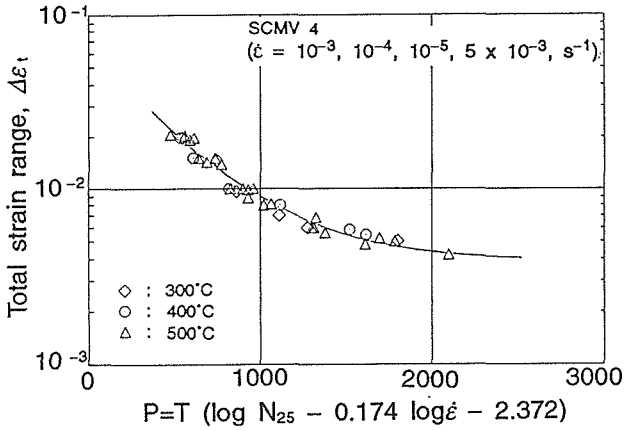

Fig. 1. A master curve representation for time-dependent low-cycle fatigue at elevated temperatures

Also, a series of Data Sheet Technical Documents is provided from NRIM to assist users for effective application of Data Sheets. It gives comprehensive analysis and guidance on data, under each selected technical subject, seven volumes are available and others are in preparation.

All these efforts contribute, together with several hundreds of scientific publications from this project, to the enrichment of knowledge in materials science and safer and effective use of engineering materials.

❒ Creep Strain-Time Characteristics in Large Welded Joint of 304 Stainless Steel

Y. Monma, 5th Research Group

Keywords: creep, creep-rupture, FEM, size effect, stainless steel, welded joint

Large Welded Joints at High Temperature

There are many examples where creep deterioration of weldment during high-temperature operation is responsible for failure in elevated-temperature components. The welded joint of the structural component typically consists of three constituents: weld metal, heat affected zone (HAZ) and the base metal. When a welded joint is subjected to creep loading, each constituent shows a different character of creep. In general the weld metal exhibits poor ductility, whereas the strain concentration takes place often in the HAZ. The creep behavior of a welded joint has been treated with the assumption that the composite modelling based on the creep properties of the three constituents is valid. Thus, the creep data of the weld metal, the HAZ and the base metal for the specimens cut from the joint can be used to predict the entire strain-time curve of the welded joint. Numerical simulation using the finite element method (FEM) is a common practice in predicting creep behavior of welded joints. However, very limited data on the practical behavior of large joint, particularly for large, thick joints, are available for the simulation.

The objectives of this research is to obtain creep strain-time data of a large welded joint using full-thickness specimens, together with the data of the weld metal, the base metal and the joint using conventional small specimens. Then, FEM calculation on the creep strain distribution of the large welded joints is made using the uniaxial data from the small specimens, in order to evaluate the creep performance of the full-thickness joint from experimental and computational points of view.

Creep Behavior of Welded Joints

The specimens were cut from a narrow-gap SAW (submerged arc welding) joint of 304 stainless steel plate (18.4%Cr-8.9%Ni-0.05%C, 50mm thick) as shown in figure 1. Creep-rupture test for the large joint, specimens (WJL) was conducted on heavy-loading 50t machines. Figure 2 compares creep strain-time curves for the constituents of the welded joint. The creep strength of the weld metal taken from the middle of the plate (WM2) is higher than that from the surface portion (WM1 and WM3). The higher strength is attributable to the local variability of carbide precipitation during the multi-layer welding process.

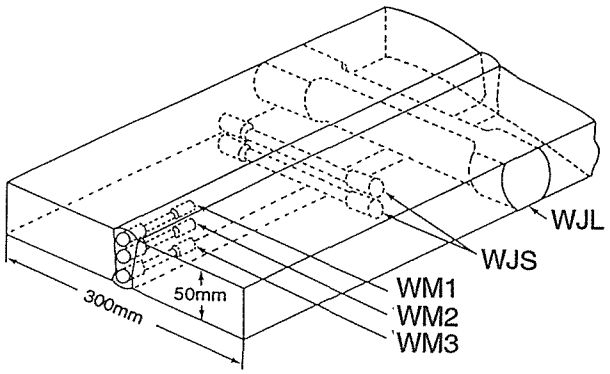

Fig. 1. Sampling of test specimens from welded joint

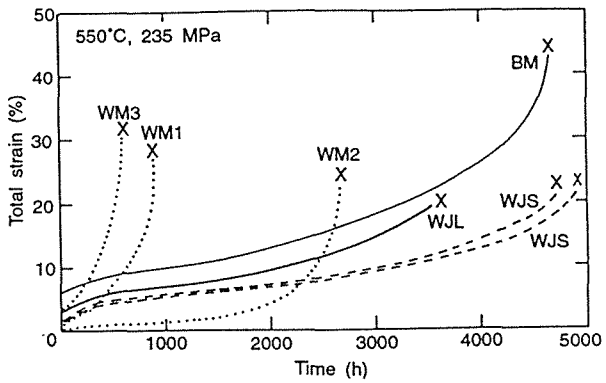

Fig. 2. Comparison of creep curves of base metal (BM), weld metals (WM1-3) and welded joints (WJS and WJL)

Strain Distribution and Specimen Size Effect

The FEM calculation allows the estimation of the strain distribution around the welded joint as well as creep strain-time curve of the large joint specimen (WJL) by assuming the isotropic hardening on the basis of the Mises rules and no residual stress due to welding. In our calculation we ignored the effect of the interaction between the plastic and creep deformation. The results was compared with the experimentally determined strain distribution using the moiré interferometry technique for the creep-interrupted specimens of the large welded joint. Although the calculated strain in the weld metal is greater than the strain from the experiment, both measured and calculated creep curves are in good agreement each other.

Concerning the specimen size effect, the fracture took place at the base metal for the small specimens, whereas it occurred at the weld metal for the large specimens. Since there was little dif-

ference in creep-rupture times between the large and small specimens, the change in location of fracture is attributed to the plastic constraint at the base metal. As shown in figure 4, the smaller the slenderness index, D/L or W/L, the larger the plastic constraint at the base metal, resulting in the fracture away from the weld metal. This index (expressing the degree of constraint) helps to predict the location of failure in practice.

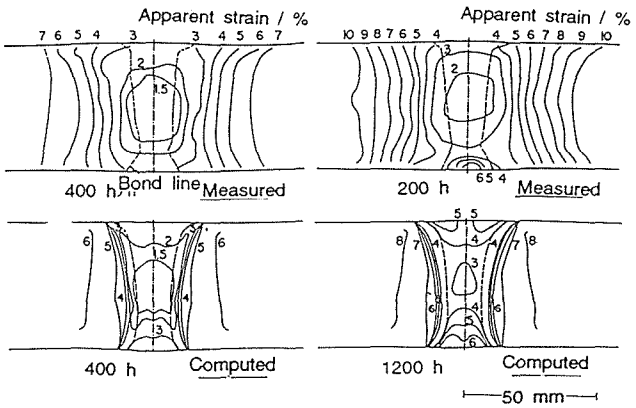

Fig. 3. Comparison of computations with measurements for contours of apparent strains in loading direction (Specimen WJL, tested at 550 °C and 235MPa)

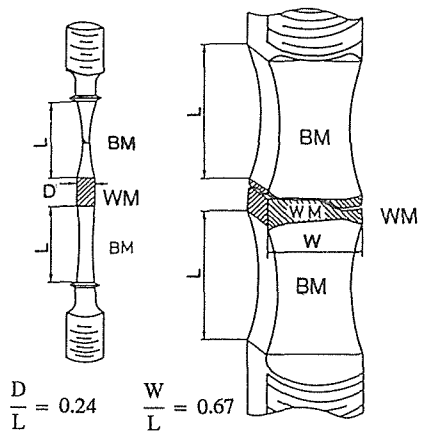

Fig. 4. Schematic comparison of fracture location for small and large joint specimens

References

1. *Computation for Creep Deformation of Welded Joint of 304 Stainless Steel by Using Finite Element Method*, Kinugawa, J., Muramatsu, Y., Monma, Y., Yamazaki, M., Hongo, H. and Watanabe, T. Quarterly J. of Japan Welding Soc. 7 (1989): 117–24 (in Japanese).
2. *Creep-Rupture Behavior of Butt Welded Joint of 304 Stainless Steel Thick Plate Using Small and Large Specimens*, Yamazaki, M., Monma, Y., Hongo, H., Watanabe, T., Kinugawa, J. and Muramatsu, Y. Trans, NRIM 33 (1991): 64–71.

❐ A New Information in Fretting Fatigue Failure in Metallic Structural Materials

K. Nakazawa, M. Sumita and N. Maruyama, Mechanical Properties Division

Keywords: fretting fatigue, contact pressure, frictional shear stress, crack initiation site, stress concentration

Introduction

Fretting damage is known to have a deleterious effect on the fatigue behavior of structural steels and alloys. Many factors control the fretting fatigue. The effect of contact pressure on fretting fatigue has been studied by several researchers. Most of these studies have shown that the fretting fatigue life decreased with an increase in contact pressure. We found that the fretting fatigue life exhibited a minimum at a low contact pressure and a maximum at an intermediate contact pressure[1]. This phenomenon was made clear in terms of stress concentration at the fretted area.

Experimental Procedure

Materials used were a high strength quenched and tempered steel and a Ti-6Al-4V alloy. The ultimate tensile strengths of the steel and the titanium alloy were about 1000 and 1100 MPa, respectively. The fretting fatigue device is shown schematically in figure 1. Bridge-type fretting pads (span length 20 mm) of the same materials as the fatigue specimens were used. When the cyclic load is applied to the fatigue specimen, small relative slip occurs between the fatigue specimen and the pads and causes fretting damage in the fretted area. The contact pressure was maintained below 160 MPa. The tests were carried out using a sinusoidal wave at a frequency of 20 Hz under tension-tension mode at a stress ratio of 0.1 in laboratory air of 40 to 70% relative humidity at room temperature. The frictional force between the fatigue specimen and the pad was measured using strain gages bonded to the side of the central part of the pad.

Effect of Contact Pressure

In fretting fatigue, the frictional shear stress acts on the fretted surface and stress concentration occurs there. The larger the frictional stress, the shorter the life would be. The effects of contact pressure on fretting fatigue life and frictional stress amplitude at axial stress amplitudes of 180, 250 and 350 MPa for the steel are shown in figures 2 and 3, respectively. At a stress amplitude of 350 MPa, the fretting fatigue life decreased monotonously with increasing contact pressure. The frictional stress amplitude increased with increasing contact pressure. There was a good correlation between the life and the frictional stress amplitude.

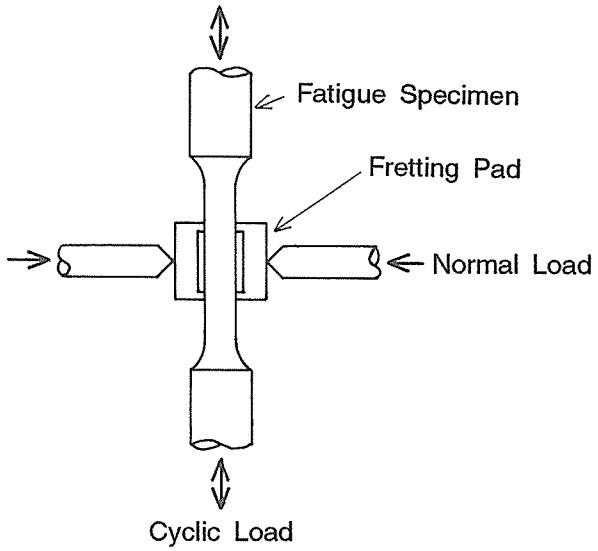

Fig. 1. Schematic representation of fretting fatigue test

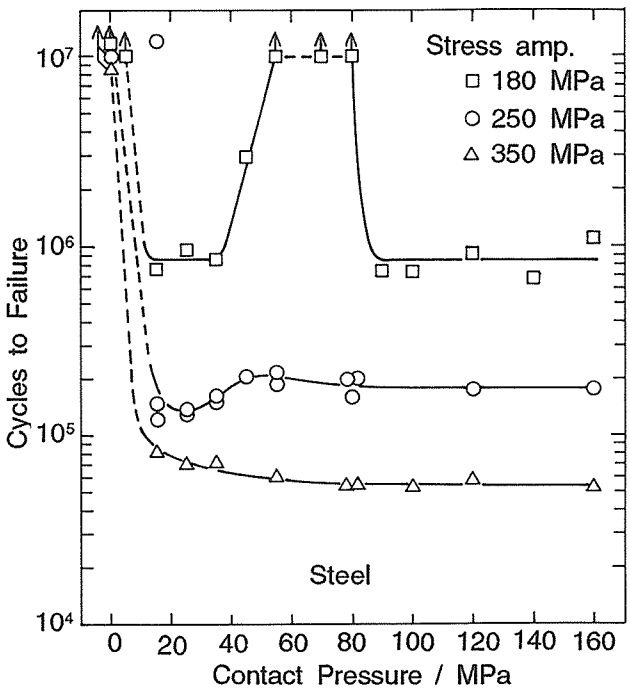

Fig. 2. Effect of contact pressure on fretting fatigue life for steel

On the other hand, the fretting fatigue lives at stress amplitudes of 180 and 250 MPa exhibited a minimum at contact pressures of 15 to 35 MPa, and a maximum at contact pressures of 55 to 80 MPa, then decreased again and became constant at high contact pressures. In the titanium alloy, the fretting fatigue life also took a minimum at low contact pressures. This phenomenon cannot be explained simply or directly by the change in frictional stress amplitude, since the frictional stress amplitude in-

creased monotonously with increasing contact pressure.

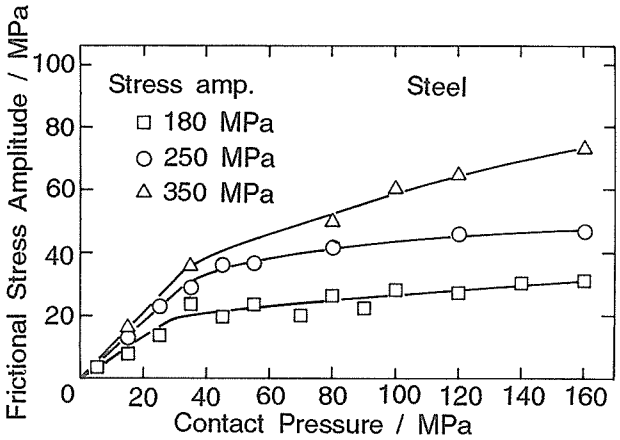

Fig. 3. Relation between frictional stress amplitude and contact pressure for steel

Mechanism of Fretting Fatigue Damage

The fretting damage is shown schematically in figure 4. Under a certain testing condition, there exists a stick region at the middle portion of the fretted area and slip regions on either side of it. The initiation sites of main cracks responsible for the failures were near boundaries between the stick and slip regions. At high contact pressures, the stick region was wide and the main cracks were initiated near the outer edge of the pad. However, at low contact pressures where the life exhibited a minimum, the stick region was narrow, and the main cracks were initiated at the middle portion of the fretted area.

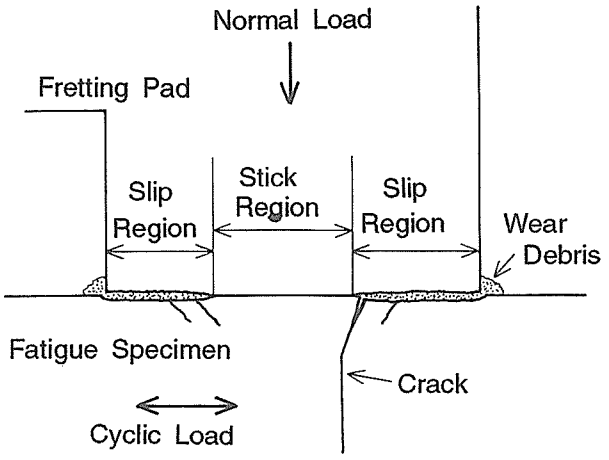

Fig. 4. Schematic representation of fretting damage

The contact pressure and the frictional stress amplitude shown in figures 2 and 3 were the average values and were calculated by dividing the normal load and the frictional force by the apparent fretted area. It was assumed that they were distributed uniformly over the whole fretted area. When the stick region was narrow, the contact pressure was concentrated at the narrow stick region, and was greater than the average. The net contact pressure and resulting net frictional stress amplitude equal to or greater than those at high contact pressures must have acted on this narrow stick region. The minimum in life was probably caused by this high concentration of frictional stress amplitude.

The effect of contact pressure on fretting fatigue life at a given stress amplitude is shown schematically in figure 5. There are two life curves. The first has ABDE drawn assuming that the contact pressure is distributed uniformly over the whole fretted area; the second with BCD assumes that the contact pressure is concentrated at narrow stick region. Point C corresponds to a minimum in life, and an intersection of the two curves D to a maximum in life at an intermediate contact pressure. Contact pressure dependence at stress amplitudes of 180 and 250 MPa can be explained by this model.

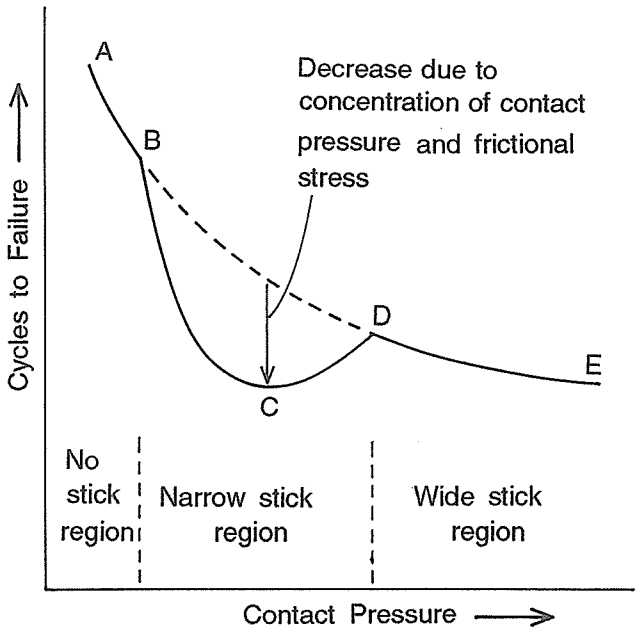

Fig. 5. Schematic representation of the effect of contact pressure on fretting fatigue life at a given stress amplitude

Reference

1. *Effect of Contact Pressure on Fretting Fatigue of High Strength Steel and Titanium Alloy,* Nakazawa, K., Sumita, M. and Maruyama, N. ASTM STP 1159 (1992): 115–25.

❒ Rutherford Backscattering and Particle Induced X-ray Spectroscopy Studies of Thin Film Oxide Superconductors

K. Nakamura and A. Ishii, Surface and Interface Division

Keywords: RBS, PIXE, oxide superconductors, thin films

Since the discovery of high-T_c oxide superconductors, numerous works have been published on the synthesis and characterization of oxide superconductors such as Y and Bi based oxides. Among the papers hitherto published, however, not so many works have been done on the reliable compositional analysis and/or on the correlation between the compositions and various properties such as phase relations, structural and physical properties of the oxide thin films. One of the reasons of this is that these films are usually very thin, and in many cases researchers cannot find reliable analytical methods such as Rutherford backscattering (RBS) analysis. Although RBS is the most reliable method for thin film analysis, its poor mass resolution for heavier elements makes it difficult to analyze the systems containing heavier elements with closer mass number. Particle Induced X-ray Emission (PIXE) combined with RBS is expected to solve these problems.

Figure 1 shows a schematic diagram of our RBS-PIXE system. He^{++} ions are accelerated by Pellertron type accelerator (Terminal voltage 1.1 MV). The maximum energy and current are 3.3 MeV and 200 nA, respectively. At the analytical chamber, surface barrier detector (bias voltage 50–75 V) for He^{++} detection is placed at a angle of 165° and Si (Li) detector (bias 600 V) for X-ray is placed at 135 detector angle as shown in the figure. Data acquisition is normally carried out with 2.00 to 3.05 MeV He^{++} or 2.0MeV H^+ of 10–20 μA influence.

To analyze the composition and thickness of oxide superconductor films using the RBS technique is a routine work in our laboratory. Since the composition from RBS acquired without a standard sample is the absolute value, the composition and thickness of our oxide films are accurately controlled by applying repeated feedback to the deposition conditions. Thus, we have successfully controlled the number of $CaCuO_2$ perovskite layers in $Bi_2Sr_2Ca_{n-1}Cu_nO_y$ films (BSCCO) with n=1 to 7, and have succeeded in getting as-grown superconductivity for N=6 and 7 phases for the first time[1].

The problems related to oxygen content in $YBa_2Cu_3O_{7-\delta}$ (YBCO) thin films is another target in this study. We have successfully controlled oxygen potential in YBCO films by equilibrating them with bulk pellets of various oxygen content (δ = 0.1 – 0.9). The oxygen content was primarily estimated from the change in the c lattice parameter. In order to determine oxygen content more directly, we have applied 3.05 MeV He^{++} resonance scattering analysis. Figure 2 shows variation of resonance scattering yield from ^{16}O in the YBCO film as a function beam energy. The observed change in the resonance scattering yield can be accounted for by the energy loss and straggling in the YBCO films. Taking these factors into account, we have succeeded in determining oxygen content in YBCO films within ±2%.

The advantage of RBS-PIXE analysis is that the data can be acquired simultaneously under the same beam conditions, and the characteristic X-ray

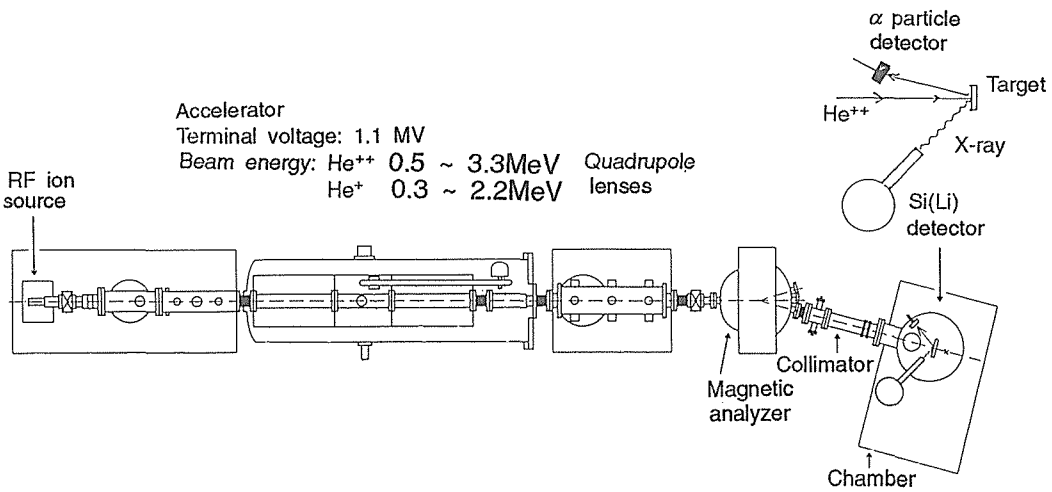

Fig. 1. Schematic diagrams of RBS-PIXE analytical system

yield can be calibrated by the backscattering yield of the projectile ions. In addition to this, the background of PIXE spectra is extremely low compared with that of the electron induced X-ray emission such as EPMA and EDX, which mainly originates from the braking radiation of incident electron beam. Thus, in PIXE analysis the detection limit in a standard condition is of the order of magnitude 10^{-6}.

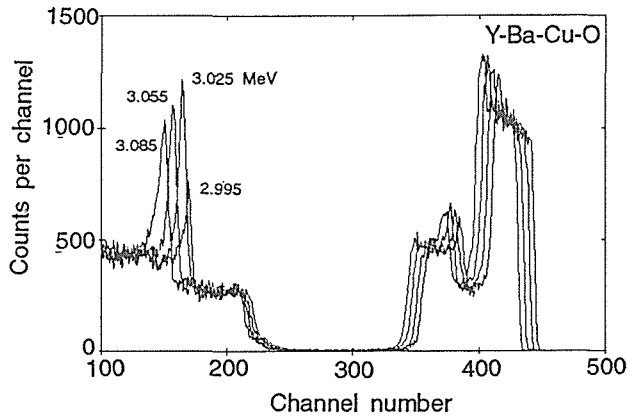

Fig. 2. Variation of oxygen resonance scattering yield vs. beam energy

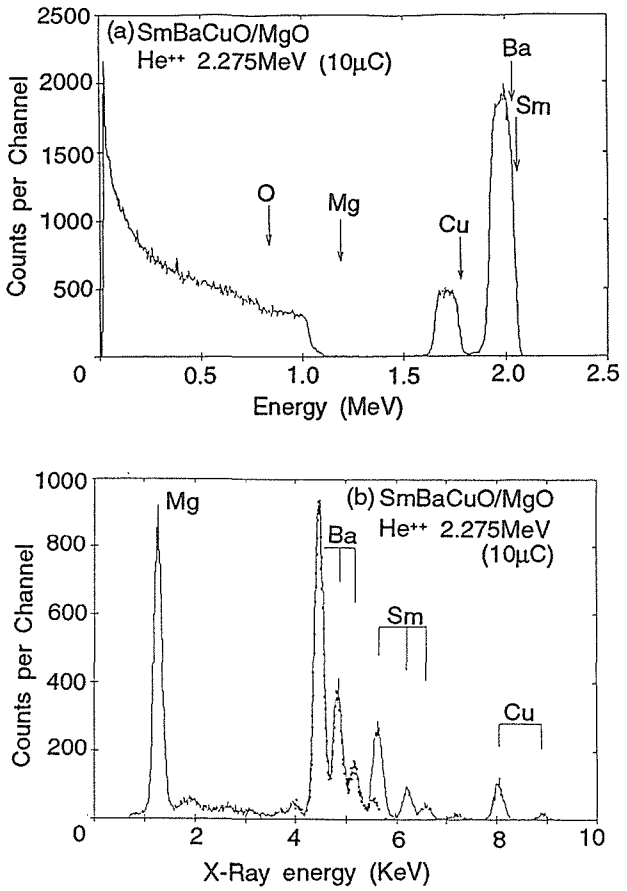

Fig. 3. RBS(a) and PIXE(b) spectra from $SmBa_2Cu_3O_y$ film[2]

An example of RBS-PIXE analysis is shown in figure 3 for the Sm-Ba-Cu oxide film sputter-deposited from $SmBa_2Cu_{3.0}O_y$ target. Since the atomic weight of Sm and Ba are 150 and 137, respectively, the backscattered spectra from Sm and Ba obtained by 2.275 Mev He irradiation almost overlaps as shown in figure 3. However, when characteristic X-ray lines from the film are acquired, we can clearly distinguish Ba $L_{\alpha,\beta}$ and Sm $L_{\alpha,\beta}$ as shown in figure 3.

Detecting a trace amount of impurities accidentally or intentionally incorporated in the film is one of the most important aspects of PIXE analysis in the present investigation. In the earlier studies on the fabrication of BSCCO films, the magnetic susceptibility of as-grown films often showed Curie-Weiss behavior and we thought that a trace amount of magnetic impurities incorporated during sputter-deposition is responsible for the observed behavior. At that time, however, EDX and other analytical methods could not detect such a small amount of impurities in the BSCCO films.

Recently we have applied PIXE analysis to the BSCCO films and have found that Curie-Weiss behavior of the BSCCO films caused not only from Fe and Ni impurities incorporated from the stainless steel cramp during sputter-deposition but also from a trace amount of Fe dissolved in single crystal MgO substrate. As described above, RBS-PIXE analysis provides us with a strong analytical meaning to a complete compositional analysis of oxide superconductor films.

References

1. *Synthesis and Characterization of $Bi_2Sr_2Ca_{n-1}Cu_nO_y$ (n = 1 to 7) Thin Films Grown by Off-Axis, Three Target Magnetron Sputtering*, Narita, H., Hatano, T. and Nakamura, K. J. Appl. Phys. 72 (1992)
2. *RBS-PIXE Analysis on Thin Films of High T_c Oxide Superconductors*, Ishii, A. and Nakamura, K. Nucl. Instr. Meth.

❒ Preparation of Carbon fiber/SiC Composite by Chemical Vapor Infiltration

T. Noda, Second Research Group

Keywords: carbon fiber/SiC composite, chemical vapor infiltration, βSiC, ethyl-trichloro-silane, methyl-trichloro-silane

SiC is an attractive material for structural components at high temperatures in the energy production area of advanced reactors because of its heat resistance, high thermal conductivity and irradiation resistivity. Moreover, since SiC does not produce radioactive nuclides with a long half-life under neutron irradiation[1], it has become of major interest as a low activation material for first wall or blanket components of a fusion reactor from the environmental safety[2]. Induced activity of SiC decreases by about 9 orders of magnitude within several days after the reactor shutdown and its fast decay allows ease of the contact maintenance[2]. However, since SiC is intrinsically brittle and it is difficult to achieve high-purity with general sintering procedures, development of materials satisfying both purity and improved mechanical properties is required.

In the present study, chemical vapor infiltration (CVI) process to produce carbon fiber/SiC is examined to obtain a composite with a proper purity and improved toughness.

Carbon fibers, TORAYCA T300, were used as base materials. Two types of carbon yarns, such as randomly oriented chopped fibers and plainly woven cloth were infiltrated with SiC. The sources of SiC were ethyl-trichloro-silane (ETS) and methyl-trichloro-silane (MTS).

MTS or ETS gas evaporated from a reservoir was carried by H_2 to the substrate and thermally decomposed to deposit SiC inside the preforms. The CVI was conducted under non-isothermal condition. The temperature at the downstream side of substrates was kept at 1273-1573K and a cooled mixture gas of MTS or ETS and hydrogen with a volume ratio of 1/30 was introduced to the upstream side. The downstream side was continuously evacuated and the pressure was controlled at 13.3kPa. The composites formed were identified by X-ray diffraction. Microstructures were observed with SEM and TEM. Mechanical properties were evaluated with bend tests at room temperature. Impurity concentration was measured by a neutron radioactivation analysis.

The composites produced at various temperatures were identified by X-ray diffraction. Main matrix of composites were β-SiC. In the case of MTS, Si deposition also occurred along with SiC. Other compounds such as α-SiC and SiO_2 were not found. The purity of materials was found to be better than 99.99% from the activation analysis. The amount of SiC deposition increases with temperature and takes maximum at around 1400K and 1523K for ETS and MTS, respectively. At higher temperatures, decomposition occurs before the reactant gas reaches the substrate and as a result the uptake of SiC decreases. In addition, the deposition rate was so fast that most of SiC deposited on the side of the upper stream of reactant gas and it was difficult to obtain a composite with a uniform texture. At temperatures lower than around 1300K, it requires longer than 100ks to achieve a sufficient infiltration. Then in the present study, the optimum temperatures were 1323-1473K for ETS and 1423-1473K for MTS, respectively. Microstructure of cross-section of the composite was shown in figure 1. SiC deposited finely around carbon fibers and more densely at lower temperatures. However, small pores are still observed. In the present condition, the maximum density was 90%.

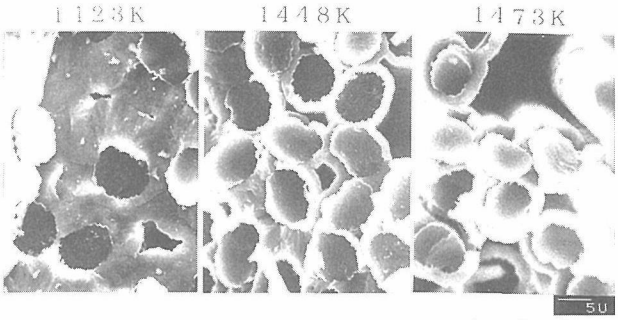

Fig. 1. Microstructures near the center of cross-section of carbon fiber/SiC composites formed with MTS for 108ks at various temperatures

The wettability of SiC to carbon fiber seems to be fairly good. Microstructures at the interface between fiber and SiC were examined with a high-solution TEM. The formation of graphite layer with a thickness of around 0.5μm was observed at the interface between carbon fiber and SiC. Carbon atoms in graphite are arranged in hexagonal rings on (0001) plane and each carbon is bonded to other three carbons with sp^2 hybrid orbitals. C-C bond distance in graphite is 0.14nm. If the neighboring carbon is replaced by Si, Si and C form sp^3 orbitals and are joined to each other with a strong covalent bond. Si-C bond distance of 0.18nm in βSiC is not much different from C-C

distance. Such electronic structural stability are considered to be closely related to the mechanism of graphite formation on carbon fibers prior to SiC deposition from chloro-silane and the growth of SiC crystal on the graphite.

The mechanical properties of the composites were examined by bend test at room temperature.

Figure 2 shows load-deflection curves of composites prepared from carbon fiber preforms with felt and woven yarn. The composites were made with ETS. Since the carbon fiber content in the composite with the felt-type preform was as low as 20%, the fracture behavior became similar to that of monolithic SiC. On the other hand, the composite with the woven-yard-type preform whose fiber content is higher than 50% showed apparent plasticity due to bridging and pullout of the fibers.

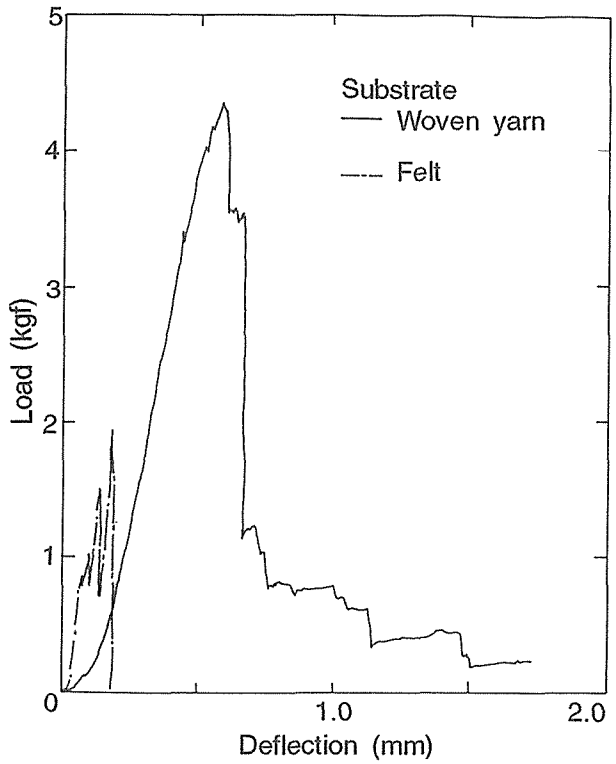

Fig. 2. Load-deflection curves of composites prepared from carbon fiber preforms with felt and woven yarn. The composites were made with ETS for 43.2ks at 1423K

The mechanical properties of composites is mainly affected by porosity. Materials prepared in the present study contained pores. The fracture strength increases with decreasing porosity. The maximum fracture strength at the present study was 800 MPa at 10-20% of porosity for the composite prepared with ETS.

The bend strength was also affected by the thickness of SiC layer coated on the composite at the final stage of the infiltration. This coated layer seemed to work as a notch for the bending. Assuming the thickness of the coated layer as a pre-crack length, apparent fracture toughness, K_Q, is calculated from the bend tests.

Figure 3 shows the fracture toughness, K_Q, as a function of the porosity. The fracture toughness increases with decreasing porosity and reaches around 10MPa.m$^{1/2}$ for ETS which were 3 times higher than that of monolithic SiC[2]. The toughness of the composites prepared with ETS is higher than with MTS. In the case of MTS, Si also deposited along with SiC and graphite. Such inhomogeneity of the matrix might affect the decreasing of strength.

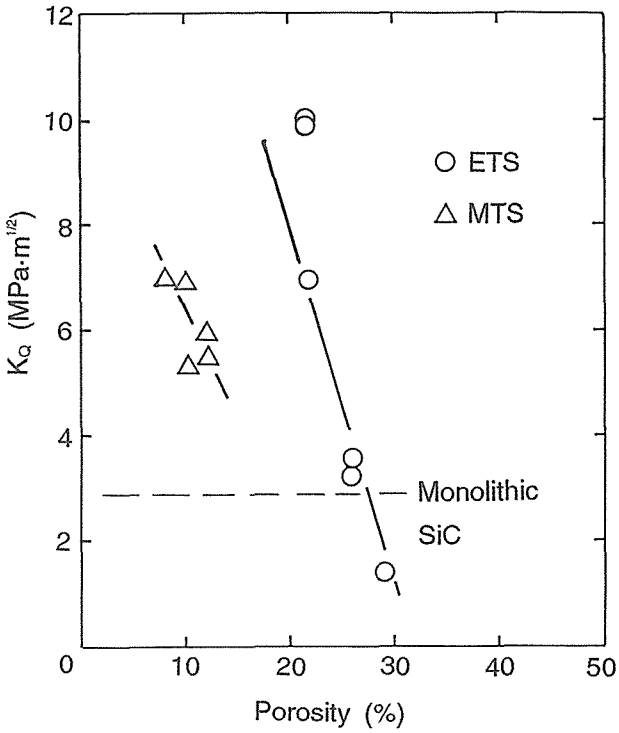

Fig. 3. Fracture toughness of the composites as a function of porosity

As a summary, the following conclusions were made:

1. Carbon fiber/SiC composite with a purity better than 99.99% and a porosity less than 20% was obtained by the CVI method.
2. Maximum fracture toughness obtained from bend tests was 10 MPa.m$^{1/2}$. This value is 3 times higher than that of monolithic SiC.

References

1. Noda, T., Araki, H., Abe, F. and Okada, M. Trans. NRIM 30 (1988): 185–215.
2. Noda, T. Netsu-shori 28 (1988): 100–5 (in Japanese).

❒ Development of a 20 T Large Bore Superconducting Magnet

T. Kiyoshi, K. Inoue, K. Itoh, T. Takeuchi, H. Wada and H. Maeda, First Research Group

Keywords: superconducting magnet, high magnetic field, superfluid helium

Introduction

As one of the major technological challenges in the Multi-Core Research Project on Superconductivity, a 20 T large bore superconducting magnet has been developed at NRIM. The main purpose for developing this magnet is to estimate performances of newly developed superconductors, such as high T_c copper oxides.

Until now, this magnet has been operated three times and generated up to a magnetic field of 20.3 T in a 44 mmØ diameter clear bore. In this paper, we describe an outline of the magnet system together with the operation results and our future plans.

Magnet System

The cryostat of this magnet is separated into two chambers. Two outer coils in the outer chamber are designed to provide stable back-up fields up to 15 T. No challenging operation is scheduled for those coils because their stored energy amounts to 45 MJ. On the other hand, various test operations are carried out in the inner chamber. By separating two chambers thermally with a vacuum, heat generation that occurred in the inner chamber, such as quenches of the two inner coils, should have no essential effect on the stability of the outer chamber coils.

High-current conductors made of twisted multifilamentary strands are used for the two outer coils. The conductor for the outermost (outer-2) coil is composed of 19 NbTi strands, while the other coil (outer-1) conductor contains 11 (Nb, $Ti)_3Sn$ strands. Both conductors are stabilized with OFHC copper and pure aluminum. They are wound into double-pancakes and stacked. Those two coils are connected in series and designed to generate a central magnetic field up to 15 T at the operating current of 4717 A. The middle coil is also made of double pancakes with monolithic conductors of multifilamentary $(Nb,Ti)_3Sn$. The $(Nb,Ti)_3Sn$ conductors used for the outer-1 and the middle coils are fabricated by the bronze process and wound after heat treatment. A contribution field of the middle coil is designed to be 3 T at 883 A and a central field as high as 18 T can be generated in a 160 mm diameter bore. The first inner coil is also made with a bronze-processed multifilamentary $(Nb,Ti)_3Sn$ conductor. It was made by the Wind & React method and impregnated with epoxy resin. By operating this coil, a central field over 20 T can be obtained.

We have chosen saturated superfluid helium as a coolant of this magnet. Each chamber contains a liquid helium tank over the coils. Liquid helium in the tank expands adiabatically through a J-T valve, absorbs the heat in a 1.8 K saturated helium bath and is decompressed with rotary pumps. The pressure of the saturated superfluid helium bath in each chamber is controlled automatically by changing the conductance of an automatic valve. A liquid level of each bath is also maintained by opening and closing the J-T valve.

Figure 1 shows the outer coils with the liquid helium tank and other upper structures. The inner chamber is already inserted.

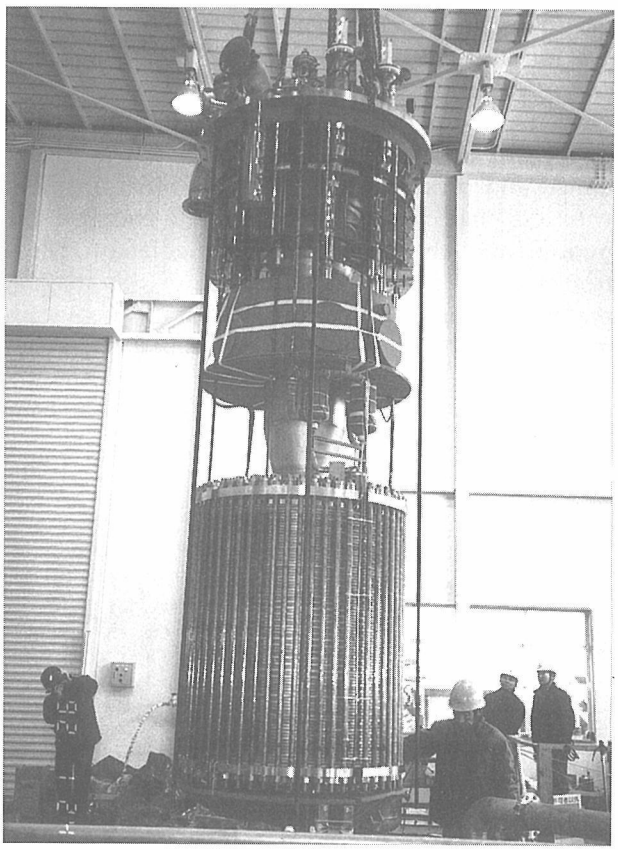

Fig. 1. A picture of the outer coils of the 20 T large bore superconducting magnet with the upper structure. The inner chamber is already inserted

Results of Operation

A new helium refrigerator will be combined with this magnet in 1994. Until then, this system has to be cooled with liquid nitrogen and liquid helium. It takes three days to cool down from ambient temperature to 4.2 K. Additional 4 hours and 1.5 hours are required to cool down to 1.8 K from 4.2

K for the outer chamber and for the inner, respectively. The temperatures for the both chambers finally reach below 1.7 K.

In the first charging up of the two outer coils, remarkable voltage was generated in them at 4573 A. Some part of the coils must have gone to the normal resistive state and a quench detector judged it was a signal of a quench. Those coils, however, could be energized to the operating current of 4717 A with no fluctuation of coil voltage in the next operation. The middle coil could be energized beyond the designed current of 883 A up to 910 A (18.06 T). Two quenches occurred at the current of 853 and 893 A before reaching 910 A. After those quenches, no more quenches due to the middle coil itself have been observed up to 910 A.

The inner coil had experienced nine quenches before its current was maintained at 255.5 A. The field of 20.3 T could finally be obtained in a 44 mmØ free bore. The highest field of a superconducting magnet in literatures is a field of 20.1 T in a 31.8 mm coil inner diameter[1]. The field obtained in our magnet exceeded this record. The training process of the inner coil is shown in the load line curve of figure 2.

Even when both the inner chamber coils quenched, the back-up field of 15 T was maintained and pressure increase of the inner chamber was less than 10 Torr. We could re-energize the middle and the inner coils immediately. These results prove a good performance of this magnet system. This magnet will provide an ideal environment for coil tests of newly developed superconductors.

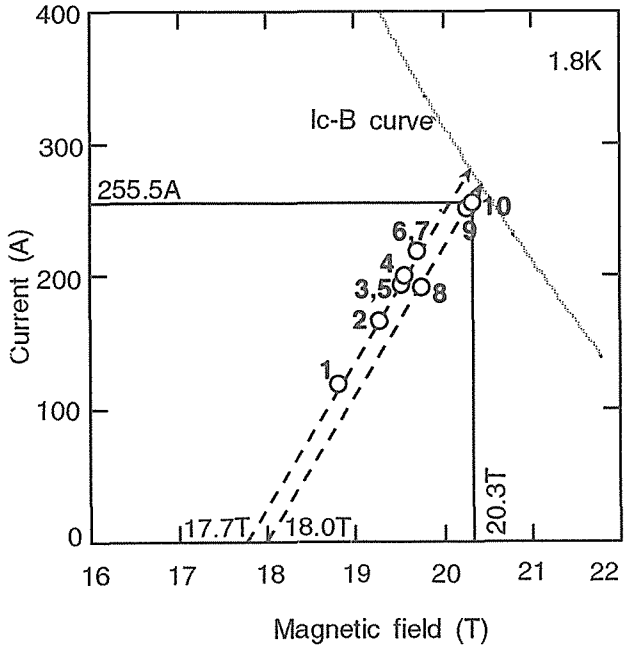

Fig. 2. Training process of the inner coil. Quenches occurred at open circles except the tenth operation. Numbers near the circles represent the order of the operations. The dotted line is an Ic-B curve extrapolated from data at 4.2 K

Figure 3 shows magnetic field distribution at the midplane of the coils when the highest field is generated. When both the inner and the middle coils are removed from the inner chamber, the fields up to 15 T are obtained in the inner chamber with a diameter of 314 mm. By inserting the middle coil, a 160 mm free bore with a magnetic field of 18 T can be obtained. When all the coils are assembled, the highest field of 20.3 T can be generated in a 44 mm free bore.

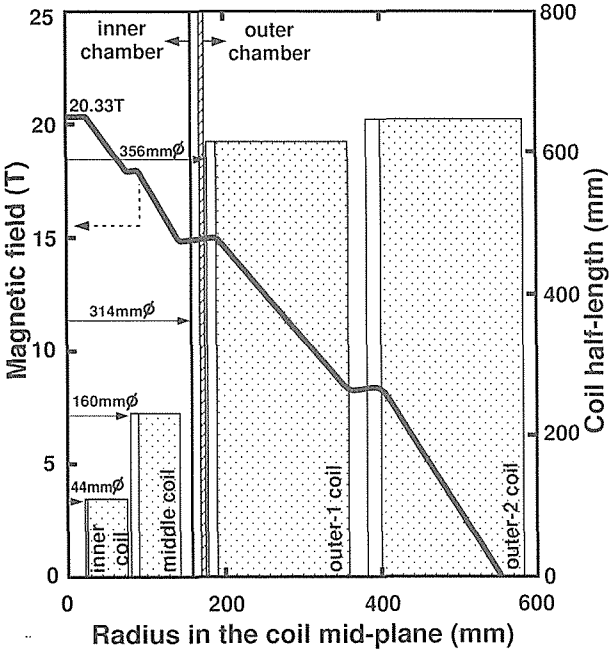

Fig. 3. Radial magnetic field distribution at the center of the magnet when a central field of 20.3 T is generated. Cross sections of the four coils overlap in this figure. Each open square on the left of a coil represents thickness of a coil bobbin

Future Plans

We plan to develop three other inner coils and their operations will be tested in 1992 fiscal year. After 1995, this magnet system will be provided to both domestic and international collaborative research programs.

Reference

1. *A 20-T Superconducting Magnet System*, Turowski, P. and Schneider, Th. Physica B 155 (1989): 87–90.

❐ Fabrication and Properties of $Bi_2Sr_2CaCu_2O_8$/Ag Tapes and Coils

*H. Kumakura, H. Kitaguchi, K. Togano** and H. Maeda, 1st Research Group

Keywords: $Bi_2Sr_2CaCu_2O_8$/Ag tape, dip-coating method, grain alignment, critical current density

Introduction

Application of superconducting materials to magnets requires the winding of tape or wire conductors with sufficient flexibility and sufficiently high critical current density J_c into a coil. Since the oxide superconductors are intrinsically brittle, as is the case of A15 intermetallic superconductors, special techniques must be developed for making flexible tape or wire conductors. We have applied doctor-blade process for the fabrication of $Bi_2Sr_2CaCu_2O_8$ (2212)/Ag tape conductors and have succeeded in obtaining grain oriented 2212 microstructure with excellent J_c values[1]. Grain alignment of 2212 phase brought about J_c values much higher than those of conventional metallic superconductors in magnetic fields above 20T at 4.2K[2]. The excellent J_c-B properties at 4.2K of the textured tapes suggest that the tapes were promising for the high field application above 20T for which no superconducting tape or wire of conventional materials is currently available.

An alternative method of fabricating oxide tape conductors is a dip-coating method[3]. The dip-coating method is more adequate than the doctor blade method because long tapes can be more easily obtained.

In this report, we summarize our recent results on the 2212/Ag tapes and coils prepared by applying the continuous dip-coating method.

Tape and Coil Fabrication

Long 2212/Ag tapes about 6m length were easily obtained by continuous dip-coating process. This is schematically shown in figure 1. Ag tape as a substrate of ~6m in length was continuously coated with slurry consisting of 2212 powder and organic materials such as binder, dispersant and solvent. In order to obtain uniform thickness of the coated slurry on the Ag tape, it is very important to adjust properly the viscosity of the slurry, by changing the volume fraction of the solvent present.

After the solvent in the slurry was completely vaporized, the coated tape was cut into four tapes of 1.5m length. Each tape was wound loosely into a pancake coil with a small gap between neighboring tape, and then heat treated. The temperature profile of the heat treatment is shown in figure 2. The coil was heated at 500 °C to remove organic materials, heated up to 885 °C, just above the melting point, and then slowly cooled down to 835 °C. This slow cooling from the partial melting state is essential for the grain alignment and the excellent J_c-value. One of the coils after the heat treatment is shown in figure 3. After the heat treatment, from two to four coils were combined together coaxially by inserting coils into a gap of another coil. Myler tapes were also inserted along each gap of the coils for insulation. Figure 4 shows the final coil composed of four conductors.

The dip-coated tape shows an excellent J_c-value with a small magnetic field dependence at 4.2K, indicating the tape is promising for the high field application. However, the J_c values of the dip-coated tape are slightly smaller than the best J_c values of the doctor blade processed tapes. This is because the uniformity of the 2212 thickness of the dip-coated tape is still not optimized, and a higher J_c-value can be obtained by the improvement of the dip-coating process.

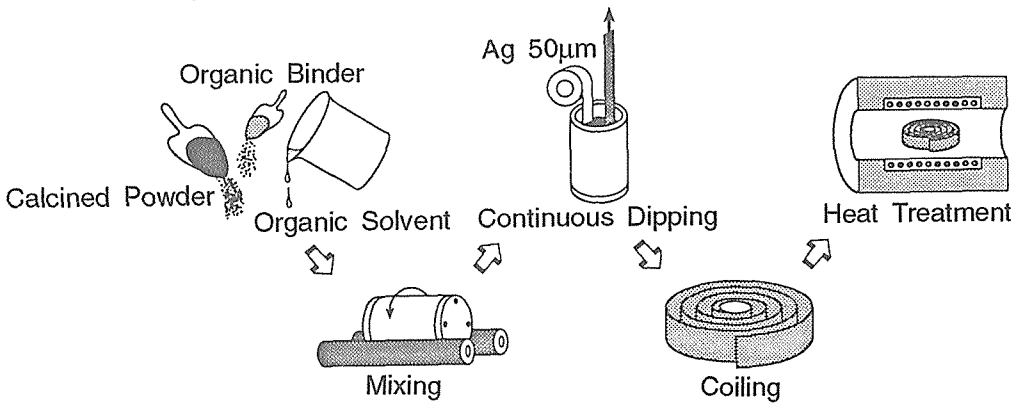

Fig. 1. Fabrication of $Bi_2Sr_2CaCu_2O_8$/Ag pancake coil applying continuous dip-coating method

*Surface and Interface Division

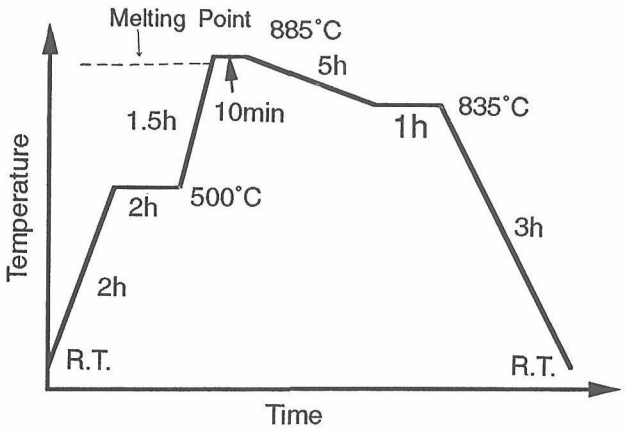

Fig. 2. Typical heat treatment schedule

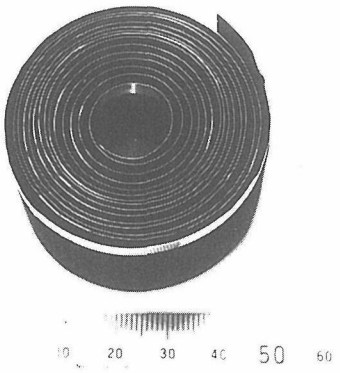

Fig. 3. $Bi_2Sr_2CaCu_2O_8$/Ag coil after the heat treatment

Fig. 4. Final coil composed of four $Bi_2Sr_2CaCu_2O_8$/Ag conductors

Coil Test

A coil performance test was carried out for the coil shown in figure 4 in magnetic fields at 4.2K. The parameters of the coil are listed in table 1. Four conductors with 1.5m length were connected in series using Ag strip. The coil was inserted at the center of the superconducting magnet, and the voltage of the four conductors was monitored simultaneously with increasing applied current in a fixed bias magnetic field. Magnetic fields induced by the coil was measured by a Hall probe set at the center of the coil.

One of the four conductors showed resistive transition, and critical current I_c defined by the $10^{-13}\Omega \cdot m$ criterion is 230A. Three other conductors showed voltages much less than the values of the criterion up to 250A, which is the maximum current available using our power supply. The results indicate that the dip-coated tape has non-uniform I_c distribution. The magnetic field generated by the coil reached 0.6T at I_c = 230A. This value is nearly equal to the magnetic field calculated from I_c and the coil parameters shown in table 1. This is one of the highest magnetic fields generated by high-T_c oxide superconducting coils. The generated magnetic field can be increased by improving the uniformity of the I_c-values.

Table 1 Parameters of the $Bi_2Sr_2CaCu_2O_8$/Ag Coil

Conductor	Dip-Coating Processed Bi-2212/Ag Tape	
Conductor Size	Width Thickness Length	13mm 0.15 1500mm
Number of Turns	64 (16 × 4)	
Number of Pancake	1	
Coil Size	Inner Diameter Outer Diameter Height	13mm 45mm 13mm

Conclusion

$Bi_2Sr_2CaCu_2O_8$/Ag tapes with excellent J_c-B properties were fabricated by applying the continuous dip-coating process. A pancake coil of 64 turns was fabricated using this long tape, and succeeded in generating a magnetic field of 0.6T in a bias field of 12T at 4.2K. The result indicates that the dip-coating method is promising for the fabrication of practical 2212 tape conductors.

Acknowledgement

This work is under collaboration with Asahi Glass Co., Ltd. and Hitachi Cable, Ltd. The authors are grateful to collaborators, Mr. J. Shimoyama and Dr. T. Morimoto of Asahi Glass Co., Ltd., Mr. K. Nomura and Dr. M. Seido of Hitachi Cable, Ltd.

References

1. *Improvement in Critical Current Density of $Bi_2Sr_2CaCu_2O_8$ tapes Synthesized by Doctor-blade Casting and Melt Growth*, Kase, J., Irisawa, N., Morimoto, T., Togano, K., Kumakura, H., Dietderich, D.R. and Maeda, H. Appl. Phys. Lett. 56 (1991): 970–72.
2. *Anisotropy of Critical Current Density in Textured $Bi_2Sr_2CaCu_2O_8$ Tapes*, Kumakura, H., Togano, K., Maeda, H., Kase, J. and Morimoto, T. Appl. Phys. Lett. 58 (1991): 2830–32.
3. *Fabrication of BiSrCaCuO/Ag Composite Superconductors by Dip-coating Process*, Togano, K., Kumakura, H., Kadowaki, K., Kitaguchi, H., Maeda, H., Kase, J., Shimoyama, J. and Nomura, K. Proceedings of ICMC '91, Huntsville, Alabama (in preparation).

Research in Progress 1991–92

❐ List of Research Subjects

Numbers with circle indicate subjects newly started from April 1992.

Numbers with square indicate subjects ended by March 1992.

Characterization/Properties

Electronic and nuclear properties

1 Electronic Structure and Superconducting Mechanism in High-Temperature Superconductors

2 Theory of Structure and Electronic States in Systems with Randomness

3 Studies on Electronic and Magnetic Properties at High Pressure

4 Database Development in Assistance of New Superconducting Materials Research

5 Relaxation Phenomena in Magnetic and Superconducting Materials

Atomistic arrangement

(6) Structures of Transition Metal Oxides from the Bonding View Point

7 High Resolution Transmission Electron Microscopic Study for Interfaces of Materials

[8] Structure and Electronic Properties of Low-dimensional Transition Metal Compounds

Phase transformation and microstructures

(9) Super-Microscopic Study on the Mechanism of Martensitic Transformation in Shape Memory Alloys

[10] Mobilities of Austenite/Martensite Interface in Fe-based Shape Memory Alloys

[11] Mechanism of Variant Selection in Stress Induced Transformation

[12] Research of Shape Memory Thin Films for Microactuator

Surface and interface properties

(13) Disintegration Phenomena in Intermetallic Compounds

14 Study on Changing the Properties of Metallic-Oxide Films for Increasing the Hydrogen Permeability

15 Effect of Oxidation on Mechanical Degradation of Metallic Material at High Temperature

16 Fabrication of Quantum Well Box Systems by Droplet Epitaxy for Advanced Optoelectronic Devices

[17] Compatibility of High Temperature Materials in Liquid Metals

Mechanical properties

(18) Fatigue Behavior of Brittle Materials at Elevated Temperatures

19 NRIM Fatigue Data Sheet Project (IV)

20 Controlling and Recovering High Temperature Damage

21 Tensile Fracture Mechanism for Long Ceramic Fibers

22 NRIM Creep Data Sheets (IV)

23 Effect of Surface Film on Deformation of Bulk Matrix Material

24 Evaluation of Crack Initiation and Growth of Superalloys under Creep and Creep-Fatigue Conditions

25 Real Time Evaluation of Fatigue Damage during Crack Propagation under Random Loadings

26 Mechanism of Fretting Fatigue Failure in Composite and Surface Modified Materials

27 Fatigue Crack Initiation Process in Corrosive Environment

[28] Crystal Growth on the Surface of Intermetallic Compounds

[29] Mechanism of Mechanical Damage Accumulation in Brittle Materials

Measurement and evaluation

(30) Study on Detection and Evaluation of Radiation Damages in Extreme Particle Fields

(31) Development of Advanced Technologies for X-ray Microtomography

(32) Evaluation of Metallurgical Structure with a Fazzy Logic

(33) Atomic Scale Evaluation of Material Damage in Aqueous Solution

(34) Quantitative Evaluation of Fracture in Materials for Casks

35 Vaporization and Ionization by Arc Plasmas

36 Characterization of Metals and Alloys Using Synchrotron Radiation

37 Characterization and Control of Elementary Functions of Materials in the Localized Fine Area

38 'In-Situ' Analysis/Evaluation of Radiation Damage in Materials

39 Advanced Techniques of Physical Analyses for Metals

40 Study on Mechanism of Ion Production in Low Temperature Plasma

41 Sensitive Instrumental-Analysis of Metallic Materials by Direct Methods and Separation Methods

42 Database Systems for R&D of Superconducting Materials

43 Sensing and Analysis of Material Damage Formation Processes

44 Research on Quantitative and Intelligent Nondestructive Evaluation Techniques for Materials and Structures of High Reliability

45 Chemical Analysis of Organotin in Marine Environmental Samples

46 Study on Measurement and Evaluation Methods for Superconducting Properties

[47] A Basic Research for In-Situ Measurement of Dynamic Strains of Materials at Elevated Temperature

[48] Investigation on Non-Contact Materials Evaluation Using Laser Beam

[49] Measurements of Transient Phenomena Due to Beam-Solid Interaction

[50] Development of Fundamental Technologies for X-ray Microtomography

[51] Image Analysis of Metallurgical Structure with a Computer Network System

[52] Fundamental Study on Initial Oxidation by Means of Light-Induced Exoelectron Emission

[53] In-Situ Quantitative Evaluation of Microreaction

[54] Fundamental Study on Quantitative Non-Destructive Evaluation of Small Defects in Materials

[55] In-Situ Observation of Fatigue Damage

[56] Quantitative Evaluation of Fracture at High Strain Rate and Low Temperature in Ferritic Steels

[57] International Joint Research on Evaluation and Standardization of Advanced Materials

Simulation and theory

58 Development of Material-Design-Technique for Mechano-Chemical Attack on Light-Weight Heat-Resistant Materials

59 Study on the Computer Aided Design Tools for the Development of Materials

60 Study on the Construction of Self-Organizing Information-Base System Used for Creative Research and Development

61 Development of Knowledge Based System for Materials Life Prediction

62 Predictions of Materials Strength and Endurance under Irradiation Using Ion Beam

Materials

Non-ferrous materials

63 Basic Research to Establish Design Techniques for Advanced Materials

64 Microstructural Refinement and Mechanical Properties of Titanium Alloys

Intermetallic compounds

(65) Improvement of Mechanical Properties of Intermetallic Compounds by Crystal Growth Control

(66) High Ionic Conductivity of Solid Electrolyte

67 Preparation of Spontaneous Exothermic Metals and Its Application

68 Fatigue Fracture Mechanisms for TiAl Intermetallic Compounds at High Temperatures

69 Production and Character Evaluation of Functional Intermetallic Compounds

70 High Performance Materials for Severe Environments- I

[71] Advanced Intermetallic Compounds for Nuclear Reactors

[72] Crystal Growth on the Surface of Single-Crystalline Intermetallic Compounds

Composites

73 Thermal Effects on the Material with Heterogeneous Phase

Materials for mechanical application

74 Intelligent Structural Materials

75 Development of Metal Matrix Composites for High Temperature Use Through Com-

binations of Advanced Powder Metallurgy Processes

[76] Development of Damping Materials

Materials for electronics application

77 Fabrication of High-T_c Superconducting Wires

78 Development and Evaluation of Advanced Superconducting and Cryogenic Materials

79 Development and Characterization of Superconducting Materials for Fusion Reactor Magnet Use

[80] Synthesis of New Functional Materials by the Application of Host-Guest Reactions

[81] Evaluation and Application of Cu-Ag Alloy as Conductor Material in High Field

[82] Studies on Fabrication Processes of BiSrCaCuO Superconductors

Magnetic materials

(83) Fabrications of Mesoscopic Scale Materials and Their Properties

[84] Fabrication and Properties of Novel Metallic Materials with Artificial Microstructures

[85] Properties and Applications of Mesoscopic Scale Materials

Opto-materials

[86] Reversible Color Change Alloys

Materials for energy application

(87) Processing and Development of Isotopically Controlled Materials (ICM)

88 Fundamental Study of Microstructures and Properties to Develop High Performance Materials for Severe Environments

89 Study on a Porous Gas-Diffusion Electrode

90 Environmental Degradation of Structural Materials for Light Water Reactors

91 Assessment of Strength and Structural Materials Database for Weldment in FBR Components

92 Fundamental Research on Application of New Functional Materials to Passive Components

93 Development of the Fusion Reactor First Wall Materials Resisting to Plasma and Radiation Damage

94 Material Chemistry in the Extreme Conditions under Irradiation

95 Research on Distributed Database for Advanced Nuclear Metals

96 R&D of Advanced Heat-Resistant Structural Materials for Very High Temperature Gas-Cooled Reactors

[97] Research on Fundamental Techniques to Develop Functionally Gradient Materials for Relaxation of Thermal Stresses (II)

[98] Research on Fundamental Techniques to Develop Functionally Gradient Materials for Relaxation of Thermal Stresses

Materials for environmental performance

(99) Improvement of Wear Properties of Metallic Medical Materials

100 Achievement, Measurement and Application of Extremely High Vacuum

[101] Study on Improvement of Metallic Biomaterials

[102] Corrosion Resistance of Synthetic Barriers in Geological Disposal of Spent Nuclear Fuels

[103] Corrosion Resistance of Coated Materials in Natural Environment

[104] Development of Low Activation Materials

Processing

Separation and synthesis

(105) Elimination of Some Specified Toxic Metallic Ions

106 Preparation of Superconducting Raw Materials Having Controlled Quality

107 Fundamental Study on Preparation and Characterization of the Metal Complexes Possessing a Peculiar Molecular Structure

108 Alloying Method Using Decomposition of Metal Halides

(109) Project Research on the Purification Techniques of Rare Metals in View of Finding New Materials Properties (Phase II)

Gaseous process

(110) Precise Composition Control Ordered Alloys by Chemical Transportation Techniques

(111) Extraction from Melt to Gas Phase

112 Synthesis and Characterization of Oxide Superconductor Films

Liquid state process

(113) Measurements, Analyses and Evaluations of Specimens Made by FMPT

114 Purification of Metals by Non-Contacting Melting Method

115 Solidification Processing for Fine-grain Structure Materials

116 Physical, Chemical and Biological Phenomena under Microgravity Environment

117 Development of Extraction Techniques of Gallium and Other Rare Metals

Solid state process

118 Materials Properties Induced by Transformation Superplasticity

119 Metallurgical Analysis of Cutting Region

120 Comprehensive Research and Development of Special Structural Ceramics Using Colloid Processing

Powder processing

(121) Development of Particles Assembly Technology for Integration of Functions

122 Coating of Fine Powders by CVD Technique in Fluidized Bed

123 Coating Formation by Molten and Electrified Powders

124 Combustion Synthesis for Production of Intermetallic Compound

125 Production and Characterization of Advanced Powders

126 Preparation and Characterization of Ultrafine Particles Used for Making Oxide Superconductors

Joining

127 Corrosion of Dissimilar Metals Joints in Reactor Fuel Reprocessing Plants

128 Joining of Intermetallic Compounds Utilizing Resistance Heating of the Compound to Be Joined

129 Low Energy Joining with Controlled Surface Composition and Misorientation Angle

130 Effect of Temperature Distribution on Capillary Flow

Composite process

(131) Forced Infiltration Process for Making Composite Structures

132 Material Processing for Making Layered Structures

Process with aid of beam technology

(133) Diagnostics of Laser Photoionization Induced Plasma

(134) Study on Evaporation Process by High Energy Density Beams

135 Development of Quantum Microstructure in Ultra Clean Vacuum

136 Study on Synthesis of Special Compounds by a Combined Use of Ion Implantation and Deposition

137 Fundamental Study on Formation of Dissimilar Surface Layer by High Energy Density Beams

138 Study on Molten Metal Behavior in Surface Modification Process with High Temperature Heat Sources

Processing in special environment

139 Development of Extremely High Field Magnets

❒ Research Programme

Characterization/Properties

Electronic and nuclear properties

1 Electronic Structure and Superconducting Mechanism in High-Temperature Superconductors

April 1988 to March 1994
T. Oguchi, Materials Physics Division
Keywords: high-temperature superconductor, theory, electronic structure

The high-temperature superconductor (HTSC) is a potential material for a variety of applications. Despite a great deal of effort of basic research on electronic structure and properties of HTSC, the superconducting mechanism has not been clarified yet. In this work, we have studied electronic structure of HTSC based on band-structure calculations with the local-density approximation (LDA).

The electronic structure of La_2CuO_4 has been investigated for two different crystal structures, K_2NiF_4 and Nd_2CuO_4. The calculated band structure shows importance of the position of oxygen atoms outside CuO_2 planes in realizing two-dimensional character of the electronic structure near the Fermi energy (E_F). The high density of states just below E_F obtained for the Nd_2CuO_4 structure implies relative instability when doping holes, being consistent with the observed fact that no hole-doping is possible in Nd_2CuO_4.

LDA band calculations have been performed for $YBa_2Cu_3O_y$ (y=6 or 7), abbreviated as Y123. Several characteristic aspects have been derived by comparing with other HTSC's. Importance of the energy separation between Cu-*d* and O-*p* states was pointed out in connection to photo-emission experiments. Significance of the *p-p* hopping between the nearest oxygen atoms was also discussed.

Recently the electronic structure of $YBa_2Cu_4O_8$ (Y124) has been calculated. Overall characteristics of the electronic structure are quite similar to those of Y123. A large energy-level lowering of oxygen *p*-states at chain sites was found. This result may explain the relative stability of the oxygen ions in Y124. Some differences in the Fermi surfaces between Y123 and Y124 were also suggested in conjunction with anisotropic transport properties.

Related Papers

Implications of Band-Structure Calculations for High-T_c Related Oxides, Park, K.T., Terakura, K., Oguchi, T., Yanase, A. and Ikeda, M. J. Phys. Soc. Jpn. 57 (1988): 3445–56.

Electronic Band Structure of $YBa_2Cu_4O_8$, Oguchi, T., Sasaki, T. and Terakura, K. Physica C 172 (1990): 277–81.

Local-Density Band Structure of Y-Ba-Cu Oxides, Oguchi, T., Sasaki, T. and Terakura, K. Physica C 185–189 (1991): 1733–34.

2 Theory of Structure and Electronic States in Systems with Randomness

April 1990 to March 1993
T. Oguchi, Materials Physics Division
Keywords: electronic structure, defects in solids, structural stability

We investigated theoretically the structure and electronic states of bulk materials which contain imperfections such as point defects, stacking faults or phase boundaries. The analysis is based on the density-functional (DF) electronic theory combined with the molecular-dynamics (MD) method (abbreviated as DF–MD method). This DF–MD method provides an useful tool to determine the optimum atomic arrangement affected by the imperfections as well as the electronic states.

First of all, physical backgrounds and concepts of the DF–MD method have been studied intensively. Numerical techniques and algorithms involved in the method have been examined in details by performing small-scale calculations for silicon molecules. It was demonstrated that the method enables us to carry out first-principle MD simulations and has several great advantages over the conventional methods for electronic-structure calculations. Some new concepts which are necessary to extend to metallic systems were also discussed.

Formation energies for stacking faults of Al have been evaluated with the DF–MD method. We considered twin and intrinsic stacking faults in the present work. To model these faults, supercell geometry which contains repeated fault planes was used. The formation energies calculated by taking full atomic relaxations into account are in fairly good agreement with the experimental values. It was found that only small atomic relaxations occur, which is consistent with close-packed structure of the faults.

It is well known that high-conductive ZnSe promises realization of new devices such as blue LED's. However, no stable *p*-type ZnSe sample has been fabricated so far. Here, the origin of the in-

stability of *p*-type ZnSe has been studied with the DF–MD method. Based on the total energies calculated for Li-doped ZnSe and host ZnSe, we have proposed a new compensation mechanism for a Li acceptor in ZnSe and have shown that Li is not suitable as the *p*-type dopant of ZnSe.

An extension of the DF–MD method has been recently carried out in order to make an application to a system with spatially localized electrons feasible. For the purpose, linear-augmented-plane-wave functions were adopted as the basis set. It was shown that atomic-force calculations for bulk silicon and copper systems can be done with the same order of computational resources. A inclusion of spin-polarization in the method is also considered.

Related Papers

Li Impurity in ZnSe: Electronic Structure and the Stability of the Acceptor, Sasaki, T., Oguchi, T. and Katayama-Yoshida, H. Phys. Rev. B43 (1991): 9362–64.

Density-Functional Molecular-Dynamics Method, Oguchi, T. and Sasaki, T. Prog. Theor. Phys. Suppl. 103 (1991): 93–117.

Density-Functional Molecular Dynamics Calculations for Defects in Si and Al, Oguchi, T. and Sasaki, T. in Molecular Dynamics Simulations Yonezawa, F., ed., (Springer-Verlag, 1992): 157–66.

3 Studies on Electronic and Magnetic Properties at High Pressure

April 1990 to March 1993

T. Matsumoto, Materials Physics Division

Keywords: pressure effect, magnetic properties, high-T_c oxides, rare-earth compounds, phase transition

We are interested in the effect of applied pressure on physical properties. One of the important purposes of this research program is to clarify the quantitative changes of physical properties under pressure. Thus, we have developed the original apparatuses in order to measure the magnetization and specific heat under pressure with a high accuracy. Our recent studies have been focused on oxides with low carriers density and rare earth compounds with valence instability and abnormal electron mass.

One of our typical results is the pressure effects on the oxide superconductor $YBa_2Cu_4O_8$ and its related materials. In this research, the pressure dependence of T_c and crystal structure has been investigated by the experiments of electrical resistivity and neutron diffraction. It is very interesting to note that the T_c of $YBa_2Cu_4O_8$ easily exceeds 100K above the pressure of 5GPa. From the analysis using the result of neutron diffraction under pressure, the increment of T_c is concluded to be caused by the carrier redistribution from CuO chains to CuO_2 planes at high pressures. Subsequently, we have investigated the pressure effects on the oxides in which Cu atoms of $YBa_2Cu_4O_8$ were partially replaced by other transition elements.

The pressure effect on valence phase transition, T_V of Yb intermetallic compounds has been studied by the magnetic measurements. Magnetic susceptibilities indicates the decrease in T_V with increasing pressure. From the results, the Yb^{3+} magnetic state at higher temperatures is explained to be stabilized by pressure.

Related Papers

Structure Changes of Superconducting $YBa_2Cu_4O_8$ under High Pressure, Yamada, Y., Jorgensen, J.D., Pei, S., Lightfoot, P., Kodama, Y., Matsumoto, T. and Izumi, F. Physica C173 (1991): 185–94.

Pressure Effects on the Transport Properties of $Ln_{2-x}Ce_xCuO_4$ (Ln= Pr, Nd, Sm, Gd) Single Crystals, Matsushita, A., Uji, S. and Matsumoto, T. Physica C185–89 (1991): 1325–26.

Pressure effects on T_c of Superconducting $La_{2-x}Ca_{1+x}Cu_2O_6$, Yamada, Y., Kinoshita, K., Matsumoto, T., Izumi, F., and Yamada, T. Physica C185–89 (1991): 1299–1300.

Magnetic Susceptibility Anisotropy in the High T_c Cuprates, Johnston, D.C., Matsumoto, T., Yamaguchi, Y., Hidaka, Y. and Murakami, T. in Electronic Properties and Mechanism in High-Tc Superconductors Oguchi, T., et al., eds., Elsevier Science Publishers B.V., North-Holland (1992): 301.

4 Database Development in Assistance of New Superconducting Materials Research

April 1988 to March 1994

S. Nishijima, Failure Physics Division

Keywords: superconducting materials, high-T_c oxides, factual materials property database, empirical properties correlation

It is not long ago that a flood of research information came out monthly from many journals and reports related to R&D of new high T_c superconducting materials. A database was thought to be helpful for scientists and engineers to put those outcomes in order. The present work was asked as a part of so-called Multicore Project by the Science and Technology Agency, where several core frames including the database are set and promoted in various ways.

The database core has two aspects: one is to develop factual materials database on new superconducting materials and the other is to study and determine possible areas for future application of those high T_c materials. The former is conducted at NRIM and the latter in collaboration of many industrial and public laboratories at the Society of

Non-Traditional Technology with coordination by and participation of NRIM staffs.

An in-house factual database system is being built by Asada, Y., and mostly used to investigate empirical relations between materials parameters and superconducting performances using data collected from open literature. The findings have been published each time in academic journals, while the accumulated data is considered to be released open as a data set for more general use.

Here may be noted as an example of data correlations reported by Asada, Y., that a linear relation exists between the lattice constants, L(a, b, c), and the oxygen content, z, for $YBa_2Cu_3O_z$ system, where c–z relation is utmost significant. The orthorhombic distortion, p = b − a, is proposed as a good index for the structural transformation which could be correlated as the source of variation in the critical temperature, T_c of the materials with different z.

Another topic is the correlation between T_c and energy gap, Δ. It is true that the relation stands basically within the range of prediction by the BCS theory, $2\Delta/kT_c = 3.52$, where k is Boltzman constant, for such materials as $La_{2-x}Sr_xCuO_4$ or $YBa_2Cu_3O_7$ and the like.

Related Papers

Dependence of Lattice Constants and Tc on the Oxygen Content in YBCO, Asada, Y., Nakada, E., Miyazaki, A. and Yokokawa, T. J. Japan Inst. Metals 5 (1991): 105–9 (in Japanese).

A Review of the Size of the Energy Gap in Superconducting Oxides, Hirata, T. and Asada, Y. J. Superconductivity 4 (1991): 171.

5 Relaxation Phenomena in Magnetic and Superconducting Materials

April 1990 to March 1993

M. Uehara, Surface and Interface Division

Keywords: magnetic relaxation, metastable state, domain wall motion, magnetic after effect

Recently much attention has been given to the dynamical nature in magnetic and superconducting systems such as spin glasses, amorphous magnets and high-T_c superconductors. We study the magnetic relaxation phenomena in which a macroscopic system in a metastable state undergoes transitions to a lower state via thermal excitation or quantum fluctuations through the barrier. It was shown that the thermal activation mechanism responsible for the diffusion of ferromagnetic domain walls in a $SmCo_{3.5}Cu_{1.5}$ single crystal shows a strong anomaly below a temperature of 50K. This effect, initially attributed to quantum fluctuations, has been studied in more detail. In particular it was shown that the evolution of the magnetic after effect at low temperature fits a simple model where an effective temperature T^* to 10K accounts for energy fluctuations of domain walls at zero Kelvin. This temperature coincides with the characteristic frequency, ω_0 to $10^{12}sec^{-1}$ of domain wall vibrations in metastable equilibrium. At lower temperature, collective jumps of magnetization in a metastable state were observed in a reversed magnetic field. Such behavior strongly suggests the existence of simultaneous wall motion on the scale of the sample, due to thermal "avalanche effect", associated with dissipation, and initiated by wall tunneling events on a microscopic scale. The studies on magnetic relaxation in superconducting $Bi(Pb)_2Sr_2Ca_2Cu_3O_y$, $YBa_2Cu_3O_7$ and in high-quality single crystalline $Bi_2Sr_2CaCu_2O_8$ are currently in progress.

Related Papers

Noncoherent Quantum Effects in the Magnetization Reversal of a Chemically Disordered Magnet, Uehara, M. and Barbara, B. J. Physique 47 (1986): 235–38.

Staircase Behavior in the Magnetization Reversal of a Chemically Disordered Magnet at Low Temperature, Uehara, M., Barbara, B., Dieny, B. and Stamp, P.C.E. Phys. Lett. A114 (1986): 23–26.

Anomalous Demagnetization Process at Low Temperature in Nd-Fe-B Magnets, Otani, Y., Coey, J.M.D., Barbara, B., Miyajima, H., Chikazumi, S. and Uehara, M. J. Appl. Phys. 67 (1990): 4619–21.

Atomistic arrangement

(6) Structures of Transition Metal Oxides from the Bonding View Point

April 1992 to March 1994

M. Okochi, Materials Physics Division

Keywords: transition metal oxides, interatomic bonds, binding nature, valence values

Transition metal oxides have characteristic physical properties which are direct consequence of the structure of the crystalline coordination compounds. The metal oxides can be imagined as an interconnecting array of atoms with interatomic bonds by the sharing of electrons between metallic atoms and the neighboring oxygen. The bonding theory is a potential conception to make the microscopic binding nature clear in the three dimensional geometrical array of atoms and gives the conceptional understanding about the binding nature in the compounds like metal oxides. The binding nature is inherently dependent on interatomic distances, the coordination number and the direction in the crystals, and does not be studied quantitatively but is limited to be qualitatively at the present time. The metal atoms appear to exist in different electronic states by different atomic surroundings in the crystals and hence the atoms possess more than one valence values.

In the third lab. of Materials Physics Div. we have a new informative knowledge about the binding nature in comtemplation as follows:

Firstly, the valence states of transition metals will be made clear by analyzing available atomic structural data; bond lengths and bond angles between metallic atoms and the neighboring oxygen. This study will be able to search new metal oxides having various valence states. Secondly, the atomic arrangement near the surface of metal oxides will be investigated using an XPS diffraction technique; XPS measurements for constituents of cleaving metal oxides inclined the angles against the direction of emitting photo-electrons. These XPS patterns in angular coordinate representation give definitive information about the local atomic arrangement such as atomic species on the cleavage plane and occupation probabilities of metal constitutents in atomic sites. Thirdly, the bond strength between metallic atoms and the oxygen will be measured by Fourier transform i.r. spectroscopy. This study gives information about the bond strength change accompanied with atomic or electronic transformation.

7 High Resolution Transmission Electron Microscopic Study for Interfaces of Materials

April 1990 to March 1993

S. Ikeda, Surface and Interface Division

Keywords: HRTEM, Y_2O_3, $Bi_2Sr_2CaCuO_y$, iodine intercalation, irradiation induced structural images

Structure images of materials are studied by means of a 400kV-type High Resolution Transmission Electron Microscope (HRTEM).

The HRTEM image of $Ia\bar{3}$ structure was first observed for a crystal of Y_2O_3. Y-atoms of Y_2O_3 are shifted by 0.035nm from the cationic position of CaF_2 structure. Using an electron microscope with a resolution of 0.17nm, structure images different from the CaF_2 type structure were obtained. A staggered configuration of the spotting image corresponding to the shifted Y-atoms was observed for the (110) plane. Positions of oxygen vacancy chains in the (111) image could be detected from the shifts of Y-atom columns caused by the presence of oxygen vacancy chain.

Anisotropic bindings in the micaceous like structure of $Bi_2Sr_2CaCuO_y$ and more particularly the existence of van der Waals couplings in the Bi_2O_2 layers allow this material to be intercalated. To analyze the effect of intercalation on the crystal structure, a slightly deficient iodine intercalated superconducting oxide $I_{0.9}Bi_2$ $Sr_2CaCu_2O_y$ has been studied by HRTEM. Iodine atoms are located between the Bi-O planes. Upon intercalation, one of the two perovskite-like blocks of a unit cell shifts by $^1/_2$ *a* and the ...ABA... stacking to ...AAA... Lattice imperfections associated with iodine deficiency and in particular, boundaries between intercalated and host material domains have been analyzed. The host material can accommodate upon intercalation, global distortions of 1.7A along the *c*-axis of the unit cell and 1.35A in the perpendicular plane, on a scale of 5 atomic distances.

Ion irradiation enhances the irreversibility fields and increases the values of the intragrain Jc of the superconducting material. Irradiation induced structural damages in $Bi_2Sr_2CaCu_2O_8$ of 15μm thick have been observed by HRTEM. Highly damaged areas consist of long continuous cylindrical columns which vary from 2 to 8nm in diameter.

Related Papers

Structure Images of Y_2O_3 corresponding to the Shift of Y-atoms, Ikeda, S. and Ogawa, K. J. Electron Microsc 41 (1992): 330.

HREM Study of Iodine Intercalated $IBi_2Sr_2CaCu_2O_8$, Chenevier, B., Ikeda, S. and Kadowaki, K. Physica C 185–89 (1991): 643.

High Resolution Electron Microscopy Observation of Defects in 180Mev Cu^{11+} Ion Irradiated $Bi_2Sr_2CaCu_2O_8$ Crystals, Chenevier, B., Ikeda, S., Kumakura, H., Togano, K., Okayasu, S. and Kazumasa, Y. Jpn. J. Appl. Phys. 31 (1992): L777.

8 Structure and Electronic Properties of Low-dimensional Transition Metal Compounds

April 1990 to March 1992

M. Okochi, Materials Physics Division

Keywords: transition metal chalcogenides, X-ray photoelectron spectroscopy, Madelung potential, Fourier transform i.r. spectroscopy, niobium oxides

In the course of pursuing our studies concerning the above subject, we have found the following:

1. An empirical formula, m/n=6/k (k=1,2, ...*n*), for transition metal chalcogenides T_mX_n, was found by analyzing a lot of available thermodynamic data; we stress that this formula is useful not only for predicting the stoichiometry of binary systems but also as a guide line into synthesizing ternal chalcogenide compounds such as Ti_2VS_2, TiV_2S, TiVS, and $TiVS_4$, etc.
2. Using X-ray photoelectron spectroscopy (XPS), the electronic structures of superconducting $YBa_2Cu_4O_8$ and $YBa_2Cu_3O_{6.9}$ oxides were investigated in detail. No appreciable difference was observed between Cu2p spectra of $YBa_2Cu_4O_8$ and $YBa_2Cu_3O_{6.9}$.

   Based on a careful analysis of Ba3d and Y3p core-level spectra, we found that the size of the binding energy (BE) shift between Ba3d spectra of the above two oxides does coincide with the difference between the Madelung potentials at Ba site, which can be calculated in such a way

that the hole distribution is most stable in terms of the Madelung energy.

On the other hand, the BE shift in Y3p spectra was turned out to be negligible, indicating a relatively large covalency of Cu-O bonding as well as some relaxation effect caused by extra holes in the Cu-O plane.

3. By Fourier transform i.r. spectroscopy, the "phonon stiffening" was found to occur between the blue bronze $K_{0.3}MoO_3$ and the red bronze $K_{0.33}MoO_3$. We also found that hydrogen insertion in Pt-impregnated V_2O_5 leads to intensification of the O-H stretching vibration mode, and results in hydrogen-induced amorphization at a certain hydrogen concentration ($x>0.3$ in $H_xV_2O_5$) by a mechanism of bond arrangement; the Bragg reflections due to V_2O_5 became invisible at $x>0.3$.
4. The structures of transition metal oxides were analyzed in view of constituent polyhedra such as octahedron or tetrahedron which share corners and/or edges, to find a general rule controlling these structures. This study enabled us to predict new oxide phase(s) in niobium oxides of pentagonal column and titanium oxides of octahedra.

Phase transformation and microstructures

(9) Super-Microscopic Study on the Mechanism of Martensitic Transformation in Shape Memory Alloys

April 1992 to March 1995

S. Kajiwara, Physical Properties Division

Keywords: transformation, interface, structure image, shape memory

In order to elucidate the mechanism of martensitic transformation in shape memory alloys, the study on the interface between martensite and parent phase on a very fine microscopic scale is needed. In the present study, we attempt to observe the atomic arrangement on the interface by high resolution electron microscope. Namely, structure image near the interface is taken to know the coherency between two lattices. We try to find the difference of structure image between shape memory alloys and ordinary alloys. The alloys employed are Fe-based shape memory alloys, such as Fe-Ni-C, Fe-Ni-Ti-Co and Fe-Mn-Si-Cr-Ni, and, for comparison, well-known NiTi. The transformation systems in these alloys are f.c.c.→b.c.t., f.c.c.→h.c.p., b.c.c.→R-phase→h.c.p., respectively. In the case of f.c.c. to h.c.p. transformation, we also examine the disorder in the stacking sequence near the interface by the lattice imaging method.

[10] Mobilities of Austenite/Martensite Interface in Fe-based Shape Memory Alloys

April 1989 to March 1992

S. Kajiwara, Physical Properties Division

Keywords: shape memory alloy, mobility, interface

One of important characteristics in Fe-based shape memory alloys is the mobility of the austenite–martensite interface. In the last fiscal year, we examined the mobility of the interface in Fe-Ni-C alloys in detail. This year, the mobility of an Fe-14Mn-6Si-9Cr-5Ni shape memory alloy which is about to practical use has been mainly studied. Phase transformation associated with the shape memory effect in this alloy is f.c.c.→h.c.p. and the interface is parallel to $(111)_{fcc}$ plane.

The specimens were first austenitized at 1320K for 30 min and cold-rolled by 10% at room temperature, and then heated at 970K for 10 min. It is known that such thermomechanical treatment produces the best shape memory effect. The thickness of specimens was 0.4mm. After inducing martensite at room temperature by stretching the specimen, it was heated in a heating stage of the high temperature microscope and the movement of the interface was measured. It was found that the interface moved approximately at a linear speed which was nearly the same as those of the other Fe-based shape memory alloys. The reverse transformation behavior of martensite produced by simple cooling seemed to be unusual, namely, the surface relief of martensite becomes invisible without accompanying the interface movement and the reverse transformation is accomplished.

On another shape memory alloy, Fe-Ni-Co-Ti, the interface movement was also studied. In this case, the associated phase transformation is f.c.c.→b.c.t., and it was found that the interface moved rather jerky.

[11] Mechanism of Variant Selection in Stress Induced Transformation

April 1989 to March 1992

H. Miyaji, Advanced Materials Processing Division

Keywords: variant selection, martensitic transformation, constraint stress, texture

Twinning Shear model and Bain Strain model for the variant selection in martensitic transformation of ferrous alloys have recently been proposed. Both models are based on the point of view that such a variant is to be selected as the lattice deformation associated with the martensitic transformation is assisted more effectively by the external applied stress. However, these models are different from each other concerning the stages of lattice deformation processes to which the external applied stress affects in the martensitic transformation.

When the transformation occurs in solid phase, the constraint stress to prevent the deformation arises from the surrounding matrix phase, and

when the constraint stress is anisotropic (in thin sheet, for example), the occurrence of variant selection is pronounced in the transformation without external applied stress.

The authors have analyzed the characteristics of the constraint stress and proposed that the application of the constraint stress to some proper crystal system would clarify the variant selection mechanism; that is, by examining which variant is selected in tetragonal ($|\varepsilon_1| \approx |\varepsilon_2|$) martensitic transformation of a cubic texture γ sheet, the validity of the variant selection model will be tested.

To verify the above remarks, Fe-30 Ni alloy was prepared which having the Ms near the room temperature seemed to be suitable for the observation of structure changes before and after transformation. Then thin sheet of the alloy having cube texture containing 0.8% C was prepared by severe cold rolling (95%) and carburization at 900 °C for 50 h. Partially transformed tetragonal ($|\varepsilon_1| \approx |\varepsilon_2|$) martensitic phase was formed by subzero-quenching into liquid nitrogen. The textures of both phases were measured by conventional X-ray pole figure method. The results that support the Bain Strain model was obtained.

[12] Research on Shape Memory Thin Films for Microactuator

April 1991 to March 1992
A. Ishida, 3rd Research Group
Keywords: shape memory alloy, Ti-Ni alloy, thin film, sputtering, microactuator

Micromachines are expected to be use in various fields such as biotechnology, medicine, semiconductor industry. In order to achieve such a micromachine, the development of an effective microactuator is essential. In this study, we have developed shape memory thin films of Ti-Ni using sputtering method[1] and demonstrated their shape memory behavior[2), (3)]. One of the examples is shown in Figure 1. This film exhibited a good shape memory behavior, which was comparable to that of bulk Ti-Ni alloy. This result suggests that a thin film of Ti-Ni is a promising candidate for a microactuator.

Related Papers

Formation of Ti-Ni Shape Memory Films by Sputtered Method, Ishida, A., Takei, A. and Miyazaki, S. Proc. of Int. Conf. on Martensitic Transformations ICOMAT-92, California (1992).

Thin Shape Memory Film of Ti-Al Formed by Sputtering, Ishida, A., Takei, A. and Miyazaki, S. Proc. of Twelfth Int. Vacuum Cong. IVC12, Netherlands (1992).

Shape Memory Characteristic of Ti-Ni Thin Films Formed by Sputtering, Miyazaki, S., Ishida, A and Takei, A. Proc. of Int. Conf. on Martensitic Transformation ICOMAT-92, California (1992).

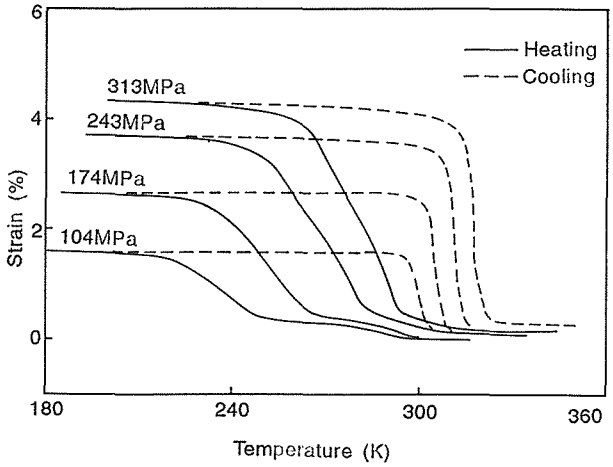

Fig. 1. Strain vs. temperature curves at constant loads for Ti-51.4at%Ni thin film

Surface and interface properties

(13) Disintegration Phenomena in Intermetallic Compounds

April 1992 to March 1995
K. Kawahara, Physical Properties Division
Keywords: manganese intermetallic compound, disintegration, pulverization

During the investigation on manganese-based alloys, we have found that a manganese intermetallic compound disintegrates spontaneously when exposed in air for a few days. Similar phenomena are known on tin, graphite crucibles, and some slags in steel making. In a manganese-aluminum compound containing carbon, the disintegration has been said to be due to the hydrolysis of an aluminum carbide. Although the detail mechanism is not clarified yet, it may be closely associated with a chemical reaction between the moisture in atmosphere and the phase dispersed in the bulk as well as exposed to the surface.

We are examining that such a disintegration occurs in what kinds of intermetallic compounds and conditions. As an example of application to the disintegration phenomena it is considered that hard materials difficult to grind can be pulverized without artificial operation.

14 Study on Changing the Properties of Metallic-Oxide Films for Increasing the Hydrogen Permeability

April 1991 to March 1994
M. Amano, Physical Properties Division
Keywords: oxide film, hydrogen penetration, reaction method, hydrogen separation

It is well known that oxide films on metals and alloys impede hydrogen penetration. The aim of this study is then to increase the hydrogen permeability of oxide films formed on metals and alloys based on V_a elements by changing the composition and structure of the films through a reaction method. The membrane of a V-15at% Ni-0.05at%Ti alloy, which was developed for hydrogen separation by our research group, was used as a substrate. Metal which has more affinity for oxygen than that of vanadium, such as yttrium, lanthanum, cerium, titanium or zirconium, was deposited on the alloy membrane, followed by further deposition of palladium over the metal layer by using an electron beam gun. The hydrogen permeability of the samples was determined by using a gas permeation method after annealing at 673K. It has been found that the deposition of lanthanum or yttrium markedly suppresses the hydrogen-trapping phenomenon below 473K only for the alloy membrane with palladium overlayer. The depth profile of Auger electron spectroscopy analysis for the oxide films revealed that the vanadium oxide was reduced and the oxide consisting mainly of lanthanum or yttrium was formed underneath the palladium overlayer.

15 Effect of Oxidation on Mechanical Degradation of Metallic Material at High Temperature

April 1991 to March 1994

Y. Ikeda, Failure Physics Division

Keywords: spalling, S segregation, Al_2O_3 coating, Y_2O_3, ODS alloy

In our previous work we proposed the model that the oxide scale spalling is promoted by S segregation at scale/alloy interface but suppressed through S trapping with REM (rare earth metal). The same model was successfully applied to Al_2O_3 coating film/alloy systems where the S segregation was suppressed by REM addition. Since it is well known that scale spalling is well suppressed by Y_2O_3 dispersion, as well as REM addition, we expected that spalling of Al_2O_3 coating film is also suppressed by Y_2O_3 dispersion. In this work surface segregation rate of S was measured with AES (Auger electron spectroscopy) on several ODS (oxide dispersion strengthened) alloys and the extent of spalling of Al_2O_3 coating film during thermal cycling was examined on them.

It was found that both S surface segregation and the spalling of coating film were well suppressed on ODS alloys. Although this result suggests strongly that S is trapped by dispersed oxide particles, there remains a question yet: while it is reasonable that a reactive element such as REM traps S to form a stable sulfide in alloy matrix, a stable oxide such as Y_2O_3 does not seem possible to turn into a sulfide or oxisulfide by S trapping. In order to confirm the S trapping by dispersed oxide particles, we measured S concentrations on the particles and in alloy matrix (MA956 alloy) with analytical electron microscope. The result showed that the S concentration was one to two orders of magnitude greater on the particles than the matrix. Thus, we consider that the dispersed particles absorb S by virtue of the high interfacial energy.

Related Papers

High Temperature Oxidation and Surface Segregation of S, Ikeda, Y., Nii, K. and Yoshihara, K. Proc. 3rd JIM Int. Symp. on High Temperature Corrosion of Metals and Alloys Suppl. to Trans. Jpn. Inst. Met. 24 (1983): 207–14.

Detrimental Effect of S Segregation to Adherence of Al_2O_3 Coating Layer on Stainless Steels and Superalloys, Ikeda, Y., Tosa, M., Yoshihara, K. and Nii, K. ISIJ Int. 29 (1989): 966–72.

16 Fabrication of Quantum Well Box Systems by Droplet Epitaxy for Advanced Optoelectronic Devices

April 1991 to March 1996

N. Koguchi, Surface and Interface Division

Keywords: quantum well boxes, molecular beam epitaxy, GaAs, InSb

Predictions of enhanced electron mobility and advanced semiconductor laser with high-monochromized and low threshold current density have been made for quantum well box systems. Recently, selective area metal organic vapor phases epitaxy for fabricating quantum well boxes was demonstrated. Molecular beam epitaxy is successful in growing finely layered structures and quantum well wires. But it has not yet been able to achieve comparable success in production of structure for quantum well boxes.

We have proposed a new MBE growth method termed Droplet Epitaxy for the fabrication of some III–V compound semiconductor quantum well boxes. This method is based on the V-column element incorporation into the III-column element droplets deposited on the inert substrate for the monolayer absorption of the III and V-column elements with a zinc-blend type surface structure. Some III–V compound surface terminated with a VI-column element like a S, Se or Te has reported for providing the inert surface for the foreign atom adhesion caused by the partially filled dangling bond at the surface. The surface of the VI-column element terminated III–V compound semiconductor is thought to be suitable for the growth of epitaxial microcrystals by Droplet Epitaxy.

We have demonstrated a three dimensional growths of GaAs epitaxial microcrystals on a Se-terminated GaAlAs substrate, InSb epitaxial microcrystals on a Te-terminated substrate and

InAs epitaxial microcrystals on a S-terminated InP substrate by Droplet Epitaxy. Numerous pyramidal shape epitaxial microcrystals were obtained on these VI-column element terminated substrate. Base size of each epitaxial microcrystals was about 30nm × 50nm and the standard deviation of the size distribution was about 10%. The growth of the microcrystals is caused by a Vapour-Liquid-Solid (VLS) mechanism.

[17] Compatibility of High Temperature Materials in Liquid Metals

April 1987 to March 1992
T. Suzuki, Mechanical Properties Division
Keywords: flowing sodium, corrosion, refluxing mercury

Corrosion in a flowing sodium

Long term behavior up to more than 8000h of austenitic and ferritic stainless steels in flowing sodium at 700 °C has been examined. The results are summarized as follows: (1) steady-state corrosion rates of austenitic steels are obtained after equilibrating dissolution of Fe, Ni and Cr into the sodium and diffusion of Ni and Cr in the steels during an initial corrosion period; (2) steady-state corrosion rates of ferritic steels are obtained after equilibrating dissolution of Cr and/or Fe, absorption of Cr and/or Ni, and diffusion of Ni and Cr in the steels during an initial corrosion period; (3) dissolution or absorption of carbon and nitrogen depending on chemical affinity and activity of carbide/nitride stabilizing elements in the steels, rapidly occurs during an early corrosion period, and; (4) differences in corrosion behavior among the steels become smaller with increasing corrosion period.

Corrosion in refluxing mercury

Long term behavior up to 5000h of Mo-base TZM alloy capsules (Mo-0.5Ti-0.08Zr-0.025C-0.025 oxygen in wt.%) and ceramic rods (ZrC, TaC, WC and SiC) exposed to refluxing mercury with a small amount of potassium has been examined. After heating the capsules and the rods at 600 °C, they were cut into pieces and distilled out the residual mercury. The inner surface of the capsules and the outer surface of the ceramic rods exposed to the refluxing mercury hardly showed corrosion. The solubility of Mo in mercury would be extremely small since no chemical reaction associated with non-metallic elements such as oxygen seemed to occur in the capsules.

Related Papers

Effect of Molybdenum Content on the Corrosion of 9Cr Ferritic Steels in a Flowing Sodium Environment, Mutoh, I. and Suzuki, T. J. Japan Inst. Metals 56 (1992): 794–801 (in Japanese).

Quasi-Equilibrium of Stainless Steel in a Non-Isothermal Sodium Loop Constructed of Type 316 Stainless Steel, Suzuki, T. and Mutoh, I. J. Nucl. Mat. 186 (1991): 20–26.

Corrosion of a Type 304 Stainless Steel and a Molybdenum-base TZM Alloy in Refluxing Mercury with a small amount of Potassium, Suzuki, T. and Mutoh, I. J. Nucl. Mat. 184 (1991): 81–87.

Mechanical properties

(18) Fatigue Behavior of Brittle Materials at Elevated Temperatures

April 1992 to March 1995
Y. Kawabe, Mechanical Properties Division
Keywords: cyclic fatigue, elevated temperatures, ceramics

The development of ceramics is being watched with knee interest, because they are very promising as structural components for engineering applications where metallic materials are not available. Since many of them are subjected to static or cyclic loading at elevated temperatures for prolonged periods, it is important to understand fatigue behavior at elevated temperatures. Nevertheless, there are very few studies on the cyclic fatigue behavior of ceramics at elevated temperatures.

In prior study, we had evaluated fatigue properties for various kinds of non-transforming ceramics at room temperature and suggested crack resisting-reactivating model as fatigue mechanisms. However, it is doubted if this mechanism is available at elevated temperatures. Recent studies have shown that cyclic loading has a beneficial effect at high temperature, compared to static loading. Such results are inexplicable by any fatigue mechanisms proposed at room temperature so far. Systematical investigation for various kinds of ceramics is, thus, required to understand the difference at room and high temperatures.

Oxidation, crack healing and viscous behavior of grain boundary glass phase are important factors affecting high temperature mechanical properties of ceramics. Moreover, for the ionic crystals such as Mg0, the effect of the motion of dislocations is important, because dislocations in them is mobile at high temperature. It is thought that they also affect high temperature fatigue behavior.

In this work, by taking into consideration the influence of the factors noted above, fatigue behavior in various kinds of ceramics will be investigated over extensive temperature range.

19 NRIM Fatigue Data Sheet Project (IV)

April 1990 to March 1994
S. Nishijima, Failure Physics Division

Keywords: fatigue, standard reference data, high strength steel, aluminum alloy, pressure vessel steel, heat-resisting alloy, on-line database

It is well known that the fatigue of metallic materials could be a cause of hazardous failure accident in machines and structures suffering fluctuating loads during use. This project is aiming at the establishment of standard reference data on the basic fatigue properties of Japanese engineering materials which are commonly used for those machines and structures.

The work has been conducted since 1975 under successive five-year-term programs for ease of periodical reviews. In the present term IV, the accent is put on the ambient properties of high strength steels and aluminum alloys, intermediate temperature properties of steels for pressure vessels, and high-temperature time-dependent properties of heat-resisting alloys. Table give a brief summary of NRIM Fatigue Data Sheets.

Series of more basic researches have been performed in parallel to understand the materials behavior and mechanisms of degradation under fatigue. Some of the latest concerns are: mode I–II transition of fracture in aluminum alloys, quantitative analysis of the effect of non-metallic inclusions in high-strength steels, effect of strain aging on cyclic properties of steels at intermediate temperatures, prediction of long-term creep-fatigue life at elevated temperatures, and so forth.

The output data thus validated by the basic researches have been published and exchanged worldwide with scientific and technical organizations. An on-line data service is currently available through Japan Information Center of Science and Technology. It is anticipated that the NRIM Fatigue Data Sheet Project contributes to the safer and more efficient use of engineering materials.

Summary of NRIM Fatigue Data Sheets, 1992

Subthemes and Items Investigated		Nos. Issued
<Machine Structural Material>		
High/Low Cycle Properties on:	Carbon and Low Alloy Steels, Stainless Steels, Carburizing Steels, Spring Steels, Tool Steels, and Aluminium Alloys	29
<Welded Joints>		
High/Low Cycle and Crack Growth Properties, looking at the effect of:	Specimen Dimensions, Welding Procedures, Stress Ratios, and Weld/HAZ Materials for Steels, and Welding in Aluminium Alloys, as well	20
<Elevated Temperature>		
Properties of Carbon and Low Alloy Steels, Stainless Steels and Heat Resisting Alloys for Regimes:	High/Low Cycle, Time Dependent Low Cycle, and Frequency Dependent Intermediate Temperatures	19

Related Papers

Effect of Inclusions on Fatigue Properties of High Strength Steels, Kanazawa, K. and Abe, T. Impact of Improved Material Quality on Properties, Product Performance and Design ASME MD-28 (1991): 139–50.

Fatigue Properties of Butt-Welded Joints for 5083-O Aluminum Alloy, Hirukawa, H., Matsuoka, S., Takeuchi, E. and Nishijima, S. Trans, Japan Soc. Mech. Eng. 58A (1992): 549.

Fatigue Strength of Butt Welded Al-Mg Alluminum Alloy: Tests with Maximum Stress at Yield Strength, Ohta, A. and Mawari, T. Fatigue Fracture Engng Mat Struct. 13 (1990): 53–58.

Creep-fatigue of 1Cr-Mo-V Steels under Simulated Cyclic Thermal Stresses, Yamaguchi, K., Ijima, K., Kobayashi, K. and Nishijima, S. ISIJ Int. 31 (1991): 1001–6.

20 Controlling and Recovering High Temperature Damage

April 1991 to March 1994

N. Shinya, Failure Physics Division

Keywords: grain boundary cavities, sintering, self-recovering, life extension

Low ductile fracture of metals after long term high temperature creep results from the progressive accumulation of grain boundary cavities throughout the creep process. Therefore, technologies for controlling and recovering the cavities are important for the development of reliable heat resisting alloys and also for the maintenance of high temperature components. In this work, a sintering mechanism and a self-recovering mechanism of the cavities are being studied, and a life extending system, based on control of the cavities, is being developed.

Sintering of grain boundary cavities

Sintering heat treatments have been undertaken in atmospheric pressure and hydrostatic pressure under compressive load to remove grain boundary cavities within a 1.3Mn-0.5Mo-0.5Ni steel following creep tests. High sensitive density measurements and microscopic metallography have been used to monitor the progressive sintering of the cavities. Experimental sintering rates were much slower than those predicted by diffusion control and coincided with those calculated by constrained diffusion control. This suggests that sintering rates depend on a relaxation process for the constraint imposed by an inhomogenious distribution of the cavities.

Self-recovering of grain boundary cavities

In a previous work it was confirmed that a BN compound is formed at the cavity surface during creep in austenitic stainless steels. Shielding by a stable compound like BN at the cavity surface is expected to suppress the surface diffusion and the cavity growth remarkably. Accordingly the precipitation of BN at the surface may provide a kind of self-recovering function to heat resisting alloys.

Extension of creep life

A rejuvenation investigation for providing a prolonged creep life is being aimed at eliminating grain boundary cavities. Effective sintering treatments were proposed and also a metallurgical technique for the prevention of surface cracks, which cannot be recovered, was developed in previous works. Using these techniques, a life extending systems for high temperature components is being developed.

21 Tensile Fracture Mechanism for Long Ceramic Fibers

April 1990 to March 1993

C. Masuda, Failure Physics Division

Keywords: tensile strength, boron fibers, fracture mechanism, silicon carbide fiber with coating, silicon carbide fiber without coating

Several kinds of long ceramic fibers are used for reinforced materials in several composites such as plastic, metal, and ceramic matrix composites. The tensile strengths of those composites are strongly influenced by the strength of the reinforcement. In order to obtain basic data of the strength for monofilament, tensile tests were performed with boron fibers in relation to the probability and with fracture mechanism. Last year the tensile strength and fracture mechanism were examined for boron fibers fabricated by two different companies.

This year two types of silicon carbide fibers were examined. One was silicon carbide fiber coated by carbon with thickness of about 3μm, and the other was silicon carbide fiber without coating. The silicon carbide fibers were about 140μm in diameter. The average tensile strength of silicon carbide fiber without coating was lower than that for silicon carbide fiber with coating. Moreover, the scatter of the tensile strength for the former was also larger than that for the latter.

On the fracture surfaces, many types of fracture origins were pointed out. For silicon carbide fiber without coating, fracture origins were observed in the core fiber, at the interface between core carbon fiber and silicon carbide fiber as well as the surface. On the other hand, for silicon carbide fiber with coating the fracture origin was seen either in the core carbon fiber or at the interface between the core carbon fiber and silicon carbide fiber. Other origins were also found near the specimen surface at the interface between the carbon coating and silicon carbide fiber. The mirror zone observed on the fracture surface of silicon carbide fiber was not so clear in comparison to that for boron fibers reported on the paper.

Related Papers

Tensile Fracture Surface for Boron Fiber, Tanaka, Y. and Masuda, C. J. Soc. Mat. Sci. Jap. 40 (1991): 869.

22 NRIM Creep Data Sheets (IV)

April 1991 to March 1995

C. Tanaka, Environmental Performance Division

Keywords: NRIM creep data sheets, heat-resistant metallic materials, long-term creep and rupture tests

The objective of this program is to obtain 10^5h creep and rupture strength data of heat-resistant metallic materials in long-term creep and rupture tests, to publish the data obtained as NRIM Creep Data Sheets, to investigate long-term creep deformation behaviour and creep rupture properties of these materials, and to develop an evaluation method of long-term creep and rupture strength at high temperature. These activities are expected to contribute to ensuring safety and reliability of structural components of high temperature plants and developing new materials.

This program was started in 1966 and is still continuing in order to obtain further long-time creep testing data of domestic steels and alloys. In the program IV which was started in last year, the tubes and plates of mod. 9Cr-1Mo and 9Cr-2Mo steels and the plates of low-carbon and medium-nitrogen 316 austenitic stainless steel were added as the testing materials. The short-time data have been already obtained for a part of these new materials.

Long-term creep and rupture strength of steels and alloys at high temperature are investigated using the data and the ruptured specimens which were obtained from the NRIM Creep Data Sheets program. The main subjects investigated are as follows: (1) the creep deformation behaviour of 1.3Mn-0.5Mo-0.5Ni steel was evaluated using a modified θ projection concept, and the heat-to-heat variation of the parameters which were obtained from this analysis was studied from the viewpoint of microstructure; (2) it was found out from the long-term data in NRIM Creep Data Sheets that the long-term creep strength of ferritic heat resistant steels was almost the same. It was thought that the creep strength at higher temperatures and lower stresses was reduced by the microstructural change and approached to an inherent value, and;

(3) the creep rupture strength of austenitic steels and Ni-base superalloys was studied in relation to microstructural change and creep damage formation, and so on.

Related Papers

Fundamental Properties of Long-Term Creep Strength for Ferritic Heat Resistant Steels, Kimura, K., Kushima, H., Yagi, K. and Tanaka, C. Tetsu-to-Hagane 77 (1991): 667–74 (in Japanese).

Evaluation of Creep Deformation and Rupture Life of 1.3Mn-0.5Mo-0.5Ni Steel by Modified θ Projection Method, Kushima, H., Watanabe, T., Yagi, K. and Maruyama, K. Report of 123rd Com. on Heat-Resisting Metals and Alloys, JSPS 32 (1991): 189–200 (in Japanese).

Life Prediction by the Iso-stress Method of Boiler Tubes after Prolonged Service, Kanemaru, O., Shimizu, M., Ohba, T., Yagi, K., Kato, Y. and Hattori, K. Int. J. Pres. Ves. & Piping 48 (1991): 167–82.

23 Effect of Surface Film on Deformation of Bulk Matrix Material

April 1991 to March 1994

K. Kanazawa, Environmental Performance Division

Keywords: fatigue crack initiation, dynamic ultra micro hardness tester

A surface crack is not easy to initiate under high-temperature, high-cycle fatigue in air environment, as films at the specimen surface prevent dislocations from slipping off from the surface. This project aims at studying the effect of surface films on deformation of bulk matrix material to evaluate the resistance of surface films to fatigue crack initiation from the surface.

As an example of surface films, oxide film formed on a matrix surface of low alloy steel has been examined. Hardness of oxide film and its thickness are measured by using a dynamic ultra micro hardness tester. The hardness is higher than that of the matrix. Effect of hard oxide film on deformation of bulk matrix is studied analytically by FEM method.

24 Evaluation of Crack Initiation and Growth of Superalloys under Creep and Creep-Fatigue Conditions

April 1991 to March 1993

K. Yagi, Environmental Performance Division

Keywords: creep crack growth, creep-fatigue crack initiation and growth and superalloys

An understanding of crack initiation and growth behaviour under creep and creep-fatigue loading conditions is one of the most important subjects in ensuring the reliability of high temperature structural components. In this study, the crack initiation and growth behaviour of superalloys under creep and creep-fatigue loadings is being investigated by taking the micro fracture mechanism into account.

1. Creep crack growth behaviour of Ni-base superalloys

   The creep and rupture properties of the testing material, which would be needed to evaluate the creep crack growth rate, were obtained from the creep tests. For Ni-base superalloy, complicated microstructural changes were observed in the specimens ruptured. The creep crack growth tests will be conducted at 900 and 1000 °C and creep crack growth behaviour will be investigated in detail from the viewpoint of microstructure and micro fracture mode.
2. Creep-fatigue crack initiation and growth behaviour of Fe-based superalloy

   The crack initiation and growth behaviour of NCF 800H alloy under creep-fatigue loading condition is being investigated. For this alloy, the wedge-type cracking was observed in the specimen ruptured. It is expected from this study that the creep-fatigue interaction under the creep damage mode condition corresponding to wedge-type cracking will be clarified.

Related Papers

Creep Crack Growth Behaviour in High Temperature Structural Steel and Alloys, Tabuchi, M. and Yagi, K. Mechanical Behaviour of Materials–VI Vol. 4 Jono, M. and Inoue, T., eds., Pergamon Press, New York (1991): 571–76.

Effect of Grain Size on Rupture Life under Creep-fatigue Loading for 321 Stainless Steel, Yagi, K., Kubo, K., Kanemaru, O. and Tanaka, C. Mechanical Behaviour of Materials–VI Vol. 4 Jono, M. and Inoue, T., eds., Pergamon Press, New York (1991): 583–88.

25 Real Time Evaluation of Fatigue Damage during Crack Propagation under Random Loadings

April 1991 to March 1994

A. Ohta, Environmental Performance Division

Keywords: fatigue crack propagation, random loading, fatigue threshold

The fatigue crack propagation properties of several metals are investigated on a crack closure free conditions by holding the maximum load during cycling. The propagation properties are tried to compare with da/dn and $\Delta K/E$, where da/dn is the fatigue crack propagation rate, ΔK is the range of stress intensity factor and E is the Young's modulus. The crack opening displacement, δ, is monitored during the whole period of random loading blocks by means of optical type displacement gage and personal computers. The

equivalent value of crack opening displacement is also calculated as $(\Sigma n_i \cdot \delta_i^m)^{1/m}$ ignoring the cycling below the fatigue threshold.

Related Papers

Effect of Young's Modulus on Basic Crack Propagation Properties near Fatigue Threshold, Ohta, A., Suzuki, N. and Mawari, T. Int. J. Fatigue 14 (1992): 224–26.

Fatigue Crack Propagation in Tensile Stress Field under Two-Step Programmed Test, Ohta, A., McEvily, A.J. and Suzuki, N. (in pression).

26 Mechanism of Fretting Fatigue Failure in Composite and Surface Modified Materials

April 1991 to March 1994

M. Sumita, Mechanical Properties Division

Keywords: fretting fatigue failure mechanism, metal matrix composite, surface modified metallic material

Fretting damage is known to have a detrimental effect on fatigue behavior of structural materials. Many factors control the fretting fatigue. This research was planned aiming a fundamental understanding of the mechanism of fretting fatigue failure from a microstructural viewpoint for metal matrix composites and surface modified metallic materials.

An important factor which influences fretting fatigue strength is a frictional stress between the specimen and the pad. According to the hypothesis on the adhesive force on the contact area, the friction coefficient is expressed as the ratio of the shearing force on the contact area to the hardness. If this is not denied, the friction coefficient is microstructurally controlled and is expected to be decreased. Another important factor is the behaviour of stick region on the contact area. We found that the fretting fatigue life exhibited a minimum at low contact pressure and a maximum at intermediate contact pressure. This phenomenon was made clear in terms of stress concentration at the fretted area. Cracks are initiated at the boundary between the stick region and the slip region on the contact area. The behavior of the stick region also seems to be microstructurally controllable.

In order to improve fretting fatigue strength according to the above idea, the structures of the materials used have to be consisted of hard phases and soft phases or of hard layers and soft layers. In addition, the design to optimize the volume fraction, the size and the shape of each phase, and the thickness and the number of layers are involved.

Using these materials, friction coefficient, the size of stick region, the roughness of contact area, the number of fretting cycles to cause the saturation of damage, and fretting fatigue life are measured.

Related Papers

Effect of Contact Pressure on Fretting Fatigue of High Strength Steel and Titanium Alloy, Nakazawa, K., Sumita, M. and Maruyama, N. ASTM STP 1159 (1992): 115–25.

27 Fatigue Crack Initiation Process in Corrosive Environment

April 1991 to March 1994

R. Hamano, Mechanical Properties Division

Keywords: corrosion fatigue, pre-crack deformation, early fatigue crack growth, high strength, slip localization

Fatigue lives of structural materials extremely decrease in corrosive environments, compared with in laboratory air. The decrease in lives has been explained by (a) the formation of stress concentration sites such as corrosion pitts, (b) the preferential corrosion of slip bands, and (c) the mechanical rupture of film exposed to the corrosive environments. However, we have no definite mechanisms that the corrosive environments play an important role on the crack initiation or crack propagation process of fatigue. Therefore, we must investigate the environmentally-assisted fatigue damages in the processes such as (a) pre-crack cyclic deformation, (b) microcrack initiation with its early propagation, and (c) long crack growth.

In the present study, the emphasis is put on the processes of pre-crack cyclic deformation and early crack propagation of high strength materials.

The fatigue crack initiation process was observed in a 3.5% NaCl aqueous solution under cathodic polarization of −1.1V(Ag/AgCl reference electrode), using notched specimen of high strength steel of SNCM 439. A load ratio of 0.1 and a sinusoidal wave of a frequency of 1.0Hz were employed. In laboratory air, fatigue cracks initially nucleated at 45 degrees to the notch root surface and propagated along slip line directions, i.e., maximum shear stress directions. But, fatigue cracks easily deviated from maximum shear stress to maximum tensile stress direction in a 3.5% NaCl aqueous solution, compared with in laboratory air. These fatigue crack behavior was reversible. That is, the fatigue crack again propagated along maximum shear stress by the change of the test environments from a NaCl aqueous solution to laboratory air. It is suggested that the environment has an effect on pre-crack cyclic deformation and crack nucleation processes.

28 Crystal Growth on the Surface of Intermetallic Compounds

April 1990 to March 1992

T. Hirano, Chemical Processing Division

Keywords: interface materials, disilicides, crystal growth

The goal of this study is to develop new interface materials. Metal disilicides exhibit clean and flat surfaces by cleaving. We focus on the crystal growth and chemical reaction of metal overlayers on the clean cleaved single-crystals of $CoSi_2$ and $CaSi_2$. These disilicides provide a characteristic surface structure by cleaving. The experimental equipments in use are floating zone furnace by infrared heating, X-ray photoemission spectroscopy, and Auger electron spectroscopy.

We have grown single crystals of many metal disilicides from IIa group through VIII group in the periodic table. It is found that $CoSi_2$ and $CaSi_2$ exhibit a different surface structure by cleaving. It is considered that the crystal growth of the metal overlayer is affected by the surface structure. We presently examine the crystal growth and chemical reactions of the metal overlayer on the disilicide surface by the surface sensitive analyses mentioned above.

Related Papers

Single-crystalline Growth and Electrical Properties of $CaSi_2$, Hirano, T. J. Less-Common Metals 167 (1991): 329–37.

Surface Analysis of Cleaved Single-crystalline $CaSi_2$ by Auger Electron Spectroscopy, Hirano, T. and Fujiwara, J. Phys. Rev. B 43 (1991): 7442–47.

[29] Mechanism of Mechanical Damage Accumulation in Brittle Materials

April 1989 to March 1992

S. Horibe, Mechanical Properties Division

Keywords: crack propagation, cyclic loading, indentation fatigue

Mode I Fatigue

Crack propagation under cyclic loading was investigated in non-transforming ceramic materials, such as silicon carbide, silicon nitride and sialon, with different microstructures produced by various processes. Cyclic fatigue crack growth was observed in the intergranular-fracture type materials and was never seen in the transgranular-fracture type ones, irrespectively of materials. The occurrence of intergranular cracking causes (i) microscale-crack branching or crack path deflection, (ii) grain-particles debonding from the matrix and (iii) production of crack surface-asperities. These have actually been observed in this study. On the basis of these observations, the most possible fatigue mechanism for the non-transforming ceramics has been proposed. The mechanism was based on the consideration that the crack resistance caused by microcrack branching or crack-path deflection during tensile loading and the crack reactivation due to the asperity-contacts during unloading occur repeatedly. These processes resulted in continuous crack growth under cyclic loading conditions.

Indentation Fatigue

Indentation fatigue in various ceramics was studied in terms of grain size, fracture appearance and ionic/covalent bonding characteristics. It has been found that there are two types of indentation fatigue behavior (Type I and Type II). Type I was characterized by slight increase of damaged zone size with increasing in number of indentation cycles, followed by the abrupt chipping of a part of surface layer. Such a Type I behavior was observed in silicon carbide, silicon nitride and sialon, which was considered to be caused by the continuous growth of lateral crack with indentation cycles. On the other hand, Type II behavior, which was seen in magnesium oxide and aluminum oxide, was characterized by pronounced enlargement of indentation-induced damaged zone in early cycles. It was assumed that this type of behavior was associated with plasticity and microcracking characteristics of materials.

Related Papers

Cyclic Fatigue of Ceramic Materials: Influence of Crack Path and Fatigue Mechanisms, Horibe, S. and Hirahara, R. Acta Metall. 39 (1991): 1309–17.

Damage Accumulation Caused by Cyclic Indentation in Ceramic Materials, Takakura, E. and Horibe, S. Proc. of 6th Int. Conf. on Mechanical Behavior of Materials Kyoto, 1991: 365–70.

Measurement and evaluation

(30) Study on Detection and Evaluation of Radiation Damages in Extreme Particle Fields

April 1992 to March 1998

N. Kishimoto, Materials Characterization Division

Keywords: combined effect of ion and photon, extreme particle field, in-situ dynamical measurements, low-temperature irradiation devices

Extreme physical conditions, such as high electric/magnetic fields and low/high temperatures etc, have been extensively applied to emphasize elementary processes in solids and also to explore novel properties of materials. As is well-known, both charged particle and photon exert strong interactions with material, and each of them has contrastive effects on the material, concerning momentum, energy, excitation modes etc. The combined effect of ion and photon is an important aspect for materials in environments of high energy devices, such as fusion reactors, MHD generators etc, but the complex effects arising from their coexistence have not been revealed, especially in the case of high particle energies. Consequently, we have focused on the strong interactions of the

combined particle environment, and have introduced a concept of "Extreme Particle Field."

A main purpose of this research program is to detect and evaluate non-equilibrium and nonlinear processes of materials in the extreme particle fields, associated with radiation damages. Technical features of this program are development of precisely-controlled condensed particle fields, in-situ dynamical measurements and their integration to a material evaluation system.

This project has just been inaugurated from April 1992 as one of basic researches of atomic energy. Prior to development of the extreme particle fields, in-situ detection techniques are now being investigated, aiming at dynamical observation of damage states generated by high-energy ions alone. To evaluate the basic electronic states and their relaxation processes, low-temperature irradiation devices to detect charge transport phenomena and photoconductivity are installed into a light-ion accelerator system (NRIM cyclotron BC1710). Specimens of crystalline and amorphous silicon are being investigated as reference materials. After the technical problems, including precise/remote measurement under high radiation field, are solved on the spot, production of the extreme particle field will be attempted in the next step.

(31) Development of Advanced Technologies for X-ray Microtomography

April 1992 to March 1995

Y. Yamauchi, Materials Characterization Division

Keywords: CT, tomography, microtomography, X-ray, three-dimension

Techniques of X-ray computerized tomography have been widely utilized in the applications for relatively large objects, such as in medical diagnostics of human bodies or in industrial inspection of manufactured components. In those applications the required spatial resolution is usually in the order of 1mm or 0.1mm at most and is limited by the number of pixels of the image. The effective number of pixels is circumscribed by the dynamic range of detected X-ray signal or the steepness of X-ray absorption. Further a mass of data storage and computational power have to be considered. However, if it is allowed to restrict the size of objects fairly small, the constraints would be alleviated. The limited number of pixels may not affect the pixel size nor the resolution of image. Based on this idea, we will develop the X-ray microtomography device.

The nondestructive characteristics of the X-ray tomography afford another important feature, i.e., three-dimensional image which is created from multi-sliced tomographies taken in a fine pitch along to the rotational axis. The three-dimensional image provides us overall information of an object. Since in the conventional microscopy, observation is made on a certain cross-section, there always remains ambiguity whether the sample is cut in the right plane containing any inherent information.

In the previous project, high resolution tomographies of a small object were accomplished with the parallel beam projection using a conventional point X-ray source. Then we extended the function of the device to three-dimensional. In this project we will study advanced technologies which improve the spacial resolution of tomographs and which provide another function to analyze chemical composition.

(32) Evaluation of Metallurgical Structure with a Fuzzy Logic

April 1992 to March 1995

M. Fukamachi, Materials Characterization Division

Keywords: computer-image analysis, fuzzy logic, electron microscopy, distribution of chemical elements on metallurgical structures

In order to carry out an accurate and rapid computer-image analysis of metallurgical structures, the feasibility of an application of fuzzy logic to a computer-image simulation has been studied. Fine metallurgical structures can be revealed with the electron microscopy. Usually, the numerical computer-image simulation is necessary to analyze and to evaluate the fine metallurgical structures. It is difficult to give accurate numerical values to many parameters which characterize the geometry of electron microscope and the operating conditions to obtain a satisfactory image simulation.

The method to simulate microscope images of the secondary and the reflected electrons has been studied with an application of fuzzy logic. Only two parameters are used in the image simulation. These are the parameters to represent the amount of generation of the signal electrons and the efficiency of detector to collect the electrons. With this method, the distribution of chemical elements on metallurgical structures can be obtained rapidly by separating the image contrast caused by the local distribution of chemical elements from that of the geometry of specimen surface.

(33) Atomic Scale Evaluation of Material Damage in Aqueous Solution

April 1992 to March 1994

H. Masuda, Failure Physics Division

Keywords: in-situ observation, STM, corrosion, electrodeposition, subtraction of STM images

In-situ observation was done by the scanning tunneling microscopy (STM) to study the corrosion behavior of steels in 1% NaCl and 0.1% HNO_3 aqueous solution and the electrodeposition behavior of copper on gold electrode in 0.1 M

$CuSO_4$ + 0.6% H_2SO_4 aqueous solution.

Both corrosion and electrodeposition rates were estimated by the subtraction of STM images. The average chemical reaction rates obtained by the STM were well coincident with those calculated from Faraday's conversion of current density, while the local reaction rates were more than 3 times bigger than the average reaction rates. The local chemical reaction rate can be estimated by STM.

㉞ Quantitative Evaluation of Fracture in Materials for Casks

April 1992 to March 1994

T. Yasunaka, Environmental Performance Division

Keywords: dynamic elastic-plastic fracture toughness, low temperature embrittlement, carbon steel, nodular cast iron

A shipping containers (casks) for radioactive materials might be subjected to impact loading at low temperature. Even such is the case, the integrity of casks must be ensured. For the materials which have low temperature embrittlement, therefore, it is necessary to evaluate brittle fracture on the basis of fracture mechanics.

In this study, a carbon steel and a nodular cast iron for casks are used. Dynamic elastic-plastic fracture toughness is measured. The objective of this study is to develop the more precise evaluation method for the integrity of casks against impact loading.

For the carbon steel, fracture toughness values in the ductile-brittle transition range scatter largely. In view of this large amount of scatter, fracture toughness in the transition range is studied.

For the nodular cast iron, on the other hand, the scatter of fracture toughness values in the transition range is relatively small because of finely dispersed graphite nodules. The quantitative evaluation of ductile and brittle fracture is studied with regard to temperature and strain rate which correspond to those under accident loading conditions.

It is desirable to evaluate nodular cast iron casks by small specimens taken from suitable locations owing to inhomogeneous microstructure. The estimation of fracture toughness using small bend specimens is attempted for the modular cast iron.

35 Vaporization and Ionization by Arc Plasmas

April 1991 to March 1993

A. Okada, Advanced Materials Processing Division

Keywords: vaporization, GTA, anodic spot, energy balance, mixed gas

Vaporization from anode spots

The vaporization behavior at the molten pool in a GTA weld can be classified into two types. In the first mode, vaporization takes place from a wide region on the molten metal surface, while in the second vaporization is restricted to the anodic spot. These phenomena are discussed on the basis of measurements of the current distribution on the molten pool.

A measurement method is being developed to measure the current and movement of the anode spot, on the basis of an experimentally observed anode spot diameter of approx. 1mm, moving on a weld pool of diameter 10mm. The spot current and the spot movement are obtained by measuring the amplitude of a voltage difference between two points in the base plate caused by the movement of the anodic spot.

It is concluded that the anodic spot current is influenced by the gross arc current and the ionization potentials of the base metal elements in the weld pool.

Energy Balance in Argon-Helium Arcs

The energy balance in argon-helium mixed gas arcs was investigated using calorimetry, radiative calorimetry and Langmuir probes. Calorimetric experiments on argon-helium mixed gas arcs showed that the heat transfer efficiency to the anode is maximum at a helium content of about 80%, and that heat losses are minimal at this gas composition. Combination with the results of the radiation measurements leads to the conclusion that this is caused by the decrease in radiative losses and the increase in the convective and conductive heat losses with increasing helium content.

From the results of the Langmuir probe experiments it was concluded that the anode voltage drop is little affected by the addition of helium to the argon shielding gas. Most of the rise in the arc voltage is due to processes near the cathode. The anode voltage drop and cathode voltage drop are believed to change significantly only when pure helium is used as a shielding gas.

Related Papers

Anodic Spot Current on Molten Pool in Stationary GTA Welding, Okada, A. and Nakamura, H. Quarterly J. Japan Weld. Soc. (in Japanese) to be published.

Evaluation of Local Plasma Composition and Temperature in GTA Plasma Column by Light Spectroscope, Hiraoka, K. Quarterly J. Japan Weld. Soc. (in Japanese) to be published.

36 Characterization of Metals and Alloys Using Synchrotron Radiation

April 1990 to March 1993

T. Saito, Materials Characterization Division

Keywords: synchrotron radiation (SR), near-surface analysis, laboratory XAFS, computed tomography, parallel-beam diffractometer

Use of Synchrotron radiation (SR) as a powerful research tool in materials characterization has grown tremendously in recent years. In the present program, from a view point of materials charactertization, new analytical techniques and apparatuses as well as their practical applications have been extensively studied.

1. Near-surface analysis using grazing incidence X-ray experiments:
   Grazing incidence X-ray techniques have been often used for near-surface study of materials and characterization of thin films. In the present study, a novel technique to determine each layer thickness of multi-layered thin films has been developed using interference oscillation observed in X-ray total external reflection. It was found that the peak positions given by Fourier transform are in good agreement with the layer thicknesses, and are determined independently from the surface/interface roughness.
2. Development of laboratory XAFS facilities and the structural study of alloys:
   The labo-XAFS is essentially important for the daily materials evaluation, and is considered to be complementary with SR based XAFS experiments. In this study a 60 kW super high power X-ray source has been employed and modified for XAFS experiments. A linear spectrometer with a curved monochromator as well as a mirror/multilayer was equipped. Practical materials such as mechanically alloyed powders have been analyzed as well. Immissible systems, which are not expected to form alloys, were studied by observing the atomic structure change. During the present study, the evidence for amorphization of Cu-Ta system was first observed.
3. Evaluation of structure and defects by X-ray computed tomography:
   In order to analyze the structure, defects, and fracture process of metal matrix composites and ceramic matrix composites during the tensile test, the nondestructive evaluation was carried out by X-ray computed tomography using SR. A tensile testing machine was fabricated to observe the inner defects and fractured fibers in composites under in-situ condition. The ability of the machine was checked and cross sectional CT images could be constructed.
4. Crystallographic analysis of superalloys by applying SR parallel-beam diffractometry:
   An SR parallel-beam diffractometer with a long parallel slit was developed to characterize Ni-base single crystal superalloys. These superalloys have γ' precipitates of an ordered FCC phase, based on Ni_3Al, in γ matrix of a disordered FCC one. Many reflections in the patterns were usually in clusters of overlapping peaks because of the very small difference in the lattice parameters of both phases. The measured data having a simple pseudo-Voigt profile shape was the highest quality to determine the lattice misfits and lattice strains of γ' precipitates in the superalloys in peak analysis, such as profile fitting and deconvolution to remove instrumental broadening of profiles.

Related Papers

Fourier Analysis of Interference Structure in X-ray Specular Reflection from Thin Films, Sakurai, K. and Iida, A. Jpn. J. Appl. Phys. 31 (1992): L113.

Observation of Solid-State Amorphization in the Immiscible System Cu-Ta, Sakurai, K. et al. Appl. Phys. Lett. 57 (1990): 2660.

Solid State Amorphization in the Cu-Ta Alloy System, Sakurai, K. et al. Mater. Sci. Eng. A134 (1991): 1414.

Determination of Lattice Parameter and Strain of γ' Phases in Nickel-Base Superalloys by SR Parallel-beam Diffractometry, Ohno, K. et al. Adv. in X-ray Anal. 34 (1991): 493.

37 Characterization and Control of Elementary Functions of Materials in the Localized Fine Area

April 1989 to March 1993
K. Furuya, Materials Characterization Division
Keywords: Focused Ion Beam (FIB), TEM, micro-lithography, in-situ analysis, cathodoluminescence spectroscopy, GaAs, low temperature

Bulk functions of materials are controlled by the physical and chemical properties in localized fine area ranging from 10^{-6} to 10^{-9} m. Especially, the electronic and magnetic properties of metals and semiconductors are considered to come from the heterogeneity in the materials such as surfaces, grain boundaries and domains. Focused ion beam (FIB) has increased usefulness for creating artificial heterogeneity by ion implantation, etching and lithography with submicron dimensions. However, the microstructural aspect and elementary functions of fabricated area by FIB could not be analyzed in the conventional experiments. The purpose of this research is to develop a new equipment for in-situ analysis of materials under the micro-lithography by FIB in the transmission electron microscope (TEM).

The equipment called "FIB/TEM" (as shown in figure 2) consists of a 200 kV standard TEM with 25 kV Ga^+ FIB. FIB system is mounted in the specimen column of TEM and the working distance for FIB reduces to 100mm for an ion beam spot smaller than 200nm diameter. In addition to TEM observation, the cathodoluminescence spectroscopy (CL), energy dispersive X-ray spectroscopy (EDS) and electron energy loss spectroscopy

(EELS) are attached to characterize the basic physical properties of the localized fine area. The FIB/TEM will be completed at the end of 1992, and the improvements will be carried out for heating and/or cooling specimens.

The effort has been conducted to install the device for CL measurements. A small paraboloidal mirror and light guide were designed to insert right above the specimen which was located into the polepiece gap of objective lens of TEM and emitted light by the electron beam. The light was extracted from the vacuum chamber and was analyzed by the monochromator which was directly attached to the TEM column. Two detectors, PMT and InGaAs semiconductor detectors, covered the wave length from 200 to 1800nm and the signal was visualized as a spectrum on the CRT of computer. Figure 3 shows the typical example of CL spectrums obtained for GaAs at low temperature. Under the electron intensity of 13 nA, the best S/N ratio could be achieved at the lowest temperature of 5 K. For the next step, EDS and EELS will be installed to get additional information on the properties in the localized fine area of materials.

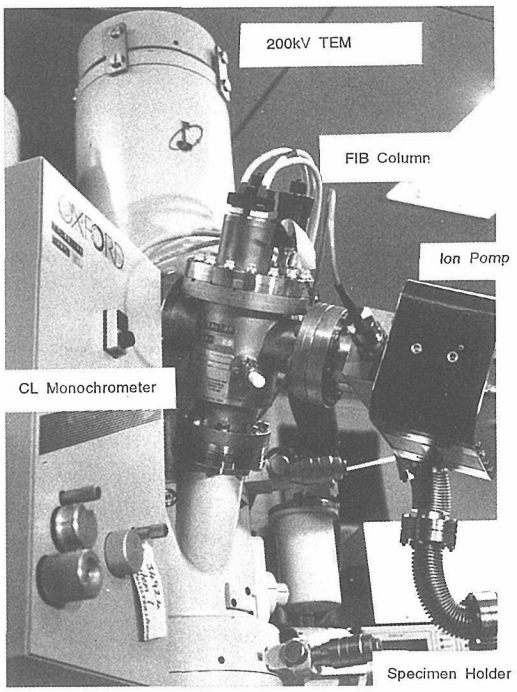

Fig. 2. Photograph of the FIB/TEM which is based on a 200 kV transmission electron microscope incorporated with 25 kV Ga^+ focused ion beam system and with cathodoluminescence spectroscopy.

Related Papers

Microscopic Observation of Si(100) TEM Film Locally Milled by Ga^+ Focused Ion Beam, Furuya, K. and Ishikawa, N. Radiation Effects and Defects in Solids 124 (1992): 61–67.

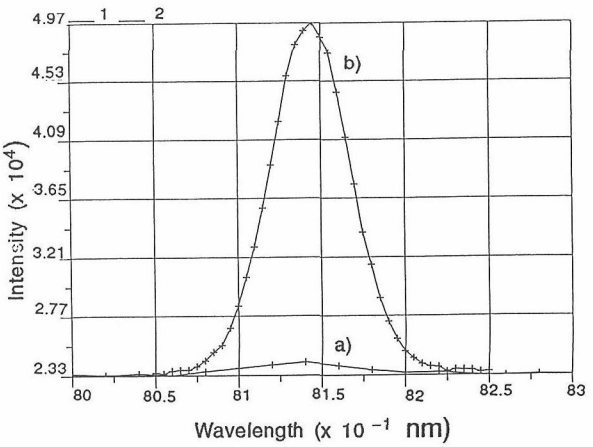

Fig. 3. A typical example of the CL spectrums for GaAs taken at a) 25 K and b) 5 K.

38 'In-Situ' Analysis/Evaluation of Radiation Damage in Materials

April 1988 to March 1994

K. Furuya, Materials Characterization Division

Keywords: radiation damage, in-situ analysis, dual-beam ion irradiation, SUBNANOTRON, 1 MV TEM, Ni, 70 KeV Ar^+, 20keV H^+

Radiation damage of metallic materials is characterized by the atomic displacements in the crystalline structure by the irradiation of energetic particles. Many types of defects and defect clusters are supposed to be produced by this atomic process and the resultant microstructure generally becomes complicated with the formations of dislocations loops, voids, precipitates and so on. For the basic understanding of radiation damage, in-situ irradiation of materials during the observation in the transmission electron microscope (TEM) is one of the fascinating ways to investigate the structural evolution induced by particles bombardments and implantations.

The purpose of this research is to develop a new facility for the in-situ analysis of the microstructural aspects of materials under dual beam ion irradiations. The facility so-called "SUBNANOTRON" consists of a 1 MV TEM with two ion accelerators. The voltage of 1 MV for electron was chosen for the resolution lower than 0.15nm, enough thickness of the specimen and enough volume at the specimen position where stressing, heating and cooling will be conducted. The attached analytical tools such as MAD, EDS and EELS are essential to characterize the complicated structural changes of irradiated materials. The construction of the SUBNANOTRON is in progress and will be completed at the end of 1993.

A special effort for SUBNANOTRON has been performed by using a standard 200 kV TEM incorporating with two types of small ion accelerators which can produced 100 keV heavy ions and 30 keV inert gas ions such as H and He (as illustrated in figure 5). Several specimens of Ni have been

irradiated in this system and the dynamic behavior of defect clusters was observed in the images taken by a fiber optically coupled TV camera, and recorded with a VTR through a real time image processor. Figure 4 shows the accumulation of secondary defects of Ni simultaneously irradiated by 70 keV Ar^+ and 10 keV H^+ at a flux of 6×10^{17} and 8×10^{17} ions/m^2/s, respectively. It is clear that many small defects which appeared as a dot at the irradiation of 60 s. grew to the loops and dislocations when the total fluence has reached to 1.7×10^{20} ions/m^2. This behavior can be compared with the results of single irradiation of Ar^+ or H^+ and implies the effects of dpa/s which may increase the mobility of Ni atoms during the irradiation. Based on these scientific results, the beam control and the data analysis system will be improved for SUBNANOTRON.

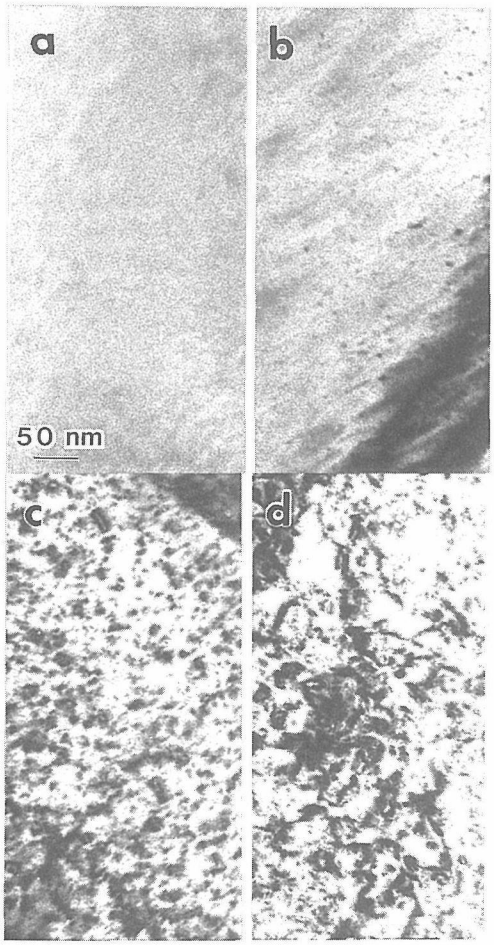

Fig. 4. The results of TEM observation of Ni simultaneous irradiation at room temperature with 70 keV Ar^+ and 20 keV H^+ at a flux of 6×10^{17} and 8×10^{17} ions/m^2/s, respectively. a) 0 sec, b) 10 sec, c) 30 sec and d) 120 sec.

Related Papers

Direct Observation of Defects Formation of Semiconductors during the Irradiation in the Electron Microscope, Furuya, K. and Ishikawa, N. Proc. 2nd Japan International SAMPE Symposium Dec. 11–14, 1991.

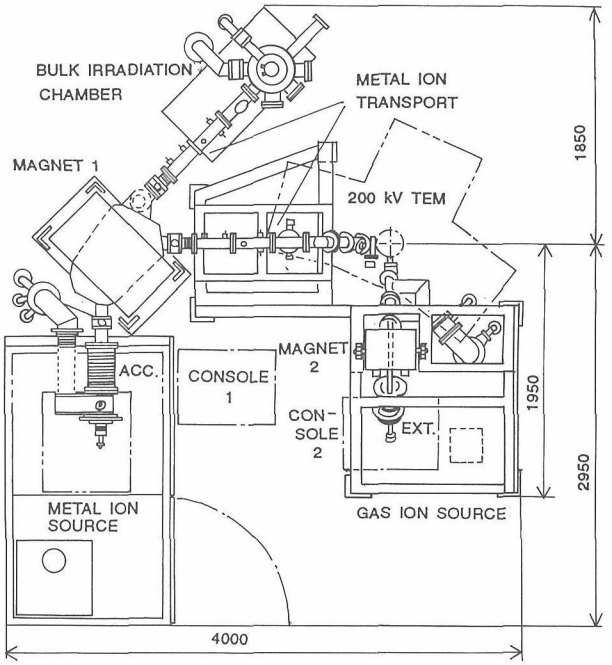

Fig. 5. Schematic drawing of SUBNANOTRON PROTOTYPE is based on a 200 kV transmission electron microscope incorporated with two ion accelerators.

39 Advanced Techniques of Physical Analyses for Metals

April 1991 to March 1994

Y. Tamura, Materials Characterization Division

Keywords: structure analysis, surface structure analysis, composition analysis

The purpose of this investigation is to develop the higher performance techniques of physical analyses for advanced materials with the help of data processing by micro-computers. Physical analyses include X-ray diffraction, electron probe microanalysis, transmission electron microscopy, scanning electron microscopy and optical microscopy.

The scope of the investigation is as follows:

1. Techniques of crystal structure analyses
   a. Crystal structure analyses by XRD
      i. Study on quantitative analysis. A computer software development is intended, by which the crystal structure of unknown substances can be identified on the basis of the X-ray diffraction data.
      ii. Study on surface structure analysis. An application technique is studied of the X-ray total reflection method in order to obtain the information of crystal surface structures.
   b. Crystal structure analyses by HREM
      Study on lattice image structure analysis. The structural analysis of lattice images are performed on metal/ceramic interfaces by means of a high resolution electron microscopy.

2. Techniques of materials composition analysis
   Study on a computer processing of EPMA data Computer softwares are developed for the purpose of highly accurate on-line micro-analysis.
3. Application
   On-request, physical anlayses and consultative function are performed.

40 Study on Mechanism of Ion Production in Low Temperature Plasma

April 1991 to March 1994
M. Saito, Materials Characterization Division
Keywords: mechanism of ionization, glow discharge plasma, determination of ultratrace elements

Using gas mixture (Ar/CH_4, Ar/O_2, etc.) for discharging, ion species were produced in direct current discharge plasma, one of the low temperature plasmas, and were analyzed with a high resolution and precision mass spectrometry (GDMS). Following results were obtained.

1. Ion intensity signals of almost elements were greatly increased by the addition of small amount of H_2 (0.1 to 0.5%) to Ar. This behavior was recognized for many elements except for P, As and Se also in the case of H_2 addition to Kr. The increase of ion intensity signals of elements was attributed to the increase of metastable argon or krypton atoms in amount of the addition of H_2. The results obtained for elements such as P, As and Se can be interpreted by taking into consideration that these elements are not ionized under the condition of metastable krypton atoms caused by H_2 addition to Kr.
2. The mechanism of ion production for molecules was found to be different from that of ion production for elements.
3. This technique is very useful not only for the determination of ultratrace elements in solid samples, but also for the investigation on the mechanism of ionization in glow discharge plasma.

41 Sensitive Instrumental-Analysis of Metallic Materials by Direct Methods and Separation Methods

April 1991 to March 1994
R. Hasegawa, Materials Characterization Division
Keywords: inert gas fusion, GD-MS, GF-AAS, ICP-AES, separation

Aiming at the development of fundamental techniques for the sensitive instrumental analysis of metals, alloys and related materials, studies on the following three items including direct methods and separation methods are carried out.

Study on direct analysis of solid samples

1. Determination of trace O and trace N in low melting point metals and in rare earth metals by inert gas fusion method using impulse heating technique
2. Evaluation of the relative sensitivity factor and the formation of ions in Ti and its alloy analyses by glow discharge mass spectrometry (GD-MS)

Study on direct analysis of liquid samples

1. High efficiency atomization of analytes in a modified graphite-furnace atomic absorption spectrometry (GF-AAS) for the determination of volatile and less-volatile elements in high melting point matrices (Ta, Ti and Mo) and/or in a solution of high concentration
2. Sensitive atomic emission spectroscopy (AES) using end-on observation and time-resolved measurement of the inductively coupled plasma (ICP) flame of the electrothermally vaporized sample
3. Application of ICP-AES to the analysis of the samples which are not easily dissolved in acids

Study on separation analysis of liquid samples

1. Determination of trace elements in Cr by co-precipitative separation and ICP-AES
2. Ion exchange separation and X-ray fluorescence spectroscopy (XRF) for the determination of trace elements in zircalloy, and absorption spectrophotometry for the determination of Hf in W
3. Simultaneous analysis of multi-elements for the determination of trace impurities in Cu and Ni by ICP-AES using a flow injection system

The investigation also includes the improvement of analytical techniques available for the chemical analysis of the various samples which are provided from other divisions of the Institute.

42 Database Systems for R&D of Superconducting Materials

April 1989 to March 1994
S. Nishijima, Failure Physics Division
Keywords: superconducting materials, High T_c oxides, factual database, common samples, common measuring practice

As one of the coordinated research programs of the Science and Technology Agency, this project aims at the development of factual data systems on the new oxide superconducting materials, which will assist researchers with more ordered information. There are 33 participants from industrial, university and national institutions, where NRIM takes part in the development itself of the database and the coordination of the group tasks.

In the first three-year term ending by March 1992, the work was oriented to improve sample

reproducibility and establish common practices for property evaluation, by comparing the results of multiple measurements on common samples shared by different laboratories. An experimental database system will be constructed and tested in the succeeding two-year term.

Various bulk, tape and film samples have been prepared for Y-Ba-Cu-O and Bi-Sr-Ca-Cu-O systems and characterized from different view points by different laboratories. All the detailed data have been collected and reviewed to be stored as premier data in the database, then processed to get characteristic values as required, and eventually re-processed according to any new theories in the future.

Common input systems for data and experimental details record have been developed with many tools such as dialog-based featuring system of curvilinear data. Figure 6 gives an outline concept of the data system under development.

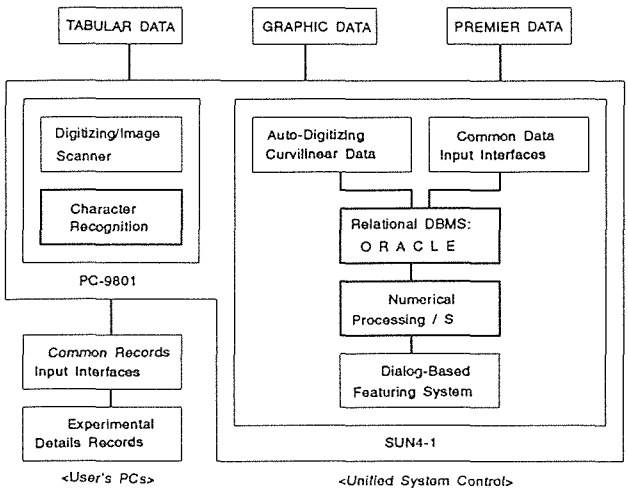

Fig. 6. Scheme for the Database Management System

Related Papers

Database Systems used for Research and Development of New Superconductors, Hoshimoto, K., Yokokawa, T., Nakada, E. and Iwata, S. Proc. Euro-Japan Seminar 92 on Database Feb. 1992, Paris (in preparation).

43 Sensing and Analysis of Material Damage Formation Processes

April 1991 to March 1994

N. Shinya, Failure Physics Division

Keywords: damage monitoring system, piezoelectric polymer, electron Moiré method

In this work, a damage monitoring system and advanced analytic techniques for damage formation processes are being developed. The main research programme is as follows.

1. A surface treatment for the detection of local strain and microcracks is being developed. As a strain sensor, piezoelectric polymers are used and coated on the metal surface. Local strain is measured by operational amplifier circuit with a scanning probe, and also observed using the voltage contrast technique in a scanning electron microscope.
2. Microcreep deformation process is observed and analyzed by an electron Moiré method which has already been developed using an electron lithography and an electron beam scan. Using this method, microcreep deformation in polycrystal metal is measured. As the creep proceeds, the strain distribution becomes more complicated and non-uniform even in a same grain, and this non-uniformity of strain distribution has a relationship to grain boundary sliding. Furthermore this method will be advanced to a highly sensitive technique with finer Moiré fringes by application of ion beam lithography. This method will make it possible to observe and analyze the damage formation process clearly.

44 Research on Quantitative and Intelligent Nondestructive Evaluation Techniques for Materials and Structures of High Reliability

April 1990 to March 1993

C. Masuda, Failure Physics Division

Keywords: nondestructive evaluation, frequency response, acoustic microscopy, laser-ultrasonics, composite materials

In this research, it is intended to develop the advanced nondestructive evaluation techniques and systems based on various ultrasonic measurement techniques to maintain the reliability of newly developed materials such as new ceramics and composites. The research is a part of the organized work of STA supported by members of various institutions, universities and companies. The following four sub-themes are carried out in our laboratory.

1. Ultrasonic measurement of highly attenuating materials

   Materials characterized by ultrasonic high attenuation, such as composites and cast metals, are difficult to be tested by traditional ultrasonic method. Development of ultrasonic measurement method for evaluation microstructure and flaws in the ultrasonic attenuative materials is the aim of this sub-theme. A new technique based on ultrasonic frequency response of the material has been developed, and good results are obtained on estimation of grain size of steels.
2. Improvement in acoustic microscopy

   Using of V-Z curve property obtained from scanning acoustic microscope (SAM), velocity of Rayleigh waves on small region of material surface can be determined. Techniques to evaluate microscopic physical property using

this information are investigated for the analysis of microscopic fracture mechanics of advanced materials. In order to obtain the more accurate information of Rayleigh wave, the SAM was modified. The residual stress and the inhomogeneous structures in the composites will be evaluated by this technique.

3. Laser-ultrasonics

   Laser-ultrasonics is a technique to perform non-contact ultrasonic measurements in which pulsed laser and laser interferometry are employed for ultrasonic generation and detection, respectively. This sub-theme is carried on to develop non-contact ultrasonic imaging system for evaluation of materials at high temperature. The current work is to design elemental mechanisms of the system, which consist of a laser beam scanner and a signal compensator for quantitative laser-ultrasonic detection.

4. Flaw evaluation in inhomogeneous and anisotropic materials

   Inhomogeneity of composite materials causes complex ultrasonic phenomena. For detection of flaws, it must be required to know the ultrasonic behaviors such as reflection and scattering. The purpose of this sub-theme is to clarify the phenomena and to develop the technique to evaluate the materials with complex structure. The development of computer simulation method and of standard specimen with the inhomogeneity were started for the analysis of this phenomena.

45 Chemical Analysis of Organotin in Marine Environmental Samples

April 1991 to March 1996

H. Okochi, Director of Special Research

Keywords: ICP-MS, organotin, hydride generation, XRFS, deep sea sediment

Speciation of organotin

Organotin compounds are highly of environmental and toxicological concern. In order to monitor trace of organotin compounds in the environment, high sensitive and precise determination method are required.

Inductively coupled plasma mass spectrometry (ICP-MS) has been used as a high sensitive detector for several organotin compounds and a simple hydride generation method has been applied to the introduction to the ICP plasma. The organotin compounds under investigation are triphenyltin (TPT), diphenyltin (DPT), monophenyltin (MPT), tributyltin (TBT), dibutyltin (DPT), monobutyltin (MBT) and inorganic tin.

Various analytical conditions have been investigated. Artificial sea water was used at experiments. At pH 2 of a sample solution in hydride generation, the highest signal of tin was obtained. Nitric acid and hydrochloric acid gave same results. Adequate amount of $NaBH_4$ were about 100 mg l^{-1} and more than 100 mg l^{-1} was useless. The more the arkyl group in arkyl (butyl or phenyl) tin compounds increase, the higher the boiling points of their hydrides are. Accordingly the optimum temperature was investigated and all the organotin compounds hydrides gave the highest signals at 60 to 70 °C. The sensitivity increased 3 to 5 times more than that at a room temperature. The organotin hydrides were collected in a gas trap cooled with liquid nitrogen and then the trap was slowly warmed.

After they were separated by fractional vaporization, they were measured with ICP-MS. A high sensitive determination method of organotin has been established.

Deep sea environmental analysis

X-ray fluorescence analysis of deep sea sediments has been investigated. Analytical elements are Si, Ti, Al, Fe, Mn, Mg, Ca, K and P as main constituents and Ca, Sr, Pb, Ni, Zn, Rb, Cu, Y, Zr, Nb and Mo as minor ones. Glass beads of sediments were prepared for analysis with X-ray fluorescence spectrometer. Preoxidation of organic materials in sediments was necessary. The matrix effects were corrected by the theoretical alpha coefficients method. The deep sea sediments were collected by "Shinkai 2000" in the Japan Marine Science and Technology Center.

46 Study on Measurement and Evaluation Methods for Superconducting Properties

April 1990 to March 1993

H. Wada, 1st Research Group

Keywords: stress effect, ac loss, critical current, superconductor simulator

This is a collaboration program of NRIM with NIST (National Institute of Standards and Technology, Boulder, Colorado), based on the Japan-US Agreement on Cooperation in Research and Development in Science and Technology, and covers the following topics:

1. stress effects on critical currents in advanced superconducting materials,
2. ac losses in advanced superconducting materials, and
3. critical currents in oxide superconductors.

In fiscal year 1991 a computer program for automated critical current (I_c) measurement was developed at NIST through collaborative work by NIST and NRIM researchers using a superconductor simulator invented at NIST. It is assumed that the second derivative of a voltage-current (V-I) curve represents a distribution of superconducting filaments with different critical current densities (J_c) within a wire. Thus, the second derivative (d^2V/dI^2) curves were calculated and plotted on

both the simulator and an oxide superconductor fabricated at NRIM using the developed program. Smooth curves were obtained which may be used for the evaluation of the wire quality. It also turned out that the d^2V/dI^2 curves thus obtained may give information on heating occurring at various places in the measurement system, such as sample current terminals. Results are being examined and will be presented at the Applied Superconductivity Conference in August, 1992.

Related Papers

Critical Current Degradation in Nb_3Al Wires due to Axial and Transverse Stress, Kuroda, T., Wada, H., Bray, S. and Ekin J. (to be published in Fusion Engnr. Design).

[47] A Basic Research for In-Situ Measurement of Dynamic Strains of Materials at Elevated Temperature

April 1991 to March 1992

Y. Muramatsu, Advanced Materials Processing Division

Keywords: laser speckle method, in-situ measurement, dynamic strain, high temperature

Laser speckles are random light and shade patterns caused by the interference of scattered laser light on the surface of an object, and we can use them to measure the surface strains without contact with high accuracy because the patterns deform with a specific relation to the deformation of the surface illuminated by the laser beam. If it can be applied to the in-situ measurement of dynamic strains at high temperatures as encountered in welding processes, it would be helpful to clarify various problems such as high-temperature cracking in a weld.

In the laser speckle method, photo-intensity distributions of the speckle patterns before and after deformation of an object surface are sampled and the strain is calculated by using cross-correlation function between two distributions.

In this research, our examination and results are as follows:

1. Basic evaluation for the laser speckle method.
2. Dynamic strain measurement at high temperatures on steel plates which are welded with the GTA welding method.
3. Evaluation of relationship among the strain rate, sampling interval and the accuracy.
4. Determination of optimal measuring condition with the relationship between the spot diameter of laser beam on the surface and the measuring accuracy.

The laser speckle method has been confirmed to be applicable to dynamic measurement at elevated temperatures when the response of the devices is sufficiently fast in relation to the strain rate. The maximum strain rate which can be measured stably was 3000 micro strain per second.

The spot diameter of the laser beam on the object surface, however, affects on the measuring accuracy depending on the amount of the information in the spot. The accuracy goes down with decreasing the spot diameter because we can expect fewer information from smaller spot diameter. On the contrary, we found the fact that the peak value of cross correlation function cannot indicate the measuring accuracy from the data obtained by several spot diameters.

[48] Investigation on Non-Contact Materials Evaluation Using Laser Beam

April 1987 to March 1992

T. Saito, Materials Characterization Division

Keywords: laser-ultrasonics, ultrasonic imaging, optical heterodyne interferometry systems

Laser-ultrasonics is a non-contact ultrasonic measurement technique using pulsed laser irradiation and laser interferometry. In this study basic technique of laser-ultrasonics have been investigated. Recent interests are on a non-contact microscopic ultrasonic imaging and on simultaneous detection of longitudinal and share ultrasonic waves by newly developed optical heterodyne interferometry systems.

Laser-ultrasonic measurement can be easily applied to the small region by means of focusing laser beams. By the combination of laser-ultrasonic and scanning techniques, it is possible to develop ultrasonic imaging techniques for microscopic materials evaluation at elevated temperature. In comparison with a scanning acoustic microscope (SAM), it has some advantages. The most important advantage is the applicability for materials in hostile environments. Another merit appears on imaging for specimens with a rough surface. On imaging by using piezoelectric transducer in SAM, the disturbance of ultrasonic waves by the specimen surface roughness causes the deformation of the imaging. On the other hand, as the non-contact detection of ultrasonic waves is performed just on the surface, as in the technique developed here, it is expected that no deformation occurs. The improvement of sensitivity is an important problem for this technique, because measurements on rough surface give very noisy images by reduction of optical interference signals.

The optical ultrasonic measurement has been applied only to the detection of vertical vibrations of surface. The newly developed optical heterodyne interferometry system is, however, constructed by combining two interferometers to detect the vertical and horizontal motions at the same point on

the specimen surface simultaneously. In the experiments, a specimen with rough surface is required for the detection of horizontal motion, so that the signal to noise ratio of the detected signals is for the present insufficient to practical use. This system is expected to use for advanced application of laser-ultrasonics techniques.

[49] Measurements of Transient Phenomena Due to Beam-Solid Interaction

April 1990 to March 1992

N. Kishimoto, Materials Characterization Division

Keywords: pulsed-beam perturbation, strain measurement under 10MeV D irradiation, resonant behavior of creep

Microstructural evolution in irradiated materials results from a dynamical balance between generation and relaxation of point defects. A transient response of a material to a pulsed-beam perturbation conveys kinetic information. The purpose of this research program is to explore a new detection technique of the dynamical processes and to estimate the microstructural parameters from the macroscopic responses.

Strain measurement under 10MeV D irradiation has been conducted for a foil specimen of Fe-Ni-Cr alloy, under uniaxial loading. After continuous irradiation for about 10 hrs, it was switched to a square-wave (pulsewidth τ = 10 msec–1000 s), at a low damage rate of 10^{-7} dpa/s.

A systematic study of pulsewidth dependences of strain change has revealed overall response behaviors of this alloy system. While the specimen showed some contraction after continuous irradiation at $\tau > 200$ s or < 1 s, a prominent increase in strain was observed around 100 s. Under continous irradiation, such large positive creep had never been observed at the low dose rate. Comparision of the peak creep between solution-annealed and cold-worked specimens showed a rather weak dependence on dislocation density.

The resonant behavior of creep is important not only technologically but also from a fundamental aspect. This result indicates that pulsed irradiation may cause a significant deformation in austenitic steels even at such low dose and slow pulsing rates. This effect would have to be taken into account in designing fusion devices such as ITER.

The resonant behavior is elucidated in terms of a point defect model based on rate equations taking dislocation networks as strong sinks and diffusion-limited recombination. The pulsing time at resonance corresponds to a characteristic time of transient enrichment of interstitial atoms resulting from vacancy lifetime. This resonant creep may be an evidence to support a creep mechanism of stress-induced interstitial nucleation, rather than conventional models of dislocation motion.

Related Papers

Helium Gas Release Due to Grain Boundary Fracture in Neutron-Irradiated High-Nickel Austenitic Alloys and a Ferritic Steel, Kishimoto, N., Clausing, R.E., Heatherly, L. and Farrell, K. J. Nucl. Mater. 179–181 (1991): 998–1002.

[50] Development of Fundamental Technologies for X-ray Microtomography

April 1989 to March 1992

Y. Yamauchi, Materials Characterization Division

Keywords: CT, tomography, microtomography, X-ray, three-dimension

Microscopes such as optical or electron type have been applied for materials research. In those applications, however, observations are limited to the cut surface of the sample. Thus, there always remains some ambiguity whether the sample is cut at the right plane containing the proper information. On the other hand, a three-dimensional image provides us overall information of the object sample. The nondestructive characteristics of X-ray tomography afford a unique feature, i.e., a three-dimensional image which consists of multi-sliced tomographs taken in a fine pitch along the rotational axis.

We have developed an in-house microtomography device for relatively small objects using a conventional X-ray source. The X-ray source using a rotating target is operated in the fine focus mode. The parallel projection configuration is adopted and transmitted X-rays are converted to visible light by the fluorescent screen before detection by a charge coupled device (CCD) still camera. The data acquisition is controlled mainly by a personal computer and the reconstruction is accomplished by a powerful computer accessible through the local area network (LAN). The performance of the appartus was examined by observing a carbon-fiber/SiC composite.

Followings are some accomplishment of this project.

1. The apparatus is compact enough to be operated in a single room of an ordinary laboratory.
2. A spatial resolution of less than 10 μm was achieved.
3. It took about 3 and a half hours in total to complete the measurement and to process the data over 256 pixels × 192 slices × 200 directions.
4. The thin SiC rich zone in the infiltered fiber layer was found by taking a vertical tomograph. The three-dimensional observation is informative and provides us more chances to get substantial facts about objects than those by surface micrographs.

51 Image Analysis of Metallurgical Structure with a Computer Network System

April 1989 to March 1992

M. Fukamachi, Materials Characterization Division

Keywords: computer-image analysis, X-ray maps of EPMA, analysis of chemical compositions

In order to carry out an accurate and rapid computer-image analysis of metallurgical structure observed with the X-ray maps of EPMA, the feasibility of a local area network system of small computers has been studied. In the system, 5 computers are connected to share application programs, X-ray maps and data-files among computers. X-ray maps are processed to reduce the image noise, to correct the image distortion and to extract the factors to evaluate the metallurgical structure. After the measurement and evaluation of X-ray maps, results are stored as a reference data-file for the future analysis.

The system can be utilized to improve the resolution of X-ray maps. The distribution of fine materials smaller than the electron probe size are revealed and these fine materials can be identified by the analysis of chemical compositions.

52 Fundamental Study on Initial Oxidation by Means of Light-Induced Exoelectron Emission

April 1991 to March 1992

Y. Ikeda, Failure Physics Division

Keywords: oxidation, Fe-Cr alloy, photoelectron

The research on the mechanism of initial oxidation at high temperature is not so well developed as that of long term oxidation because of experimental difficulties. We tried to follow the initial oxidation process by measuring photoelectrons emitted by the ultraviolet irradiation in air. Some Fe-Cr alloys were oxidized at 1000K in air and the photoelectron current was measured on the surfaces. The current increased initially, reached a maximum and decreased with the mass gain. This process was found on all alloys examined in this work. The maximum value on low Cr alloys agreed with the value on prepared Fe_2O_3 and the photoelectron current from other probable oxides was negligible in comparison with Fe_2O_3. In addition, Auger electron spectroscopy revealed that the surface concentration of Fe changed in the same manner as the current. These results show that the photoelectron current reflects the thickness of Fe_2O_3 layer on the surface. The maximum value of photoelectron current decreased with increasing Cr content. This decrease is reasonably attributed to the formation of Cr-enriched oxide which prevents the growth of Fe_2O_3 layer.

53 In-Situ Quantitative Evaluation of Microreaction

April 1991 to March 1992

H. Masuda, Failure Physics Division

Keywords: electrodeposition, STM, tunnel current

We studied on the initial stage of electrodeposition for copper on gold electrode in 0.1 M $CuSO_4$ + 0.6% H_2SO_4 aqueous solution by a scanning tunneling microscope (STM). It was found that the enhanced electrodeposition occurred under STM tip when the tunnel current was increased. The electrodeposition rate was dependent on the tunnel current but not on the potential of gold electrode, and it became more than 2 order faster than that estimated from cathodic polarization curve of copper as the tunnel current was increased. The STM observation after the test showed that the electrodeposition of copper occurred only under the STM tip. It is concluded from these results that the tunnel current was consumed to the electrochemical reaction.

54 Fundamental Study on Quantitative Non-Destructive Evaluation of Small Defects in Materials

April 1990 to March 1992

C. Masuda, Failure Physics Division

Keywords: reliability, advanced material, damage, defect, non-destructive evaluation

To know the reliability of advanced materials to be applied for practical use is very important. Particularly, the detection and evaluation of damage or small defects in the materials is a key problem, which is highly demanded for the reliability. The main object in this study is to get fundamental information to develop a non-destructive evaluation method to detect and characterize small defects in the material with high accuracy.

Two types of approaches have been carried out in this study, which are ultrasonic and electro-magnetic non-destructive evaluation methods.

As for the study by ultrasonics, the major concern is the detection and evaluation of inner defects in metals and advanced materials such as ceramics and composites. Ultrasonic non-destructive testing approach has been theoretically examined by the numerical simulation and frequency response analysis method developed by us, looking at the fundamental problems in measuring condition of angle beam method that affect the detection precision, and the problems in the echo response from defects or creep damages produced in the material. An acoustic microscopic approach using SAM has also been attempted to study the mechanism of failure in composite materials.

As for the study by electro-magnetics, useful results have been brought about to detect and evaluate surface defects of the materials with high accuracy. Magnetic flux leakage testing method has

been studied theoretically by using a dipole model and experimentally as well by using Hall element sensors for determining the dimension of defects quantitatively. Furthermore, the fundamental information has been obtained on the defect leakage flux by AC magnetizing which is useful in further progress of accuracy in the method. Material evaluation by incremental permeability techniques has also been studied successfully showing a possibility for steel classification. (This research work will be continued in another related theme in next term).

Related Papers

Detection of creep damage by ultrasonicwave, Fukuhara, H., Shinya, N. and Kyono, J. Journal of JSNDI 40 (1991): 450–55 (in Japanese).

Effect of sensor size on results of magnetic flux leakage testing, Uetake, I., Ito, H. and Saito, T. Journal of JSNDI 40 (1991): 291–97 (in Japanese).

Effect of several factors on evaluation of damage for metal-matrix composites using SAM, Tanaka, Y. and Masuda, C. (to be published in Japanese in the Journal of SMSJ).

55 In-Situ Observation of Fatigue Damage

April 1989 to March 1992

S. Matsuoka, Environmental Performance Division

Keywords: metallic materials, fatigue, scanning tunnelling microscope, exso-electron

In order to clarify the fatigue mechanism of metallic materials, the observation of slip markings and fatigue and brittle fracture surfaces with the scanning tunnelling microscope (STM), and the measurement of exso-electron emission from the bare surface are being carried out.

The STM observation was done with a tunnel current of 1 nA and a tunnel bias of 25 mV in air. STM images of slip markings were obtained for seven pure metals of Au, Ag, Cu, Fe, Zn and Al and three kinds of engineering materials of SB42 carbon steel, SUS304 stainless steel and Ti-6Al-4V titanium alloy. The slip interval and step were about 2 and 0.2 μm, respectively. STM images of fatigue fracture surfaces for Ti-6Al-4V titanium alloy and brittle fracture surfaces for chromium and molybdenum had a fractal character (i.e., self-similarity) up to very high magnification where scanning range of 40 nm in X and Y directions corresponded to about 150 atoms for the three metals. However, the fractal character is expected to break down when scanning range is below 20nm.

The exso-electron emission from the bare surface, which is very sensitive to the material and its oxidation rate, was measured for eleven pure metals of Au, Pt, Ag, Cu, Ni, Fe, Cr, Ti, Al, Pb and Zn, and two ceramics of SiC and Si_3N_4 in air and vacuum (10^{-4} to 10^{-6} Torr). The amount of exso-electrons decreased with decreasing water vapour pressure. This result explained the dependence of the fatigue life on the water vapour pressure for lead and aluminum alloys.

Related Papers

Application of Scanning Tunneling Microscope to Metal Fatigue, Matsuoka, S. J. Iron and Steel Inst. Jpn. 75 (1989): 1943–46 (in Japanese).

Fractal Character of Scanning Tunneling Microscopic Images of Brittle Fracture surfaces on chromium, Matsuoka, S., Sumiyoshi, H. and Ishikawa, K. Trans. Jpn. Soc. Mech. Eng. 56 (1990): 2091–97 (in Japanese).

Fatigue Threshold and Low-Rate Crack Propagation Properties for Structural Steels in 3% Sodium Chloride Aqueous Solution, Matsuoka, S., Masuda, H. and Shimodaira, M. Metall, Trans. A 21A (1990): 2189–99.

56 Quantitative Evaluation of Fracture at High Strain Rate and Low Temperature in Ferritic Steels

April 1989 to March 1992

T. Yasunaka, Environmental Performance Division

Keywords: low temperature embrittlement, dynamic elastic-plastic fracture toughness, nodular cast iron, carbon steel

Ferritic steels are embrittled at low temperature and higher strain rates accelerate the embrittlement. For the integrity of structures such as containers of spent nuclear fuel, it is important to evaluate fracture quantitatively on the basis of fracture mechanics. The objective of this study is to clarify the effect of temperature and strain rate on fracture toughness and to lead to accurate evaluation of fracture.

For the measurement of dynamic elastic-plastic fracture toughness, a drop-weight type and a electrohydraulic type tensile testing machines were used. The materials used were a nodular cast iron and a carbon steel.

In the ductile fracture region, fracture toughness of nodular cast iron increased with decreasing temperature. However, it decreased abruptly with the occurrence of low temperature embrittlement. The higher strain rate led to increase in fracture toughness in the ductile fracture region in addition to the increase in ductile-brittle transition temperature. The increase in strength with decreasing temperature or with increasing strain rate is responsible for the increase in fracture toughness. Ductile-brittle transition temperature was linearly related to stress intensity rate.

With regard to carbon steel, the effect of strain rate on ductile-brittle transition temperature was also clarified. In addition, the relationship between low temperature embrittlement and generation of

deformation twins was studied.

Related Papers

Determination of dynamic elastic-plastic fracture toughness by a drop-weight impact testing machine, Yasunaka, T., Nakano, K. and Saito T. ISIJ International 31 (1991): 298–303.

Effect of graphite nodule spacing and temperature on fracture toughness in a thick walled ferritic spheroidal graphite cast iron, Nakano, K. and Yasunaka, T. Tetsu-to-Hagane 78 (1992): 926–33 (in Japanese).

[57] International Joint Research on Evaluation and Standardization of Advanced Materials

April 1989 to March 1992

H. Maeda, 1st Research Group

Keywords: standard measurement methods, superconducting material, cryogenic structural materials, surface chemical analysis, mechanical property at high temperature, material database

NRIM has participated in the studies on the establishment of standard measurement methods in several technical working area (TWA) of VAMAS, such as superconducting materials, cryogenic structural materials, surface chemical analysis, mechanical properties at high temperature and inter-operability between materials databases, and has been acting as the central laboratory in the TWA of superconducting and cryogenic structural materials. Useful recommendations for these standard measurement methods will be presented soon and new programs for them will be started.

For superconducting materials, standard measurement methods on critical current and ac losses are being developed through measurement intercomparison programs. Critical current measurement intercomparisons were completed in 1992 and results are being examined for a final report. A special Technical Working Party (TWP) meeting was held in Brussels last October, whereby details of the second intercomparison programs were determined. In the second ac loss measurement intercomparison, 7 NbTi sample wires different in filament diameter, matrix materials, etc were supplied by NRIM and 20 institutes participated. Results are being reported to NRIM and will be presented at the next TWP meeting in June, 1992 in Vienna.

A second international round robin (RR-) tensile and fracture toughness test program at liquid helium temperature was conducted in order to refine procedures of the test and clarify remaining problems under limited testing conditions. The results were considerably improved compared to the those in first RR-test; average yield strength was 1065 MPa with a standard deviation of 15 MPa (1.4% to the average) and fracture toughness was 263 MPa$\sqrt{m}$ with a standard deviation of 15.3 MPa$\sqrt{m}$ (5.8%). The second stage of strain gage measurements at cryogenic temperature was also carried out using the same lot gages and common instruments which apply designated stress at liquid helium temperature.

For surface chemical analysis, the software has been constructed to translate spectral data acquired on different machines to VAMAS-SCA Standard Data Transfer Format and to Manipulate AES and XPS spectra in a standard manner. We called this software THE COMMON DATA PROCEEDING SYSTEM. The software also has the spectra data banks in which 450 spectra are now stored. At present, everybody can use this software by connecting to ASTM electrical bulletin board.

The RR-tests of creep crack growth were carried out on IN 100 superalloy, a brittle material, at 850 °C, and the creep crack growth rate obtained was evaluated using the non-linear fracture mechanism parameter C*. From these experiments, it was verified that the appropriate data could be also obtained for IN 100 superalloy on the guideline which was modified from one for 1Cr-Mo-V steel. The creep crack growth rate in IN 100 superalloy was about 10 times as fast as that in 1Cr-Mo-V steel. For IN 100 superalloy, the effect of specimen thickness on creep growth rate was little recognized.

With the cooperation of fifteen experts from five countries, an interlaboratory comparison of data evaluation methods for creep and fatigue data of typical engineering steels and alloys was conducted as a project of the VAMAS TWA10. The RR-work identified various aspects of procedures in data analysis with computational modeling. In 1991 we launched a follow-up project, another international collaboration, that aims at the establishment of an inventory of data evaluation methods and models commonly used in factual materials data systems. The NRIM is working with the NMC (New Materials Center) on the data evaluation modeling for steels and alloys.

Related Papers

Results on the First VAMAS Intercomparison of AC Loss Measurements, Itoh, K., Wada, H. and Tachikawa, K. Advances in Cryog. Engineer. Mater. 38A (1992): 459–67.

VAMAS Second Round Robin Test of Structural Materials at Liquid Helium Temperature, Ogata, T., Nagai, K., Ishikawa, K., Shibata, K. and Murase, S. Advances in Cryog. Engineer. Mater. 38A (1992): 69–76.

Quantitative Surface Chemical Analysis of Au-Cu Alloys with XPS, Yoshitake, M. and Yoshihara, K. Surface and Interface Analysis 17 (1991): 711–15.

Effect of Specimen Size on Creep Crack Growth Rate Using Ultra-large CT Specimen for 1Cr-Mo-V steel, Tabuchi, M., Kubo, K. and Yagi, K. Engineer. Frac-

ture Mech. 40 (1991): 311–21.

Significance of Data Evaluation Models in Materials Databases, Nishijima, S., Monma, Y. and Kanazawa, K. VAMAS Technical Report 6 October 1990.

Simulation and theory

58 Development of Material-Design-Technique for Mechano-Chemical Attack on Light-Weight Heat-Resistant Materials

April 1989 to March 1993

I. Tomizuka, Physical Properties Division

Keywords: material design, mechanochemical attack, light-weight heat-resistant material, intermetallic material, C/C-composite material, oxide-dispersion-strengthened superalloy

Current subjects handled in this research are in the following:

1. Mechano-chemical attack on intermetallic materials

   This section is concerned with mechanical degradation of Ni_3Al-based intermetallic materials in high-temperature air and with anodic dissolution of TiAl-based materials in 5N sulfuric acid. While the first topics is still at its initial stage, the second one could elucidate an anodic dissolution of TiAl-based materials, which were qualitatively similar to that of titanium.
2. Mechano-chemical attack on carbon-fibre-reinforced carbonaceous composite materials

   This section is concerned with an attempt to account for mechanical degradation of C/C-composite-materials by weight-decrease-behavior to be observed in a thermobalance. The attempt was partly successful. Not all the mechanical degradation was accounted for by weight decrease observed in a thermobalance.
3. Mechano-chemical attack on light-weight super-heat-resistant oxide-dispersion-strengthened alloys

   This section is concerned with analysis of effect of gamma-prime-phase-content on yield strength at various temperatures of oxide-dispersion-strengthened nickel-based superalloys. The effect was found to be significant at high temperatures.

59 Study on the Computer Aided Design Tools for the Development of Materials

April 1991 to March 1994

K. Hoshimoto, Materials Design Division

Keywords: computer aided development of materials, sensory test, micrographic data, materials database, knowledge on materials, materials design

The objective of the study is to extend fundamental tools used for the computer aided development of materials. The following three subjects have been studied.

1. Development of statistical tools for materials design

   Sensory tests followed by the analysis by using a multi-dimensional scaling method have been adopted in order to investigate the relationship between the micrographic data of structure and of fracture surface. The results have shown that the procedure should possibly be applied to relate the information of microstructure with the materials properties using computer. The procedure should be applied further to the automatic recognition of graphical data in the materials design works.
2. Optimization of the implementation of materials data

   As a part of the scheme for optimization of the structure of the materials database, the most efficient way to computerize binary phase diagrams obtained from literatures has been studied. An intelligent man-machine interface for the retrieval of data has been developed which accept the user who lacks the knowledge on the special language of database management.
3. Organization of knowledge on materials and its application to materials design

   Information expressed by different format or recorded by different media have been analyzed and an optimal way has been explored for organizing the knowledge of the materials so as to be the most suitable for the application to materials design.

60 Study on the Construction of Self-Organizing Information-Base System Used for Creative Research and Development

April 1991 to March 1994

K. Hoshimoto, Materials Design Division

Keywords: self-organizing, information-base, materials design, dictionary, knowledge converter

In the domain of metals and alloys one can never find any two species that have precisely identical internal structure even if the chemical composition and outer shape are the same; which means that one can not specify the object exactly in the database of materials properties. Therefore the specification of materials has inevitably an ambiguity. Specialists create new materials by combining basic theories, factual data and qualitative knowledge with their full skill and experiences. But information on materials today is increasing day by day beyond the quantity which one person can deal with. The objective of the present study is to develop a self-organizing information-base sys-

tem for materials design. To realize the system, the investigation of fundamental procedures to select and organize various types of information automatically with the aid of computer to produce new materials has been made.

The knowledge on materials being fuzzy ones, the answer that the system can offer contains fuzziness inevitably to some extent. For these reasons, a knowledge retrieval system has been constructed in the previous study by which the knowledge included in the research articles are collected and stored in the computer, and in the response to the queries expressed by natural language (Japanese in this case) of user, the system retrieves and shows the related knowledge to the user. Information on the data source and experimental procedures were also stored together with the experimental results and conclusions.

The system to be developed in the study will treat the fundamental knowledge on materials and the actual data of materials properties in addition to the above mentioned information. In 1991 fiscal year, two tools for gathering information into the computer have been developed. The first searches for new words from the text fed into the computer by using OCR and put them in the dictionary automatically. It also assists to construct a thesaurus in consultation with the user. The second is a knowledge converter by which a text cut out from a document is transformed to a knowledge treatable by the computer.

61 Development of Knowledge Based System for Materials Life Prediction

April 1988 to March 1993

N. Nagata, 5th Research Group

Keywords: life prediction, database, knowledge base

This research program aims at building an integrated system for advanced materials life prediction, by combining the factual database on materials strength with the knowledge base including scientific and empirical predictions on materials deformation and fracture processes.

An integrated database management system, DIMS (Dialogical Integrated system for Material Strength database), which works in a UNIX operating environment with X-Windows, was newly developed. This system allows easy access to any combination of particular data among the analyzed data as well as factual data of materials. So far we have applied this system to the three fields of fatigue, creep and corrosion, independently, for the life prediction.

The DIMS allows us to find a good correlation among particular characterized items and strength properties of materials. For example, fatigue strength of carbon steel was able to be predicted from the combination of the chemical compositions and its tempering temperature. By using these good combinations we have proposed several empirical models and developed a new algorithm for predicting the fatigue strength of materials. This algorithm has been applied to the prediction of lives of notch members and to the construction of the computer aided fatigue design system of machinery in cooperation with companies.

In the field of creep, a new approach to look into the heat-to-heat variations of creep rupture strength has been proposed taking a fact into account that the scatter in creep rupture times in a single heat was about 0.04 in logarithm. The strength ratio curve, the ratio of long-time strength to tensile strength at the same temperature in ordinate versus temperature indicates a new way of extrapolation and interpretation of the variation.

In the field of corrosion, significant efforts have been made on two items for the construction of knowledge base: corrosion fatigue (CF) in high temperature water and stress corrosion cracking (SCC) in high temperature aqueous solution. Evaluation of SCC-related data of which testing methods were varied is also being made assisted by some tools for construction of an expert system.

62 Predictions of Materials Strength and Endurance under Irradiation Using Ion Beam

April 1988 to March 1993

J. Nagakawa, 2nd Research Group

Keywords: irradiation creep, stress relaxation, computer simulation

Among the various changes in materials properties induced by neutron irradiation, a change in mechanical properties is one of the most important property alterations in the structural materials for nuclear reactors. The change causes a significant reduction in endurance of the structural components. It is, however, almost impossible to obtain a complete set of irradiation data necessary for the endurance assessment of the currently operated reactors as well as reactors to be developed for the next generation such as the fusion reactors, because of technical difficulties and a high cost of irradiation tests.

Materials behavior under irradiation is especially difficult to be evaluated, and, in most cases, it cannot be estimated from the pre- and/or post-irradiation results. In order to cope with this difficulty, it is highly desirable to develop a prediction method to interpolate and/or extrapolate the limited number of existing data under irradiation. A calculational method has been developed to predict the radiation induced deformation, based on a computer simulation of point defect kinetics under stress. This has been applied

to the examination of the low-temperature irradiation creep and the irradiation induced stress relaxation. Following are the results of the calculation;

1. Low-temperature irradiation creep, which is regarded as a serious problem for the experimental fusion reactor like ITER, was explained from the transient behavior of point defect kinetics. Inclusion of the transient climb-glide model improved the prediction and diminished the previously predicted difference in the induced creep strain between the cold worked and the solution annealed materials. Linear stress dependence and weaker-than-linear dependence on damage rate of the low-temperature irradiation creep deformation at 60 °C lead to about 30% stress reduction in one month and about 50% in one year at the outer portion of the fusion blanket structure.
2. Irradiation induced stress relaxation in a light-water fission reactor was calculated for Inconel X-750 at 300 °C and 3×10^{-8} dpa/s, and it was revealed to be very significant due to the linear stress dependence of the induced deformation. The tightening stress in the fuel assembly bolt was predicted to be almost completely relaxed in several years.

Related Papers

Computer Simulation of Early-Stage Irradiation Creep, Nagakawa, J., Yamamoto, N. and Shiraishi, H. J. Nucl. Mater. 179–81 (1991): 986–89.

Calculational Evaluation of Radiation Induced Deformation, Nagakawa, J. (to be published in Proc. of the 4th Int'l Symp. on Advanced Nuclear Energy Research).

Materials

Non-ferrous materials

63 Basic Research to Establish Design Techniques for Advanced Materials

April 1989 to March 1994

M. Yamazaki, Materials Design Division*

Keywords: system for advanced materials design, cluster variation, thermodynamics

The objective of this research is to establish the system for advanced materials design using both calculations such as cluster variation and thermodynamics, and experimental knowledge on alloy design. The systems is mainly constituted with two subsystems: one to estimate microstructures through alloy composition and processes, and other to estimate properties from the compositional parameters such as alloy compositions of phases of alloy and structural parameters such as volume fraction and lattice parameters of the phases. This study has currently been carried out for Ni-base superalloys, titanium alloys and C/C composites.

Related Papers

Creep Properties of $\alpha + \alpha_2$ High Temperature Titanium Alloys Designed by the Aid of Thermodynamics, Onodera, H., Nakazawa, S., Ohno, K., Yamagata, T. and Yamazaki, M. ISIJ Int. 31 (1991): 875–81.

64 Microstructural Refinement and Mechanical Properties of Titanium Alloys

April 1991 to March 1994

T. Kainuma, Mechanical Properties Division

Keywords: Ti-3-8-6-4-4, mechanical properties, microstructural refinement, hydrogen absorbing

Recently, metastable beta-type titanium alloys have drawn attention because of their excellent formability. However, a rapid grain growth is known to occur when they are annealed at temperatures, above the beta transition temperature T_β. Then, a metastable beta-type alloy with a composition of Ti-3Al-8V-6Cr-4Mo-4Zr (Ti-3-8-6-4-4), which is resistant to grain growth even at temperature above T_β, was developed for applications requiring cold formability and high strength.

The aim of this work is to reveal the mechanism of microstructure refinement of grain size, substructure and alpha phase precipitation due to thermomechanical treatment and the hydrogen absorbing treatment in Ti-3-8-6-4-4 alloy. The mechanical properties of the alloy with the refined microstructures will also be evaluated.

1. Microstructural refinement and mechanical properties.

   The grain refinement for Ti-3-8-6-4-4 alloy is mainly achieved by heavy cold-rolling, followed by short time recrystalization method. The addition of silicon to the alloy substantially help refine the grain size. The substructural refinement in the alloy are achieved by the combination of various annealing condition and various reduction ratios of cold rolling. The relationship between the grain refinement and the alpha precipitate morphology is currently being determined.
2. Microstructural refinement by hydrogen addition.

* Present address: NASDA

Previously we have shown that hydrogen absorption and formation of dislocation structures induced by the absorption, occurs during the specimen preparation of the beta-type titanium alloy, such as the cold rolling, the emery polishing, the diamond cutting and the water quenching.

In this work, we have tried to understand the absorption mechanism of hydrogen by changing composition of atmosphere. In addition, the dislocation structure has been examined for the Ti-3-8-6-4-4 alloy charging with hydrogen, and revealing that the high dislocation density is caused by pinning effect due to hydrogen atoms which retards the recovery of dislocations introduced by the thermomechanical treatments. The possibility of the further refinement of microstructure using hydrogen effect is also studying.

Intermetallic compounds

(65) Improvement of Mechanical Properties of Intermetallic Compounds by Crystal Growth Control

April 1992 to March 1997

T. Hirano, Chemical Processing Division

Keywords: unidirectional solidification, floating zone method, Ni_3Al, room-temperature ductility

The objective of this study is to improve the mechanical properties of intermetallic compound by crystal growth control. Recently, we have found that unidirectional solidification using a floating zone method is remarkably effective in enhancing the room-temperature ductility of Ni_3Al without addition of alloying elements such as boron. The details are described in Research Topics. It exhibits more than 60% tensile elongation at room temperature. It indicates that brittleness of intermetallic compounds can be solved by crystal growth control. We call this method FZ-UDS. FZ-UDS is a new promising method to improve brittle intermetallic compounds.

In this study three subjects are stressed. First, crystal growth technique is developed in detail. Columnar grained Ni_3Al is grown by FZ-UDS, which is closely related to the large ductility mentioned above. Favorable growth conditions for such stucture are investigated. Secondly, the solidified structures are characterized, paying a much attention on the grain boundary structure. Thirdly, the mechanical properties are to be evaluated. Deformation mechanism is also studied. These studies are expected to clarify the mechanism of improving the ductility of intermetallic compounds by FZ-UDS.

(66) High Ionic Conductivity of Solid Electrolyte

April 1992 to March 1995

H. Nakamura, Environmental Performance Division

Keywords: ionic conductor, solid electrolyte, charge carrier, electrical conductivity

Recently, research works on the solid high ionic conductor have been mainly focused on the oxygen ion conductor such as ZrO_2, the proton conductor such as $SrCeO_3$ and sodium ion conductor such as $\beta - Al_2O_3$. One of the reasons why no other solid electrolytes has been developed as high ionic conductor is that the sintered materials prepared for the solid electrolyte tend to initiate cracks caused by the grain growth or voids along the grain boundary.

The purpose of this study is to synthesize a new solid electrolyte consisting of oxides and sulfates ($M_2O - B_2O_3 - M_2SO_4$ M = Li, Na, K) that posesses grain boundaries or voids as little as possible by a rapid quenching method, and to investigate the suitable composition of the compound in solid-liquid coexisting composition range by various thermal analytical methods.

Furthermore, the electrical properties for the electrolyte can be evaluated by the measurement of the electrical conductivity, the investigation of the polarzing behavior, the determination of the charge carrier, the comparison of the electro motive force of the concentration cell with that of the theoretical one, etc.

67 Preparation of Spontaneous Exothermic Metals and Its Application

April 1990 to March 1993

T. Fujii, Chemical Processing Division

Keywords: skelton structure, exothermic metals, compound

We have previously shown that a spontaneous generation of heat can easily be taken place in the air from the bulk material of Ni-Al alloys after leaching. These materials are called "Spontaneous Exothermic Metals". This year Co-Al alloys with the composition of 30 to 60 wt%Co-Al were prepared by a self-propagating high-temperature synthesis (SHS) method under a vacuum of 1×10^{-3} Pa for the purpose of refinement of microstructure. These alloys are leached to dissolve the Al element in an alkaline aqueous solution at about 373K. The measurement of the exothermic characteristics was conducted with a newly disigned thermobalance.

The results obtained at present stage are summarized as follows.

1. The alloys produced by SHS were composed of two or three kinds of intermetallic compounds with Co_5Al_{13}, Co_2Al_9 and Co_xAl_y phases.
2. After leached, the X-ray diffraction pattern showed all intermetallic compounds with a

large line broading, indicating the skelton structure.
3. The leached compounds had stable spontaneous exothermic reaction in air atmosphere and maximum spontaneous exothermic temperatures were 998K to 1058K in inverse proportional to the amounts of Co.
4. On the leached surface of Co_2Al_9 phase the particles consisting of CoO less than 70nm in diameter are presented much more frequently after spontaneous exothermic reaction.

68 Fatigue Fracture Mechanisms for TiAl Intermetallic Compounds at High Temperatures

April 1991 to March 1994
K. Yamaguchi, Failure Physics Division
Keywords: TiAl intermetallic compound, fatigue strength, fatigue fracture surface

The TiAl intermetallic compound has a potencial for high temperature structual applications due to its low density, high strength and good oxidation resistance. The poor ductility at room temperature has been improved by recent R&D. To make use of the attractive and unique properties, it is important to study the dynamical behavior such as fatigue strength as well as the static one.

Samples for fatigue experiments were prepared from a 7 kg ingot by skull melting and casting. The chemical composition is 36.1 and 33.9wt%Al. This material has the maximum tensile fracture elongation by 2.2% among the as-cast materials from 28wt% to 38wt% with the aluminum content.

The microstructure of the as-cast Ti-33.9%Al consisted of large grains containing full lamellar morphology of γ(TiAl) and α_2(Ti_3Al) phases.

The material showed a good fatigue resistance at room temperature and 800 °C. Especially, the fatigue strength at 800 °C is comparable to that at room temperature. The fatigue fracture surface consisted mainly of transgranular mode reflecting the lamellar structure. Intergranular fracture mode was not observed, though the intergranular mode was occationally observed in full annealed TiAl intermetallic compounds of γ single phase.

Related Papers

"Fatigue Properties and its Mechanisms of Ti-Al-V Intermetallic Compounds", Yamaguchi, K., Shimodaira, M. and Nishijima, S. J. Iron and Steel Inst. 78 (1992): 134–40 (in Japanese).

69 Production and Character Evaluation of Functional Intermetallic Compounds

April 1988 to March 1993
M. Nakamura, 3rd Research Group
Keywords: coatings, thermoelectric, combustion synthesis, TiAl, effect of weightlessness

Many intermetallic compounds are candidates for new functional and structural materials with peculiar and excellent properties which conventional metals and alloys are not endowed with. The basic research work on intermetallic compounds like aluminides, silicides, etc. for functional and structural applications have been carried out. Fabrication and application of the intermetallic compounds like TiAl, NiTi, $FeSi_2$, etc. have also been studied. The following items are the research subjects:

1. Coating of Intermetallic compounds for High Temperature Corrosion Resistance.
2. Development of High Performace Thermoelectric Intermetallic Compounds.
3. Combustion Synthesis of Intermetallic Compounds.
4. Development of Light-weight Heat-resisting Materials Based on TiAl Intermetallic Compound.
5. Effect of Weightlessness on Microstructure and Strength of Ordered TiAl Alloys.

Related Papers

Structure and Properties of Ni-TiC Cermet Films Formed by Ion Plating, Ishida, K., Ogawa, K., Kimura, T. and Takei, A. Thin Solid Film 191 (1990): 69–76.

Studies on the Holes of p-type $Bi_2Te_{2.85}Se_{0.15}$ Single Crystal, Kaibe, H.T., Sakata, M. and Nishida, I.A. J. Phys. Chem. Solid 51 (1990): 1083–87.

Superplasticity of TiAl Intermetallics, Nobuki, M. and Tsujimoto, T. Advanced Structural Materials Vol. 2, Han, Y., ed., Elsevier Science Publishers B. V., Amsterdam (1991): 791–96.

70 High Performance Materials for Severe Environments-I (Microstructure and Properties of Intermetallic Compounds with High Specific Strength)

April 1990 to March 1994
M. Nakamura, 3rd Research Group
Keywords: TiAl, heat-treatment, thermomechanical processing, microstructure, mechanical properties, environmental effect.

Light-weight, heat-resisting intermetallic compound TiAl is a candidate for a structural use in severe environments such as space plane, etc. In this research program, the mechanical properties are systematically studied for TiAl base alloys, of which composition and microstructure are well controlled. The fundamental methods to control microstructure which gives the optimum properties for a practical use to materials are discussed. TiAl base alloys with various microstructures and compositions have been prepared by heat-treat-

ment and thermomechanical processing using isothermal forging above 1000°C, and the effect of microstructure on mechanical properties like strength, ductility, etc. has been studied. The environmental effect on mechanical properties like room temperature tensile properties, etc. and high temperature oxidation behavior have been also studied.

Related Papers

Microstructures and Deformation Properties in TiAl Intermetallics Containing Ti_3Al, Nobuki, M. and Tsujimoto, T. Proc. Int. Symp. on Intermetallic Compounds Izumi, O., ed., The Japan Institute of Metals (JIMIS-6) (1991): 451–55.

Effect of Heat-Treatment on Tensile Properties of Forged TiAl-Base Alloy with Addition of Manganese, Hashimoto, K., Nobuki, M., Doi, H., Nakamura, M., Tsujimoto, T. and Suzuki, T. The Japan Institute of Metals (JIMIS-6) (1991): 457–61.

[71] Advanced Intermetallic Compounds for Nuclear Reactors

April 1987 to March 1992

T. Hirano, Chemical Processing Division

Keywords: intermetallic compounds, electrical properties, elastic properties, unidirectional solidification, irradiation

The objective of this study is to develop intermetallic compounds for advanced nuclear reactors, focussing on transition metal disilicides and aluminides. These compounds have attractive high-temperature mechanical properties and corrosion resistance and, therefore, are considered to be candidate materials for the advanced nuclear reactors. However, these favorable properties have not been clarified because it is very difficult to fabricate good samples. Our major efforts are in the field of single crystal growth, characterization of crystal structures, and evaluation of physical and mechanical properties of these compounds. The effect of irradiation on the mechanical properties is also examined. The experimental equipment in use are floating zone furnace with infrared heating, X-ray diffractometer, cyclotron irradiation facility, and mechanical testing equipment.

Single crystals of transition metal disilicides, from group IVa through VIII, have been successfully grown by a floating zone method. The electrical and elastic properties of these compounds have been measured and their crystallographic anisotropy have been discussed. The high-temperature mechanical properties of $MoSi_2$ and WSi_2 showed that these compounds are attractive materials for high-temperature applications.

Unidirectional solidification of Ni_3Al using a floating zone method showed a remarkable improvement of the room-temperature of this compound without addition of alloying elements such as boron. We named this method as FZ-UDS. Cold rolling is possible. It also shows a good resistance to helium ion irradiation. The details are described in Research Topics.

Related Papers

Electrical Resistivities of Single-crystalline Transition Metal Disilicides, Hirano, T. and Kaise, M. J. Appl. Phys. 68 (1990): 627–33.

High Temperature Deformation Behavior of $MoSi_2$ and WSi_2 Single Crystals, Kimura, K., Nakamura, M. and Hirano, T. J. Mater. Sci. 25 (1990): 2487–92.

Cold Rolling of Boron-free Polycrystalline Ni_3Al Grown by Unidirectional Solidification, Hirano, T. and Mawari, T. Scripta Metall. et Mater. 26 (1992): 597–600.

[72] Crystal Growth on the Surface of Single-Crystalline Intermetallic Compounds

April 1991 to March 1992

T. Hirano, Chemical Processing Division

Keywords: intermetallic compound, single crystal, Schottky barrier height

The purpose of this study is to investigate a formation mechanism and properties of the metal/semiconductor interfaces which are formed on intermetallic compound surfaces, by measurements of schottky barrier height (SBH) at various temperatures. Cobalt disilicide ($CoSi_2$) and calcium disilicide ($CaSi_2$) were chosen as substrate materials for the following reasons:

1. SBH of Si/metal silicide (MSi_2) is sensitive not only to the kind of metals but also to interface structure.
2. For the above reason, MSi_2 has used in electrodes and gates of very-large-scale intergrated circuits.
3. Lattice mismatch to Si is small for both disilicides and they epitaxially grow on Si.
4. Chemical bonding characteristics of Si-Si bond in $CoSi_2$ are different from that in $CaSi_2$.

We designed the apparatus for precise measurements of SBH at high temperatures. Since it is important to keep cleanness of the sample during heating and to eliminate the leakage current, we chose combination of a chamber fabricated from stainless steel with BNC connectors, an infrared heating system with halogen lamp and a picoammeter. The sample is heated by infrared rays introduced into the chamber through a quartz rod. A shutter between the rod and the sample enable us to heat the sample locally by changing the diameter of the rays. Resistivity measurements at high temperatures are carried out under high vacuum in this chamber.

The (111) silicide substrates were cut from single crystals grown in a flowing Ar atmosphere by a

floating zone method with infrared heating[1, 2].

We plan to measure the temperature dependence of SBH of Si/MSi_2 interface by current-voltage method. These results will be discussed in relation to a formation process of Si/MSi_2 interface.

Related Papers

Electrical Resistivities of Single Crystalline Transition-Metal Disilicides, Hirano, T. and Kaise, M. J. Appl. Phys. 68 (1990): 627–33.

Single -Crystal Growth and Electrical Properties of $CaSi_2$, Hirano, T. J. Less-Common Met. 167 (1991): 329–37.

Composites

73 Thermal Effects on the Material with Heterogeneous Phase

April 1990 to March 1993

I. Shiota, Physical Properties Division

Keywords: MMC, heterogeneous phase, thermal stability, interfacial reaction, pit

Metal matrix composites (MMCs) consist of heterogeneous phases, and are hopeful for high-temperature applications in various fields such as aero-space and atomic reactors, as they have high specific strengths, high specific moduli, high heat resistivities and so on. However, MMCs are not thermodynamically in a state of equilibrium, and often deteriorates by chemical reactions at the interface between the reinforcement and matrix when they are exposed at elevated temperatures. Therefore, improving the thermal stability is most essential for high-temperature applications.

From the above-mentioned viewpoint, we have been trying to reveal the mechanism of interfacial reactions in order to improve MMCs. In this work, pure Ti and its alloys were used as matrices of composites. SiC fiber was used as a reinforcement. The reinforcement was a continuous fiber of SiC with carbon core which was produced by chemical vapor deposition. The diameter of SiC fiber was 140 μm. The composites were fabricated by hot-pressing. The fiber volume fractions were 40%. The alloy matrix composites had room temperature tensile strengths more than 2 GPa and densities slightly lighter than Ti, which were two times stronger than the ordinary steels and nearly a half of the density of them.

The effects of interphases formed at the interface on the tensile strength of the composites were investigated. Relationship between the tensile strength and heat-treatment time was also examined for extracted-fibers from composites. Tensile strengths were measured at a room temperature. Heat-treatments were carried out at 1123K for 32.4–360 ks. The tensile strength of composites decrease with increasing the thickness of the reaction products. Several reaction products were formed at the interface, and they showed a layer by layer structure. The composition of the inner layer was mainly TiC, whereas the outer was Ti_5Si_3. The total thickness lineally increases as a function of square root of heat treatment time, indicating that the rate determining process of the reaction is diffusion of Si or C. When the total thickness of the reaction products reaches to 3 μm, the tensile strength of composites abruptly decreased. The tensile strength of the as-received fibers and the extracted-fibers from as-fabricated composites showed a typical Weibull distribution. On the other hand, the extracted-fibers from the heat-treated composites were classified into a slight-loss group and a large-loss group. A pit was observed on the edge of fracture surface of an extracted fiber with the large-strength loss group. The pit was considered to be caused by a local growth of reaction product.

From these results, the critical thickness of reaction products at the interface was 3 μm for composites of pure Ti matrix and alloy matrices. The degradation of fiber was caused by stress concentration at the pit of surface. It is considered that the strength of composites are abruptly deteriorated by pits formed at the surface of fibers when the total thickness of reaction products reaches to 3 μm.

Related Papers

The relationship between interfacial reaction and tensile strength of SiC filament reinforced Ti alloy composites, Imai, Y., Shinohara, Y., Ikeno, S. and Shiota, I. Proc. 5th Japan–US Conf. Compos. Mater Jpn. Soc. Compos. Mater., Tokyo (1990): 347–54.

Deterioration Factor of SiC/Ti Alloy Composite after heat Treatment, Imai, Y., Shinohara, Y., Ikeno, S. and Shiota, I. ISIJ International 32 (1992): No. 8: 928–33.

Materials for mechanical application

74 Intelligent Structural Materials

April 1991 to March 1996

S. Matsuoka, Environmental Performance Division

Keywords: intelligent material, sensing, processing, actuating, damage

A concept "intelligent material" was originated in Japan. The intelligence of the material is being defined as self-detectablity for environmental changes and feasibility of sensing, processing and actuating, just like living creatures.

In this study, fundamental research has been carried out in order to impart the intelligent functions to the metallic materials for structural use. Small cavities which do not deteriorate the mechanical properties exist in the structural materials. An at-

tempt has been made to implant the sound-emitting material or phase-transformed material into the cavities. The implantation could make the material possible to self-sense and self-restore the damage during operation. A nano-technology based on the scanning tunneling microscope and atomic force microscope has also been developed to evaluate the intelligent functions of the materials from atomic scale viewpoint.

75 Development of Metal Matrix Composites for High Temperature Use Through Combinations of Advanced Powder Metallurgy Processes

April 1991 to March 1994
M. Hagiwara, Mechanical Properties Division
Keywords: titanium, powder metallurgy, rapid solidification, titanium matrix composite

Titanium alloys are ideally suited for airframe and gas turbine engine components because of their unique mechanical properties. However, the service temperature is limited to 600 °C due to a rapid degradation of creep strength, metallurgical stability and environmental resistance. However, there still has much room to develop advanced titanium alloys having superior combinations of high-temperature strength, creep resistance, stiffness, corrosion resistance and thermal stability for future aircraft components available at temperatures up to 1000 °C.

The application of advanced powder metallurgy processes such as rapid solidification (RS) can be considered as one possible route to expand the service temperature of titanium alloys. RS could improve high-temperature properties of conventional titanium alloys because post thermal exposure results in a fine distribution of insoluble dispersoid particles such as carbides, oxides and borides. Powder metallurgy also provides a flexible process for manufacturing composites reinforced with relatively large size (1 to 40 μm) ceramic particles.

Our research group has been devoted to the production of RS titanium powders using plasma rotating electrodes process (PREP) and melt spinning apparatus. We are also engaged in the research and development of a new class of particle reinforced RS titanium matrix composites, with emphasis on relationship between composition/microstructure and high-temperature mechanical properties.

Related Papers

Mechanical Properties of Particulate Reinforced Titanium-based Metal Matrix Composites Produced by the Blended Elemental P/M Route, Hagiwara, M., Emura, S., Kawabe, Y., Arimoto, Y. and Suzuki, H.G. ISIJ Int. 32 (1992): 906–16.

Microstructures and Tensile Properties of Titanium-Based Composites Produced by Powder Metallurgy, Hagiwara, M., Emura, S., Takahashi, J., Kawabe, Y. and Arimoto, N. Proc. 6th World Conf. Titanium (1992) (in preparation).

76 Development of Damping Materials

April 1989 to March 1992
K. Kawahara, Physical Properties Division
Keywords: aluminum bronze, damping material

Aluminum bronze alloys, which are known as shape memory alloys, have been examined for the purpose of developing high-strength and high-quality damping materials. These alloys have generally higher strength than manganese-based damping alloys, though the former have difficulties in cold workability. We have evaluated the effect of alloying elements on the mechanical properties and damping characteristics of the Al-Cu alloy. The damping capacity was measured under a cantilever beam method, using plate-like specimens. The alloys containing nickel, iron, manganese, cobalt, vanadium and chromium individually, were prepared and tested. These alloying elements were chosen from the following viewpoint:

1. Whether the amount of their solubility in manganese or copper is large or small
2. Whether the intermetallic compounds of manganese or copper are formed or not by additive elements.

Addition of elements having a large solubility in copper or aluminum showed a tendency to increase in the damping quality. To guarantee the best quality, a quenching was required for the alloys containing nickel, while slow cooling was neccessary for the alloy containing manganese. Manganese was more effective in improving the damping quality than nickel. We have yet obtain the logarithmic decrement data of less than 0.1 for smooth sample, although the highest value was reported to be more than 0.4. However, we have found that the value increases up to over 0.15 for the notched samples as notch depth, made near vice, increases from the edge to the center of the specimen, suggesting that the value increases as the testing condition approaches that of a single crystal.

Materials for electronics application

77 Fabrication of High-T_c Superconducting Wires

April 1988 to March 1993
H. Maeda, 1st Research Group
Keywords: high-T_c oxide superconducting wire, Y-Ba-Cu-O, Bi-Sr-Ca-Cu-O

The goal of this study is to fabricate long high-T_c oxide superconducting wires and tapes with sufficient flexibility and high critical

current density, J_c. As the oxide superconductors are intrinsically brittle, we have been studying on various potential wire fabrication techniques based on vapour phase, solid phase and liquid phase reaction process, and the increase in J_c, especially, in magnetic fields, for Y-Ba-Cu-O and Bi-Sr-Ca-Cu-O superconductors.

$Bi_2Sr_2CaCu_2O_8$(2212)/Ag composite tapes were prepared by applying dip-coating method and powder-in-tube method. High grain alignment of the 2212 layer is attained by partial melting and slow cooling process. In this process, it turns out that the silver substrate plays an important role for the grain alignment. By this way, J_C of the tape is significantly improved. The J_C-values larger than $1 \times 10^5 A/cm^2$ is easily obtained in magnetic fields above 20T at 4.2K. These values are much larger than those of conventional metallic superconductors Nb-Ti and Nb_3Sn. Fabrication of coil is now in progress. Details of the coil fabrication procedure are presented in "Topics" of this volume. Moreover, for Bi-oxides, other techniques such as plasma spraying, suspension-spinning and chemical coating combined with laser irradiation annealing, glass crystallization and internal oxidation have been studied to apply the fabrication of superconducting tapes and magnetic shielding sheets or vessels. To further improve J_c, we have been studying on the fundamental problems such as the flux motion in high-T_c materials using 2212 single crystals and the introduction of pinning center to prevent the flux motion by applying ion irradiation.

For Y-oxide superconductors, vapour deposition techniques such as sputtering, laser ablation and hot plasma flash evaporation (HPFE) have been employed. Especially, by applying the HPFE technique, we have been studying the deposition of Y-oxide thick films on metallic substrate with a buffer layer of YSZ, and obtain excellent superconducting properties such as T_c of 91K and a J_C of $4.3 \times 10^4 A/cm^2$ at 77K and 0T. In the HPFE process, one of the most important factors is continuous feeding the fine powders of around 1μm radius. To attain the continuous deposition, further modification of the feeder system is now in progress.

Related Papers

Improvement in Critical Current Density of $Bi_2Sr_2CaCu_2O_8$ Tapes Synthesized by Doctor-blade Casting and Melt Growth, Kase, J., Irisawa, N., Morimoto, T., Togano, K., Kumakura, H., Dietderich, D.R. and Maeda, H. Appl. Phys. Lett. 56 (1991): 970–72.

Fabrication of BiSrCaCuO/Ag Composite Superconductors by Dip-coating Process, Togano, K., Kumakura, H., Kadowaki, K., Kitaguchi, H., Maeda, H., Kase, J., Shimoyama, J. and Nomura, K. Proceedings of ICMC 91 Huntsville, Alabama (in preparation).

Fabrication of Bi-Based Oxide Superconductors by YAG-Laser Irradiation, Yuyama, M., Wada, H., Itoh, K. and Kuroda, T. Cryog. Engineer 26 (1991): 288.

Preparation of YBa_2Cu_3Oy Superconducting Thin Films by Radio-Frequency Plasma Flash Evaporation, Fukagawa, W., Komori, K., Fukutomi, M., Tanaka, Y., Asano, T., Maeda, H. and Hosokawa, N. Jpn. J. Appl. Phys. 30 (1991): 1216–17.

78 Development and Evaluation of Advanced Superconducting and Cryogenic Materials

April 1990 to March 1993

H. Maeda, 1st Research Group

Keywords: Nb_3Al multifilamentary superconductors, magnetic refrigerator, high cycle fatigue

Three major materials have been studied to contribute to the development of advanced superconducting technologies.

The microstructure of Nb_3Al multifilamentary superconductors was studied with XRD, TEM, etc., and its effect on superconducting properties was revealed from the viewpoints of Al-core sizes, heat treatments and additive elements. With decreasing the Al-core size, the critical current initially increases, reaches a maximum, and then decreases. The small diffusion spacing between Nb and Al increases the volume fraction of A15 phase to other intermediate phases, decreases the lattice parameter of A15 phase, and hence facilitates to form the metastable A15 phase with the composition near stoichiometry. The filament "sausaging", however, brings about the degradation in superconducting properties at smaller Al-core sizes (<50nm). The additive elements of Ag and Mg increase the formation rate of Nb_3Al, which suggests that these elements are suitable for the development of ac superconductors heat treated at low temperatures.

A compact and hightly efficient magnetic refrigerator to form below 1K have been developed. Specially designed components of the refrigerator are pulsed superconducting magnets, a magnetic refrigerant and two thermal switches; a Ti alloy heat pipe and a mechanical contact switch for expelling the heat generated during magnetization. Large scale rare earth garnet single crystals of $(Dy_{1-x}Y_x)_3Ga_5O_{12}$ with x of 0.4 – 0.6, which have low magnetic transition temperatures of about 200 mK, have been grown and tested as magnetic refrigerants. Graphite was found to be one of the most promising candidates for the mechanical thermal switch and the graphite switch is now tested.

For SUS347 stainless steel (0.05C-8.98Ni-17.97Cr-0.60Nb), the effects of cold rolling and

sensitization, simulated Nb_3Sn formation (SNF) heat treatment (973K × 200h), have been examined on high cycle fatigue properties. The SUS347 steel is much less severely sensitized than Nb free austenitic stainless steels; however, the toughness is still deteriorated due to the occurrence of intergranular dimple fracture. The cold rolling accelerates the sensitization. When high cycle fatigue strength was measured in terms of one-million-cycle fatigue strength (FS), the FS increases as the test temperature decreases for all specimens: unrolled, unrolled + SNF treated, 10% cold-rolled, and 10% cold rolled + SNF treated. No significant difference among the FS's is recognized at 77K or 4K, although the 10% cold-rolled specimens show higher FS's than unrolled specimens at 293K. All the fatigue crack initiation sites are at the specimen surface and no feature of intergranular fracture is seen in fatigue fracture surface even at 4K.

Related Papers

Microstructure and Superconducting Properties of Nb_3Al Multifilamentary Wires Processed by Nb-Tube Method, Takeuchi, T., Kosuge, M., Iijima, Y., Hasegawa, A., Kiyoshi, T., Matsumoto, F. and Inoue, K. J. Japan Inst. Metals 55 (1991): 472–80.

A Carnot Magnetic Refrigerator Operating Temperature between 1.4 K and 10 K, Numazawa, T., Kimura, H., Sato, M. and Maeda, H. (in preparation Cryogenics).

Cryogenic Mechanical Properties of Ti-6Al-4V Alloy with Three Levels of Oxygen Content, Nagai, K., Yuri, T., Ogata, T., Umezawa, O., Ishikawa, K., Nishimura, T., Mizoguchi, T. and Ito, Y. ISIJ Intern. 31 (1991): 882–89.

79 Development and Characterization of Superconducting Materials for Fusion Reactor Magnet Use

April 1989 to March 1994
H. Wada, 1st Research Group
Keywords: Nb_3Al wires, critical temperature, critical current, strain

The purpose of this study is to develop high-field superconducting materials for fusion reactor use by characterizing and evaluating new, promising superconducting materials under those conditions that may be experienced by them when wound to a superconducting magnet which should confine and control plasma in the reactor.

In fiscal year 1991, effects of tensile strain on superconducting properties of multifilamentary Nb_3Al wires were studied. Multifilamentary Nb_3Al wires fabricated by a modified composite diffusion process show high critical current densities at high fields, comparable to those for practical Nb_3Sn wires. Degradations of both critical temperature and critical current with strain were smaller for Nb_3Al wires than for Nb_3Sn wires. The strains for the occurrence of permanent degradation in the critical current, the irreversible strain, were beyond 1%, which are comparable to those for in situ processed Nb_3Sn wires. Large irreversible strains for Nb_3Al may be attributed to Nb_3Al filament diameter sizes which are in the range of submicron.

Power losses in ac fields and effects of neutron irradiation on the critical current in Nb_3Al wires are to be studied.

Related Papers

Strain Effects on Superconducting Properties in Nb_3Al Ultra-Thin Filamentary Wires, Kuroda, T. and Wada, H. J. Japan Inst. Metals 55 (1991): 344–50 (in Japanese).

80 Synthesis of New Functional Materials by the Application of Host-Guest Reactions

April 1990 to March 1992
M. Amano, Physical Properties Division
Keywords: insertion/extraction reactions, ionic-conductor materials, hydrous pentavalent oxides

The aim of this project is to synthesize new functional materials by applying insertion/extraction reactions. We are trying to synthesize new ionic-conductor materials by using ion exchange processes. Hydrous pentavalent oxides have been selected as the object materials, because they are known to possess interesting ion exchange properties and some hydrous oxide of Sb, Nb and Ta, e.g., $HSbO_3 \cdot xH_2O$ and $HNbO_3 \cdot xH_2O$, are known as ionic conductors. These compounds can be prepared by acid treatment of the corresponding alkali metal compound such as $LiSbO_3$, $KSbO_3$ and $LiNbO_3$. Different crystal structures of hydrous oxide can be obtained by changing the preparation process.

Proton conduction in the prepared samples has been studied by making use of an impedance analyser. The mechanism of the proton conduction in the prepared samples has been investigated by means of NMR, TGM and FTIR. The applicability of the synthesized materials to fuel cells will be also investigated.

81 Evaluation and Application of Cu-Ag Alloy as Conductor Material in High Field

April 1991 to March 1992
H. Maeda, 1st Research Group
Keywords: Cu-Ag alloys, high ultimate tensile strength, high electrical conductivity

The development of conductor material with high mechanical strength is very important for making resistive high-field magnets, such as a

pulsed magnet and a water cooled magnet. Recently, we have found that the heavily-cold worked Cu-Ag alloys show excellent properties as a conductor materials. When the Cu-Ag alloys including 10 to 16at% Ag were cold-drawn into wires with several intermediate annealings at 450 °C, they exhibited high ultimate tensile strength above 1GPa and high electrical conductivity above 80% IACA at room temperature.

In this year we have established the fabrication process of the Cu-Ag alloy wire with net weight up to 40kg, including the optimized conditions of high-frequency melting, die casting, hot forging, annealing, and cold-drawing. Because the spring-back force of the Cu-Ag alloy wire is very strong, it is very hard to wind the thick wire into a coil. However, we have succeeded in fabrication a small pulsed magnet by winding a rectangular Cu-Ag alloy wire of 2mm × 3mm. The performance of the pulsed magnet is now testing. For winding thicker Cu-Ag wires into coils, we have designed a powerful winding machine and it is ready for fabricating it now.

Collaborating with the Francis Bitter National Magnet Laboratory (FBNML), USA, we measured the resistivities of the Cu-Ag alloy wires and plates in high fields, which are very important to design the high-field resistive magnets. Application of the Cu-Ag alloy plates to the Bitter-type water-cooled magnets are also being discussed with the magnet designers of FBNML.

Related Papers

Development of High-Strength, High-Conductive Copper-Silver Alloys, Sakai, Y., Inoue, K., Asano, T. and Maeda, H. "J. Japan Inst. Metals" 55 (1991): 1382–91 (in Japanese).

Development of High-Strength, High-Conductivity Cu-Ag Alloys for High-Field Pulsed Magnet Use, Sakai, Y., Inoue, K., Asano, T., Wada, H. and Maeda, H. "Appl. Phys. Lett." 59 (1991): 2965–67.

[82] Studies on Fabrication Processes of BiSrCaCuO Superconductors

April 1991 to March 1992

H. Maeda, 1st Research Group

Keywords: BiSrCaCuO oxide superconductor, powder-in-tube method, AgCu alloy-sheathed tapes

In order to utilize the BiSrCaCuO oxide superconductor for high field magnets, high mechanical strength as well as high superconducting critical current density, J_C are required. In the study, which has been carried out in collaboration with the University of Illinois, efforts have been focused on optimizing the raw powder compositions and finding new sheath materials for the BiSrCaCuO oxide tapes. After final sintering treatment, conventional pure Ag-sheathed tapes becomes so soft as the oxide core within the sheath being easily cracked during handling. AgCu alloy sheaths have been investigated. Both Bi2212 and Bi2223 phase tapes have been fabricated using the AgCu alloy sheaths with various Cu concentration by the powder-in-tube method. The critical temperature, T_C's of AgCu alloy sheathed tapes (AgCu-tape) with Cu concentration upto 20at% for Bi2212 and 13at% for Bi2223 tapes are equivalent with those of pure Ag sheathed tapes (Ag-tape). The J_C values for the AgCu2212 tapes are nearly equal to those of the Ag-tape while those for the AgCu2223 tapes are greatly differed from those of Ag2223 tape. Relations between the J_C and microstructures on both 2212 and 2223 tapes have been studied. Furthermore, the AgCu alloy sheathed tapes can be cold worked rather easily and the Vickers hardness of AgCu tapes increases upto about 200, which is two times larger than that of Ag tape. Lithium addition or pratial substitution to the 2212 raw powders produces the interesting changes in melting temperature, T_C and resistive transition curve. AgCu tapes using the lithium doped powders are being studied.

Related Papers

Fabrication and Superconducting Properties of AgCu Alloy-Sheathed BiSrCaCuO Oxide Tapes, Tanaka, Y., Asano, T., Yanagiya, T., Fukutomi, M., Komori, K. and Maeda, H. Jpn. J. Appl. Phys. 31 (1992): L235–L238.

Magnetic materials

(83) Fabrications of Mesoscopic Scale Materials and Their Properties

April 1992 to March 1995

I. Nakatani, Physical Properties Division

Keywords: mesoscopic scale materials, high-resolution electron-beam lithography, ferromagnetic fine-particle lattices, micromagnetic studies, iron-nitride magnetic fluids, sub-nanometer microclusters, whiskers of titanium diboride (TiB_2), metastable new phases of iron nitride

Mesoscopic scale materials are such materials that have sizes intermediate between atomic or molecular sizes and sizes of bulk materials. The interest of this project is focused on the fabrications and the magnetic properties of mesoscopic materials with sophisticated structures. The project involves basic research on novel properties of the mesoscopic scale materials and applied research on them.

The research program is divided into the following 5 items.

1. High-resolution electron-beam lithography is applied to fabricate the ferromagnetic fine-particle lattices that are arrays of deep sub-micron particles of Fe-Ni alloy or Co-Cr alloy with controlled sizes, distances and symmetry. Using ferromagnetic resonances, Bitter pattern observations and accurate measurements of magnetization, micromagnetic studies are made on the fine-particle lattices in which single-domain fine particles have controlled magnetic interaction.
2. Research on synthesize of iron-nitride magnetic fluids, having the highest magnetization exceeding 0.3Tesla and the lowest viscosity of 2000 mPa·s, is on going by the method of vapor-liquid reaction. Superparramagnetic properties of the magnetic fluids are studied by magnetization measurements, ferromagnetic resonances and Mössbauer effect measurements. New type of magnetic composites that ultrafine particles of iron-nitride are dispersed and suspended in resins is studied. Some applications of magnetic fluids to active dumper for automoble, inductors for radio frequency circuits, magnetic toners for xerography and cosmetic colors are being made cooperating with Japanese private companies.
3. Preparations of microclusters of ferromagnetic metals, sub-nanometer in size, are tried by the vacuum evaporation on the cold substrate of liquid. The size effects on cooperative phenomenon of ferromagnetism will be clarified by measurements of magnetization and Mössbauer spectroscopy on those fine particle systems.
4. Whiskers of titanium diboride (TiB_2), with high toughness and high electric conductivity, were grown by CVD reactions. Their crystallographic, electric and mechanical properties are being studied.
5. Microwave-plasma CVD reaction is applied to synthesize metastable new phases of iron nitride. Magnetic properties of the new phases are studied in terms of the ferromagnetic interaction between the iron atoms.

[84] Fabrication and Properties of Novel Metallic Materials with Artificial Microstructures

April 1989 to March 1992
I. Nakatani, Physical Properties Division
Keywords: micromagnetics, ultrahigh-resolution electron-beam lithography, fine particle lattices, new magnetic excitation modes of magnetic dipolar waves

Ferromagnetic fine particles are widely applied to recording media, permanent magnets and magetic fluids. Micromagnetics is concerned with magnetic particles whose dimensions lie in the same order of magnitude as the thickness of the Bloch walls. At present, an accurate description of the magnetic properties of ferromagnetic single-domain particles, however, remains an unsolved problem. If the microscopic status of the individual particles can be specified in terms of magnetization, magnetic anisotropy and dynamic motion of magnetic spins, considerable progress of micromagnetics and their applications is foreseen. For clarifying these problems, suitable samples require the control of their particle sizes, shapes, morphology, relative orientations and spacing. In this project, making use of ultrahigh-resolution electron-beam lithography, we fabricated fine particle lattices of submicron particles or stripes of permalloy or Co-Cr alloy. The lattices are well controlled and consist of 10^5 – 10^6 identical particles arrayed in the manner of rectangular or triangular symmetries with identical spacing between the particles. Highly accurate magnetization measurements, ferromagnetic resonances and Lorentz transmission microscopy are employed to investigate micromagnetism for the fine particle lattices. Recently, in the fine particle lattice we have found new magnetic excitation modes of magnetic dipolar waves, which the precession motion of a dipole can propagate in the plane of the fine particle lattice in the form of waves with the amplitude changes from dipole to dipole. The physical description is provided to the magnetic dipolar waves.

[85] Properties and Applications of Mesoscopic Scale Materials—Metallic Magnetic Fluids, Ultrafine Particles of Metals and Thin Whiskers of Semimetal

April 1989 to March 1992
I. Nakatani, Physical Properties Division
Keywords: iron-nitride magnetic fluids, ultrafine particles, TiB_2 whiskers

The objectives of this project are research and development on metallic magnetic fluids of iron-nitrides, ultrafine particles of metals and thin whiskers of semimetal TiB_2.

It is unlikely that any type of liquid will be found that is intrinsically ferromagnetic. Ferromagnetic substances—for example, iron, iron alloys or iron oxides—are only ferromagnetic in a solid state. Magnetic fluids are liquids that can be strongly magnetized by applying magnetic fields and they have all sorts of fascinating features. Magnetic fluids are composed of ferromagnetic fine particles of several nanometers colloidally dispersed in a liquid carrier. In most of magnetic fluids that are currently used, magnetite (Fe_3O_4) or ferrites are used as ferromagnetic particles. The purposes of this study is to develop new types of

magnetic fluid of ferromagnetic metals, alloys or iron nitrides with higher magnetizations than the magnetizations of the magnetite or ferrites.

We have developed the following three methods: (1) Vacuum evaporation method, (2) plasma chemical vapor deposition and (3) vapor-liquid chemical reaction. The method (1) is used for preparing the magnetic fluids of metals or alloys, and the method (2) and (3) are for iron-nitride magnetic fluids. In the method of the vapor-liquid chemical reaction (3), iron carbonyl ($Fe(CO)_5$) is reacted to ammonia gas in a carrier liquid of kerosine added with a dispersant such as a surfactant. The magnetic fluids obtained by the method have the saturation magnetization $4\pi M_s$ exceeding 0.23T, which is 5 times larger in magnitude than the maximum value of the magnetic fluids in the past.

Magnetic properties of ultrafine particles in the magnetic fluids prepared by these method were also examined. It was shown that the particles of iron, cobalt and nickel were ferromagnetic down to the size of 2nm.

Titanium diboride (TiB_2) is a compound having high hardness and high electric conductivity. Whiskers of titanium diboride were prepared by chemical vapor deposition (CVD) from $TiCl_4$ and BBr_3. It is essential for growing whiskers to use fine particles of Ti-Ni alloy or fine particles of Si as catalysts during the deposition. At present, the whiskers are expected to be useful for heat resisting composite materials or electric conductive materials.

Related Papers

Preparation and Magnetic Properties of Colloidal Ferromagnetic Metals, Nakatani, I., Furubayashi, T., Takahashi, T. and Hanaoka, H. J. Mag. Mag. Mater 65 (1987): 261–64.

Iron-Nitride Magnetic Fluids Prepared by Plasma CVD Technique and Their Magnetic Properties, Nakatani, I. and Furubayashi, T. J. Mag. Mag. Mater 85 (1990): 11–13.

Mössbauer Studies of Colloidal Ultrafine Particles of Iron, Furubayashi, T. and Nakatani, I. IEEE Trans. Mag. 26 (1990): 1855–57.

Magnetic Properties of Ni Fine Particles, Furubayashi, T. and Nakatani, I. Solid State Commu. 74 (1990): 821–24.

Ferromagnetic Resonances of Metallic Fine Particles, Nakatani, I., Furubayashi, T. and Nose, H. Proc. Inter. Sympo. Phys. Mag. Mater (1987): 182–85.

Preparation and Magnetization of Colloidal Ferromagnetic Metals, Furubayashi, T. and Nakatani, I. Proc. Inter. Sympo. Phys. Mag. Mater (1987): 186–89.

Titanium-Diboride Whiskers, Nakatnai, I. and Ozawa, K. Ceramics 24 (1989): 307–12 (in Japanese).

Opto-materials

86 Reversible Color Change Alloys

April 1989 to March 1992

H. Sasano, Physical Properties Division

Keywords: reversible color change alloy, optical recording, 1.5 electron compound, vapor-solid diffusion couple method

An Ag-50mol%Zn alloy quenched from a temperature above 570K shows a pink color. The alloy exhibits a color change to silver color on aging around 450K. The color change is reversible depending on the heat treatments. Such an alloy is called a reversible color change alloy and a candidate for optical recording material.

The main aim of this research program is to look for new alloys of this kind. There are many alloy systems which have 1.5 electron compound (electron/atom ratio = 1.5) of B2 or DO_3 crystal structure. It is well known that the compounds such as NiAl and Cu_3Al show a unique color. Therefore, our investigation was focused on the optical properties of these compounds.

It was found that the Cu-Zn-Al, Ag-Zn and Ag-Cd alloys having a specific composition, show the drastic color change with phase transformations. It was also found that these alloys can be easily synthesized by the vapor-solid diffusion couple method which was invented by our group. We examined the effects of aluminum addition to Ag-Zn and Ag-Cd B2 alloys on the spectral reflectivity and the solubility range. We also succeeded in synthesizing thin film of NiAl alloys by RF sputtering.

Materials for energy application

(87) Processing and Development of Isotopically Controlled Materials (ICM)

April 1992 to March 1996

T. Noda, 2nd Research Group

Keywords: isotopically controlled materials, ICM processing facility, laser CVD, chemical vapor infiltration

Project Description

Materials composed of isotopically selected elements realize the essential solution of subjects such as induced activity, He embrittlement, and compositional change caused by reactions with energetic particles.

The objectives of the program are (1) R&D of in-situ ICM processing facility utilizing infrared multi-photon decomposition reaction, (2) search of working materials for isotope separation, (3) development of in-situ synthesis of isotopically

controlled SiC, Si_3N_4, BN etc. and (4) development of ceramics and their composites with advanced properties. The program contains the following main subjects.

1. R&D of in-situ ICM processing facility (IC-MPF).
2. Search of working materials for isotope separation
   search or synthesis of Si, B and N working gases with a high selectivity for isotopes
3. Development of in-situ synthesis of ICM
   low temperature synthesis of ICM such as SiC, Si_3N_4 and BN using laser CVD
4. Development of ceramics and composites with advanced properties
   evaluation of neutron-irradiated properties of ICM by using a simulation code
   physical properties of ICM
   improvement of mechanical properties by chemical vapor infiltration process

Major Products

The designing of infrared laser beam line of IC-MPF was accomplished. The simulation code, IRAC, calculating transmutation and induced activity, and decay heat under various neutron irradition conditions covering thermal to 14MeV neutrons predicted superiority of ICM to conventional materials.

Low temperature synthesis of SiC film using laser CVD was studied. Polycrystalline SiC film could be formed even at 518K under a proper mixture condition of Si_2H_6 and C_2H_2.

Chemical vapor infiltration process to obtain SiC composite with a high purity and improved mechanical properties is being developed. Carbon fiber/SiC composite with a toughness three times higher than that of monolithic SiC was obtained.

Related Papers

Prospect of Material Processes for Low Activation, Noda, T., Abe, F., Araki, H., Suzuki, H. and Okada, M. Proc. 4th Int'l Symp. Advanced Nucl. Energy Res. Feb. 5-8 (1992).

Formation of Polycrystalline SiC Film by Excimer-Laser Chemical Vapor Deposition, Noda, T., Suzuki, H., Araki, H., Abe, F. and Okada, M. J. Mat. Sci. Let. 11 (1992): 477–78.

88 Fundamental Study of Microstructures and Properties to Develop High Performance Materials for Severe Environments (II High Temperature Intermetallic Compounds)

April 1990 to March 1997

*M. Yamazaki,** Materials Design Division

Keywords: niobium aluminide, mechanical and oxidation properties, powder metallugy

This research is to make clear the fundamentals about niobium aluminide intermetallic compounds. Three different approach are in practice, cast materials for mechanical and oxidation properties, and powder metallugy for process technology. In order to improve the brittleness of Nb_3Al intermetallic compound, two phase alloys composed of Nb_3Al phase (A15) and ductile Nb phase (A2) that are equilibriated at 1800 °C, were examined in Nb-Al binary and Nb-Al-X ternary alloys. In Nb-18at%Al binary alloy and three Nb-18Al-X (X; Co,Ta,W) ternary alloys, two phase structures were observed.

89 Study on a Porous Gas-Diffusion Electrode

April 1990 to March 1993

M. Kobayashi, Chemical Processing Division

Keywords: fuel cell, antimonic acid, lithium

Fuel cells have many attractive features for power utilities desiring urban power generation, and are promising in the following decades. Pilot plant of phosphoric acid fuel cell have already been operated in several places in the world. They are operated at ca. 200C, which poses severe problems for the constituent materials. Though operating condition of an alkaline fuel cell is milder, the rate of oxygen reduction and hydrogen oxidation is slow. The aim of this study is to seek an effective electrocatalyst and electrode material to overcome above disadvantage.

A simple test is considered to screen out good electrocatalysts from many candidate materials. The catalytic properties are roughly evaluated by measuring the cathodic polarization curve of suspension in an alkaline solution under 0_2 bubbling at 50C. Following the rough screening, disk samples are prepared by a hot press. The disk is installed in the cell, one side of the disk is in contact with an alkaline solution and the opposite side of the disk is exposed to a pure oxygen atmosphere. Cathodic polarization is measured at 50C. Noble metals on the activated carbon are used to prove the effectiveness of the above two step screening. As an electrode material, antimonic acid is prepared from lithium antimonate. A particular sample of lithium antimonate is packed in a column and a nitric acid solution flows down through the sample bed to exchange the lithium ion by hydrogen ion. The ion exchanged antimonic acid is a selective absorbent of lithium ion, and is also expected as the electrode material of the fuel cell. The kinetic study is carried out, and it is found that the ion exchange rate is strongly dependent on the temperature.

*Present address : NASDA

90 Environmental Degradation of Structural Materials for Light Water Reactors

April 1991 to March 1996
N. Nagata, 5th Research Group
Keywords: acoustic emission, AC-impedance, straining electrode

In order to clarify the initiation and growth mechanism of environmentally assisted cracking (EAC) in structural materials under high temperature pressurized water and to systematize the related data for the life prediction of components, following research items have already started: (1) Development of monitoring techniques for the initiation and growth of localized corrosion damage such as pits and SCC in high temperature water, and (2) clarifying the elemental EAC process and its modeling. As one of the monitoring techniques acoustic emission technique applicable to high temperature water condition is being developed. Prior to the fatigue test in high temperature water several basic experiments in air were conducted resulting in that AE signals associated with fatigue crack growth could be successfully measured.

As one of the electrochemical approaches, a new challenge to monitoring the localized corrosion damage by using an AC-impedance technique for WOL-type specimen is also being carried out. As a strong point of this system, a luggin tube of the reference electrode was mounted to a long and narrow hole machined in the center of thickness of the WOL-type specimen so that measurements of electrochemistry in the vicinity of the crack tip could be carried out. It was found that the AC-impedance technique might be applicable to the evaluation of localized corrosion damage in high temperature water. In addition, designing and fabrication of hydrogen electrode applicable to high temperature water are now underway. A new device of straining electrode testing machine was set up for the evaluation of submicroscopic reactions through measuring corrosion rate and repassivation rate of fresh metal surfaces disclosed in high temperature water.

91 Assessment of Strength and Structural Materials Database for Weldment in FBR Components

April 1991 to March 1996
Y. Monma, 5th Research Group
Keywords: creep, stainless steel, welded joint

Creep strain distribution of weldment is an important information to ensure the structural integrity of FBR (fast breeder reactor) components. Our goal is to predict the creep behavior of weldment components at high temperature in long times from the uniaxial creep strain-time equation. The materials used are austenitic stainless (304 and 316) and high Cr steels. Butt welded joints of GTAW (gas tungsten arc welding) were prepared using 50mm thick 316 steel plate with low C and medium N. Creep strain-time tests are being conducted at 550 °C using full-thickness as well as conventional small size specimens. Initial data up to 3000h suggests that we need refinement of existing constitutive equations for creep. In order to measure the strain distribution of the welded joint, an image processing technique using moiré interferometry of a CCD (charged couple device) camera has been developed for the creep interrupted specimens. We plan to improve this technique to be applied at high-temperatures. A computer simulation using FEM (finite element method) calculation to predict entire creep curve was partly successful. But we must take into account for the local variability of weldment for better accuracy of the prediction. A special stage has been installed to measure the hardness of the large joint specimens. The hardness distribution of the welded joint specimen is considered to reflect the local variabilty.

92 Fundamental Research on Application of New Functional Materials to Passive Components

April 1990 to March 1994
T. Ishihara, 5th Research Group
Keywords: shape memory characteristics, recovery stress, thermal and stress cycles, martensitic transformation

Evaluation of the shape memory characteristics under thermal and stress cycles in the environments is indispensable to ensure applicability and reliability of shape memory alloys used in nuclear power reactors. Then the effects of $\gamma \Leftrightarrow \varepsilon$ cyclic transformation on the shape memory characteristics were investigated on a commercial Fe-14Mn-6Si-9Cr-5Ni(wt%) alloy. ε martensite was stress-induced by deforming specimens at room temperature, and then it was reversely transformed to γ by heating under various stresses. The change of surface relief during reverse transformation was observed by a high temperature optical microscope equipped with a tensile testing machine. The recovery stress was measured by this apparatus after the "cyclic transformation" was repeated various times.

The characteristics in thermal and stress cycles in this alloy were further studied in details. The results are as follows. (1) In bending tests, nearly 100% shape recovery is observed in the case of small amount of strains, while in the case of large initial strains, the shape recovery is not good in the first thermal cycle, but it is soon increased in subsequent cycles. Decline in shape memory function

is much larger in the latter case as expected. (2) The recovery stress is proportional to the transformation strain produced by tension. The temperature at which the recovery stress shows a maximum becomes higher with increasing transformation strain. (3) When the specimens are stretched to induced martensitic transformation, the recovery stress is increased twice in the first transformation cycle, and then in the subsequent cycles the level of recovery stress is kept constant. (4) Easiness of the martensitic formation determines the level of recovery strength, namely, when the stress to induce the martensite is high, the amount of martensite become small and then the recovery strength will be low. Studies on thermal cycle characteristics and shape memory characteristics of Ti-Ni alloy are now in progress.

93 Development of the Fusion Reactor First Wall Materials Resisting to Plasma and Radiation Damage

April 1987 to March 1993

H. Shiraishi, 2nd Research Group

Keywords: C-B-Ti composites, thermal shock test, functionally gradient material, Ni_3Al, helium embrittlement, ZrO_2, microstructure control by phase transformation

1. **High Heat Flux Materials**
   In order to develop first wall and diverter plate materials for fusion reactor, C-B-Ti composites were manufactured by hot press followed by the sintering at 2000 °C and HIP. The physical and thermo-mechanical properties of the products were obtained. The thermal diffusivity is dependent on the TiC/TiB_2 ratio and showed maximum at 1:1 composition at the temperature range from 300 to 1800K. The produced specimens consisted of graphite, TiC and TiB_2 and the low density graphite rich sample was tougher to mechanical fracture than $TiC+TiB_2$ sample in thermal shock test. The functionally gradient material in which the density of plasma side is lower than that of the coolant side was manufactured and the resistance to thermal shock is superior to the single composition material.
2. **Radiation damage resistance of microstructure controlled materials**
   For the further development of high temperature structural alloys, it is essential to reduce the susceptibility of materials to helium embrittlement due to grain boundary fracture. Several low activation martensitic steels and directionally solidified Ni_3Al alloy were estimated from the standpoint of helium embrittlement using helium injection with cyclotron and high temperature tensile test. Helium desorption during tensile test was measured with mass analyzer. In the 9Cr steels, helium was trapped at the lath boundary and it is inferred that this resulted in improvement of helium embrittlement in these alloys. Ni_3Al also showed excellent ductility at high temperature and this is because of non-existence of grain boundary normal to tensile stress axis. This result shows possibility of single crystal application for high temperature helium embrittlement.
3. **Study on microstructure control for function generation of high melting point materials**
   ZrO_2 material with addition of Y_2O_3, MgO, Al_2O_3 were melted and the possibility of microstructure control using phase transformation is being investigated.

Related Papers

Thermal Shock Behavior of Sintered Mixtures of Carbon, Boron and Titanium, Shinno, H., Fujitsuka, M. and Tanabe, T. AIP Conf. Proc. 231 Emin, B.D., et al. Boron Rich Solids (1991): 570.

Induced Radioactivity of Commercial Isotropic Graphite for High Heat Flux Tiles, Shikama. T., Kayanao, H., Fujitsuka, M. and Tanabe. T. J. Nucl. Mater. 179–81 (1991): 209.

Creep Rupture Properties of Helium Implanted Precipitation Strengthened Alloy, Yamamoto, N., Nagakawa, J., Shiraishi, H., Kamitsubo, H., Kohno. I. and Shikata, T. J. Sci. & Tech. 28 (1991): 1001.

94 Material Chemistry in the Extreme Conditions under Irradiation

April 1989 to March 1994

M. Kitajima, 2nd Research Group

Keywords: irradiation, dynamic process, surface reaction, surface damage

Materials are subject to both chemical and physical attacks by particle bombardment at the same time under irradiation. The main purpose of this research is to elucidate the mechanism of surface reaction processes activated by irradiation, and to develop new analytical methods for that with emphasis of real-time observation for dynamic process. Kinetic or phenomenological modeling on the surface reaction and damage processes is also our target. From this viewpoint, we are investigating a lattice disordering kinetics of graphite and silicon surfaces during ion irradiation by using a real-time *in situ* Raman measurement technique. *In situ* ellipsometry is also being performed to study growth kinetics on surface oxide film during oxygen plasma discharge. In order to compare plasma oxidation rate with plasma characteristics, Langmuir probe measurements and emission spectroscopy have been performed. Recently, we have started studies on laser stimulated desorption and reactive scattering of molecules on irradiated surface.

Related Papers

Ion-Irradiation Effects on the Phonon Correlation Length of Graphite Studied by Raman Spectroscopy, Nakamura, K. and Kitajima, M. Phys. Rev. B45 (1992): 78.

Initial Damage of Graphite Under Ion Irradiation by Real-Time Raman Measurements, Kitajima, M. and Nakamura, K. J. Nucl. Mater. (in preparation).

Real-time Raman Measurements of Si Under Ion Irradiation, Nakamura, M. and Kitajima, M. J. Appl. Phys. 71 (1992): 3645.

Plasma Density Dependence of the Oxidation Rate of Si by in situ During Process Rapid Ellipsometry, Kuroki, H., Shinno, H., Nakamura, K.G., Kitajima, M. and Kawabe, T. J. Appl. Phys. 71 (1992): 385.

Study of Surface Under Ion Irradiation by Real-Time Raman in situ Measurements, Kitajima, M. Proc. Mater. Chem '92 March 12-13, 1992 (Mitsubishi Research Lab.), p 157.

95 Research on Distributed Database for Advanced Nuclear Metals

April 1991 to March 1996

M. Fujita, 2nd Research Group

Keywords: Data-Free-Way, distributed database, advanced nuclear materials, to share data

New material-searching using database systems is required for nuclear technology. But it is very difficult at present to describe numerous nuclear materials properties because of their complexity in nature and pre-standardized status of information on new materials. The stored data consist of the properties under environments from normal to severe states, such as high temperature, stress loading and/or corrosive ones under heavy irradiation. Therefore a wide spectrum of special knowledge of different fields is necessary.

A distributed database system, for designing and selecting has been built under the cooperation of National Research Institute for Metals (NRIM), Japan Atomic Energy Research Institute (JAERI) and Power Reactor and Nuclear Fuel Development Corporation (PNC). The system is called as "Data-Free-Way" and has been built since April of 1990. This project is to build the system within five years, focusing on advanced nuclear materials, such as new structural metals, intermetallic compounds, ceramics and composites. Input data will be captured from results of Fundamental Research on Nuclear Materials supported by Science and Technology Agency of Japan.

In the pilot system, a new method to share data and meta data among the databases of the respective institutes is demonstrated. The merits to share data and the methods to obtain the knowledge in the distributed data system were discussed through irradiation data on tensile properties of type 316 stainless steel. Comprehensive data sets were established on the basis of the system; thermal neutron data from JAERI, fast neutron data from PNC and ion irradiation data from NRIM. It is concluded that the major merits are that the knowledge of material technology is able to be expressed by numercial values, since a large number of data examined under various conditions are considered in analysis. The merits to share data and the methods to obtain the knowledge in the distributed data system were discussed through irradiation data on tensile properties of type 316 stainless steel. Comprehensive data sets were established on the basis of the system; thermal neutron data from JAERI, fast neutron data from PNC and ion irradiation data from NRIM.

96 R&D of Advanced Heat-Resistant Structural Materials for Very High Temperature Gas-Cooled Reactors

April 1990 to March 1995

T. Tanabe, 2nd Research Group

Keywords: high temperature gas-cooled reactor, material design, testing-and-evaluation

In order to fulfill the national request for advanced structural materials for high temperature gas-cooled reactors, we have been carrying out the R & D of new heat-resistant materials for very high temperature use of up to 1,373K by combining the material-design and the testing-and-evaluation technologies. The present status of the R & D is as follows.

1. Development of Advanced Heat-Resistant Materials: The design of new materials have been conceived through the testing and evaluation of existing heat-resistant materials such as nickel-base superalloys, oxide dispersion strengthened (ODS) superalloys, intermetallic compounds. The most promising material is considered to be the ODS superalloy of our Ni-Cr-W alloy. The manufacture of the new superalloy is now in progress.
2. Development of Advanced Material Testing-and-Evaluation Technologies: Various types of the tests and evaluations have been made and clarified the environmental and/or the microstructural effects on the properties of the materials; i.e., creep crack growth tests, conventional creep rupture tests, interruption creep tests, varying stress and temperature creep tests, high-temperature tensile tests, high-temperature corrosion tests, EPMA analysis, carbon analysis, statistical creep damage analysis, etc.

Related Papers

Creep Crack Growth Behavior in a Ni-base Superalloy in 1,273K Helium Gas Environment, Nakasone, Y. et al. Proc. 1st JSME/ASME Joint Int. Conf. Nucl. Eng. (1991): 549–52.

Creep Crack Growth Behavior in Ni-base Superalloys in 1,273K Helium Gas Environment, Nakasone, Y. et al. J. Nucl. Sci. & Tech. (in preparation) 29-5 (1992).

Effects of Product Form and Boron Addition on the Creep Damage in the Modified Hastelloy X Alloys in a Simulated HTGR Helium Gas Environment, Nakasone, Y. et al. Proc. 4th Int. Symposium Advanced. Nucl. Energy Research (in preparation) (1992).

Creep Damage of Hastelloy XR at Very High Temperatures in Simulated HTGR Helium Gas , Nakasone, Y. et al. Proc. CREEP5 (in preparation) (1992).

Creep Crack Growth Behavior of Ni-26% Cr-17% W-0.5% Mo Alloy in Air and in Helium Gas Environment at 1,273, Tabuchi, M. Proc. CREEP5 (in preparation) (1992).

[97] Research on Fundamental Techniques to Develop Functionally Gradient Materials for Relaxation of Thermal Stresses (II)

April 1990 to March 1992

I. Shiota, Physical Properties Division

Keywords: functionally gradient material, thermal stress, thermal stability

A Functionally Gradient Material (FGM) is defined as a material of which functionality changes continuously with space or time. Generally speaking, ceramics are heat resistive, and metals are tough structural components. Ceramics are often coated or sticked on the metal surface for thermal protection. However, in the case of the space shuttle, the ceramic tiles sometimes came off from the fuselage because of thermal stresses at the interface. A space-plane (SP) is expected to fly at much higher speed than a shuttle. The SP is anticipated to be subjected to intense heat of 2000K, which may cause enormous thermal stresses in nose cones, turbines, combustion chambers and so on. At such elevated temperatures, no traditional heat protective system is reliable.

Relaxing the stresses is the most essential to construct the SP. FGM is the most hopeful candidate. It does not contain stress concentration parts, because functionality changes continuously as the composition varies gradually from ceramics on the face to metals on the back. However, the FGM is a heterogeneous material and is thermodynamically in non-equilibrium. Therefore, thermal stability is the most important factor for its practical application. We are carrying out an investigation of thermal stability of metal-ceramics FGMs. The following are recommended to fabricate FGMs with higher thermal stability.

1. It is very important to find the stabilizing system of FGM structure.
2. Porosity of FGM should be decreased to restrain the volume change by sintering.
3. It is important to control the distribution of pores and the thickness of ceramics part to restrain crack initiation.
4. When optimum FGM is selected, it is necessary to mention the diffusion between the FGM and the substrate at an elevated temperature.

Related Papers

Effect of Crystal Structure on Thermal Stability of Ti-TiC FGM, Shinohara, Y., Imai, Y., Ikeno, S. and Shiota, I. Proc. 1st Int. Symp. FGM. (1990): 225–30.

Thermal Stability of Ti and TiC Related with Substrates, Shiota, I., Shinohara, Y., Imai, Y. and Ikeno S. Proc. 1st Int. Symp. FGM (1990): 219–24.

[98] Research on Fundamental Techniques to Develop Functionally Gradient Materials for Relaxation of Thermal Stresses

-Study on densification of graded materials by thermal spraying process-

April 1990 to March 1992

T. Fukushima, Advanced Materials Processing Division

Keywords: thermal spraying, graded coating, composit coating, densification, heat-treatment, low pressure plasma spraying (LPPS)

In the case of ordinary plasma-sprayed coating of ceramics on the metal surface, peeling from the substrate or cracking in the coating by thermal and residual stresses due to the difference in thermal expansion of metal and ceramics has often occurred in actual service conditions.

Application of graded coatings are anticipated in order to solve is expected these problems. Graded coating (Functionally Gradient Materials (FGM)) has a gradually changing mixed compostions from 100% of metal to 100% of ceramics layer by layer. For fabrication of such graded coating, application of two torches (named as plasma twin torch process (PTTP) is advantageous, compared with the conventional single torch method, since it is possible to feed independently each spraying powder of metal and ceramics and to select suitable spraying conditions for each powder in the former process.

In the first stage (1988 to 1990), formation of graded coatings and composit coatings were tried using the PTTP.

Ni-base alloy (NiCrAlY alloy) and ZrO_2-base ceramics (ZrO_2 -Y_2O_3 8%, named as 8YSZ) powders with particle size from 10 to 44 μm were used as spraying materials in this study.

Graded coatings were obtained by step-wise control of the feeding rate each powder, which was calculated from each deposition efficiency, layer by layer.

Porosity, thermal expansion, thermal diffusivity, thermal shock characteristic, tensile strength and

hardness of the coating were investigated.

It was clarified that the capability to withstand thermal shock of the graded coating was higher than that of 8YSZ mono-layer coating, because relaxation of thermal stress could occur in the graded coating, due to gradually changing thermal properties such as thermal expansion and thermal diffusivity.

In the second stage (1990 to 1992), formation of coatings in the low pressure atmosphere (LPPS) by the PTTP and heat-treatment of the coatings were studied for the purpose of densification and strengthened coatings.

It was recognized that the LPPS and heat-treatment of the graded coating of NiCr-AlY alloy and 8YSZ were effective to improve the density, uniformity and bonding strength of the coatings.

Apparent porosity of 8YSZ coating was decreased from about 22% (under atmospheric pressure) to about 6% (after heat-treatment), bonding strength of NiCrAlY alloy and 8YSZ coatings by LPPS also increased by heat-treatment by from 2 to 10MPa compared with the coating formed under atmospheric pressure and NiCrAlY alloy was protected against oxidation in LPPS.

Related Papers

Formation of Graded Coatings by Plasma Spraying, Fukushima, T., Kuroda, S. and Kitahara, S. Pro. 5th Int. Symp. JWS. (1990): 393–98.

Gradient Coatings Formed by Plasma Twin Torches and those Properties, Fukushima, T., Kuroda, S. and Kitahara, S. Proc. Int. Symp. FGM (1990): 145–50.

Thermal Stability of NiCrAlY→PSZ FGM by Plasma Twin Torches Method, Shinohara, Y., Imai, Y., Ikeno, S., Shiota, I. and Fukushima, T. Application Form for Publication in ISIJ International 32 (1992): 893–901.

Materials for environmental performance

(99) Improvement of Wear Properties of Metallic Medical Materials

April 1992 to March 1994

A. Hoshino, Physical Properties Division

Keywords: medical materials, titanium alloy, fretting corrosion test, tribological properties, coupling effect

Although titanium alloys are excellent corrosion resistant materials under static condition, their wear resistance are known to be poor under the fretting condition. In order to improve the tribological properties of titanium alloys for surgical implants, an *in vitro* fretting corrosion test of Ti-6Al-4V alloy was conducted in a simulated body fluid environment at controlled potential.

The objects of this study are to analyse the degradation mechanism due to fretting corrosion of titanium alloy devices in human body environment, and subsequently to investigate the effect of coupling with stainless steel or the effect of microstructural control on tribological properties of this α-β type titanium alloy in order to minimize the toxicity by wear particles..

100 Achievement, Measurement and Application of Extremely High Vacuum

April 1991 to March 1993

M. Tosa, Surface and Interface Division

Keywords: extremely high vacuum, boron nitride, hydrogen permeation, sliding friction

Extremely high vacuum system less than 10^{-10} Pa is the key technology to advance surface analyses and thin film preparations remarkably. Low outgassing is the necessary property of the material for the achievement and application of the extremely high vacuum system. Boron nitride with hexagonal structure is inert to the adsorption of gases, but it was difficult to prepare boron nitride layer on the surface of stainless steels directly at low temperature. We previously found that the precipitation temperature of boron nitride went down to 900K on the surface of type 304 stainless steel doped with boron and nitrogen and also found that the precipitation temperature went down to 600K on the surface of deposited film of mixed boron nitride and stainless steel. The purpose of this work, therefore, is to apply the surface precipitation of boron nitride to the barrier layer against the diffusion of doped atom and to the lubricant layer suppressing adhesion during sliding manipulation in the extremely high vacuum. We prepared the rf-magnetron sputtered film of mixed boron nitride and type 304 steel on the type 304 steel substrate and annealed the specimen in the vacuum of 10^{-6}Pa at 800K for an hour. Scanning Auger electron spectroscopy analysis showed that precipitated boron nitride successfully covered the whole surface of the sputtered film and that a little oxygen and carbon was absorbed on the surface of the film even after the exposure to the atmosphere. We developed an apparatus for the measurement of hydrogen permeating rate and estimated the permeating rate through thin film of type 316L stainless steel dividing two chambers of two different hydrogen pressure. We found that the hydrogen permeating rate of film covered with boron nitride was less than one-thirds of the rate of film covered with no boron nitride. This shows that precipitated boron nitride can be a barrier layer against the hydrogen permeation. A pin on a plate type tester for sliding friction showed that the frictional resistance of boron nitride precipitated film on the type 304 stainless steel substrate was lower by half than that of no boron nitride precipitated film. This shows that pre-

cipitated boron nitride can be a good lubricant for smooth specimen manipulation system causing little outgassing.

101 Study on Improvement of Metallic Biomaterials

April 1989 to March 1992
A. Hoshino, Physical Properties Division
Keywords: metallic biomaterials, stainless steels, titanium alloys, fretting enhanced crevice corrosion, corrosion fatigue

Metallic biomaterials are susceptible to degrade in human living body by crevice corrosion, fretting corrosion and corrosion fatigue. In this study, fretting corrosion and corrosion fatigue tests have been carried out on stainless steels and titanium alloys.

For fretting corrosion, Pin-on-Flat type fretting corrosion testing apparatus was constructed for *in vitro* testing of stainless steels for surgical uses, in order to acquire the useful information for improvement. In continuous fretting corrosion test of 316L stainless steel, it was found that the fretting enhanced crevice corrosion did not occur. However, during the intermittent fretting corrosion test, crevice corrosion occurred remarkably at the resting stage, and the anodic current corresponding to release of metal ions was one order of magnitude higher than that at fretting stage. High Mo stainless steel was found to be more effective for suppressing such crevice corrosion.

For corrosion fatigue test, the effects of some additional elements on corrosion fatigue behaviour of titanium alloys have been evaluated by using tensile specimens in saline solution.

102 Corrosion Resistance of Synthetic Barriers in Geological Disposal of Spent Nuclear Fuels

April 1988 to March 1992
T. Kodama, Environmental Performance Division
Keywords: geological disposal, corrosion rate monitoring, electrochemical impedance, chemical potential diagrams

In the nuclear fuel cycle system proposed by Atomic Energy Commission of Japan, high level nuclear waste separated from spent fuel after reprocessing is molded into metallic containers in the form of solidified glass which is to be disposed of in deep geological repositories. In this system, radioactive waste must be isolated safely until radioactivity has been reduced to a nonhazardous level and a durability of 1000 years is expected for metallic containers. In advance of the proposed construction of a nuclear disposal and repository in the forthcoming century, it is desirable that sufficient data be prepared for the guarantee of nuclear safety. For this purpose we have studied corrosion and life prediction of metals for the use of nuclear waste disposal containers.

1. Corrosion monitoring in simulated geological environment

   Electrochemical impedance measurements have been carried out in simulated geological environment for corrosion rate monitoring. A simulated solution for electrochemical measurement was prepared by adding sodium-bentonite clay to water at a concentration of 10g kg^{-1} followed by the separation of the clay by filtration and centrifugal method. For electrochemical impedance measurement the small sinusoidal potential polarization was impressed on electrode using a potentiostat and the response in current was analyzed by a frequency response analyzer. In the impedance spectrum of carbon steel sample in the simulated geological solution as a parameter of frequency (Nyquist plot), two semicircles were observed indicating that the corrosion process proceeds via two rate processes; the first process with small time constant corresponds to adsorption without electrical charge transfer and the second one is attributed to the electrochemical process with charge transfer.
2. Water chemistry in geological environments

   For the description of chemical environments of geological disposal sites, acidity in terms of pH and redox parameter in terms of Eh are thought to be the most fundamental parameters which affect corrosion of metals, dissolution of glass and adsorption of fission products to minerals and clays. For predicting these parameters in a geological environment, we have developed a new computer code for the automatic construction of chemical potential diagrams. The system was applied for the construction of Eh-pH diagrams of fission products and actinide element in geological environment using a new prediction method of chemical stability constants of complex ion formation. Various diagrams have been prepared including U-H_2O, U-CO_3-H_2O, Pu-H_2O, PuCO_3-H_2O systems.

103 Corrosion Resistance of Coated Materials in Natural Environment

April 1989 to March 1992
T. Kodama, Environmental Performance Division
Keywords: atmospheric corrosion, paint/metals, pollutant analysis, combined acceleration tests

As a part of Japan-ASEAN Cooperation on Science and Technology, which is in progress under auspices of the Japan International Cooperation Agency (JICA), NRIM has been in charge of supporting projects on atmospheric corrosion carried out at national research institutes in Thailand

and the Philippines by participating in the planning of experiments and technical discussion and by dispatching to these countries. In parallel with the overseas experiments on atmospheric corrosion, laboratory works on metal/polymer adhesion, mass transfer through paint films and surface treatment have been carried out at NRIM with participants from ASEAN countries.

Progress in Research

1. Atmospheric Corrosion in Tropical Areas
   In Thailand and the Philippines, atmospheric exposure tests are in progress for bare metals and steels with organic and inorganic coatings at several exposure sites selected from different atmospheric conditions. In parallel with the exposure tests, meteorological and pollution data are collected periodically. In this connection a new technique for the pollutant analysis using ion chromatography has been developed. Pollutants collected onto alkaline filter papers were soaked in water and extracted to form a pollutant containing solution. The extract was treated by calcium-modified cation exchanger prior to ion chromatography to remove excessive carbonate in the test solution in the form of calcium carbonate. The removal of carbonate eliminated the interference effects in chromatography and it allowed the use of ion chromatographic technique to be the most rapid analytical method by which almost all pollutants can be determined in single pass.
2. Corrosion Control at Metal/Coating Interface
   For the simulation of the atmospheric deterioration and corrosion of paint/metals systems, combined acceleration tests were carried out using irradiation of ultraviolet (UV) light in a Xenon lamp weather meter and salt spray test. Samples of carbon steel, aluminum and zinc were pre-treated and were coated both with primers and top coats. Deterioration of paint films was evaluated by visual observation and electrical impedance change after the irradiation to UV light. In all samples rusting of metals and blistering of paint films occurred more frequently with increasing exposure to UV light. For carbon steels, conversion treatment showed the highest corrosion resistance among three different pretreatments. Electrical impedance of paint films decreased with the time of UV irradiation. Among polymer films tested, polyurethane resin enamel showed the highest resistance to UV irradiation.

104 Development of Low Activation Materials

April 1987 to March 1992

T. Noda, 2nd Research Group

Keywords: low activation materials, induced activity, ferritic steels, carbon fiber/SiC composites, chemical vapor infiltration

Project Description

The use of low activation materials is one of key issues in fusion reactors from the viewpoint of reactor safety, waste management, and environmental aspects. The primary objectives of the program are (1) selection and design of low activation materials and (2) materials development including iron-base alloys, refractory alloys, and ceramics composites. The program contains the following main subjects.

Selection and design of low activation material
- development of the simulation code calculating induced radioactivity of materials
- evaluation of materials

Materials developments
- development of reduced activation iron base austenitic and ferritic steels with high-temperature strength and toughness
- development of new process for ceramics composites with a high purity and favorable mechanical properties

Major Products

The simulation code, IRAC, calculating transmutation and induced activity, and decay heat of elements and alloys under various neutron irradiation conditions covering thermal to 14MeV neutrons was developed.

Based on the evaluation of induced activity, reduced activation ferritic and austenitic alloys were developed. Reduced activation Fe-9Cr-1W-0.2V-0.1Ta alloys superior to conventional Cr-Mo steels in resistivity against neutron irradiation as well as in phase stability, toughness and high-temperature strength under non-irradiation conditions.

Chemical vapor infiltration method was applied to prepare ceramic composites. Carbon fiber/SiC composite with a purity >99.99% and improved fracture toughness 3 times better than monolithic SiC could be obtained.

Low temperature synthesis of SiC using laser CVD also examined. Polycrystalline SiC film could be formed even at 518K.

Related Papers

Carbon Fiber/SiC Composite for Reduced Activation, Noda, T., Araki, H., Abe, F. and Okada, M. J. Nucl. Mat. 179–81 (1991) 379–82.

Alloy Composition Selection for Improving Strength and Toughness of Reduced Activation 9Cr-W Steels, Abe, F., Noda, T., Araki, H. and Nakazawa, S. J. Nucl. Mat. 179–81 (1991) 663–66.

Low Temperature Synthesis of SiC by UV Laser CVD, Noda, T., Suzuki, H., Araki, H., Abe, F. and Okada, M. Proc. 2nd Japan Intl SAMPE Symp." Dec. 11-14 (1991): 1209–14.

Separation and synthesis

⑩⑤ Elimination of Some Specified Toxic Metallic Ions

April 1992 to March 1993

I. Tomizuka, Physical Properties Division

Keywords: environmental contamination, Chernobyl accident, toxic metallic ions, decontamination, adsorption

The aim of this research on the following items:

1. Current situation of environmental contamination caused by Chernobyl accidents.
2. Maneuvers adopted in Ukraina to eliminate the contamination.
3. Current situation and feasibility of eliminating the highly-diluted contamination species through processes based on adsorption.

The survey will largely depend on the sources to be supplied from Ukrainian Academy of Sciences.

106 Preparation of Superconducting Raw Materials Having Controlled Quality

April 1988 to March 1994

T. Fujii, Chemical Processing Division

Keywords: purification, superconducting oxide, consolidation, ultrafine particles, powders

Four kinds of studies are included in this research

1. Purification of Chemically Active Elements for Superconductors: Rare earth metals usually contain much impurities or like elements. In this study, the methods for impurity reduction have been studied, e.g. by vaporization under high vacuum. Superconducting oxides are made from high purity materials thus obtained, and the effects of impurities on the properties are being studied.
2. Physical Properties and Consolidation Behavior of Powders Used for High Pressure Forming of Superconductors: Hot isostatic pressing and sintering behavior of superconducting oxide powders has been studied in view of obtaining the low porosity solids with high superconducting critical current densities (Jc).
3. Preparation and Characterization of Powders Used for Making Y- and Bi-Series Oxides Superconductors: The 'Reactive Plasma-Metals Method' developed in this Institute has been successfully applied to prepare elemental ultrafine particles for constructing superconducting oxides. Powders by a Rapid-Solidification using the 'Centrifugal Atomization Method' has also been applied to make superconducting powders directly. Characterization and consolidation behavior of these powders, and superconducting properties of solids have been studied.

107 Fundamental Study on Preparation and Characterization of the Metal Complexes Possessing a Peculiar Molecular Structure

April 1991 to March 1994

H. Isago, Chemical Processing Division

Keywords: phthalocyanine, preparation, cerium, mixed valence, bismuth

Phthalocyanine and its related compounds containing metal elements have been known as one of the most important organic pigments so far and also have been intensively studied as a group of new materials in recent years. Indeed, it was found in this laboratory that bis(phthalocyaninato)lanthanoid(III) complexes exhibited remarkable electrochromic properties in organic solvents and in solid state as thin film. In these compounds, a hole is created in the complex molecule.

This research work consists of the following two subjects; 1) preparation and characterization of bis(phthalocyaninato)cerium complex and its derivatives which show exceptional properties among a series of bis(phthalocyaninato)lanthanoid(III) complexes and 2) an attempt to prepare the first bismuth complex ligating a phthalocyaninate ring or rings.

In the former subject, our interest is mainly placed on the behavior of the 4f electron on the cerium ion in the bis(phthalocyaninato)cerium complex. In this complex, the cerium is found to be in mixed valence state between trivalent and tetravalent states by electronic, infrared, ESR, and XPS spectra. It is probable that the 4f orbital of the cerium is largely hybridized with a phthalocyanine π orbital. In the latter subject, it is of interest whether the bismuth-phthalocyanine complex has a similar structure to those of the bis(phthalocyaninato)lanthanoid(III) complexes and whether the bismuth complex shows similar properties. It is because that a bismuth(III) ion has a close ionic radius to those of lanthanoid(III) ions with the same coordination number. Moreover, coordination chemistry of the phthalocyanine complex of the other group 15 elements in the periodic table as well as bismuth has been scarcely studied and hence a development of a new field of chemistry and material science is expected.

108 Alloying Method Using Decomposition of Metal Halides

April 1991 to March 1994
G. Omori, Advanced Materials Processing Division
Keywords: magnesium, zirconium, alloying, decomposition, metal halides

An investigation is now conducted on the merits of several zirconium containing materials for the alloying of this metal to magnesium.

Magnesium alloys containing zirconium have been used extensively in application requiring the high strength, where zirconium being an important grain refiner of alloy matrix. There are, however, some problems in the practical alloying procedure. Elemental zirconium is not an efficient agent to use because of its high melting point and high oxidation tendency.

The purpose of this work is to examine thoroughly the problem of alloying method in adding zirconium to magnesium, using various zirconium containing materials as the supplier of the element.

Magnesium metal was melted in a crucible of mild steel under SF_6 atmosphere with electric furnace. For the first step, adding zirconium to magnesium was done by using the powder of $ZrCl_4$ or briquet fixed with phosphorizer. With regard to alloying efficiency, no difference was found between these two $ZrCl_4$ agents.

It was found that zirconium dissolved once in magnesium was segregated to the bottom of the crucible in the form of zirconium rich compounds or free zirconium during the process and cooling of the melt, and that zirconium tended to be segregated some what more with an increase of killing time.

The above results will serve as basic information on an alloying method using decomposition phenomena of metal halides.

It can be said that, if moisture is excluded completely from the atmosphere, zirconium metal liberated by magnesium reduction should be very pure and alloy well with the rest of host metal.

$ZrCl_4$ powder is light, fluffy and extremely hygroscopic, and sublimates easily at 604 K. Whence, the treatment of $ZrCl_4$ requires circumspection.

[109] Project Research on the Purification Techniques of Rare Metals in View of Finding New Materials Properties (Phase II)

April 1990 to March 1992
E. Furubayashi, Chemical Processing Division
Keywords: rare earth metals, elemental separation, electro-transport, superconducting state, laser photo-ionization method

In succession to the previous study (Phase I; Apr. 1987 to March 1990) of the same program, the purification of rare metals, particularly Rare Earth Metals, and the evaluation of their purity have been studied comprehensively in cooperation with some industrial laboratories and universities. The materials thus obtained are found to have much lower contents of oxygen or other interstitial elements, and such materials are used to study the intrinsic physical properties of rare earth metals having higher purities than before.

1. Superconducting Properties of Y-Oxides: Effects of ferromagnetic impurities like Fe, Ni, Co substituting Cu in Y-Oxides on the superconducting properties have been studied. The superconducting state has been found to coexist with the spin glass state from the measurements of the Mössbauer effect and magnetic susceptibilities.
2. Preparation of Rare Earth Metal Standard Materials by Electro-Transport Method: The refining of La metal with preliminary deoxidation using calcium offered a low oxygen sample of less than 100 ppm O. Electromigration of O and N solutes suggesting capable of purifying was also found for Er_3Ni material.
3. Mutual Separation of Chemically Similar Rare Earth Metals by Laser Photo-ionization (Laser Materials Purification (LMP)) Method: Tunable Laser beam has been directed to the mixed atomic beam of Nd and Pr from a Nd-Pr alloy, and the way of selective ionization and following extraction with electric field of Nd atoms has been studied. Multiple step resonance excitation processes for Nd atoms have been clarified in collaboration with Nippon Steel Corporation. The method has been successfully applied to the efficient separation of Nd from Pr and to obtain the purified Nd films.

Gaseous process

(110) Precise Composition Control of Ordered Alloys by Chemical Transportation Techniques

April 1992 to March 1995
H. Sasano, Physical Properties Division
Keywords: ordered alloys, shape memory alloys, reversible color change alloys, chemical transportation technique

Ordered alloys are expected to have attractive properties. However, the properties are very sensitive to the composition of the alloys. It is hard to control the composition precisely by usual methods. We succeeded in controlling zinc or cadmium concentration in shape memory alloys and reversible color change alloys with accuracy of 0.1 percent by solid-vapor diffusion couple method. In this method, components to be used are restricted to the ones which have high vapor pressure. In this

study we try to control the concentration of component which has low vapor pressure.

This project is divided into two parts. In the first part aluminum concentration in copper or nickel base alloys is controlled by a chemical transportation technique using aluminum trichloride as a transport medium. In the other part oxygen concentration in electroconductive ceramics is controlled. We will also examine the physical properties changes with the deviation of concentration from the stoichiometry of the ordered alloys.

(111) Extraction from Melt to Gas Phase

April 1992 to March 1994

A. Fukuzawa, Chemical Processing Division

Keywords: thermal plasma, low pressure plasma jet, vaporization

Thermal plasma produced by transfer or non transfer type torch is widely used for melting metals and surface lining. However, its operating pressure is usually at atmospheric pressure because of the existence of plasma jet. In some case low pressure plasma jet is used, but its pressure is not less than 100torr.

This research work is to investigate the behavior of plasma jet in lowered pressure of 10torr order and apply to the extraction of so called tramp elements like Cu, Sn, Ga or Cr from liquid iron or steel by the vaporization of these elements by the help of ultra high temperature given by the plasma jet. According to the theoretical calculation, the vaporization rate of Sn in the testing pressure will be 3 times higher than the conventional condition, and the final Sn level in the melt is expected to be lowered.

The behavior of plasma of this aimed pressure range is not used so much in these days. However, when the effectiveness of lowering the pressure is revealed, this technology can be applied for the extraction of various kinds of elements from molten metals and alloys, and especially for renewal of recycled scrap.

112 Synthesis and Characterization of Oxide Superconductor Films

April 1988 to March 1994

K. Togano, Surface and Interface Division

Keywords: high-T_c oxide superconductors, thin films, Rutherford backscattering, MBE

Since the discovery of high T_c oxide superconductors, extensive efforts have been made by a number of research groups to fabricate thin films of the oxides, especially Y and Bi based superconductors, available for electronic devices. Our major interests are the formation of artificially layered structure and the exploration of growth mechanism of oxide thin films.

Concerning the artificially layered structure, we have concentrated on the control of the number of CuO layers, n, in a unit cell of $Bi_2Sr_2Ca_{n-1}Cu_nO_{2n+4}$. Until now, we have succeeded to synthesize the films with n of up to 7, all of which show superconductivity except n=1[1]. The crystal quality of the films is characterized by means of X-ray diffraction, high resolution TEM[2], Rutherford backscattering (RBS) and particle induced X-ray emission (PIXE). In these, RBS channeling measurement is extensively used to characterize the epitaxy of the films as well as the composition change with depth.

In order to investigate the growth mechanism of oxide film during deposition, we have developed a reactive MBE system having an energy dispersive X-ray spectroscopy combined with reflective high energy electron diffraction. Using this system, we have succeeded to detect the variation of surface composition and surface structure simultaneously, which is very useful information to investigate the growth mechanism.

Based on the above-mentioned results, we have a plan to fabricate films with super/normal and super/insulator superlattices and to characterize them.

Related Papers

Synthesis and Characterization of $Bi_2Sr_2Ca_{n-1}Cu_nO_y$ (n=1 to 7) Thin Films Grown by Off-axis Three Targets Magnetron Sputtering", Narita, H., Hatano, T. and Nakamura, K. to be published in Dec. 15 issue of J. Appl. Phys.

Cross-sectional High-resolution TEM Studies of Superconducting Oxide Films of the Bi System, Ikeda, S., Sato, J. and Nakamura, K. Material Transactions, JIM 31 (1990): 602–7.

Liquid state process

(113) Measurements, Analyses and Evaluations of Specimens Made by FMPT

April 1992 to March 1994

A. Sato, Advanced Materials Processing Division

Keywords: microgravity, solidification, fluid flow

First Material Processing Test of Japan under microgravity environment is performed in September, 1992 in the space shuttle/space lab of NASA (National Aeronautics and Space Administration of the United States of America) during the 7-day flight. Researchers of our Institute are responsible for following five themes including 22 materials processings out of total 34 themes;

1. Production of compound semiconductor crystals by floating zone melting: A large single crystal of indium antimonide compound semiconductor will be made in an infrared image furnace. The crystal will be examined by an

X-ray diffraction topography, and the electric property will also be measured.

2. Production of new superconducting materials: Al-Pb-Bi and Ln-Ba-Cu eutectic alloys are to be produced. The effect of gravity on structures, properties, critical currents, and phase compositions will be examined.
3. Formation mechanism of oxide inclusions in a complex-deoxidized steel: Samples to be made in the space lab is examined by a SEM, an EMPA, an EDX, and a wet chemical analysis. The effect of gravity on distribution and configuration of the inclusions in the steel will be discussed in terms of a computer-aided fluid flow simulation.
4. Preparation of particle dispersion alloys: Ni-Mo-TiC type dispersion alloys will be melted and solidified. Their physical properties will be examined, and compared with those of alloys solidified at the ground lab. The feasibility of a castable dispersion alloy through melting and solidification in microgravity will be discussed.
5. Diffusion in melt binary alloys: Diffusion couple of two different metals, Au and Ag, will be melted in order to examine interdiffusion behavior. Since the thermal convection and buoyancy are suppressed under microgravity conditions, the results will be compared with those from the ground experiments.

114 Purification of Metals by Non-Contacting Melting Method

April 1991 to March 1994

A. Fukuzawa, Chemical Processing Division

Keywords: cold crucible, levitation melting

The purpose of this study is to develop the electromagnetic levitation melting process of reactive metals and refractory metals using the cold crucible type non-contacting induction furnace. Up to now, the reaction between metal and crucible has made it difficult to purify the reactive metals and there has been no crucible materials for homogeneous melting of refractory metals. The cold crucible type melting method will solve these problems.

In these several years, we have made various kinds of trials on the cold crucible type non-contacting induction furnace and many fundamental results concerning to the cold crucible have been obtained. And, we have been developing the levitation control techniques; supplying different two frequencies in order to obtain optimum levitating conditions corresponding to any molten metals and alloys that have various physical properties such as density, electrical resistance, and melting point.

In this term we are going to carry out further study by setting the cold crucible in an atmosphere controlling vessel for optimum levitating and purification of molten metals such as titanium and its alloys. The shape of the cold crucible and the high frequency coil and the electric output power will be examined in order to obtain the optimum levitating conditions in the vessel.

Next, we are going to develop the levitation technique concerning high-purification melting of reactive metals and refractory metals.

115 Solidification Processing for Fine-grain Structure Materials

April 1991 to March 1994

A. Sato, Advanced Materials Processing Division.

Keywords: grain structure, rapid solidification, vigorous agitation

The grain structure of solidified materials has a great effect on various properties of materials. Solidified materials are composed of one of three types of grain structures, namely, coarse, conventional, and fine grain structures. Materials solidified slowly have coarse grain structures, and single crystal structure in the extreme case. Materials solidified in usual cooling speeds have conventional poly-crystal structures. Materials solidified rapidly have fine grain structures, and amorphous structures in the extreme case. We studied a technique to produce materials composed of coarse grains by a moldless upward continuous casting process for these several years. Though materials composed of coarse grains or single crystals have many advantages and merits over materials composed of conventional poly-crystal grains or fine grains, their usage in practical industries are very slight at the present time. On the other hand, materials composed of fine grains are used in many fields of practical industries. Then, we concluded that researches on methods to produce materials composed of fine and coarse grain structures are equally important. Materials composed of fine grain structures are produced by many methods. We are proposing a new method to produce large ingots composed of fine grain structures. Large ingots have usually coarse grain structures because the solidification rate of the ingots is rather slow. An apparatus for a rapid solidification along with vigorous agitation is constructed, and experiments using aluminum and its alloys are being performed.

116 Physical, Chemical and Biological Phenomena under Microgravity Environment

April 1987 to March 1992

*M. Yamazaki,*Materials Design Division*

Keywords: microgravity environment, solidification, superconducting alloys, dispersion alloys, fluid flow

---

*Present address: NASDA

One of the most important object of researches and developments in the materials science is the discovery of materials which have new functions. Materials processing on a micro scale are very essential in the discovery of new functions of materials. A microgravity environment has some special merits, namely, no natural convection, no floating and sinking, no static pressure, and containerless melting and solidification.

This research is composed of a lot of sub-themes carried on by researchers in government research institutes, universities and private companies. Three sub-themes of them had been performed in these two years, and described briefly below.

1. Formation mechanism of monotectic and eutectic composite structures: Multi-component superconducting alloys of Al-Cu with additions of Ba, Yb, Eu, etc. were crystallized by rapid or directional solidification on the earth and in the microgravity environment realized by drop-towers, airplanes or small rockets. Effects of gravity on structures and properties of samples obtained were examined.
2. Uniform dispersion mechanism of particles in dispersion alloys: Two different dispersion alloys, Cu-5 vol%Al_2O_3 and Cu-5 vol%W, were melted and solidified in the microgravity environment (sounding rocket flight) as well as on the ground in order to investigate the uniform dispersion mechanism of particles in dispersion alloys. The experimental results showed that melting and solidification in the microgravity environment was favorable for a uniform dispersion.
3. Effect of the fluid flow in melts on the properties of crystals grown: Embryos of crystals in melts formed just before its solidification was attempted to observe using an ultramicroscope. During the construction of the ultramicroscope, the lattice defects in a single silicon crystal made in an infrared image floating zone furnace were measured, analyzed and estimated with an X-ray diffraction topography.

117 Development of Extraction Techniques of Gallium and Other Rare Metals

April 1987 to March 1992

A. Fukuzawa, Chemical Processing Division

Keywords: gallium, iron ore, iron and steelmaking

Iron ore produced in the Panzihua area in south-western China's Sichuan Province is famous for the typical vanadium bearing titanoferrous magnetite and in Panzihua Iron and Steel Co. Vanadium is removed from the spray steelmaking method in the hot metal pretreatment stage as a byproduct. Besides, the titanium rich part is separated during the dressing process. This ore also contains rare metals such as nickel, chromium, cobalt or gallium.

To recover these rare metals, especially for gallium, we, NRIM and the University of Science and Technology, Beijing, have carried out this joint research project since 1986. Gallium is one of the most important elements for semiconductors such as Ga-As, magnetic bubble and others.

Gallium, whose content in iron ore is 40 to 50 ppm, is enriched a little in the blast furnace during reduction as high as 70 to 80 ppm in Panzihua Iron and Steel Co. In the steelmaking stage gallium is partially oxidized when the hot metal is treated for vanadium extraction, but the most of gallium is retained in the molten steel. Therefore, our research work covered all of the iron and steelmaking processes from iron ore to molten steel to investigate the suitable points in the process line to recover gallium effectively. Then the following two subjects were examined as the final stage of joint project.

Extraction from vanadium slag: As gallium is also oxidized in the spray steelmaking stage for vanadium recovery and gallium content in the vanadium slag is as much as 150 to 200 ppm, a wet extraction method has been applied after soda roasting of vanadium slag. At first, gallium and vanadium were extracted from soda slag into NaOH solution, then both elements were effectively separated by solvent extraction method.

Recovery by flux from hot metal: Since from the preliminary tests, flux with CaO has shown a potential to retain gallium oxide in slag, simultaneous extraction of gallium and vanadium from hot metal was tested at first by 1kg hot metal, then the continuous operation with 3t hot metal. This process is more advantageous for vanadium extraction than the conventional process from the points of not to make spinel structure with high melting point and less soda pollution problem.

Solid state process

118 Materials Properties Induced by Transformation Superplasticity

April 1990 to March 1993

H. Nakajima, Advanced Materials Processing Division

Keywords: transformation superplasticity, microstructures, mechanical properties

There are two types of superplastic behaviour, known as fine-grained and transformation superplasticity. In the latter, large elongations are generated by a thermal cycle of a material through a phase transformation. The purpose of this

investigation is to elucidate a change in the microstructures and the mechanical properties of ferrous materials which have been elongated by transformation superplasticity. Test material is 0.4% carbon steel JIS S40C. Specimens were heated to a temperature of 750 or 820 °C in order to austenitize only pearlite or both pearlite and ferrite, and then they were cooled in air under tensile load up to 49MPa. Superplastic strain were greater than linear function of applied stress, when the stress increasing above 30MPa. The microstructure after cooling was composed of ferrite and pearlite. In heating to 820 °C the morphology of pearlite was lamellar, while in austenitizing to 750 °C some carbides of pearlite presented a spheroidal form. These microstructural features affected the mechanical properties of specimens. In the former, strength was a little higher than that of the latter, and ductility was lower. Superplastical deformation, however, did not work a change in the microstructures nor in the tensile properties at room temperature.

119 Metallurgical Analysis of Cutting Region

April 1989 to March 1993

S. Yamamoto, Advanced Materials Processing Division

Keywords: chip shear region, micro-machining device, cutting force

The deformation behavior of the chip shear region in machining of various materials is being investigated from a metallurgical point of view.

A cutting region was first cut off from the work material of which machining had been suddenly stopped by a quick stop device.

Then the cutting region was cut (depth of cut: 10μm, feed of tool: 5μm) using a micro-machining device, from the undeformed zone of the work material to the chip. The cutting force measured in micro-cutting corresponded to the amount of work hardening. The cutting force in the chip was higher than that in the work material, owing to heavy work hardening. However, variation of the cutting force within each zone was small, while in the chip shear region an increase of the cutting force was observed in a direction from the starting line to the end line. The width of the chip shear region measured by above methods had a close relation to a radius of the built-up edge or a contact length between tool and chip.

Machinability of the austempered high strength ductile iron (ADI) developed for lightening of car parts was investigated. Spheroidal graphite cast iron which was composed of upper bainite structure had the tensile strength of 1000N/mm^2 and the elongation of 10 ~ 12%. In machining of the above material the tool wear was large because the contact length between tool and chip was much shorter than in machining of steel, and therefore, the crater wear was generated in the neighborhood of the cutting edge and it connected easily to the flank wear.

120 Comprehensive Research and Development of Special Structural Ceramics Using Colloid Processing

April 1990 to March 1993

Y. Kaieda, 3rd Research Group

Keywords: combustion synthesis, WC, chemical furnace

The purpose of this theme is forming of the elemental powders, instant synthesizing of the special structural compound composite using the heat of formation and its propagation, and revealing its mechanical properties. The study of the synthesis of the special compound with high melting temperature as a matrix of the composite using the chemical furnace, which is conducted by combustion synthesis, has been continued in this fiscal year. The very hard WC with high melting point is selected as an objective chemical compound in this fiscal year.

The chemical furnace consist of titanium and carbon which are both solid state below 1993K. Three matters are in condensed state below the adiabatic temperature. Namely, carbon and titanium carbide are solid state and titanium is liquid state. While the combustion synthesis is occurred, a part of the starting powder is heated up by the propagation of heat from the adjacent part in which the combustion synthesis has already started. Since titanium and carbon keep in contact with each other in solid state below the melting point of titanium, it is difficult for both powder to make a solid solution by mutual diffusion of titanium and carbon in a short time. However, above the melting point of the titanium, the solid particles of carbon are surrounded by molten titanium. Accordingly, above this temperature up to the adiabatic temperature, the synthesis becomes possible because of the classical reaction process in which the spherical particle is surrounded by liquid.

On the other hand, when the oxide starting powders are used in the chemical furnace and the following formula is applied,

$$3TiO_2 + 3C + 4Al = 3TiC + 2AL_2O_3,$$

solid state TiC and liquid Al_2O_3 are synthesized because the mutual diffusion becomes possible by the reaction, and the diffusion occurs in solid carbon particle surrounded by liquid aluminum and liquid TiO_2. This case is not favorable for synthesis of WC because the adiabatic temperature is too low.

Powder processing

(121) Development of Particles Assembly Technology for Integration of Functions

April 1992 to March 1996
N. Shinya, Failure Physics Division
Keywords: intelligent materials, multiple functions, particle assembly technology

For creation of intelligent materials, technologies for systematization and integration of multiple functions should be developed in advance. Systematically coordinated multiple functions will lead to manifestation of intelligent functions, such as self-repair, self-diagnosis, feedback and so on, which can respond to environmental conditions.

In order to provide materials with the systematically coordinated multiple functions, a new approach is made through a development of particles assembly technology in this work. Each particle has a primitive function such as sensor, processor and actuator. Therefore, coordinations and systematizations of these primitive functions may be realized through three dimensional particles arrangement. For the arrangement it is necessary to develop the technology which make it possible to assemble several kinds of particles according to structural designs for the manifestation of the coordination and systematization.

As elemental technologies for the three dimensional particles arrangements, particle designs, particle preparation, controls of particle movement and treatments of assembled particles are studied at the first stage.

122 Coating of Fine Powders by CVD Technique in Fluidized Bed

April 1991 to March 1994
T. Itagaki, Materials Design Division
Keywords: fluidized bed, CVD, hafnium carbide, tungsten powder

This research is aimed at preparing various types of very fine powders coated with very thin layer of a second substance. The fine coated powders have various advantages when they are used for sintering. For example, if the powder is coated with a sintering agent, the sintering will finish in much shorter time or will be performed at a lower temperature as compared with the case when the agent is added as powder, because the agent is much more finely dispersed. When an alloying element is coated on powder of a refaractory metal, the alloying will be more homogeneous by the same reason.

A chemical vapour deposition technique in a fluidized bed is planned to be applied to make the coating layer comprising ceramic materials. The particle size of the powder will be 1-10 microns, and thickness of the coated layer will be several nanometers. Based on the research work performed previously, we have been convinced that coating by CVD technique in a fluidized bed is technically feasible.

The first experiment was concerned with coating of hafnium carbide on tungsten powder. Until present, we attained coated layer of about 7 nanometers thickness on the surface of tungsten powder in diameter of 4 microns. The obtained powder will be sintered at a high temperature to obtain tungsten alloy dispersed with hafnium carbide.

Next experiment will be concerned with coating of sintering agent on ceramics such as silicon nitride or silicon carbide. This coating will be more difficult because the density of the powder is much smaller than that in the first experiment.

123 Coating Formation by Molten and Electrified Powders

April 1991 to March 1994
S. Kuroda, Advanced Materials Processing Division
Keywords: plasma spray, surface coating, deposition phenomena, interface, electrostatic force

This research aims to clarify the deposition phenomena of molten particles onto solid surface with a special interest for spray deposition of coatings in mind. The collision of a high velocity molten particle onto a solid surface and the subsequent solidification are very fast and complicated phenomena, on which various coating processes such as plasma spraying are based. How a particle spreads and looses heat to the underlying solid seems to be critically dependent on the temperature and velocity of the impinging particle as well as the surface state of the substrate. With the aid of a technique developed to measure the velocity and temperature of flying particles, morphology of quenched splats will be related to those parameters. The mechanical property as well as the microstructure of thus formed coating/substrate interface will be examined by using various mechanical testing methods and microscopic techniques such as TEM. In addition, feasibility of employing electrostatic force to control the motion of fine powders will be examined.

Related Papers

The Quenching Stress in Thermally Sprayed Coatings, Kuroda, S. and Clyne, T.W. Thin Solid Films 200 (1991): 49–66.

Measurement of temperature and velocity of thermally sprayed particles using thermal radiation, Kuroda, S., Fujimori, H., Fukushima, T. and Kitahara, S. Trans. Jpn. Welding. Soc. 22 (1991): 82–89.

Significance of the quenching stress in the cohesion and adhesion of thermally sprayed coatings, Kuroda, S., Fukushima, T., and Kitahara, S. Thermal Spray: International Advances in Coatings Technology. Proc. 13th Int. Thermal Spray Conf. Orlando, June, 1992: 903–909.

124 Combustion Synthesis for Production of Intermetallic Compound

April 1989 to March 1993
Y. Kaieda, 3rd Research Group
Keywords: combustion synthesis, heat of formation, shape memory

Combustion synthesis is a production process to produce chemical compounds from elemental powders in a short time using the heat of formation of component elements. The industrial technology to produce intermetallic compounds using the combustion synthesis has been being developed since last fiscal year in National Research Institute for Metals. The differences in melting point and specific gravity of the component elements are vital factors in producing the intermetallic compounds by conventional process. However, there is a possibility to produce the intermetallic compounds in combustion synthesis process, which are difficult to be produced in conventional process because the difference in specific gravity in the component powders does not affect the synthesis process and the difference in melting point affects in some degree the synthesis process.

We have studied mainly the technology to produce the NiTi system shape memory intermetallic compounds by combustion synthesis in this fiscal year. This material is produced usually by high frequency induction melting and casting in vacuum. Since the martensitic transformation temperature changes by 10 K against a change of 0.1 mass% in Ni content, the accurate control of the transformation temperature of the material made by the high frequency induction melting is said to be difficult. Two powder metallurgical methods, sintering of alloy powder process and sintering of elemental powder process, were once tried as methods to control easily the chemical composition of the material. In the method of sintering of alloy powder, the arc-melted alloy was gas-atomized to make alloy powder and the powder was hot isostatically pressed and underwent plastic working. In this method, the plastic working to make wires and plates was possible but the industrialization was not realized because the production cost was too expensive. In the elemental powder method, the production cost was low but the plastic working to make wires and plates was impossible because the contents of impurities in the material were too high.

125 Production and Characterization of Advanced Powders

April 1988 to March 1993
K. Yoshihara, 4th Research Group
Keywords: atomization, ultrafine particle, sintering, composite, rapid diffusion

Six sub-themes are included in this research.

1. Production of rapidly solidified alloy powders by super high pressure liquid atomization; Fine powders (<5 μm in diameter) of Cu, Fe, Ni, and Al base alloys are produced by a high pressure water atomization. Their properties and sintering conditions are investigated. These powders are expected to be used as raw materials for metal injection molding. Mechanical alloying characteristics are also investigated to produce metal carbides.
2. Synthesis and consolidation of ultrafine composite particles; Metal-ceramic ultrafine composite particles such as Ni-TiN and Ni-TiO_2 etc. are synthesized by an reactive plasma-metal reaction method or a RF-plasma CVD method. Sintering characteristics and catalytic (especially photo-catalytic) properties are investigated. Various powders are also prepared by a sol-gel method and their characterization are conducted.
3. Characterization of ultrafine particles and their bonded bodies; Surface chemistry of ultrafine particles, especially gas adsorption and desorption characteristics, are investigated by specially developed thermal desorption method. Electron discharged sintering characteristics are conducted to make porous or dense nanonstructured materials.
4. Production of advanced powders by centrifugal atomization; Fundamentals of centrifugal atomization are investigated. The atomization mechanisms and atomizing parameters are elucidated. The solidicated structure of atomized powders is studied in details. The importance of super-cooling is pointed out in the solidification of centrifugally atomized powders.
5. Sintering of metal-ceramic mixed powders; Wettablility and sintering characteristics of Cu-Al_2O_3 and Cu-W mixed powders are investigated to produce high strength and high conductivity alloys. Physical properties of liquid-solid interfaces are measured from a viewpoint of controlling the liquid phase sintering.
6. Reaction in metal thin film; Roll of surface free energy on the rapid diffusion and the formation of new phase in thin film are investigated by observing the reaction in Nb/Ti/Cu multi-thin films in a vacuum.

Related Papers

Slip Casting of Duplex Stainless Steel Fine Powders, Takeda, T. and Minagawa, K. J. Jpn. Soc. Powder Powder Metall. 37 (1990): 198–202 (in Japanese).

Synthesis of the Composite Ultrafine Particles of Ni-TiC by Reactive Plasma-metal Reaction, Ohno, S., Chun-Sheng, J., Okuyama, H. and Honma, K. J. Jpn. Powder Powder Metall. 39 (1992): 221–26 (in Japanese).

Sintering and Gas Desorption Characteristics of Copper Ultrafine Powders, Sakka, Y., Uchikoshi, T. and Ozawa, E. Mater. Trans. JIM 31 (1990): 802–9.

Centrifugal Atomization of Iron-Rare Earth Alloys, Halada, K., Suga, H. and Kiyama, T. Mater. Trans. JIM 31 (1990): 322–26.

Solid-Liquid Interfacial Tension of the W-Cu System, Muramatsu, Y., Halada, K., Dan, T. and Isoda, Y. J. Jpn. Inst. Met. 54 (1990): 679–84 (in Japanese).

126 Preparation and Characterization of Ultrafine Particles Used for Making Oxide Superconductors

April 1988 to March 1994

S. Ohno, 4th Research Group

Keywords: superconducting oxide, ultrafine particle, gas desorption

The finer of particle size of superconducting raw materials, the improvement of homogeneity, sinterability, and preferable orientation is expected. We have been progressing the studies on the preparation of ultrafine powders suitable for making superconducting oxide and their characterization. Following two subjects are conducted: (1) Effect of Ag addition on the growth of superconducting phase in the Bi oxide system, and (2) Stability of the superconducting oxide in air.

1. Bi, Sr $(OH)_2$, $Ca(OH)_2$ and Cu ultrafine particles are synthesized by a reactive plasma-metal reaction method. After mixing and calcinating the raw materials, the composition of which is fixed as Bi:Sr:Ca:Cu = 4:3:3:6, they are immersed in $AgNO_3$ aqueous solution. The calcinated powders with different amounts of Ag contents are heated at 860 °C for 60 h in air. The quantity of the high-Tc phase increase as increase in Ag addition to approximately 1 mass % and is saturated with adding Ag beyond 1 mass %. This phenomenon might be explained partially by the result that the liquidus temperatures are lowered by adding Ag.
2. For technological applications of superconductors, information about their stability under open environmental conditions is essential. We have demonstrated that gas adsorption and desorption measurements are suitable for estimating the surface compounds of fine powders. Gas desorption spectra of $YBa_2Cu_3O_{7-y}$ powders exposed to water vapor show two desorption peaks of water. The quantity of the water desorption increase as increase in water vapour pressures exposed and increase in oxygen vacancy concentration (y). The quantity of water desorption from the superconducting powders in the Bi oxide system is extremely smaller than that in the Y oxide system. This result indicates that the superconducting Bi oxide powders are relatively stable in air.

Related Papers

Uniformity of Sintered Superconductive Bi-Sr-Ca-Cu-O Ceramics, Ohno, S., Okuyama, H., Honma, K., Halada, K. and Ozawa M. J. Jpn. Soc. Powder and Powder Metall. 38 (1991): 263 (in Japanese).

Sorption and Desorption Characteristics of Water Vapour on $YBa_2Cu_3O_{7-y}$ Powders, Sakka,Y. and Uchikoshi, T Jpn. J. Appl. Phys. 29 (1990): L2022.

Joining

127 Corrosion of Dissimilar Metals Joints in Reactor Fuel Reprocessing Plants

April 1991 to March 1996

H. Nakamura, Advanced Materials Processing Division

Keywords: diffusion welding, titanium, zirconium, stainless steel, laser speckle method

Dissimilar metals joints are to be used in a new reactor fuel reprocessing plant in Japan. The joints composed of stainless steels and valve metals are made by solid state joining. It is necessary for the safety of plant to assure sufficiently high corrosion resistance and also corrosion fatigue strength of the joints.

Diffusion welding, friction welding and explosion welding are promising joining methods for the purpose. In diffusion welding a minimum input energy to get a sound joint is preferable for keeping the residual stresses and the formation of intermetallic compounds minimal. It was possible to make a joint of titanium and 304L stainless steel under the conditions that welding temperature, welding pressure and welding time are 750 to 800 °C, 10 MPa and 15 minutes, respectively. The tensile strength of the joint is about 300 MPa in the case of surface roughness before welding is 0.05 to 0.1 μm. It could be possible to increase the tensile strength by the aid of cleansing treatment of the surface.

Joints between zirconium and 304L stainless steel were also made under a similar condition and the strength of joints was the same level as in the titanium/304L joint.

Friction welding and explosion welding were applied to welding of zirconium and 304L stainless steel. These joints showed satisfactory tensile strength.

Laser speckle strain measurement was useful to detect a local strain in the narrow zone such as diffusion welded interface.

128 Joining of Intermetallic Compounds Utilizing Resistance Heating of the Compound to Be Joined

April 1991 to March 1993

S. Fukushima, Advanced Materials Processing Division

Keywords: joining technique, titanium aluminide, microscopic observation

The aim of this study is to pursue the possibility of the joining of intermetallic compounds which are to be used as an advanced structural material. An applied joining technique in this study consists of reaction sintering process and liquid-phase diffusion bonding process. The two processes proceed simultaneously under a certain welding force and welding current.

In this study, a casting of titanium aluminide, TiAl, was picked up as a base metal, and green mould disks compacted from the mixture of titanium and aluminium powder in the ratio of 1:1 in mol were used as an intermediate metal. Welding was carried out in argon gas atmosphere. Joining parameters to be examined are welding force, welding temperature, welding time, abutting surface condition, welding atmosphere and so forth.

Microscopic observation of the joint crosssections revealed the following items. No crack was recognized at the joint produced at the temperature of 1473K and the welding forces in the range from 0.98kN to 1.76kN. No crack was recognized at the joint produced at the temperature of 1373K and the welding force of 0.98kN, while cracks were recognized at the joints under welding forces over 1.37kN and the same temperature. Cracks were detected at all of the joints produced at the welding temperature of 1273K. These results may suggest that an adoptable welding force exists for each of welding temperatures.

Analyses of titanium and aluminium in some crystallines along the joints by EPMA suggested coexistance of alpha-two (Ti_3Al) and gamma (TiAl) phases near the joint interface.

This study will follow a series of experiments on confirmation of the joint strength.

129 Low Energy Joining with Controlled Surface Composition and Misorientation Angle

April 1990 to March 1993

O. Ohashi, Advanced Materials Processing Division

Keywords: surface composition, misorientation, diffusion welding, hydrogen permeability

The aim of our research is to develop a technique of low energy joining with the use of controlled surface composition and misorientation angle. In the second fiscal year, we constructed the surface doping chamber with an Auger analyzer and connected the ultra-high vacuum chamber. The following results have been obtained.

1. With nickel-base cast alloy single crystal of which the surface orientation to be joined is (001), it is found that creep rupture strength depends on the misorientation angle at bonded boundaries and there are peaks in strength around the coincidence boundaries. In the case of the twist angle above 3 degree, the precipitate phase is formed at the bonded boundary and bond strength is very low.
2. We have clarified the relationship between surface composition before contact and bond formation in diffusion-welding of SUS304 stainless steel. Bond formation at the contact area depends on the disappearance of the surface film which consists of oxygen and carbon. The film disappears above 800 °C, and sulfur in steel segregates to the surface. The thickness of sulfur-rich layer is 0.3-2nm. SUS304 stainless steel with sulfur-rich layer can be joined above 650 °C, since the sulfur diffuses from the contact surface to base metal.
3. The hydrogen permeability of the Pd-coated V-15at%Ni alloy membrane increases by La-coating before Pd-coating. The hydrogen trapping phenomenon is markedly improved by the reaction between La and oxides at interface.

Related Papers

Model Calculation of Electronic Property near Transition Metal Interfaces, Suga, S. and Ohashi, O. Physica Scripta 45 (1992): 458–62.

Effects of Metallic Atoms on Insulator Surfaces, Suga, S. and Ohashi, O. Physica Status Solidi 169 (1992): k13–k15.

Effects of Twist Angle on Tensile Strength of Diffusion-welded Joints in Molybdenum Single Crystal, Ohashi, O. and Suga, S. Quarterly J. of JWS 10 (1992): 53–58 (in Japanese).

Effect of Surface Composition on Diffusion Welding in Stainless Steel, Ohashi, O. and Suga, S. J. Japan Inst. Metals 56 (1992): 579–85 (in Japanese).

Hydrogen Permeation Characteristics of Palladium-Plated V-Ni Membranes, Amano, M., Komaki, M. and Nishimura, C. J. Less-Common M. 172–74 (1991): 727–31.

Hydrogen Permeation Characteristics of Vanadium-Nickel Alloys, Nishimyra, C., Komaki, M. and Amano, M. Mater. Trans. JIM 32 (1991): 501–7.

130 Effect of Temperature Distribution on Capillary Flow

April 1991 to March 1993

K. Sasabe, Advanced Materials Processing Division

Keywords: brazing, capillary penetration, micro

gravitation, computer simulation, temperature distribution

The purpose of this study is to establish a brazing technique in the space.

Brazing is the very suitable joining method for building and repairing constructions in the space, because brazing is carried out by lower energies and lower temperatures. Moreover the particular conditions of the space, i.e. high vacuum and micro gravitation, are very helfpful for brazing.

Whereas, it is well known that the strength of surface tension, which is the driving force of capillary penetration, depends on temperature. Therefore, the penetration of filler metal during brazing under a micro gravitation would not be stable when the temperature distributions on joint interfaces are not uniform.

For the first step of our study, we have investigated to establish a simulation method using personal computer to know the temperature distribution change on joint interfaces depending on the time during brazing.

By our simulation method developed, we can recognize the temperature distributions of joint of an arbitrary shape for an arbitrary time during heating by inputting material constants (heat conductivities, heat capacities and densities of base metals and filler metal, melting temperature of filler metal) and heating conditions.

The two possibilities to input heating conditions are prepared. The one is for isothermal and the other is for constant calorie heating, which correspond to furnace heating and chemical reaction heating (including solar heating), respectively.

Some studies on the temperature distribution change of thin wall cylinder joints proved to be possible to estimate the real temperature distribution during brazing by this method.

Composite process

(131) Forced Infiltration Process for Making Composite Structures

April 1992 to March 1994

T. Dendo, Advanced Materials Processing Division

Keywords: infiltration, semi-molten state, intermetallic compound

Forced infiltration technique is applied to two different processing purposes in this theme.

The first is to make a layer structure in surface portion of a porous ceramic compact by infiltration under semi-molten state.

The infiltrating metals are Pb-Sn alloys having wide region of semi-molten state in which liquid and solid co-exist. The porous compact is made of loosely-sintered alumina powder. Feature and feasibility of this new process are explored by examining the effects of process parameters such as volume fraction of liquid, porosity of ceramic compact, infiltration pressure and so on.

The other is to synthesize intermetallic compounds by infiltration into metallic powder compact. At present, synthesis of Ti-Al compound have been attempted through solid-liquid reaction in-process.

[132] Material Processing for Making Layered Structures

April 1989 to March 1992

T. Dendo, Advanced Materials Processing Division

Keywords: layered structure, large-scale and multi-layer crystal, sag test, pressure infiltration, metal-ceramic composite material

In this study, two different methods of material processing for making layered structures are attempted, and the feasibility of each process is explored through fundamental experiments.

Multi-layer crystal of refractory metals

The large-scale and multi-layer crystal, have been developed from a hot rolled multi-laminated molybdenum sheet doped with CaO and/or MgO by means of secondary recrystallization. To investigate mechanical property of the multi-layer crystal, at high temperature, a sag test was performed. Sag value in this test was measured by deflection angle of specimen. Sag value of the multi-layer crystal was lower than that of the single crystal. This improvement in mechanical property was interpreted in term of the difference in morphology of grain boundary and in distribution state of dopant between the multi-layer crystal and the single crystal.

Metal-ceramic composite material having layer structures

Pressure infiltration of molten metal into porous ceramics has been employed to manufacture a metal-ceramic composite material with layer structure. Some experiments using molten Pb-Sn alloy and semi-sintered alumina compact were performed, and morphology of the layer structure was examined in relation to the process parameters. Under the condition above 160 kgf/cm^2 of infiltration pressure, a composite structure infiltrated with the alloy can be formed in the surface portion of ceramic compact. The alloy infiltrated was uniformly distributed in thickness direction. Thickness of the layer structure formed depended strongly on the pressure of molten metal and the porosity of compact, but scarcely on the temperature of molten metal.

Related Papers

Preparation of Large-Scale and Multi-Layer Molybdenum Crystal and its Characteristics, Fujii, T. 12th

International Plansee Seminar, Proc. 1 (1989): 343–59.

Effect of Plastic Deformation on Bonding Behavior between Liquid and Solid Metals, Shirota, T., Kojima, S., Dendo, T. and Kiuchi, M. Advanced Technology of Plasticity 3 (1990): 1611–16.

Process with aid of beam technology

⑬③ Diagnostics of Laser Photoionization Induced Plasma

April 1992 to March 1995

Y. Ogawa, Chemical Processing Division

Keywords: laser photoionization, laser induced plasma, drift velocity, ion and electron temperatures, plasma density

Resonance stepwise photoionization method has acquired a wide variety of applications. Novel applications of laser photoionization include its emergence as a feasible method for the processing of high-purity materials and the separation of commercially valuable isotopes, when using as the detection of trace elements, and ion sources for ion implantation, etc. Furthermore, the extraordinary sensitivity and versatility of resonance photoionization spectroscopy have already applied to the identification of high-lying atomic levels, the measurement of transition cross sections, and the studies of chemical reactions, etc.

These applications are mainly based on laser stepwise excitation of atoms and on extraction of ions from weakly ionized plasma produced by the photoionization. The method of laser stepwise resonant photoionization of atoms was suggested more than ten years ago and the basic features and characteristics of this method have been fundamentally realized. However, little is known about the microscopic and macroscopic properties of the laser induced plasma (such as drift velocity, ion and electron temperatures, plasma density and so on) or about the extraction behavior of ions under the applied electric field. We have planned this research work to establish the diagnostic techniques for the weakly ionized plasma, which will contribute in full understanding of ion extraction behavior.

⑬④ Study on Evaporation Process by High Energy Density Beams

April 1992 to March 1995

H. Irie, Advanced Materials Processing Division

Keywords: electron beam, laser, PVD, CVD beam, arc

The electron beam PVD or CVD process has been widely used in coating process of glasses and camera lenses due to its clean environment and recently the laser PVD or CVD process has been researched and developed. In electron and laser beams evaporation process, the material does not necessarily evaporate in atomic or molecular but often accompanies dissolution of molecular, spattering, cluster, or these mixture especially under high energy density irradiation. Owing to these phenomena, electron and laser beams CVD or PVD has been done by low power and large diameter beams and often cannot obtain a desirable chemical compositions layer or fine powder at high production rate. It is necessary to analyze an evaporation process with respect to beam characteristics on the very fundamental basis.

In this study, very fundamental aspects of evaporation phenomena with high energy density beams, such as evaporation and diffusion rate, composition of vapor, recombination and deposition processes of evaporated materials will be observed and analyzed in order to realize rapid formation process of relatively thick layer or fine powder with desirable chemical composition.

Observation of vapor will be made by spectroscopic methods with and without of additional laser, time-of-flight method, high-speed movie for molten state of material and so far.

In electron beam process, evaporation process in a high and soft vacuum environment between ca 10^{-2} to 10 Pa will be investigated with typical materials of pure metal, ceramics and intermetallic compounds. Not only single beam, but also two beams system will be used in order to investigate the feasibility study on the usage of two vapor sources.

In laser beam process using a high power CO_2 laser, the laser heating process of plasma consisting of evaporated and shield gases will be investigated in order to make a sure of feasibility of laser reheating the evaporated material vapor in addition to basic evaporation process.

135 Development of Quantum Microstructure in Ultra Clean Vacuum

April 1990 to March 1995

K. Yoshihara, 4th Research Group

Keywords: quantum microstructures, extremely clean, magnetic levitation transport system

It is expected that materials with quantum microstructures will possess new and useful properties. However, to create these materials, it is necessary to handle the materials in extremely clean and high vacuum environment. Otherwise, impurities from the environment will deteriorate the material properties. This project is divided into two phases. In the first phase (Apr. 1990 - Mar. 1993), we will introduce the sample transfer system by a magnetic levitation system. By using this system, we will transfer specimens from one sta-

tion to the other station without any exposure to contaminating environment. In the second phase (Apr. 1993 - Mar. 1995), we will create materials with quantum microstructures by using this ultra clean vacuum system.

Since April 1990, we have constructed the extremely high vacuum system with new type vacuum pumps and special gate valves. In 1991, we developed two types of magnetic levitation transport system operated in the extremely high vacuum system. One is a linear motor system which carries three samples with high velocity. The other system uses couples of the magnets made of superconductive material and a permanent magnet. We manufactured a large cryostat in which a superconductive magnet moved at a temperature lower 100 K. The former type (linear motor system) is suitable for transferring rather heavy sample for long distance with high velocity. However, it is complicated and expensive. The latter type (superconductive material type) is suitable for transferring the sample for a short distance with precise position control. However it can carry only a sample under 50 grams. Both levitation transport systems have lower out-gassing rate than that of the traditional transport systems using a 'feed-through' manipulator or an all-metal magnet coupling.

The whole system will be completed until the end of March 1993.

136 Study on Synthesis of Special Compounds by a Combined Use of Ion Implantation and Deposition

April 1991 to March 1993

K. Saito, Surface and Interface Division

Keywords: ion implantation, sputter deposition, $Fe_{16}N_2$, BiSrCaCuO

A combined use of ion implantation and sputter deposition is a promising technique for synthesizing novel materials with specific atomic and electronic structures in highly controlled manner. In this study we synthesized a magnetic $Fe_{16}N_2$ compound films with a giant magnetization. Fe (001) thin films of 200nm thickness were deposited by ion beam sputtering and were implanted with nitrogen ions at low temperatures below 30K. It was found that the implanted films contained disordered martensite phase and transformed into an ordered martensite phase of $Fe_{16}N_2$ by annealing at 423 ~ 473K. Magnetization measurements of these magnetic films have been in progress. On the other hand, we succeeded in the fabrication of 30nm thick superconducting films of the BiSrCaCuO system by means of sputter deposition and Ar ion implantation 1, 2. Although the film thickness corresponds to only ten unit cell length of this system, the obtained value of T_c was raised up to 108 K, a highest value for this system. The role of the Ar ions was discussed in terms of atomic mixing and reordering within the low energy collision cascades.

Related Papers

Fabrication of 300 Å thick BiSrCaCuO Thin Films with T_c of 108 K by Use of Ion Implantation, Saito, K. and Kaise, M. Jpn. J. Appl. Phys. 31 (1992): L1047–50.

High-Quality 300 Å thick BiSrCaCuO Thin Films produced by a Magnetron Sputtering, Kaise, M. and Saito, K. submitted to J. Japan Inst. Metals.

137 Fundamental Study on Formation of Dissimilar Surface Layer by High Energy Density Beams

April 1989 to March 1992

H. Irie, Advanced Materials Processing Division

Keywords: electron beam, laser, surface modification, cladding, alloying

High energy density beams such as electron beam and high power laser have been expected to have excellent characteristics as a tool of surface modification. When these heat sources are applied to cladding and alloying, they can form a new or a different property surface layer without considerable damage to base material and with long irradiation distance, not depending on configuration or properties of base materials. In this research, fundamental study on formation processes for wide and uniform clad or alloyed surface is carried out, observing melting and flowing process of base metal and additional materials.

In laser cladding process using 5kW CO_2 laser, continuous and pulse irradiations of laser beam were applied in order to obtain very low diluted clad layer by base material. In laser cladding process of self-fluxing material such as stellite and others, which have been widely used in the arc cladding process, it is easy to accomplish a sound clad layer by a continuous laser irradiation because of no crack formation. On the other hand, in the case of the material combination of base metal and additional alloy, in which some brittle intermetallic compounds will be formed and induce cracks, it is very difficult to produce cladding layer with no mixing both materials and the method to minimize the dilution of clad layer by base metal should be essential. In the combination of WC-12Co powder and stainless steel, for example, the continuous irradiation of laser induced molten metal flow and mixing of both material. Then a reputation process of a pulse irradiation of laser on a rest specimen and movement of specimen by a certain distance under no irradiation was used. Many sorts of observation of this process, such as high speed movie and so on, indicated that this pulse irradiation of laser can melt only the added powder material at

the first step and melt the base material due to thermal diffusion from top surface, then it can minimize the melt of and the dilution by the base metal because of little flow of molten metal.

Related Papers

Formation mechanism of Locally Delayed Solidification Pattern in Electron Beam Welding, Tsukamoto, S. and Irie, H. Qu. J. Jpn. Weld. Soc. 8 (1990): 179–85 (in Japanese).

Fusion Property of CO_2 Laser in Stainless Steels, Irie, H. and Tsukamoto, S. Doc. IIW Meeting in Montreal, IIW Doc. IV-547–90 (1990).

Effect of Molten Metal Behavior on Melting Process in Electron Beam Welding, Tsukamoto, S. and Irie, H. Qu. J. Jpn. Weld. Soc. 9 (1991): 348–54 (in Japanese).

138 Study on Molten Metal Behavior in Surface Modification Process with High Temperature Heat Sources

April 1991 to March 1992

H. Irie, Advanced Materials Processing Division

Keywords: electron beam, laser, surface modification, rapid solidification

This research has been carried out under a collaboration program of bilateral science and technology agreement between Australia and Japan involving mutual exchange of scientists of each country.

In surface modification, especially rapid solidification or quenching techniques using high temperature heat sources such as laser, electron beam and arc, the surface roughness is an important factor for practice. Among various factors, the influence of sulfur content and power distribution of heat sources on the surface roughness were investigated. Grey and nodular cast irons containing several grades of sulfur content, which are used in sugar industry in Australia, were used for specimen. The Australian experiments with high speed arc melting indicated that low sulfur content produced smooth and flat molten zone whereas high content periodically humped molten metal. On cast irons of typical sulfur content in those experiments, laser high speed melting were carried out. With varying various parameters of irradiation, the melting speed along was the influencing parameter on formation of humping in high sulfur content iron whereas the smooth fusion zoned was always formed in low sulfur content as in the case of arc melting experiments.

In order to investigate the formation process of the humping fusion zone, observations of shape of fusion zone by a microscope and behaviour of molten metal by a high speed movie were carried out. And also analogous experiments were carried out in stainless steels, in which two kind of molten metal flows occur in the quite opposite direction depending upon its sulfur content due to the opposite incline of surface tension with respect to temperature in each specimen. The results showed that each hump was formed right under the laser irradiation point and grew with absorbing following molten metal until it went through the irradiation point. It indicated that humping or smooth molten metal is caused from the unbalance between the surface tension and the interfacial tension similar to the wettability of molten metal in welding. At the same time it was recognized that surface tension flows observed in arc melting of stainless steels, seem to occur, especially in smooth fusion zone.

Processing in special environment

139 Development of Extremely High Field Magnets

April 1988 to March 1994

H. Maeda, 1st Research Group

Keywords: 80 T class long-pulsed magnet, 40 T class hybrid magnet, 20 T class large-bore superconducting magnet, homogeneous-field magnet

For evaluating the high-field properties of high-T_c oxide superconductors, we are developing several high-field facilities, such as 80 T class long-pulsed magnet, 40 T class hybrid magnet, 20 T class large-bore superconducting magnet, and homogeneous-field magnet.

We found that Cu-(5–30)at%Ag alloys show the excellent properties as a conductor material for the long-pulsed magnet. It is, however, very difficult to wind the thick Cu-Ag alloy wire into a coil because of its strong spring-back force. We have succeeded in fabricating a small pulsed magnet by winding a rectangular Cu-Ag alloy wire of 2mm × 3mm. The performance test of the pulsed magnet is under way. For winding thicker Cu-Ag wires into coils, we have designed a powerful winding machine to be purchased.

The 40 T class hybrid magnet system is composed of a 15 T superconducting magnet with a clear bore of 400mm, and a polyhelix-type water-cooled resistive magnet with an incremental field of 25 T in a clear bore of 30mm. The design of the superconductor has been performed. The fabrication of the water-cooled magnet will be continued this year.

Test operation of the 20 T class large bore superconducting magnet system was performed successfully this year. The outer coil could generate a back-up field of 15 T in a 314mm free bore. The middle coil could generate an incremental field of 3 T in a 160mm free bore. In the back-up field of 18 T generated by the outer and the middle coils, the inner coil could generate 20.3 T in a 44mm free

bore. The free bore is much larger than those of other 20 T class superconducting magnets fabricated up to date and convenient for high field experiments. More details results are shown in the Research Topics.

We have performed measurements of the physical properties such as de Haas-van Alphan effect of UGe_2, NMR spectrum of ^{63}Cu in $YBa_2Cu_3O_6$, and high-resolution NMR of ^{17}O in glycine by using the high homogeneous-field magnet systems.

Related Papers

Development of 40 Tesla Class Hybrid Magnet System, Inoue, K., Takeuchi, T., Kiyoshi, T., Itoh, K., Wada, H., Maeda, H., Fujioka, T., Murase, S., Wachi, Y., Hanai, S. and Sasaki, T. IEEE Trans. on Magne. 28 (1992): 493–96.

Development of 20 Tesla Class Superconducting Magnet with Large Bore, Kiyoshi, T., Inoue, K., Itoh, K., Takeuchi, T., Wada, H., Maeda, H., Kuroishi, K., Suzuki, F., Takizawa, T. and Tada, N. IEEE Trans. on Magne. 28 (1992): 497–500.

High -Field Facilities under Development and Construction in NRIM, Japan, Inoue, K., Asano, T., Kiyoshi, T., Sakai, Y., Takeuchi, T., Itoh, K. and Maeda, H. Physica B 177 (1992): 7–15.

Development of High Resolution Magnet System and Applications - A Step toward NRIM High Field Magent Laboratories, Aoki, H., Uji, S. and Shimizu, T. Cryog. Engineer. 27 (1992): 21–9 (in Japanese).

Publications

❒ Papers Published in 1991

Characterization/Properties

Electronic and nuclear properties

1. *Superconducting Fluctuations in High-Tc Superconductors*, Kadowaki, K. Butsuri 46 (1991): 863–66 (in Japanese).
2. *Tellurides as the Thermoelectric Material*, Nishida, I. Ceramics 26 (1991): 1275–79 (in Japanese).
3. *Fabrication, Current Density and Strain Dependence of Sintered, Ag-Sheathed Bi-Sr-Ca-Cu-O (2212) Single Filament and Multifilamentary Tape Superconductors*, Schwartz, J. (Illinois Univ.), Sekine, H., Asano, T., Kuroda, T., Inoue, K. and Maeda, H. IEEE Trans. Mag. 27 (1991): 1247–49.
4. *New High Frequency dHvA Branch of CeSb*, Aoki, H., Crabtree, G.W. (Argonne Natl. Lab.), Joss, W. (Max Planck Institute) and Fulliger, H. (ETH). J. Mag. Mag. Mater. 97 (1991): 169–70.
5. *Positron Lifetime in Oxide Superconductors* $YBa_2(Cu_{1-x}M_x)_3O_{7-y}(M=Fe, Ni, Zn)$, *Ishibashi, S., *Yamamoto, R., *Doyama, M. (*Univ. of Tokyo) and Matsumoto, T. J. Phys. Condens. Matter 3 (1991): 9169–84.
6. *Torque Study of Layered Superconducting Oxide* $Bi_2Sr_2CaCu_2O_8$, *Okuda, K., *Kawamata, S., *Noguchi, S., *Itoh, N. (*Univ. of Osaka Prefecture) and Kadowaki, K. J. Phys. Soc. Jpn. 60 (1991): 3226–29.
7. *Localization in As-grown Single Crystals of* $Sm_{2-x}Ce_xCu_4$, Uji, S., Shimizu, T., and Aoki, H. Physica C 185 (1991): 1309–10.
8. *Pressure Effect on the Transport Properties of* $Ln_{2-x}Ce_xCuO_4$ *(Ln=Pr, Nd, Sm, Gd) Single Crystals*, Matsushita, A., Uji, S. and Matsumoto, T. Physica C 185 (1991): 1325–26.
9. *Local Density Band Structure of Y-Ba-Cu-Oxides*, Oguchi, T., Sasaki, T., and Terakura, K. (Univ. of Tokyo) Physica C 185 (1991): 1733–34.
10. *Two Dimensional Superconducting Properties in Single Crystalline* $Bi_2Sr_2CaCu_2O_{8+\delta}$, Kadowaki, K. Physica C 185 (1991): 1811–12.
11. *Superconducting Diamagnetic Magnetization of Single Crystalline* $Bi_2Sr_2CaCu_2O_{8+\delta}$, Kadowaki, K. Physica C 185 (1991): 2249–50.
12. *Theoretical Study on the Structural Stability of CuPd and CuPt Alloys: Pressure Induced Phase Transition of CuPt Alloy*, *Takizawa, S., *Blügel, S., *Terakura, K. (*Univ. of Tokyo) and Oguchi, T. Phys. Rev. B 43 (1991): 947–55.

Atomistic arrangement

13. *Redetermination of the Structure of the 80K Superconductor* $YBa_2Cu_4O_8$ *by Time-of-Flight Neutron Powder Diffraction*, *Lightfoot, P., *Pei Shiyou, *Jorgensen, J.D. (*Argonne Natl. Lab.), Yamada, Y., Matsumoto, T., Izumi, F. (NIRIM) and Kodama, Y. (GIRI). Acta Cryst. C47 (1991): 1143–45.
14. *Structure Images of* Y_2O_3 *by High Resolution Electron Microscopy*, Ogawa, K. and Ikeda, S. Bull. Jpn. Inst. Met. 30 (1991): 355 (in Japanese).
15. *Structure Images of* Y_2O_3 *by High Resolution Electron Microscopy*, Ogawa, K., Ikeda, S. and Sakata, K. (Science Univ. of Tokyo). J. Jpn. Inst. Met. 55 (1991): 272–78 (in Japanese).
16. *Amorphization in Immiscible Cu–Ta System by Mechanical Alloying*, *Lee C.H., Sakurai, K., *Fukunaga, T. and *Mizutani, U. (*Nagoya Univ.). J. Jpn. Soc. Powder Metall. 1 (1991): 83 (in Japanese).
17. *Helium Gas Release due to Grain Boundary Fracture in Neutron-Irradiated High Nickel Austenitic Alloys and a Ferritic Steel*, Kishimoto, N., *Clausing, R.E., *Heatherly, Jr., L. and *Farrell, K. (*Oak Ridge Natl. Lab.). J. Nucl. Matter. 179 (1991): 998–1002.
18. *Neutron Diffraction Study of the Ferromagnetic Copper Oxide* $La_{1.8}Ba_{1.2}CuO_5$, Mochiku, T., Asano, H. (Univ. of Tsukuba), Izumi, F. (NIRIM), *Mizuno, F., *Masuda, H., *Hirabayashi, I. and *Tanaka, S. (*ISTEC). J. Phys. Soc. Jpn. 60 (1991): 1959–63.
19. *Solid State Amorphization in the Cu–Ta Alloy System*, Sakurai, K., Yamada, Y., *Lee, C.H., *Fukunaga, T. and *Mizutani, U. (*Nagoya Univ.). Mater. Sci. & Eng. A134 (1991): 1414.
20. *Structural Changes of Superconducting* $YBa_2Cu_4O_8$ under High Pressure, Yamada, Y., *Jorgensen, J.D., *Pei Shiyou, *Lightfoot, P. (*Argonne Natl. Lab.), Kodama, Y. (GIRI), Matsumoto, T. and Izumi, F. (NIRIM). Physica C 173 (1991): 185.

21. *Correlation Between the Pressure-induced Changes in the Hall Coefficient and Tc in Superconducting Cuprates*, *Murayama, C., *Iye, Y., *Enomoto, T., *Mori, N. (*Univ. of Tokyo), Yamada, Y., Matsumoto, T., †Kubo, Y., †Shimakawa, Y. and †Manako, T. (†NEC Corp.). Physica C 183 (1991): 277–85.

22. *HREM Study of Iodine Intercalated $IBi_2Sr_2CaCu_2O_8$*, Chenevier, B. (École Nationale Supérieure de Physique de Grenoble), Ikeda, S. and Kadowaki, K. Physica C 185 (1991): 643–44.

23. *Pressure Effects on Tc of Superconducting $La_{2-x}Ca_{1+x}Cu_2O_6$*, Yamada, Y., *Kinoshita, K., Matsumoto, T., *Yamada, T. (*NTT Basic Res. Lab.) and Izumi, F. (NIRIM). Physica C 185 (1991): 1299–1300.

24. *Prediction for the Site Occupation of Third Element in TiAl Phase*, Hashimoto, K., Doi, H., Tsujimoto, T. and Suzuki T. (Tokyo Inst. Technol.). Trans. JIM 32 (1991): 574–79.

25. *The Local Structure of Cu–Ta Alloys Synthesized by Mechanical Alloying*, Sakurai, K., Yamada, Y., Itoh, M. (RIKEN), *Lee, C.H., *Fukunaga, T. and *Mizutani, U. (*Nagoya Univ.). X-Ray Absorption Fine Structure (1991): 543.

Phase transformation and microstructures

26. *On the Abnormally Large Tetragonality of Martensite in Fe-Ni-C Alloys*, Kajiwara, S. and Kikuchi, T. Acta. Metall. Mater. 39 (1991): 1123–31.

27. *Solute Partitioning during the Proeutectoid α Reaction in Ti-X_1-X_2 Alloys*, Enomoto, M. and Yoshida, T. (Shibaura Inst. Technol.). ISIJ International 31 (1991): 767.

28. *Deformation Behaviour of TiAl Base Alloy Containing Manganese at Elevated Temperature*, Hashimoto, K., Nobuki, M., Tsujimoto, T. and Suzuki, T. (Tokyo Inst. Technol.). ISIJ International 31 (1991): 1154–60.

29. *Degradation of 12Cr Steel due to High Temperature Creep Deformation*, Watanabe, T., Monma, Y., *Matsuo, T. and *Kikuchi, M. (*Tokyo Inst. Technol.). Jpn. Soc. for the Promotion of Sci., 123rd Committee Rep. 32 (1991): 123–36 (in Japanese).

30. *Degradation of 12Cr-1Mo-1W-0.3V Steel due to High Temperature Creep Deformation*, Watanabe, T., Monma, Y., *Matsuo, T. and *Kikuchi, M. (*Tokyo Inst. Technol.). Jpn. Soc. for the Promotion of Sci., 123rd Committee Rep. 32 (1991): 137–48 (in Japanese).

31. *Cation Interdiffusion and Phase Stability in Polycrystalline Tetragonal Ceria-Zirconia-Hafnia Solid Solution*, Sakka, Y., Ohishi, I. (Kyocera Corp.), Ando, K. (Toshiba Corp.) and Morita, S. (Mitsubishi Heavy Industries, Ltd.). J. Am. Ceram. Soc. 74 (1991): 2610–14.

32. *The Structure of Interphase Boundaries and the Ledgewise Growth of Precipitates in Metals and Alloys*, Enomoto, M. and Furuhara, T. (Kyoto Univ.). J. Iron and Steel Inst. Jpn. 77 (1991): 735 (in Japanese).

33. *Morphology of α_2 Phase in γ-TiAl-base Alloy Ingots*, Aritomi, N., Ogawa, K., Honma, K., Sato, K. and Tsujimoto, T. Mater. Sci. Eng. A149 (1991): 41–51.

34. *Martensitic Transformation in Ultra-fine Particles of Metals and Alloys*, Kajiwara, S., Ohno, S. and Honma, K. Phil. Mag. A 63 (1991): 625–44.

35. *Effect of Heat-Treatment on Tensile Properties of Forged TiAl Base Alloy with Addition of Manganese*, Hashimoto, K., Nobuki, M., Doi, H., Nakamura, M., Tsujimoto, T. and Suzuki, T. (Tokyo Inst. Technol.). Proc. of JIMIS–6 (1991): 457–61.

36. *Effect of Heat-Treatment of Physical Properties of Ti-6Al-4V Alloys at Cryogenic Temperatures*, Umezawa, O., Nagai, K. and Ishikawa, K. Proc. RASELM 91 (1991): 91–96.

37. *Raman Study of the Phase Separation in ZrO_2 –12mol% CeO_2 Ceramic* , Hirata, T., Zhu, H. (Zhejiang Univ.), Nakamura, K. and Kitajima, M. Solid State Commun. 80 (1991): 991–94.

Surface and interface properties

38. *Enhanced Adherence of Al_2O_3 Coating Layer by Concurrent S Suppression and TiC Surface Precipitation*, Ikeda, Y., Yoshitake, M., Yoshihara, K. and Nii K. ISIJ International 31 (1991): 162–67.

39. *Mechanism for Beneficial Effect of Y_2O_3 Dispersion for Protective Coating*, Ikeda, Y. and Yata, M. ISIJ International 31 (1991): 750–52.

40. *Indoor Corrosion of Copper and Silver Exposed in Japan and ASEAN Countries*, Fukuda, Y., Fukushima, T. (Univ. of the Ryukyus), *Sulaiman, A., *Musalam, I. (*RDCM, Indonesia), Yap, L.C. (SISIR Singapore), †Chotimongkol, L., †Judabong, S., †Potjanart, A., †Keowkangwal, O. (†TISTR, Thailand), Yoshihara, K. and Tosa, M. J. Electrochem. Soc. 138 (1991): 1238–43

41. *Hydrogen Permeation Characteristic of Palladium-Plated V-Ni Alloy Membranes*, Amano, M., Komaki, M. and Nishimura, C. J. Less-Common Met. 172 (1991): 727–31.

42. *Corrosion of a Type 304 Stainless Steel and a Molybdenum-based TZM Alloy in Refluxing Mercury with a Small Amount of Potassium,*

Suzuki, T. and Mutoh, I. J. Nucl. Mater. 184 (1991): 81–87.

43. *Quasi-Equilibrium of Stainless Steel in Non-Isothermal Sodium Loop Constructed of Type 316 Stainless Steel*, Suzuki, T. and Mutoh, I. J. Nucl. Mater. 186 (1991): 20–26.

44. *Dissolution Behavior of MnS Inclusion in Low Alloy Steels in High Temperature Water*, Matsushima, S., Katada, Y., Sato, S. and Nagata, N. Proc., of 7th APCCC 1 (1991): 112–17.

45. *Performance Assessment of Certain Solutions Chemical Removing of Corrosion Products*, Fukuda, Y., Fukushima, T. (Univ. of the Ryukyus) and Meechumnarn, K. (TISTR, Thailand) Rust Prevention & Control 35 (1991): 333–37 (in Japanese).

46. *In-Situ Observation on Metal Surfaces in Aqueous Solutions with an Electrochemical STM*, Masuda, H., Nagashima, N. and Matsuoka, S. Trans. Jpn. Soc. Mech. Eng. 57 (1991): 328–35 (in Japanese).

47. *STM Images of Films Produced at Elevated Temperatures*, Matsuoka, S., Masuda, H., Ikeda Y., *Akaike, K. and *Ochi, Y. (*Univ. of Electro-Communications). Trans. Jpn. Soc. Mech. Eng. 57 (1991): 2602–7 (in Japanese).

48. *Fractal Character of Fracture Surfaces on Metals*, Matsuoka, S. Zairyo to Kankyo 40 (1991): 498–505 (in Japanese).

49. *Study on Micro-Corrosion Mechanism for Low Alloy Steel by Scanning Tunneling Microscope*, Masuda, H., Matsuoka, S. and Nagashima, N. Zairyo to Kankyo 40 (1991): 754–59 (in Japanese).

Mechanical properties

50. *Fatigue and Fracture Mechanism in Polycrystalline Aluminum Oxide*, Horibe, S. and Takakura, E. Ann. Chim. Fr. 16 (1991): 403–12.

51. *Effect of Inclusions on Fatigue Properties of High Strength Steels*, Kanazawa, K. and Abe, T. ASME MD. 28 (1991): 139–50.

52. *Deformation and Fracture Behavior in High Cycle Fatigue at Cryogenic Temperatures*, Nagai, K., Umezawa, O. and Ishikawa, K. Bull. Jpn. Inst. Met. 30 (1991): 669–76 (in Japanese).

53. *Specimen Temperature Rise and Testing Conditions during Fatigue Tests at Cryogenic Temperatures*, Ogata, T., Ishikawa, K., Nagai, K., Yuri, T. and Umezawa, O. Cryogenic Engineering 26 (1991): 190–96 (in Japanese).

54. *High Cycle Fatigue Properties of Cryogenic Structural Alloys*, Nagai, K., Yuri, T., Umezawa, O., Ogata, T. and Ishikawa, K. Cryogenic Engineering 26 (1991): 255–62 (in Japanese).

55. *Subsurface Crack Initiation in High Cycle Fatigue at Cryogenic Temperatures*, Umezawa, O., Nagai, K., Yuri, T., Ogata, T. and Ishikawa, K. Cryogenic Engineering 26 (1991): 263–71 (in Japanese).

56. *Effect of Specimen Size on Creep Crack Growth Rate Using Ultra-large CT Specimens for 1Cr-Mo-V Steel*, Tabuchi, M., Kubo, K. and Yagi, K. Eng. Fract. Mech. 40 (1991): 311–21.

57. *Internal Crack Initiation in High Cycle Fatigue at Cryogenic Temperatures*, Nagai, K., Umezawa, O., Yuri, T. and Ishikawa, K. Eng. Fract. Mech. 40 (1991): 957–65.

58. *Evaluation of Fatigue Crack Propagation Properties under Random Loading Avoiding Crack Closure*, Suzuki, N., *Takeda, H., Ohta, A. and *Ohuchida, H. (*Kogakuin Univ.). Fatigue Fract. Eng. Mater. Struct. 14 (1991): 815–21.

59. *Fatigue Properties of Titanium Alloys in Liquid Helium*, Ishikawa, K., Nagai, K., Umezawa, O., Yuri, T. and Ogata, T. Int. J. JSME 34 (1991): 347–50.

60. *Optical Observations of Fatigue Crack Growth Behaviour of a Low Alloy Pressure Vessel Steel in High Temperature Water*, Katada, Y., Nagata, N. and Sato, S. Int. J. Press. Vessels & Piping 48 (1991): 37–52.

61. *Life Prediction by the Iso-Stress Method of Boiler Tubes after Prolonged Service*, Kanemaru, O., Shimizu, M., Ohba, T., Yagi, K., *Kato, Y. and *Hattori, K. (*Chubu Electric Power Co. Inc.). Int. J. Press. Vessels & Piping 48 (1991): 167–82.

62. *Low Cycle Fatigue Behavior of Pressure Vessels Steels in High Temperature Pressurized Water*, Nagata, N., Sato, S. and Katada, Y. ISIJ International 31 (1991): 106–14.

63. *Cryogenic Mechanical Properties of Ti-6Al-4V Alloys with Three Levels of Oxygen Content*, Nagai, K., Yuri, T., Ogata, T., Umezawa, O., Ishikawa, K., *Nishimura, T., *Takashima, T., *Mizoguchi, T., *Ito, Y., Ohyama, H. (*Kobe Steel Ltd.). ISIJ International 31 (1991): 882–89.

64. *Creep-Fatigue of 1Cr-Mo-V Steels under Simulated Cyclic Thermal Stresses*, Yamaguchi, K., Ijima, K., Kobayashi, K. and Nishijima, S. ISIJ International 31 (1991): 1001–6.

65. *Evaluation of Creep Deformation and Rupture Life of 1.3Mn-0.5Mo-0.5Ni Steel by Modified θ Projection Method*, Kushima, H., Watanabe, T., Yagi, K. and Maruyama, K. (Tohoku Univ.). Jpn. Soc. for the Promotion of Sci., 123rd Committee Rep. 32 (1991): 189–200 (in Japanese).

66. *Evaluation of Creep Rupture Strength for Ni-base 26Cr-17W Alloy by Intergranular Creep Damage Measurement*, Ohba, T., Yokokawa, K., Baba, E., Hiraga, K., Yagi, K. and Tanabe, T. Jpn. Soc. for the Promotion of Sci., 123rd Committee Rep. 32 (1991): 275–87 (in Japanese).

67. *Effect of Testing Environments on Fretting Fatigue Strength of Ti–6A1–4V*, Maruyama, N., Sumita, M. and Nakazawa, K. J. Iron and Steel Inst. Jpn. 77 (1991): 290–97 (in Japanese).

68. *Fundamental Properties of Long-term Creep Strength for Ferritic Heat Resistant Steels*, Kimura, K., Kushima, H., Yagi, K. and Tanaka, C. J. Iron and Steel Inst. Jpn. 77 (1991): 667–74 (in Japanese).

69. *Effect of Volume Fraction on Fatigue Strength of SiC Whisker or SiC Particle Reinforced Aluminum Composites*, Masuda, C., Tanaka, Y., *Yamamoto, M. and Fukazawa, M. (*Tokai Carbon Ltd.). J. Jpn. Compos. Mater. 17 (1991): 66–73 (in Japanese).

70. *Nodal Formulation for Computer Simulation of Elastic Waves and its Application to Rayleigh Waves*, Yamawaki, H. and Saito, T. J. JSNDI. 40 (1991): 791–7 (in Japanese).

71. *Statistical Experiment of Fatigue Crack Growth Rate Using DC Electrical Potential Method and Examination of Stochastic Models (2024-T3 Al Alloy)*, *Ichikawa, M., *Takamatsu, T. (*Univ. of Electro-Communications), Matsumura, T. (NEC Corp.), Suzuki, N. and Nishijima, S. J. Soc. Mater. Sci. Jpn. 40 (1991): 283–88 (in Japanese).

72. *Fractography and Fracture Analysis on Ceramics/Metal Joint*, Kobayashi, H. (Tokyo Inst. Technol.), Arai, Y. (Saitama Univ.) and Nagashima, N. J. Soc. Mater. Sci. Jpn. 40 (1991): 689–94 (in Japanese).

73. *Fatigue Fracture Surface at High Temperature for SiC Wisker Reinforced A2024 Matrix Composite*, Tanaka, Y., Masuda, C., *Yamamoto, M. and *Fukazawa, M. (*Tokai Carbon Ltd.). J. Soc. Mater. Sci. Jpn. 40 (1991): 748–54 (in Japanese).

74. *Tensile Fracture Surface Analysis for Boron Fiber*, Tanaka, Y. and Masuda, C. J. Soc. Mater. Sci. Jpn. 40 (1991): 869–74 (in Japanese).

75. *Fatigue Crack Propagation in Welded Joints under Random Loading*, Ohta, A., Maeda, Y., *Machida, S. and *Yoshinari, H. (*Univ. of Tokyo). J. Soc. Mater. Sci. Jpn. 40 (1991): 1442–46 (in Japanese).

76. *Fatigue Strength and Fatigue Crack Initiation and Propagation of High Strength Steels*, Abe, T. and Kanazawa, K. J. Soc. Mater. Sci. Jpn. 40 (1991): 1447–52 (in Japanese).

77. *Fatigue in Ceramics and Elucidation of its Phenomena*, Horibe, S. Maintenance Monthly 135 (1991): 32–36 (in Japanese).

78. *Indentation Fatigue of Silicon Carbide and Silicon Nitride*, Takakura, H. and Horibe, S. Mater. Trans. JIM 32 (1991): 495–500.

79. *Subsurface Crack Initiation in High Cycle Fatigue of 0.1N-32Mn-7Cr Steel at Cryogenic Temperatures*, Umezawa, O., Nagai, K., Yuri, T. and Ishikawa, K. Mechanical Behaviour of Materials–IV 4 (1991): 301–6.

80. *Creep Crack Growth Behavior in High Temperature Structural Steel and Alloys*, Tabuchi, M. and Yagi, K. Mechanical Behaviour of Materials–IV 4 (1991): 571–76.

81. *Effect of Grain Size on Rupture Life under Creep-fatigue Loading for 321 Stainless Steel*, Yagi, K., Kubo, K., Kanemaru, O. and Tanaka, C. Mechanical Behaviour of Materials–IV 4 (1991): 583–88.

82. *Correlation Between Short-Time Tensile Strength and Long-Time Creep-Rupture Strength of Commercial Superalloys*, Monma, Y., Sakamoto, M. and Yoshizu, H. Proc. First Int. Conf. on Heat-Resistant Materials (1991): 349–53.

83. *Creep Crack Growth Behavior in a Ni-Base Superalloy in 1273K Helium Gas Environment*, Nakasone, Y., Hiraga, K. and Tanabe, T. Proc. 1st JSME/ASME Joint Int. Conf. Nucl. Eng. (1991): 549–52.

84. *Relationship between the Primary and Secondary Recrystallized Textures in Multi-layer Molybdenum Crystals*, Fujii, T. Proc. of Grain Growth in Polycrystalline Materials (1991): 96–99.

85. *Fatigue Crack Growth in Welded Joints under Random Loading*, Ohta, A., Maeda, Y., *Machida, S. and *Yoshinari, H. (*Univ. of Tokyo). Proc. of ISMS' 91 (1991): 329–34.

86. *Discontinuous Deformation of Austenitic Stainless Steels at Liquid Helium*, Ishikawa, K., Ogata, T., Nagai, K., Yuri, T. and Umezawa, O. Proc. Stainless Steel 91 1 (1991): 449–56.

87. *High Cycle Fatigue of Some Austenitic Steels at Cryogenic Temperatures*, Nagai, K., Umezawa, O., Yuri, T., Ishikawa, K. and Ogata, T. Proc. Stainless Steel 91 1 (1991): 465–72.

88. *Effect of Carbon on Creep Rupture Strength and Ductility of a 10%Cr-30%Mn Austenitic Steel*, Abe, F., Nakazawa, S., Araki, H. and Noda, T. Proc. Stainless Steels 916 (1991): 610–17.

89. *Creep Embrittlement and its Prevention Catalytic Reformer Equipment*, Nomura, T. (Nippon Mining Co., Ltd.), Tanaka, H., Kushima, H., Tabuchi, M. and Yagi, K. Proc. 3rd NACE Int.

on Life Prediction of Corrodible Structures (1991): 1.

90. *Fatigue Life Prediction for Metallic Materials,* Nishijima, S. J. Jpn. Soc. Safety Engineering 30 (1991): 400–6 (in Japanese).

91. *Environment Embrittlement in Li_2-Ordered (Fe, Co)$_3$V, Nishimura, C. and Liu, C.T. (Oak Ridge Natl. Lab.).* Scr. Metall. Mater. 25 (1991): 791–94.

Measurement and evaluation

92. *Determination of Lattice Parameter and Strain of γ ′ Phases in Nickel–base Superalloys by Synchrotron Radiation Parallel Beam Diffractometry,* Ohno, K., Ohsumi, K. (Natl. Lab. for High Energy Physics), Harada, H., Yamagata, T. and Yamazaki, M. Advances in X–Ray Analysis 34 (1991): 493–499.

93. *Analysis of Minute Amounts of Solid Sample by Spark Source Mass Spectrometry,* Saito, M. Anal. Chim. Acta 242 (1991): 117.

94. *Determination of Traces of Impurities in Molybdenum Disilicide by Inductively Coupled Plasma-Atomic Emission Spectrometry after Coprecipitation,* Kujirai, O., Yamada, K., Kohri, M. and Okochi, H. Analytical Sciences 7 (1991): 99–102.

95. *Enhancement of Sensitivity by Ar/H_2 Gas Mixture in Glow Discharge Mass Spectrometry,* Saito, M. Analytical Sciences 7 (1991): 541–43.

96. *Determination of Impurities in Vanadium Disilicide and Vanadium Pentoxide by Atomic Absorption Spectrometry and Inductively Coupled Plasma-Atomic Emission Spectrometry after Matrix Separation,* Kohri, M., Kujirai, O. and Okochi H. Analytical Sciences 7 (1991): 767–71.

97. *Quantification of Surface Chemical Analysis by AES,* Fujita, D. and Honma, T. (Univ. of Tokyo) Bull. Jpn. Inst. Met. 30 (1991): 587–94 (in Japanese).

98. *The Reliability of the Quantitative Analysis with AES,* Yoshihara, K. and Ichimura, S. (Electrotechnical Lab.). Bull. Jpn. Inst. Met. 30 (1991): 595–600 (in Japanese).

99. *Quantitative Analysis of Surface Composition Co-Ni Alloys with AES,* Fujiwara, J. and Yoshihara, K. Bunseki Kagaku 40 (1991): 151–55 (in Japanese).

100. *Determination of Aluminium and Calcium in Silicon Carbide by ICP–AES after Matrix Isolation,* Yamaguchi, H., Haraguchi, H. (Nagoya Univ.) and Okochi, H. Bunseki Kagaku 40 (1991): 271–76 (in Japanese).

101. *Determination Condition of Probe Index and Beam Angle using IIW Type Standard Test Block,* Fukuhara, H. First Far East Nondestructive Testing Conference (1991): 9–16.

102. *Influence of Alloy Composition on Hot Deformation Properties of Ti-Al Binary Intermetallics,* Nobuki, M. and Tsujimoto, T. ISIJ International 31 (1991): 931.

103. *X–Ray Fluorescence Analysis of Titanium Alloys by Acid Dissolution/Glass Bead Technique,* Sato, K., Itoh,S. and Okochi, H., J. Iron and Steel Inst. Jpn. 77 (1991): 179–86 (in Japanese).

104. *Determination of Rare–Earth Elements in Metallic La, Pr, Nd, Gd and Tb by Glow Discharge Mass Spectrometry,* Hirose, F., Itoh, S. and Okochi, H. J. Iron and Steel Inst. Jpn. 77 (1991): 598–604 (in Japanese).

105. *Determination of Trace Elements in Iron and Steels by GF–AAS,* Kobayashi, T., Ide, K., Okochi, H., *Abiko, K. and *Kimura, H. (*Tohoku Univ.). J. Iron and Steel Inst. Jpn. 77 (1991): 1916–21 (in Japanese).

106. *Determination of Trace Amounts of Aluminum in Iron and Steels by GF–AAS,* Kobayashi, T., Ide, K., Okochi, H. and Shimada, Y. (Kawasaki Steel Techno-Research Corp.). J. Jpn. Inst. Met. 55 (1991): 970–74 (in Japanese).

107. *Effect of Sensor Size on Results of Magnetic Flux Leakage Testing,* Uetake, I., Ito, H. and Saito T. J. JSNDI. 40 (1991): 291–97 (in Japanese).

108. *Detection of Creep Damage by Ultrasonic Wave,* Fukuhara, H., Shinya, N. and Kyono, J. J. JSNDI 40 (1991): 450–55 (in Japanese).

109. *Application of Ultrasonic Detection by Optical Heterodyne Interferometry to Microscopic Material Evaluation,* Yamawaki, H. and Saito, T. J. JSNDI. 40 (1991): 616–23 (in Japanese).

110. *Effect of Transducer Crystal Size on Beam Angle of Ultrasonic Angle Probe,* Fukuhara, H., Hoshino, M. (Japan Probe Co., Ltd.), Kato, I. (KGK Co., Ltd.). and Takahashi, M. (Nippon Chutetsukan Co., Ltd.). J. JSNDI. 40 (1991): 646–51 (in Japanese).

111. *Observation of Micro-Deformation by a Moiré Method using a Scanning Electron Microscope,* Kishimoto, S., Egashira, M. and Shinya, N. J. Soc. Mater. Sci. Jpn. 40 (1991): 637–41 (in Japanese).

112. *Photo-Electron Emission from Bare Surface of Metals,* Nagashima, N., Masuda, H. and Matsuoka, S. J. Soc. Mater. Sci. Jpn. 40 (1991): 1100–4 (in Japanese).

113. *Drop-weight Type Impact Tensile Machine and Determination of Dynamic Elastic-plastic Fracture Toughness,* Yasunaka, T., Nakano, K. and Saito, T. Material Testing Technique 36 (1991): 23–29 (in Japanese).

114. *Determination of Boron in Iron Disilicide and High Purity Iron by Inductively Coupled Plas-*

ma-Atomic Emission Spectrometry after Anion Exchange Chromatography, Yamada, K., Yamaguchi, H., Kujirai, O. and Okochi, H. Mater. Trans. JIM 32 (1991): 480–84.

115. *In Situ Deformation of Proton-Irradiated Molybdenum in a High-Voltage Electron Microscope*, *Suzuki, M., *Fujimura, A., *Sato, A. (*Tokyo Inst. Technol.), Nagakawa, J., Yamamoto, N. and Shiraishi, H. Phil. Mag. A 64 (1991): 395–411.

116. *Fourier Analysis of Interference Structure Observed in X-Ray Specular Reflection from Thin Films*, Sakurai, K. and Iida, A. (Natl. Lab. for High Energy Physics). Photon Factory Activity Report 1991 9 (1991): 48.

117. *Grazing Exit X-Ray Fluorescence Spectrometry*, Noma, T. (Canon Inc.), Iida A. (Natl. Lab. for High Energy Physics), Sakurai, K. Photon Factory Activity Report 1991 9 (1991): 49.

118. *Structure of Ball-Milled Powders of the Immiscible System Cu-V*, Sakurai, K., *Mori, M., *Mizutani, U. (*Nagoya Univ.) Photon Factory Activity Report 1991 9 (1991): 126.

119. *Current Distribution on Molten Pool in Stationary TIG Arc Welding of Ti Alloy*, Okada, A. and Nakamura, H. Q. J. Jpn. Weld. Soc. 9 (1991): 216 (in Japanese).

120. *Quantitative Surface Chemical Analysis of Au-Cu Alloys with XPS*, Yoshitake, M. and Yoshihara, K. Surface and Interface Analysis 17 (1991): 711–18.

121. *In Situ Deformation of Proton-Irradiated Metals*, *Suzuki, M., *Fujimura, A., *Sato, A. (*Tokyo Inst. Technol.), Nagakawa, J., Yamamoto, N. and Shiraishi, H. Ultramicroscopy 39 (1991): 92–99.

Simulation and theory

122. *Creep Properties of $\alpha+\alpha_2$ High Temperature Titanium Alloys Designed by the Aid of Thermodynamics*, Onodera, H., Nakazawa, S., Ohno, K., Yamagata, T. and Yamazaki, M. ISIJ International 31 (1991): 875–81.

123. *Adaptability of TTP Methods for Creep-Rupture Data*, Monma, Y., Yoshizu, H. and Sakamoto, M. Jpn. Soc. for the Promotion of Sci., 123rd Committee Rep. 32 (1991): 177–88 (in Japanese).

124. *New Data Processing for the Sessile Drop Technique and the Application to Cu-20mass%Ni/Al_2O_3 System*, Dan, T., Halada, K. and Muramatsu, Y. J. Jpn. Inst. Met. 55 (1991): 1123–29 (in Japanese).

125. *Computer Modeling of the Growth of the Second Phase Particles in Binary Alloys*, Enomoto, M. J. Jpn. Weld. Soc. 60 (1991): 767 (in Japanese).

126. *Computer Simulation of Early–Stage Irradiation Creep*, Nagakawa, J., Yamamoto, N. and Shiraishi, H. J. Nucl. Mater. 179–181 (1991): 986–89 (in Japanese).

127. *Characterization of Optical Microstructure by Sensory Test*, Kurihara, Y., Kaneko, T., Hoshimoto, K. and Fujita M. J. Soc. Mater. Sci. Jpn. 28 (1991): 245–51 (in Japanese).

128. *Round-Robin Comparison of Data Evaluation Models for Fatigue Properties of Metallic Materials*, Kanazawa, K., Monma, Y. and Nishijima, S. Mechanical Behaviour of Materials–IV 2 (1991): 3–10.

129. *Thermodynamics Aided Design of $\alpha+\alpha_2$ High Temperature Titanium Alloys*, Onodera, H., Nakazawa, S., Ohno, K., Yamagata, T. and Yamazaki, M. Proc. of Computer Aided Innovation of New Materials (1991): 835.

130. *Density-Functional Molecular-Dynamics Method*, Oguchi, T. and Sasaki, T. Prog. Theor. Phys. Suppl. 103 (1991): 93–117.

131. *Fractal Character of Scanning Tunneling Microscopic Images of Brittle Fracture Surfaces on Molybdenum*, Sumiyoshi, H., Matsuoka, S., Ishikawa, K. and Nihei, M. Trans. Jpn. Soc. Mech. Eng. 57 (1991): 2237–43 (in Japanese).

Materials

Ferrous materials

132. *Effect of Stress on the Variant Selection in Martensitic Transformation*, Miyaji, H. and Furubayashi, E. Textures and Microstructures 14-18 (1991): 561–66.

Intermetallic compounds

133. *Fabrication Technique of TiAl Intermetallics for Structural Material*, Nobuki, M., Hashimoto, K. and Tsujimoto, T. Bull. Jpn. Inst. Met. 30 (1991): 49 (in Japanese).

134. *Elastic Properties of Intermetallic Compounds*, Nakamura, M. Bull. Jpn. Inst. Met. 30 (1991): 404–12 (in Japanese).

135. *Elastic Constants of $TiAl_3$ and $ZrAl_3$ Single Crystals*, Nakamura, M. and Kimura, K. J. Mater. Sci. 26 (1991): 2208.

136. *Microstructures and Deformation Properties in TiAl Intermetallics Containing Ti_3Al*, Nobuki, M. and Tsujimoto, T. Proc. of JIMIS–6 (1991): 451–55.

137. *Influence of Growth Rate on Microstructure and Tensile Properties of Directionally Solidified TiAl Alloys*, Takeyama, M., Hirano, T. and Tsujimoto, T. Proc. of JIMIS–6 (1991): 507.

138. *Elastic Properties of Transition Metal Di-silicides and Tri-aluminides*, Nakamura, M. Proc. of JIMIS–6 (1991): 655–59.

139. *Microstructure and Hardness of $NiAl/Ni_2Al_x$ Two-Phase Ordered Intermetallic Alloys*, Takeyama, M., *Liu, C.T. and *Sparks, Jr., C.J. (*Oak Ridge Natl. Lab.) Proc. of JIMIS–6 (1991): 871.

140. *Tensile Ductility of Stoichiometric Ni_3Al Grown by Unidirectional Solidification*, Hirano, T. Scr. Metall. Mater. 25 (1991): 1747–50.

Composites

141. *Polarization Curves of the Nickel-Base Alloys on a Single Tie-Line*, Numata, H., Tomizuka, I. and Koizumi, Y. Zairyo to Kankyo 40 (1991): 729–35 (in Japanese).

Materials for Mechanical application

142. *Titanium Alloys—The Alloy to Challenge Improved Properties*, Kawabe, Y. Chemical Education 39 (1991): 405–9 (in Japanese).

143. *Strengthening and Toughening of Titanium Alloys*, Kawabe, Y. and Muneki, S. ISIJ International 31 (1991): 785–91.

144. *Fatigue Property Enhancement of α-β Titanium Alloys by Blended Elemental P/M Approach*, Hagiwara, M., Kaieda, Y., Kawabe, Y. and Miura, S. (Showa Denko K.K.). ISIJ International 31 (1991): 922–30.

145. *Fabrication of Functionally Gradient Material*, Shinohara, Y., Shiota, I. and Watanabe, R. (Tohoku Univ.). J. Compos. Mater. 17 (1991): 179–85 (in Japanese).

146. *Production of Ti-5Al-2.5Fe Alloys by the Blended Elemental Method with Microstructural Modification and Their Mechanical Properties*, Hagiwara, M., Kaieda, Y., Kawabe, Y., *Miura, S., *Hirano, T. (*Showa Denko K.K.) and Nagasaki, S. (Showa Titanium Co., Ltd.). J. Iron and Steel Inst. Jpn. 77 (1991): 139–46 (in Japanese).

147. *Effect of Prior-Austenite Grain Size on Hydrogen Attack of 2¼Cr-1Mo Steel*, Nakajima, H., Miyaji, H. and Yamamoto, S. J. Iron and Steel Inst. Jpn. 77 (1991): 1320–27 (in Japanese).

148. *Property Enhancement of α-β Titanium Alloys by Microstructure-controllable New Blended Elemental P/M Method*, Hagiwara, M., Kaieda, Y., Kawabe, Y., Yamaguchi, K., Shimodaira, M. and Miura, S. (Showa Denko K.K.). J. Iron and Steel Inst. Jpn. 77 (1991): 2131–38 (in Japanese).

149. *Effect of Beta Grain Size and Aged Structure on Strength and Toughness in a Ti-15V-3Cr-3Sn-3Al Based Alloy*, Muneki, S., Kawabe, Y., Kainuma, T. and Takahashi, J. J. Jpn. Inst. Met. 55 (1991): 158–65 (in Japanese).

150. *Compositional Dependence of Dislocation Loop Development and Microstructures in Austenitic Fe-Ni-Cr Alloys under Proton Irradiation*, Kimoto, T., Furuya, K. and Shiraishi, H. J. Nucl. Mater. 179 (1991): 507–10.

151. *Alloy Design in Titanium Alloys*, Kawabe, Y. New Materials 2 (1991): 28–31 (in Japanese).

152. *The Effect of Aging Treatment on the Mechanical Properties of β-Titanium Alloys*, Muneki, S., Kawabe, Y., Kainuma, N. and Takahashi, J. Proc. 2nd Jpn. Int. SAMPE Symp. (1991): 418–24.

153. *Thermal Stability of FGM in Uniform and Gradient Temperature Fields*, Shinohara, Y., Imai, Y., Ikeno, S. and Shiota, I. Proc. 4th Symp. on FGM (1991): 173 (in Japanese).

154. *Strength and Toughness of Austenitic Stainless Steels at Cryogenic Temperatures*, Ogata, T., Ishikawa, K., Nagai, K., Yuri, T. and Umezawa, O. Proc. Stainless Steel 91 1 (1991): 457–64.

Materials for electronics application

155. *Anisotropy of Critical Current Density in Textured $Bi_2Sr_2Ca_1Cu_2O_x$ Tapes*, Kumakura, H., Togano K., Maeda, H., *Kase, J. and *Morimoto, T. (*Asahi Glass Co., Ltd.). Appl. Phys. Letters 58 (1991): 2830–32.

156. *Development of High-Strength, High-Conductivity Cu-Ag Alloys for High-Field Pulse Magnet Use*, Sakai, Y., Inoue, K., Asano, T., Wada, H. and Maeda, H. Appl. Phys. Letters 59 (1991): 2965–67.

157. *Processing, Microstructures, and Critical Currents of BiSrCaCuO Superconducting Tapes*, Togano, K., Kumakura, H., Dietderich, D.R., Maeda, H. and Kase, J. (Asahi Glass Co., Ltd.). High Temperature Superconducting Compounds III (1991): 363–73.

158. *Nb Tube Processed Nb_3Al MF Superconductors*, Takeuchi, T., Kosuge, M., Iijima, Y., Hasegawa, A., Kiyoshi, T. and Inoue, K. IEEE Trans. Magnetics 27 (1991): 2045–48.

159. *Strain Tolerance of Doctor Blade Processed $Bi_2Sr_2Ca_1Cu_2O_{8-\delta}$ Tapes*, Togano, K., Kumakura, H., Kase, J. (Asahi Glass Co., Ltd.), *Li, Q., *Ostenson, J.E. and *Finnemore, D. (*Iowa State Univ.) J. Appl. Phys. 70 (1991): 6966–69.

160. *Comparison of Bi-System 2223 and 2212 Thick Superconducting Tapes*, Sekine, H., Schwartz, J. (Illinois Univ.), Kuroda, T., Inoue, K., Maeda, H., *Numata, K. and *Yamamoto, H. (*Mitsubishi Heavy Industries, Ltd.). J. Appl. Phys. 76 (1991): 1596–99.

161. *New MBE Growth Method for InSb Quantum Well Boxes*, Koguchi, N., Takahashi, S. and Chikyow, T. J. Crystal. Growth 111 (1991): 688–92.

162. *Strain Effects on Superconducting Properties in Ultra-thin Filamentary Wires*, Kuroda, T. and Wada, H. J. Jpn. Inst. Met. 55 (1991): 344–50 (in Japanese).

163. *Microstructure and Superconducting Properties of Nb_3Al Multifilamentary Wires Processed by Nb-tube Method*, Takeuchi, T., Kosuge, M., Iijima, Y., Hasegawa, A., Kiyoshi, T., Matsumoto, F. and Inoue, K. J. Jpn. Inst. Met. 55 (1991): 472–80 (in Japanese).

164. *Development of High-Strength, High-Conductive Copper-Silver Alloys*, Sakai, Y., Inoue, K., Asano, T. and Maeda, H. J. Jpn. Inst. Met. 55 (1991): 1382–91 (in Japanese).

165. *Mössbauer Studies on Superconducting $La_{1.82}Ca_{1.18}(Cu_{0.99}Fe_{0.01})_2O_6$*, Furubayashi, T., Matsumoto, T., *Kinoshita, S. and *Yamada, T. (*NTT Basic Res. Lab.). Physica C 185 (1991): 1231–32.

166. *Critical Current Density and Flux Pinning in Textured $Bi_2Sr_2Ca_1Cu_2O_x$ Tapes*, Kumakura, H., Togano, K., Kitaguchi, H., Maeda, H., Kase J. (Asahi Glass Co., Ltd.) and Nomura, K. (Hitachi Cable, Ltd.). Physica C 189 (1991): 2341–42.

167. *Preparation of Bi-Sr-Ca-Cu-O Superconducting Tape by Pyrolysis of Organic Acid Salts*, *Hasegawa, T., *Kitamura, T., *Kobayashi, H., *Takeshita, F. (*Showa Electric Wire & Cable Co., Ltd.), Kumakura, H., Kitaguchi, H. and Togano, K. Physica C 190 (1991): 81–83.

168. *Fabrication of Bi(2212)/Ag Superconducting Tapes and Coils*, Kumakura, H. Proc. of the 7th US–Japan Workshop on High-Field Superconducting Materials (1991): 249–53.

169. *Growth of InSb Microcrystals on a Te Terminated InSb Substrate by Droplet Epitaxy*, Ishige, K. and Koguchi, N. Symp. Record of Alloy Semiconductor Physics and Electronics 10 (1991): 255–62.

Magnetic materials

170. *Magnetic Properties of $(Dy_{1-x}Gd_x)_3Ga_5O_{12}$* Garnet Single Crystals, Kimura, H., Numazawa, T., Sato, M. and Maeda, H. J. Mater. Sci. 26 (1991): 3753–57.

Materials for energy application

171. *Real-time Raman Measurements of Graphite under Ar^+ Irradiation*, Nakamura, K. and Kitajima, M. Appl. Phys. Letters 59 (1991): 1550–52.

172. *UV Photoemission Study on the Valence Band of Mo(110) During Argon Ion Bombardment*, Kitajima, M., Nakamura, K., Fujitsuka, M., Shinno, H., *Katoh, H. and *Miyahara, T. (*Natl. Lab. for High Energy Physics). Hyomen Kagaku 12 (1991): 36–40 (in Japanese).

173. *Creep Rupture Properties and Microstructures of Ni-Base ODS Superalloys*, Kawasaki, Y., Kusunoki, K., Nakazawa, S. and Yamazaki, M. Jpn. Soc. for the Promotion of Sci., 123rd Committee Rep. 32 (1991): 301–11 (in Japanese).

174. *Study of Raman Spectroscopy on Carbon Materials Irradiated with a High Current Density Electron Beam*, Kitajima, M., Nakamura, K., Fujitsuka, M., Shinno, H. and Tanabe, T. J. Nucl. Mater. 179–181 (1991): 81–83.

175. *Carbon Fiber/SiC Composite for Reduced Activation*, Noda, T., Araki, H., Abe,F. and Okada, M. J. Nucl. Mater. 179–181 (1991): 379–82.

176. *Alloy Composition Selection for Improving Strength and Toughness of Reduced Activation 9Cr-W Steels*, Abe, F., Noda, T., Araki, H. and Nakazawa, S. J. Nucl. Mater. 179–181 (1991): 663–66.

177. *Creep Rupture Properties of Helium Implanted γ Precipitation Strengthened Alloy*, Yamamoto, N., Nagakawa, J., Shiraishi, H., *Kamitsubo, H., *Kohno, I. and *Shikata, T. (*RIKEN). J. Nucl. Sci. Technol. 28 (1991): 1001–13.

178. *Hydrogen Permeation Characteristics of Vanadium-Nickel Alloys*, Nishimura, C., Komaki, M. and Amano, M. Mater. Trans. JIM 32 (1991): 501–7.

179. *The Effect of Tungsten on Dislocation Recovery and Precipitation Behavior of Low-Activation Martensitic 9Cr Steels*, Abe, F., Araki, H. and Noda, T. Metall. Trans. A 22A (1991): 2225–35.

180. *High Temperature Strength of Vanadium Alloys*, Kainuma, T. Metals & Technology 61-9 (1991): 19–25 (in Japanese).

181. *Electronic Structure in the Valence Band of Molybdenum being Bombarded with Argon Ions*, Kitajima, M., Nakamura, K., Fujitsuka, M., Shinno, H., *Katoh, H. and *Miyahara, T. (*Natl. Lab. for High Energy Physics). Phys. Rev. B 45 (1991): 8338–41.

182. *Time-Resolved Raman Study on Graphite under Ion Irradiation*, Kitajima, M. and Nakamura, K. Proc. of 9th ICRR 1 (1991): 299.

183. *UPS Study of Mo(110) under Ar^+ Irradiation*, Nakamura, K. and Kitajima, M. Radiation Research 1 (1991): 299.

Processing

Separation and synthesis

184. *High Purification Techniques for Rare Metals*, Hasegawa, R. Kinzoku 61 (1991): 12–15 (in Japanese).

185. *Laser Material Purification of Neodymium*, Ogawa, Y., Ozaki, T., Yoshimatsu, S. (Kobe Steel, Ltd.), *Chiba, K.*Umeda, H. and *Saeki, M. (*Nippon Steel Corp.). J. Jpn. Inst. Met. 55 (1991): 545–52 (in Japanese).

Gaseous process

186. *Preparation of $YBa_2Cu_3O_y$ Superconducting Thin Films on Metallic Substrates by Excimer Laser Ablation*, Saitoh, J. (Mitsuba Electric Mfg. Co., Ltd.), Fukutomi, M., Komori, K., Tanaka, Y., Asano, T., Maeda, H. and Takahara, H. (Mitsui Mining & Smelting Co., Ltd.). Jpn. J. Appl. Phys. 30 (1991): 898–900.

187. *Preparation of $YBa_2Cu_3O_y$ Superconducting Thin Films by Radio Frequency Plasma Flash Evaporation*, *Fukagawa, W., Komori, K., Fukutomi, M., Tanaka, Y., Asano, T., Maeda, H. and *Hosokawa, N. (*Anelva Corp.). Jpn. J. Appl. Phys. 30 (1991): 1216–17.

188. *Synthesis of Pd-Te Intermetallic Compound Films on 2H-MoS_2(0001) by Molecular Beam Epitaxy*, Yata, M., Nakamura, K. and Ogawa, K. (Yokohama Natl. Univ.). J. Vac. Sci. Technol. A9 (1991): 3019–24.

189. *Low Temperature Synthesis of SiC by UV Laser CVD*, Noda, T., Suzuki, H., Araki, H., Abe. F. and Okada, M. Proc. 2nd Jpn. Int. SAMPE Symp. (1991): 1209–14.

190. *Fabrication of Oxide Superconductor Films by Sputtering*, Nakamura, K. Surface Technique 42 (1991): 24–25 (in Japanese).

Liquid state process

191. *Moldless Upward Continuous Casting Process*, Sato, A., Ohsawa, Y. and Aragane, G. Jpn. Soc. for the Promotion of Sci., 19 Committee Rep. (1991): 2-1–2-17 (in Japanese).

192. *Production of Al-Cu and Al-Si Alloy Rods by a Moldless Upward Continuous Casting Process*, Sato, A., Ohsawa, Y. and Aragane, G. Mater. Trans. JIM 32 (1991): 77–83.

Powder processing

193. *Development of New Production Process of Intermetallic Compounds*, Kaieda, Y., Otaguchi, M., Oguro, N., *Oie, T. and *Hirayama, T. (*Kyoritsu Ceramic Materials Co., Ltd.). Bull. Jpn. Inst. Met. 30 (1991): 554–56 (in Japanese).

194. *Surface Phases of Iron Ultrafine Powders Estimated from Thermal Desorption Measurements and Their Reduction Characteristics*, Sakka, Y. and Uchikoshi, T. J. Jpn. Inst. Met. 55 (1991): 219–26 (in Japanese).

195. *Gas Evolution Characteristics and Passivity in Air of Iron Ultrafine Powders*, Uchikoshi, T. and Sakka, Y. J. Jpn. Inst. Met. 55 (1991): 558–63 (in Japanese).

196. *Uniformity of Sintered Superconductive Bi-Sr-Ca-Cu-O Ceramics*, Ohno, S., Okuyama, H., Honma, K., Halada, K. and Ozawa, M. J. Jpn. Soc. Powder Powder Metall. 38 (1991): 263–66 (in Japanese).

197. *Reaction of Sr-Ca-Cu-O Ceramics with Molten Bi_2O_3*, Ohno, S., Okuyama, H., Honma, K. and Ozawa, M. J. Jpn. Soc. Powder Powder Metall. 38 (1991): 267–70 (in Japanese).

198. *Gas Atomization and Heat Treatment of Bi-Sr-Ca-Cu Oxide*, Minagawa, K., Okuyama, H. and Harada, K. J. Jpn. Powder Powder Metall. 38 (1991): 308–11 (in Japanese).

199. *Water Atomizing Conditions and Properties of Spherical Iron Fines*, Takeda, T. and Minagawa, K. J. Jpn. Soc. Powder Powder Metall. 38 (1991): 790–99 (in Japanese).

200. *Effects of Ag-Doping on the Formation of Superconductive Phase in Bi-Sr-Ca-Cu-O Ceramics*, Ohno, S., Okuyama, H., Honma, K. and Ozawa, M. J. Jpn. Soc. Powder Powder Metall. 38 (1991): 1035–38 (in Japanese).

201. *Crystalization of Bi-Sr-Ca-Cu Oxide Atomized from Molten State*, Halada, K., Minagawa, K., Okuyama, H. and Honma, K. J. Jpn. Soc. Powder Powder Metall. 38 (1991): 1083–88 (in Japanese).

202. *Sintering Characteristics of Cobalt Ultrafine Powders*, Sakka, Y. J. Less-Common Met. 168 (1991): 277–87

203. *Effects of Cold Isostatic Pressure on the Sintering Behavior of Iron and Copper Ultrafine Powders*, Sakka, Y. J. Mater. Sci. Letters 10 (1991): 426–29

204. *Effects of Heating on the Densification, Structure and Magnetic Properties of Fe-Co Alloy Ultrafine*

Powders, Sakka, Y. J. Mater. Sci. Letters 10 (1991): 987–91

205. *Characterization of the Hydroxyapatite Precursor Synthesized by Wet Process*, Aoki, A., Ohno, S., Uchikoshi, T. and Muramatsu, Y. Phosphorus Research Bulletin 1 (1991): 31–34

Joining

206. *Effect of Molten Metal Behavior on Melting Process in Electron Beam Welding—A Study on Electron Beam Welding Phenomena (Report IV)*, Tsukamoto, S. and Irie, H. Q. J. Jpn. Weld. Soc. 9 (1991): 348–53 (in Japanese).

Composite process

207. *The Effect of Oxidizing Agents on the Formation of Chemical Conversion Coatings on Mild Steels in an Na_2MoO_4 Type Aqueous Solution*, Kurosawa, K. and Fukushima, T. (Univ. of the Ryukyus). Corros. Sci. 32 (1991): 893–902.

208. *Application of Plasma Twin Torch Process for Formation of FGM*, Kitahara, S., Fukushima, T. and Kuroda, S. Jpn. Soc. for the Promotion of Sci., 123rd Committee Rep. 32 (1991): 89–90 (in Japanese).

209. *Gradient Coatings Formed by Plasma Twin Torches and those Properties*, Fukushima, T., Kuroda, S., and Kitahara, S. Jpn. Soc. for the Promotion of Sci., 123rd Committee Rep. 32 (1991): 91–96 (in Japanese).

210. *The Origin and Quantification of the Quenching Stress Associated with Splat Cooling during Spray Deposition*, Kuroda, S. and Clyne, T.W. (Univ. of Cambridge). Proc. 2nd Plasma-Technik-Symp. 3 (1991): 273–83.

211. *Oxidation Resistant Coating on Titanium Alloys and TiAl Intermetallic Compound*, Takei, A. and Ishida, A. Proc. of 7th APCCC 2 (1991): 718.

212. *The Quenching Stress in Thermally Sprayed Coatings*, Kuroda, S. and Clyne, T.W. (Univ. of Cambridge). Thin Solid Films 200 (1991): 49–66.

213. *Measurement of Temperature and Velocity of Thermally Sprayed Particles Using Thermal Radiation*, Kuroda, S., Fujimori, H. (Keio Univ.), Fukushima, T. and Kitahara, S. Trans. Jpn. Weld. Soc. 22 (1991): 82–89.

Process with aid of beam technology

214. *Fabrication of Bi-Based Oxide Superconductors by YAG-Laser Irradiation*, Yuyama, M., Wada, H., Itoh, K. and Kuroda, T. Cryogenic Engineering 26 (1991): 288–95 (in Japanese).

215. *Fabrication of Bi-Based Oxide Superconductors by YAG-Laser Irradiation*, Yuyama, M., Wada, H., Itoh, K. and Kuroda, T. Cryogenics 31 (1991): 900–5.

216. *The State-of-The Art of Laser Apparatus for Material Processing*, Irie, H. J. Jpn. Weld. Soc. 59 (1991): 22–26 (in Japanese).

217. *Direct Observation of Defects Formation of Semiconductors During the Irradiation in the Electron Microscope*, Furuya, K. and Ishikawa, N. Proc. of JISSE–2 (1991): 323–30.

Processing in special environment

218. *Fatigue Testing System and Result of Long-Term Operation*, Yuri, T., Nagai, K., Ogata, T., Umezawa, O. and Ishikawa, K. "Cryogenic Engineering" 26 (1991): 184–89 (in Japanese).

219. *Diffusion Behavior of Ti in Cu Films Deposited on Ti Substrate*, Yoshitake, M. and Yoshihara, K. J. Jpn. Inst. Met. 55 (1991): 773–78 (in Japanese).

220. *The Gas Desorption Behavior From BN Coated Vacuum Chamber*, Tosa, M., Yoshitake, M. and Yoshihara, K. J. Vac. Soc. Jpn. 34 (1991): 62–64 (in Japanese).

❒ NRIM Publications (Apr. 1991 to Mar. 1992)

1. Bulletin of National Research Institute for Metals, in Japanese.
   No. 13 (Feb. 1992)
2. Annual Report of National Research Institute for Metals, in Japanese.
   For fiscal year of 1990 (Dec. 1991)
3. Kinzaigiken News, in Japanese.
   Nos. 4 to 12 (1991) and Nos. 1 to 3 (1992)
4. NRIM Research Activities, in English.
   (Nov. 1991)
5. NRIM Special Report, in English.
   (Mar. 1992)
6. Material Strength Data Sheet, in English.
   NRIM Creep Data Sheet,
   Nos. 8B and 38A (Sep. 1991)
   Nos. 7B and 12B (Mar. 1992)
   NRIM Fatigue Data Sheet,
   Nos. 67 and 68 (Dec. 1991)
7. Guide to National Research Institute for Metals, in Japanese and in English.
   For fiscal year of 1992 (May 1992)

International Exchange Apr.1991 to Mar. 1992

❒ International Collaboration Research

Australia

1. Study on Surface Modification of Metals with Ultra-High Temperature Heat Sources. (CSIRO)

Brazil

1. Study on Ni-Base Superalloys. (Fundacao De Technologia Industrial)

Canada

1. Damage Evaluation and Residual Life Prediction of Structural Materials. (Energy Miles and Resources Physical Metallurgy Research Laboratory)

China

1. Study on Preventing Methods of Welding Defects in Electron Beam Welding. (Chengdu Electrical Welding Machine Research Institute)
2. Investigation of High Temperature Titanium Alloy for Application over 600 °C. (Northwest Institute for Non-Ferrous Metal Research)

Finland

1. Development of High-T_c Oxide Superconducting Thin Films. (Tampere University of Technology)

France

1. Superconducting and Cryogenic Materials. (Service National des Champs Intenses, Centre National de la Recherche Scientifique Grenoble and Others)

Germany

1. Development of Superconducting Materials. (Kernforschungszentrum Karlsruhe)
2. Exchange of Creep and Fatigue Data Sheet. (5 Institutes)

Italy

1. Mechanism of Deformation, Fracture and Corrosion in Ni-Based Superalloys. (Instituto per la Tecnologia dei Materiali Metallicinon Tradizionali)
2. Superconducting Properties of Advanced Superconductors in Time-Varying Magnetic Fields. (CISE Spa, Technologia Innovative Thermophysics & Cryogenics Sec.)
3. Intercomparison of Methods and Materials for Strain Measurements at Cryogenic Temperatures. (Instituto di Metrogia "G. Colonettie" - C.N.R.)

Korea

1. Application of Thermoelectric Materials to Energy Conversion. (Korea Advanced Institute of Science and Technology)
2. Processing Technology and the Characterization of Advanced Aluminium Alloys. (Korea Institute of Machinery and Metals)
3. On the Application of the Recrystallization Phenomena in Refractory Metals. (Korea Institute of Science and Technology)
4. Characterization of the Composite Film with Dispersion of Carbide Phase by PVD and CVD Process and the Establishment of the Process Parameters Leading to Fabrication Techniques. (Korea Institute of Machinery and Metals)
5. Fabrication Process for High-T_c Superconductors. (Korea Institute of Machinery and Metals)
6. Aluminide Intermetallic Compounds for High Temperature Structual Materials. (Korea Institute of Machinery and Metals)
7. Information Exchange on Materials Strength Data. (Korea Standards Research Institute)

Philippines

1. Evaluation of Corrosion Resistance of Metals by Atmospheric Exposure Test. (Materials Science Research Institute and Other Institutes)

Sweden

1. Application of Advanced Electromagnetic Technology to the Metallurgical Processing. (Royal Institute of Technology)

Thailand

1. Evaluation of Corrosion Resistance of Metals by Atmospheric Exposure Test. (Thailand Institute of Scientific and Technological Research, and Other Institutes)

U.K.

1. Prediction of the Life and Remaining Life of Huge Structure. (Welding Institute)

U.S.A.

1. Exchange of Creep and Fatigue Data Sheets. (National Institute of Standards and Technology)
2. US-Japan Fusion Cooperation Program. (Research Institute of Fusion in U.S.A.)
3. Studies of High-Strength/High-Conductive Materials and Their Application to High Field Magnet. (Francis Bitter National Magnet Laboratory)
4. Evaluation Methods for Superconductors. (National Institute of Standards and Technology)
5. Combustion Synthesis for Production of Ceramic, Intermetallic and Composite Materials. (Alfred University)
6. Research and Development on Systems and Materials for Magnetic Refrigerators. (Francis Bitter National Magnet Laboratory)

EC

1. EC-Japan Fusion Cooperation Program. (Research Institute of Fusion in EC)

International

1. Versailles Project on Advanced Materials and Standards. (Summit Working Group on Technology)

❒ List of Guest Researchers

*STA Fellowship

Nationality and Name	Affiliation	Term	Research Subject
Australia			
Dr. D. A. Scott	Institute of Industrial Technology, CSIRO	1992.1.12. to 1992.2.1.	Study on Molten Metal Phenomena in High Power Density Beam Processing
Belgium			
Dr. D. Vanderschueren*	University of Leuven	1992.3.1. to 1993.2.28.	Hot Deformation Properties of Titanium Aluminide TiAl Intermetallics
China			
Mr. Jiang Chun Sheng	Institute of Metal Research, Academia Sinica	1990.11.27. to 1991.11.26.	Synthesis of Composite Ultrafine Particles by "Reactive Plasma-Metal" Reaction
Dr. Wang Xinhua*	University of Science and Technology, Beijing	1990.5.9. to 1991.5.8.	Complex Ore for the Rare-Metal Resources
Dr. Haiyan Zhu*	Zhejiang University	1991.5.15. to 1992.5.14.	Structure and Electric Properties of Transition Metal Compounds
Mrs. Zhao Xiu-Ping	Harbin Normal University	1991.8.9. to 1991.11.8.	Development of high performance thermoelectric intermetallic compound
Mr. Jin Chu-Ji	Harbin Normal University	1991.8.9. to 1991.11.8.	The same as above
Mr. Zhang Yong-Chang	Harbin Normal University	1991.8.9. to 1991.11.8.	The same as above
Mr. Li Jiang-Lu	Harbin Normal University	1991.8.9. to 1991.11.8.	The same as above
Mrs. Ma Minya	Institute of Metal Research, Academia Sinica	1991.11.3. to 1992.3.31.	Environmental Degradation of Structural Materials for Light Water Reactors
Dr. Zhao Hanxie	Shanghai Jiaotong University	1992.2.24. to 1992.4.12.	The same as above
Denmark			
Dr. S. Tougaard	University of Odense	1991.11.10. to 1991.12.30.	Research on the Rapid Diffusion in Thin Metal Films
France			
Dr. B. Chenevier*	Ecole Nationale Superieure de Phsique de Grenoble	1991.1.11. to 1991.10.10.	High Resolution Electron Microscope Study of Superconducting Oxide
Dr. Balette-Pape*	Université de Bordeaux I	1992.1.9. to 1993.7.8.	Damage Modeling near Crack Tip in Metal Matrix Composites

Nationality and Name	Affiliation	Term	Research Subject
Germany			
Dr. H. Norenberg*	Rostock University	1992.3.3. to 1993.3.2.	Fabrication of Quantum Well Boxes by Molecular Beam Epitaxy
India			
Dr. P. Mahajan*	Montana State University	1991.1.15. to 1992.1.14.	Characterization of Metals and Alloys Using Synchrotron Radiation
Iran			
Mr. M. Goodarzi	Iran University of Science and Technology	1991.10.7. to 1991.12.21	Training in Powder Metallurgy
Mr. A. J. Gharebagh	Iran University of Science and Technology	1991.10.7. to 1991.12.21.	The same as above
Korea			
Mr. Kim Seung-Eon	Korea Institute of Machinery & Metals	1992.2.1. to 1992.3.31.	Microstructure and Mechanical Properties of TiAl-bases Alloys
Netherlands			
Dr. J. P. Zijp*	Technische Univeriteit Delft	1990.11.11. to 1992.11.11.	Vaporization Phenomena in Arc Plasmas
Philippines			
Ms. L. A. D. Guzman	Industrial Technology Development Institute	1991.7.15. to 1992.6.10.	Japan-ASEAN Cooperation Program on Materials Science and Technology, Philippine Project on Atmospheric Corrosion (Inorganic Coating)
Ms. C. I. D. L. Pena	Industrial Technology Development Institute	1991.7.15. to 1991.12.4.	The same as above
Russia			
Dr. A. P. Kuprin*	Moscow State University	1992.3.31. to 1993.9.30.	Hydrogen and Its Isotope Effects on the Electronic Properties of Metals and Semiconductors by Using the In-Situ Analysis in the Electron Microscop
Thailand			
Mr. C. Nitipanyawong	King Mongkut Institute of Technology, Thonburi	1991.11.5. to 1992.3.18.	Japan-ASEAN Cooperation Program on Materials Science and Technology, Thai Project on Atmospheric Corrosion (Organic Coating)
Ms. N. Thanuddhanusilp	Thailand Institute of Scientific and Technological Research	1992.3.9. to 1992.7.3.	The same as above
U.S.A.			
Dr. D. C. Johnston	Ames Laboratory, Iowa State University	1991.6.10. to 1991.8.1.	Magnetic Properties of Rare Earth Compounds
Dr. G. C. Stangle*	Alfred University	1991.6.28. to 1991.8.5.	Combustion Synthesis of Intermetallics
Prof. P. G. McCormick	University of Western Australia	1991.10.14. to 1991.10.29.	Shape Memory Characteristics of Ti-Ni Thin Films Formed by Sputtering
Dr. L. F. Goodrich	National Institute of Standards and Technology	1991.12.10. to 1991.12.23.	Study on Measurement and Evaluation Methods for Superconducting Properties
Dr. Y. Iwasa	Francis Bitter National Magnet Laboratory	1992.3.1 to 1992.3.20.	Application of Cu-Ag Alloys to High-Field Magnets
Dr. H. Ledbetter	National Instutute of Standards and Technology	1992.3.14. to 1992.3.28.	Elastic Constants and Mechanical Properties of Oxide Superconductors at Low Temperatures
Dr. J. Schwartz	Illinois University	1992.3.16. to 1992.3.25.	Discussions on the Results of Ag-Sheath Bi-Oxides Superconducting Wires
Dr. J. Lewis	Illinois University	1992.3.16. to 1992.3.25.	Discussions on the Results of Doctor-Blade Processed Bi-oxide Superconducting Wires
Dr. D. K. Finnemore	Iowa State University	1992.3.23. to 1992.3.28.	Studies on the Critical Current Characteristics of High Temperature Superconductors

❒ List of Visitors

M: Meguro Main Site T: Tsukuba Laboratories

Nationality and Name	Affiliation	※	Date
Australia			
Dr. D. Phelan	Monash University	T	Feb. 1992
Austria			
Prof. Brigitte Weiss and his party	Institute of Physical Chemistry University. of Viena	M, T	Sep. 1991
Brazil			
Mr. L. S. Messias and his party	Sao Paulo State Institute for Technological Research	T	Dec. 1991
Canada			
Mr. J. P. Monchalin and his party	IMI, NRCC	T	Jun. 1991
Mr. Julian Cave	Hydro-Quebec Research Center	T	Oct. 1991
Dr. Jacques G. Martel	Industrial Materials of National Research Council of Canada	T	Dec. 1991
Prof. W. R. Patars	MacMaster University	T	Feb. 1992
China			
Dr. Yong-Gang Zhang	Beijing University of Aeronautics and Astronautics	M	Jun. 1991
Dr. Zhang Qirui and his party	Zhejiang University	T	Aug. 1991
Mr. Lu Sinien	Chinesu Academy of Science	T	Aug. 1991
Dr. Wang Jing-Tang	Institute of Metal Research, Academia Sinica	M, T	Sep. 1991
Prof. Heugrong Guan and his party	Institute of Metal Research, Academia Sinica	M, T	Sep. 1991
Dr. Wei Wen-Duo	Institute of Metal Research, Academia Sinica	M, T	Oct. 1991
Mrs. Zhao Xiu-Ping and her party	Harbin Normal University	T	Oct. 1991
Dr. Zhou Rongzhang and his party	University of Science and Technology, Beijing	M	Oct. 1991
Dr. Li Yi-Yi	Institute of Metal Research, Academia Sinica	M, T	Nov. 1991
Dr. Lin Dongliang	Shanghai Jiaotong University	M	Nov. 1991
Mrs. Ma Minya and her party	Institute of Metal Research, Academia Sinica	T	Dec. 1991
Dr. Zhang Guo-Ding and his party	Shanghai Jiaotong University	M, T	Dec. 1991
Prof. Jian Hong Chen and his party	Ganzu Technical University	M	Dec. 1991
Prof. Yunwen Lu and his party	Tsinghua University	T	Feb. 1992
Mr. Riu Baoxia and his party	Beijing Shi Jiaoyu Xueyuan	T	Feb. 1992
Czecho Slovakia			
Dr. M. Jergel	Electrotechnical Institute	T	Mar. 1992
Egypt			
Mr. M. A. Abbas and his party	Central Metallurgical Research & Development Institute	T	Dec. 1991
Formosa			
Prof. M. K. Wu	National Tsing Hua University	T	Oct. 1991
France			
Dr. O. Dimitrov	Cantre National de La Recherche Scientifique	T	Jun. 1991
Dr. Gean M. Fried	Air Liquide Laboratory	T	Jun. 1991
Dr. M. Gomina	Cantre National de La Recherche Scientifique	T	Jul. 1991
Mr. Bai Jinbo and his party	Ecole Centrale de Paris	T	Aug. 1991
Prof. Paul Merle	Lyon National Institute of Applied Science	M	Oct. 1991
Mr. Philippe Boch and his party	Cantre National de La Recherche Scientifique	M	Nov. 1991
Mr. Robert Capitini	Atomic Energy Commission	T	Dec. 1991
Germany			
Dr. R. P. Huebener	Universitat Tubingen	T	Jul. 1991

Nationality and Name	Affiliation	※	Date
Mr. Hang Leonhard and his party	Allianz Zentrum fuer Techik Gmbh	T	Aug. 1991
Prof. D. Löhe	Universitat Gesamthochshule Paderboru	T	Aug. 1991
Mr. Christian Boller	MBB-Deutsche Aerospace	T	Aug. 1991
Dr. Christian Hartig	University of Hamburg-Harburg	M	Nov. 1991
Dr. Harald Bolt and his party	Institute for Reactor Materials	T	Feb. 1992
Iceland			
Dr. Hans Kr. Gudmundsson	Technological Institute of Iceland	M	Oct. 1991
India			
Dr. Easo P. George	Oak Ridge National Laboratory	M	Dec. 1991
Dr. Krishan Lal and his party	National Physical Laboratory	T	Feb. 1992
Indonesia			
Mr. W. H. Manfadipura and his party	BPPT	M	Aug. 1991
Ms. E. M. Wigayati and her party	Research & Development Centre of Applide Physics Fisika Terapan-LIPI	T	Dec. 1991
Mr. Achmad Sulaiman	Indonesian Institute of Science	T	Feb. 1992
Iran			
Mr. S. M. L. Moossavi and his party	Esfahan Steel Company	M	Feb. 1992
Israel			
Dr. Meir Weinstein	Tel Aviv University	M	May 1991
Korea			
Mr. Shin and his party	POSCO	M	Oct. 1991
Mr. Park Moon Su and his party	Korea Association of Steel	T	Nov. 1991
Mr. Ko and his party	Sammi Special Steel Co. Ltd.	M	Nov. 1991
Dr. Gun-Woong Bahng and his party	New Materials Evaluation Center, KRISS	T	Feb. 1992
Malaysia			
Dr. A. G. Ramli and his party	Unit Tenage Nuklear	T	Feb. 1992
Netherlands			
Prof. Ir. B. H. Kolster and his party	Foundation for Advanced Metals Science	M	Jul. 1991
Mr. Baker Ad and his party	Delft University. of Technology	T	Aug. 1991
Norway			
Prof. P. J. Haagensen	University of Trondheim	M	Aug. 1991
Philippines			
Mr. S. T. Bernardo and his party	Industrial Technology Development Institute	T	Feb. 1992
Poland			
Mr. R. B. Said and his party	Warsaw University of Technology	T	Aug. 1991
Russia			
Dr. A. Merzhanov and his party	Institute of Structural Macrokinetics	M	Oct. 1991
Dr. A. Virtser and his party	Soviet Academy of Sience	T	Dec. 1991
South Africa			
Mr. Kotze Theunis G. N and his party	Consulting Engineer	T	Aug. 1991
Sweden			
Mr. P. Chirisfer and his party	Linkoqing University	T	Aug. 1991
Prof. Janne Carlsson	Royal Institute of Technology	T	Aug. 1991
Switzerland			
Mr. Irimescu Barbu and his party	Swiss Federal Institute of Technology	T	Aug. 1991

Nationality and Name	Affiliation	※	Date
Thailand			
Mr. C. Poorakkiat and his party	Chulalongkorn University	T	Dec. 1991
Dr. A. Euapermkiati and his party	National Center for Metals and Materials Technology	T	Feb. 1992
Turkey			
Mr. Unal Alkis and his party	Asil Celik	T	Dec. 1991
U.K.			
Dr. Bryan Roebuck	National Physical Laboratory	T	Apr. 1991
Dr. G. Donaldson	University of Strathclyde	T	Jul. 1991
Dr. Carter Faith and his party	Aston University	T	Aug. 1991
Dr. Anthony Barrett and his party	CODATA Task Group on Materials Database	T	Feb. 1992
U.S.A.			
Prof. James R. Thompson	University of Tennessee	T	May 1991
Prof. Ryoichi Kikuchi	University of California, Los Angeles	M	May 1991
Prof. N. S. Stoloff	Rensselaer Polytechnic Institute	M	Jun. 1991
Dr. Young-Won Kim	Wright-Patterson Air Force Base	M	Jun. 1991
Mr. Kim Yetter Bottimor	Kodak Japan Ltd.	T	Jun. 1991
Mr. Werner G. Kontara	Jet Proqulsion Laboratory	T	Jul. 1991
Dr. John Rumble	National Institute Standards and Technology	M	Jul. 1991
Dr. A. P. Malozemoff and his party	American Superconductor Corporation	T	Jul. 1991
Prof. Frederick S. Pettit	University of Pittsburgh	M, T	Jul. 1991
Dr. R. B. Poeppel	Argonne National Laboratory	T	Aug. 1991
Prof. Dabid T. Shaw	New York State Institute on Superconductivity	T	Sep. 1991
Dr. A. L. Bement, Jr. and his party	Science and Technology TWD Inc.	T	Sep. 1991
Dr. Charles W. Allew	Argonne National Laboratory	T	Sep. 1991
Prof. Richard M. Spriggs	Alfred University	M	Oct. 1991
Prof. Paul G. McCormick	University of Western Australia	M, T	Oct. 1991
Dr. M. Suenaga and his party	Brookhaven National Laboratory	T	Oct. 1991
Dr. Simon Foner	Francis Bitter National Magnet Laboratory	T	Oct. 1991
Mr. Alan M. Wolsky	Argonne National Laboratory	T	Nov. 1991
Mr. Alan McGowan	Scientists' Institute for Public Information	T	Mar. 1992

❐ Brief Introduction of STA Fellowship

The Science and Technology Agency (STA), an administrative organ of the Government of Japan, offers opportunities for promising young foreign researchers in the fields of science and technology to conduct research at Japan's national laboratories and public research corporations (excluding universities and university-affiliated institutes). The program is managed by the Research Development Corporation of Japan (JRDC), a statutory organization under the supervision of STA in cooperation with the Japan International Science and Technology Exchange Center (JISTEC).

Fellowship qualifications are as follows:

1. Possession of doctor's degree.
2. Less than 35 years of age, in principle.
3. Sufficient good health for research work and life in Japan.
4. Sufficient language ability in Japanese or English.

The tenure will be 6 months to 2 years. JRDC provides expenses for round-trip, monthly living with family, initial setting-in and travel in Japan. Research expenses willl be paid for the host institute. Further information can be obtained at:

Japan International Science and Technology Exchange Center (JISTEC)
Port One Building 6F, 1-7-6, Minato-machi,
Tsuchiura City, Ibaraki Pref. 300, Japan
Phone +81-298-24-3355
Fax +81-298-24-3214

Organization of NRIM

❒ Organization

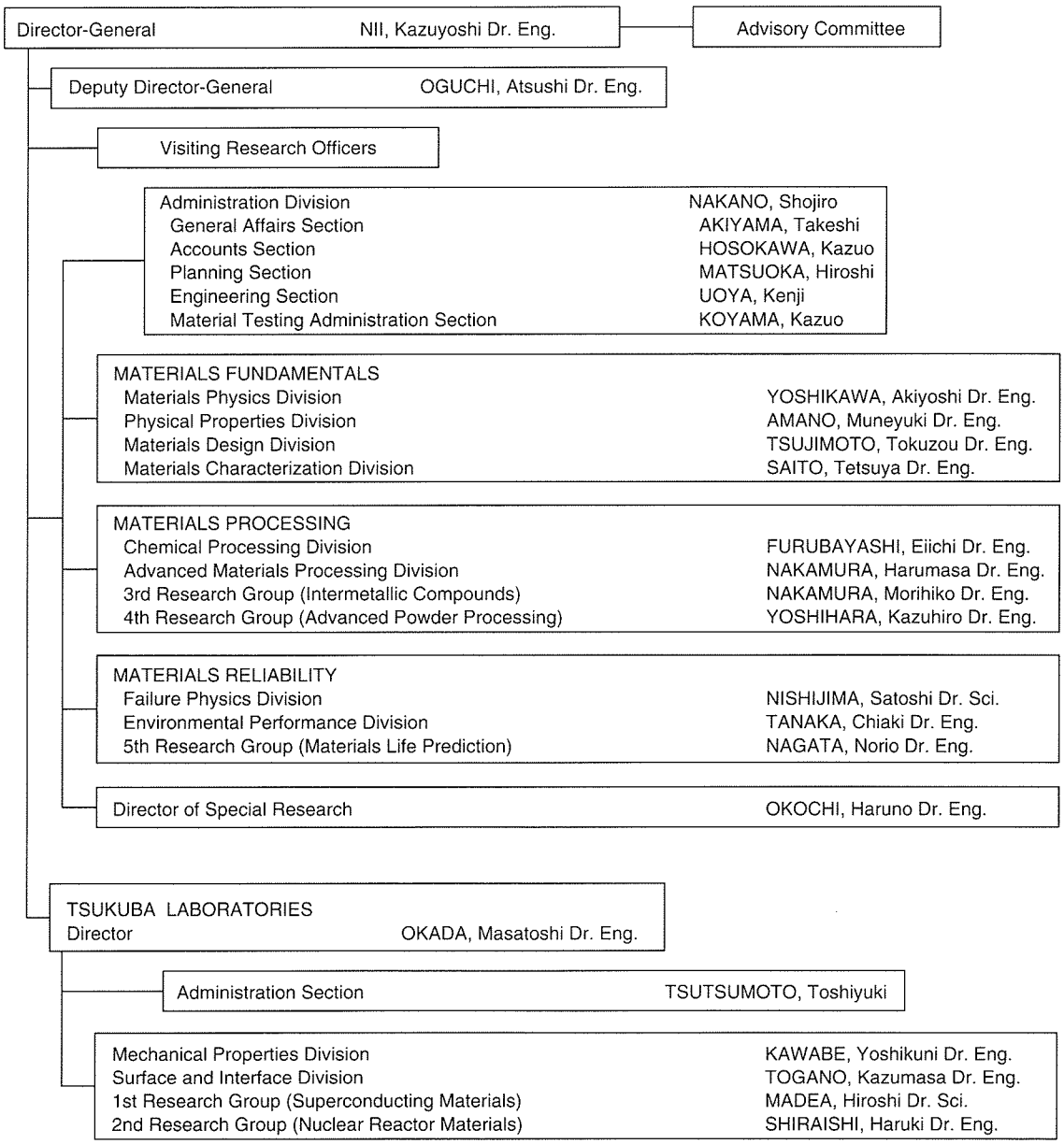

❒ Budget and Personnel in Fiscal Year of 1992

Budget	
Research and facilities	3,414
Personnel expenses	3,518
Total	6,932

unit: million yen

Personnel	
Administrative staffs	97 (8)
Researchers	330 (100)
Total	427 (108)

Number in parenthesis: Tsukuba laboratories

How to get to NRIM

To NRIM Meguro Main Site
2-3-12, Nakameguro, Meguro-ku, Tokyo 153
Phone +81–3–3719–2271 Fax +81–3–3792–3337

Narita Airport
↓ by train, JR Narita Express <60 min.>
Tokyo Station
↓ by train, JR Yamanote Line <25 min.>
Ebisu Station
↓ by taxi <5 min.> or on foot <15 min.>
NRIM

To NRIM Tsukuba Laboratories
1–2–1, Sengen, Tsukuba-shi, Ibaraki 305
Phone +81–298–51–6311 Fax +81–298–51–4556

Narita Airport
↓ by train, JR Narita Express <60 min.>
Tokyo Station
Tokyo Station Yaesu-Minami-Guchi
↓ by bus, Joban Highway Bus for Tsukuba Center <70 min.>
Tsukuba Center Bus Terminal
↓ by taxi <5 min.> or on foot <15 min.>
NRIM

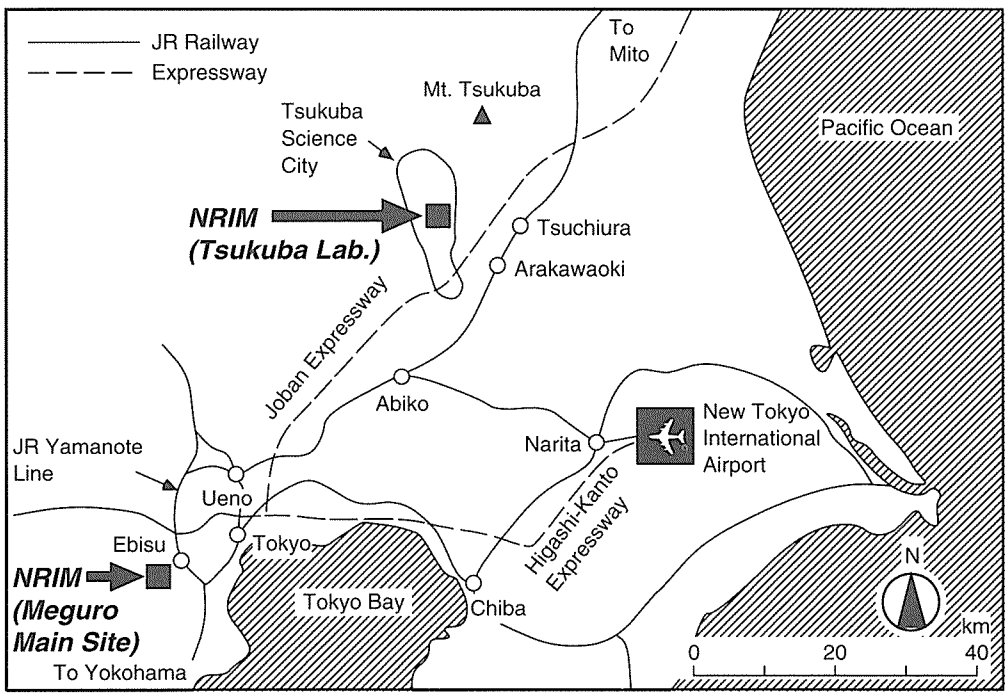

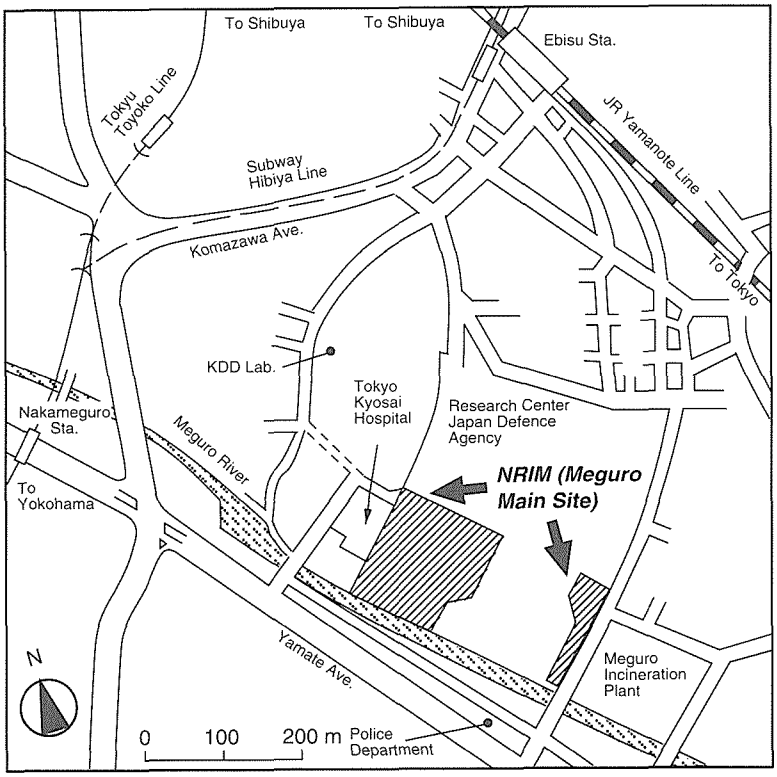

Meguro Main Site

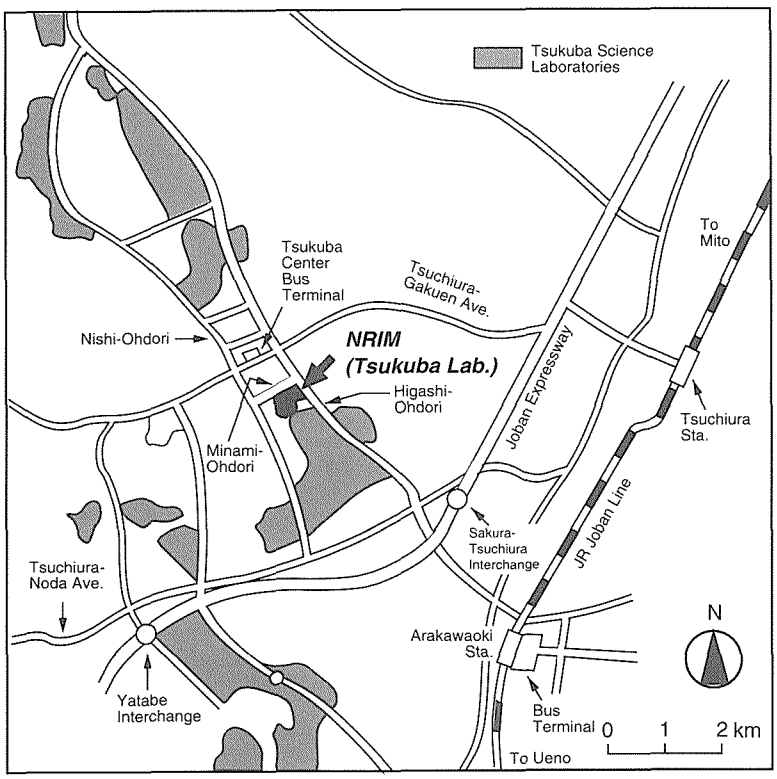

Tsukuba Laboratories

List of Keywords

E

F

G

H

NRIM Research Activities
1992
Date of Issue: 31 October, 1992

Publisher:
MATSUOKA, Hiroshi
Planning Section of Administration Division
National Research Institute for Metals
2-3-12, Nakameguro, Meguro-ku, Tokyo 153 Japan
Phone: +81-3-3719-2271 Fax: +81-3-3792-3337

Typeset using SGML by Uniscope Inc., Tokyo

NRIM Research Activities

1992